UNIVERSITY OF LONDON THESIS

Degree PhD Year 2008 Name of Author PRABHU, Gita

Neural mechanisms of object-orientated action

Gita Prabhu

Institute of Neurology

University College London

Submitted for PhD

May 2008

Supervisors: Professor R.N. Lemon & Professor P. Haggard

ProQuest LLC
789 East Eisenhower Parkway
P.O. Box 1346
Ann Arbor, MI 48106-1346

Abstract

The ventral premotor cortex (area F5, in the macaque monkey) plays an important role in the control of hand shape during object grasp. F5 neurones can encode the selection of different grasps, and are excited by vision of graspable objects. However, it is not clear how F5 influences the motor outputs to the hand and arm that control hand shape. By using linked neurophysiological studies in macaque monkeys and humans, this thesis examined, firstly, how visual information for action is encoded in area F5 and, secondly, the transmission of this information from F5 to the primary motor cortex (M1).

The relationship of F5 activity to the observation and movement stages of a visuomotor grasping task was examined. Single units from M1 and F5 and electromyographic (EMG) activity were recorded from macaque monkeys. Recordings from F5 revealed evidence for object- and grasp-related activity, suggesting that initially neurones are activated by the visual characteristics of the object and later represent the specific hand configuration for grasp of the object. M1 activity was consistent with encoding of grasp, but was uninfluenced by object. Secondly, using the same task, the pathways used to transmit visuomotor information from F5 to M1 were investigated by intracortical microstimulation of these cortical regions. The facilitation and suppression of the M1 test response from F5 conditioning was highly specific, evoked only in particular muscles and certain object-grasp combinations. Furthermore, the timing of the evoked response supports late I-wave pathways mediating F5-M1 interactions in visuomotor grasp.

In the final set of experiments a paired-pulse transcranial magnetic stimulation paradigm, previously shown to enhance the late I-wave components of the corticospinal volley, was used to examine object-orientated grasp in healthy human subjects. The results suggest excitability of cortico-cortical inputs to M1 was transient and contributed to action selection only when immediate sensory information specified which action to make.

Results from this thesis expand our knowledge of the role of F5 in visuomotor grasp, by showing F5 single unit activity is compatible with encoding the physical properties of an object to be grasped as well as the motor prototype used for grasp. Evidence is also provided for a possible route for transmission of visuomotor information from F5 to M1. Overall, there was a highly specific task-related pattern of object/grasp-related activity present in F5 and M1 single units and the EMG activity evoked from stimulation of these regions during the preparation and execution stages of visuomotor grasp.

Contents

List of Figures

List of Tables

Abbreviations

1DI – First Dorsal Interosseous

AD – Anterior Deltoid

ADM – Abductor Digiti Minimi

AbPL – Abductor Pollicis Longus

AIP – Anterior Intraparietal Area

AS – Arcuate Sulcus

BrR – Brachioradialis

CM – Corticomotoneuronal

CS – Central Sulcus

CST – Corticospinal Tract

ECR – Extensor Carpi Radialis

ECRL - Extensor Carpi Radialis Longus

ED 4,5 - Extensor Digitorum 4,5

EDC – Extensor Digitorum Communis

EMG – Electromyogram

FCU - Flexor Carpi Ulnaris

FDP – Flexor Digitorum Profundus

FDS – Flexor Digitorum Sublimis

F5 – Rostral Ventral Premotor Cortex

HAPEX – Hydroxyapatite Polyethylene

HPR – Homepad Release

ICMS - Intracortical Microstimulation

IPS – Intraparietal Sulcus

LED – Light Emitting Diode

M1 – Primary Motor Cortex

MEP – Motor Evoked Potential

MRI – Magnetic Resonance Imaging

PL –Palmaris Longus

PT- Pyramidal Tract

PTN – Pyramidal Tract Neurone

SD- Standard Deviation

SE – Standard Error

Th - Thenar

TMS – Transcranial Magnetic Stimulation

Declaration of Conjoint Work

The work to be presented in this thesis is my own original work. It was completed without assistance, apart from:

1. Critical stages of the surgical procedures were performed by Professor R N Lemon and members of his research team.
2. The experimental work was performed as part of an ongoing research programme in Professor R N Lemon's laboratory, with scientific and technical assistance from members of his research group.
3. I took the lead role in conducting all of the human experiments and most of monkey experiments reported in this Thesis; the only exceptions are the data analysed and presented in Chapter 3 (experiment M39) and Chapter 4 (experiment CS15) which were collected from a previous experiment by Professor R N Lemon and members of his team.
4. The similarity matrix and polar plots were produced by Dr T Brochier, Sobell Department, ION.
5. Assistance with programming was received from Dr T Brochier and Dr A Kraskov.
6. Post-mortem histology was performed by Mr J Dick, Sobell Department, ION.
7. MRIs were acquired from Mr D MacManus, NMR Unit, UCL Institute of Neurology.

Acknowledgements

It is a pleasure to thank all the people who have helped me over the past four years. First I would like to thank my lab, who have not only encouraged and advised me, but provided a fun and stimulating environment to work in. In particular I would like to thank Professor Roger Lemon, his knowledge and enthusiasm has been inspirational. I am extremely grateful to Dr Thomas Brochier for his endless patience and support, Dr Luigi Cattaneo and Dr Martin Voss without whom the TMS work would not have been possible. I am also extremely fortunate to have benefited from support and friendship of Dr Rachel Spinks, Sam Shepherd, Dr Alexander Kraskov and Dr Ben Townsend. I would also like to give special thanks to Professor Patrick Haggard for his greatly appreciated advice, encouragement and excellent knowledge of statistics.

This work would not have been possible without the help and support of the staff of the Sobell Department. I am indebted to the Kirkwood, Greensmith, Wolpert, Day and Rothwell labs, for their advice, friendship and letting me borrow their equipment. I would also like to thank Dr Chris Seers, Jim Dick, Richard Symonds, Ed Bye and Victor Baller who provided technical expertise and Deborah Hadley, Kully Sunner and Molly Cureton for guiding me through the intricacies of UCL administration.

Finally I would like to give special thanks to my mother and brother for their patience and support throughout these four years.

1. Introduction

The human hand is a powerful instrument of the mind. Flexible and versatile, the hand is the major route by which we interact with the world. We are able to execute rapid, accurate movements such as catching a ball, delicate manipulations when playing an instrument, and are capable of generating powerful forces to crush, twist and tear objects. Humans have used the capacity of our motor system to make our hands the effectors of cultural and technological outpourings, literally shaping our environment. Central to skilled hand function is the ability to guide the hands using the dominant sensory modality of vision. From vision of an object we can rapidly and precisely orientate and shape our hand, using the correct amount of force to hold the object securely and undamaged. As this transformation is not a conscious process, we are unencumbered in daily life by the complex processing that is being carried out, unaware of the fine motor control required each time we reach out and grasp a visible object.

1.1 The corticospinal tract

The numerous configurations we can make with the hand have been described in terms of relatively independent finger movement (RIFM). Primates show varying degrees of RIFM. For instance, the great apes, humans, and some Old World monkeys, including macaques, have a large repertoire of independent finger movements whilst New World monkeys, for example marmosets and squirrel monkeys, despite sharing a strong resemblance in hand shape, generally perform whole hand grasping actions, with a few important exceptions (e.g. capuchin monkeys) (Porter and Lemon, 1993). Among other

factors, these differences have been attributed to the descending system through which the cortex controls the hand muscles, the corticospinal tract (CST).

The descending pathways from the cerebral cortex and brain stem provide the anatomical substrate by which the brain governs spinal motoneurones and so movement (Kuypers, 1981). The importance of the CST in RIFM has been highlighted by lesion studies in macaque monkeys. Animals with a complete bilateral pyramidotomy, which interrupts all CST fibres, showed rapid postoperative recovery of walking, climbing and running, but a sustained deficit in RIFM (Lawrence and Kuypers, 1968). There is also a correlation between dexterity in mammals and the cross sectional area of the pyramidal tract (PT) through which all the CST fibres pass (Heffner and Masterton, 1975; Heffner and Masterton, 1983). However the number of fibres in the CST, and the cross sectional area, are also related to body size, so in itself a large PT is not well correlated with increased dexterity (Heffner and Masterton, 1975; Heffner and Masterton, 1983). Rather, the connections made by the CST within the spinal cord are thought to be a more important determinant of the level and type of control exerted by the cortex over the hand muscles (Kuypers, 1981).

The CST is formed from the axons of the pyramidal cells deep in layer V of the primary motor cortex (M1), secondary motor areas and parietal cortex (Galea and Darian-Smith, 1994; Jones and Wise, 1977; Matelli *et al.*, 1998). In humans and macaque monkeys, laminae V, the main source of efferent fibres, is thicker than the other M1 laminae, with widely spaced pyramidal cells (Rockel *et al.*, 1980). This

enhanced thickness reflects the extensive spiny dendritic trees of the pyramidal cells and the numerous synaptic linkages with them. The dense neuropil provides the adaptability that allows a wide variety of sensory inputs to interact with a wide range of motor outputs, which is needed to perform different motor tasks (Porter and Lemon, 1993). Around 60% of the CST arises from the frontal lobe. Though a large proportion of frontal CST fibres originate from M1, approximately 49%, there are contributions from the cingulate motor areas (21%), supplementary motor cortex (18%) and the regions in and around the arcuate (4%) and superior precentral (7%) sulci (Dum and Strick, 1991). The axons pass below the cortex as part of the corona radiata, then through the internal capsule, and descend, ipsilaterally, through the midbrain (visible as part of the cerebral peduncles), the fibres fragment into smaller bundles in the pons. On reaching the medulla oblongata the corticospinal axons, and also some axons of the corticobulbar tract, merge to form the pyramids, giving the name 'the pyramidal tract'. At the most caudal end of the medulla there is the pyramidal decussation, where the majority of corticospinal fibres cross to the contralateral side (Figure 1.1). From here the CST descends in the lateral white matter of the spinal cord as the lateral corticospinal tract and of these 50% terminate at the cervical level of the spinal cord (Weil and Lassek, 1929). The CST also projects numerous axon collaterals as it descends through cortical, sub-cortical and spinal levels that can influence other descending pathways (Armand, 1982; Canedo, 1997; Kuypers, 1981; Nathan and Smith, 1955; Porter and Lemon, 1993).

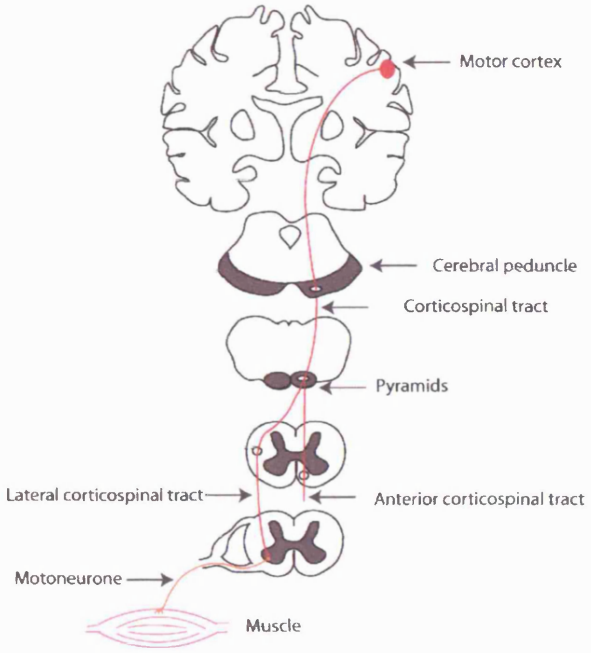

Figure 1.1 The corticospinal pathway.
Diagram includes the monosynaptic projection from M1 to the contralateral spinal neurones via the pyramidal tract.

The connections made by CST neurones to the spinal motoneurones are either monosynaptic, from corticomotoneuronal (CM) projections (Bernhard and Bohm, 1954b) or oligosynaptic. Synapses provide points where signals from propriospinal and descending motor pathways, sensory afferents and local segmental interneurones can be modified (Lemon *et al.*, 2004; Lemon and Griffiths, 2005); for instance, cortical commands may require updating to reflect late changes in peripheral input. Premotoneuronal integration of these signals, through spinal interneuronal networks, could ensure the appropriate activation of motoneuronal pools, for instance by resolving conflicts command signals originating from different pathways (Jankowska, 2001; Lemon *et al.*, 2004; Lemon and Griffiths, 2005). While oligosynaptic connections provide greater opportunity for such premotoneuronal adjustments, both oligosynaptic

and CM connections are likely to work synergistically to bring motoneurones to discharge in skilled hand movements (Lemon *et al.*, 2004; Lemon and Griffiths, 2005), it is the CM connections that are considered essential for RIFM (Bernhard and Bohm, 1954a; Lawrence and Hopkins, 1976; Lawrence and Kuypers, 1968). Primates with less developed dexterity, such as the squirrel monkey, have excitatory oligosynaptic connections and few CM connections, whilst macaque monkeys, that are capable of a higher degree of RIFM, show the opposite pattern with excitatory oligosynaptic connections less evident and clear CM projections (Lemon *et al.*, 2004; Maier *et al.*, 1998).

CM connections provide the cortex with direct access to the basic unit through which all the motor activity is mediated, the α-motoneurone of the spinal cord (Sherrington, 1947) (Figure 1.1). Described by Charles Sherrington as the 'final common pathway', contraction of a muscle can only occur via the α-motoneurone. To maintain posture and in defensive movements and locomotion, hardwired segmental motor mechanisms act upon the α-motoneurone to produce reciprocal stereotyped motor patterns between antagonistic muscles at a joint (Phillips and Porter, 1997). These relatively fixed segmental motor patterns do not allow the novel configurations of the hand and digits that are required for RIFM. The capacity to perform fractionated movements of the hand and digits, inherent in skilled hand movements, would therefore require these rigid motor patterns to be broken down, a process Sherrington described as 'analytical' motor control (Denny-Brown, 1979). These fractionated movements could then be synthesised to form a new motor act. Sherrington also noted that the discrete representation of

'movements' was increasingly evident from macaque, to baboon and to gibbon and the great apes; primates showing increasing levels of RIFM (Denny-Brown, 1979).

Direct evidence for a role for CM connections in RIFM comes from a variety of physiological studies in macaque monkeys. Spike-triggered averaging (StA) of the activity in the intrinsic hand muscles demonstrate CM neurones fire in a pattern that would support fractionated movement (Bennett and Lemon, 1996). Additionally, CM neurones are known to be primarily active during precision grip, which requires a fractionated muscle pattern, rather than power grip that produces greater muscle force (Muir and Lemon, 1983). Furthermore, CM connections can provide a significant input to hand and finger muscles. It has been estimated that 60% of the facilitatory drive needed for wrist extensor motoneurones to maintain a steady discharge was due to CM cell input (Cheney *et al.*, 1991). Injection of horseradish peroxidise (HRP) into neurones in the M1 hand area of the macaque monkey produced labelling of motoneurones in multiple muscles (Shinoda *et al.*, 1981) and electrophysiological studies show CM cells facilitate activity in discrete sets of muscles (Bernhard and Bohm, 1954a; Buys *et al.*, 1986; Fetz and Cheney, 1980). These divergent projections of CM cells influence functional groupings of muscles, such as the first dorsal interosseous (1DI) acting on the index finger and the adductor pollicis (AdP) acting on the thumb, which are commonly used together in precision grip (Buys *et al.*, 1986). The CM connections are complemented, in the hand, by a decreased level of pre-synaptic inhibition of the CM terminals, thereby allowing CM signals to influence motoneurones unaffected by local spinal mechanisms (Lemon, 1993; Nielsen and Petersen, 1994). The

greater cortical control attributed to CM connections, supported by the decreased pre-synaptic inhibition, may be required for the complex and demanding movements used in skilled hand movements (Bernhard and Bohm, 1954a; Kuypers, 1981).

There is also evidence from comparative anatomy and physiology and developmental studies, for a role of CM connections in RIFM. In macaque monkeys, the ontogeny of the connections of the CM system correlates with the development of fine finger movement (Armand *et al.*, 1997; Kuypers, 1962; Lawrence and Hopkins, 1976; Olivier *et al.*, 1997). CM connections have a greater influence over the distal rather than proximal muscles in the great apes and Old World monkeys (Lemon and Griffiths, 2005) and are more numerous in humans and the great apes compared to macaque monkeys, compatible with the superior dexterity shown by the former species (Heffner and Masterton, 1975; Kuypers, 1981). The relationship between increasing CM connections in primates and the capacity to execute RIFM was recognised by Kuypers (1981) who suggested that CM connections could be the substrate for the fractionated movements of the digits, by allowing direct, selective activation of a discrete *set of muscles*.

The spinal termination pattern of the CST shows a strong correlation with the degree of skilled hand movements shown by different primates (Heffner and Masterton, 1975; Heffner and Masterton, 1983; Kuypers, 1981). This correlation is seen both in terms of the level of the spinal cord to which the CST extends, and the spinal laminae in which it terminates. In all mammals, the CST terminates in the dorsal horn, and in those mammals with a low level of dexterity, such as goats, the CST terminates only in the

dorsal horn and does not extend below the thoracic segments (Kuypers, 1981) (Figure 1.2). At the next level of dexterity, as in the cat, the dorsal horn innervations extend throughout the length of the spinal cord along with innervation to the intermediate zone, where most of the interneurones that are part of reflex pathways are located, but not ventral horn where the motoneurones are situated (Figure 1.2), and there are still no CM connections (Kuypers, 1981). The increased dexterity shown by Old World monkeys, such as macaques, is accompanied by a more extensive pattern of terminations. There are bilateral CST projections to laminae VIII, which include some ipsilateral connections to the proximal limb muscles, and CM connections with the dorsolateral α-motoneurones in the ventral horn which innervate the more distal (hand and digit) muscles (Kuypers, 1981; Liu and Chambers, 1964; Ralston and Ralston, 1985). Humans and chimpanzees, have a still higher level of dexterity and exhibit more abundant CM connections, which include additional CM connections to ventromedial α-motoneurones that innervate the proximal muscles and those of the pectoral girdle (Figure 1.2), and there is also a reduction in the number of projections to the dorsal horn (Kuypers, 1981).

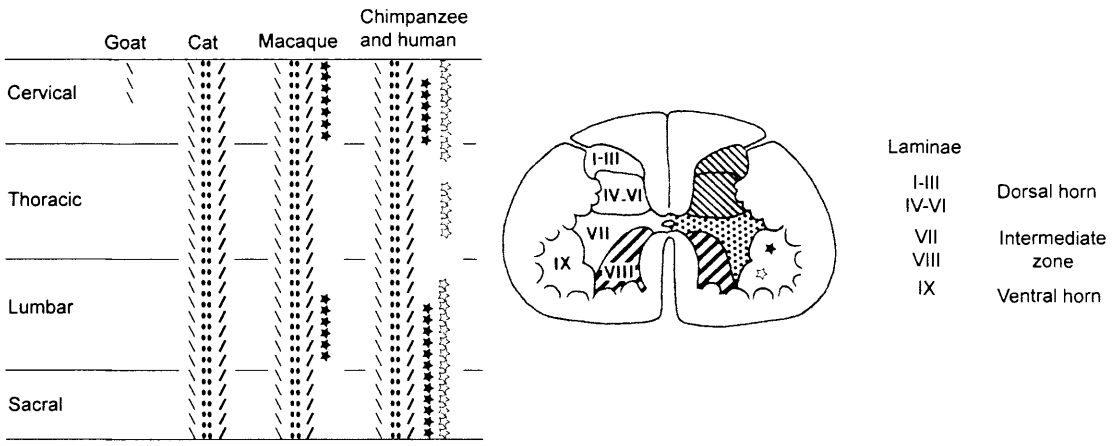

Figure 1.2 Diagram illustrating termination of corticospinal fibres in the goat, cat, macaque and chimpanzee and human.

The spinal level reached by projections to different parts of the spinal grey matter. Filled stars represent dorsolateral motoneurones to the extremities and open stars ventromedial motoneurones of the axial and trunk muscles (adapted from Porter and Lemon, 1993).

The CST is formed from axons from a wide range of cortical regions (Dum and Strick, 1991) and their cortical origins are related to their pattern of spinal termination. The corticospinal projections from the primary somatosensory region provide descending control of the main sensory relay in the spinal cord, the dorsal horn (Kuypers, 1981; Liu and Chambers, 1964; Ralston and Ralston, 1985). As all mammals possess these CST projections to the dorsal horn, this projection is likely to represent an evolutionarily older function of the CST (Lemon and Griffiths, 2005). The CST may have a role in controlling sensory inputs produced by movement; removing predictable sensory inputs associated with motor commands (Lemon and Griffiths, 2005). Certainly, control of sensory feedback is required for fine finger movement (Porter and Lemon, 1993), with PT lesions in macaque monkeys causing errors in tactile placing and difficulty in releasing grip (Lawrence and Kuypers, 1968; Tower, 1940). CM projections to the ventral horn, in which neurones from M1 terminate preferentially (Armand *et al.*, 1997;

Shinoda *et al.*, 1981), appears to be a later evolutionary development, seen in mammals that show increased dexterity (Kuypers, 1981; Lemon and Griffiths, 2005).

The diameter of CST fibres is poorly correlated with the level of digital dexterity (Heffner and Masterton, 1975; Heffner and Masterton, 1983), indicating that it is not just the largest, and therefore fastest, fibres that make CM connections. StA experiments have confirmed this finding. PTNs with fast and slow conduction times have CM connections, although these were more widespread in fast (54%) rather than slow PTNs (30%) (Porter and Lemon, 1993). However, it has been noted that those mammals in which the CST is restricted to the cervical and thoracic levels have generally thin fibres of quite uniform diameter, while species with CM connections have a wider range of diameters (Armand, 1982) which are likely to reflect different functions (Lemon and Griffiths, 2005).

There is strong evidence that the CST, and in particular CM connections, acts as the main conduit for cortical signals related to skilled hand movements. As such, changes in corticospinal activity can be used to investigate cortical outputs related to control of the hand. Notably, while the amount of neocortex that contributes to the CST does not correlate with digital dexterity, the total amount of neocortex does show a strong correlation (Nudo and Masterton, 1990b). This may reflect the contribution from cortico-cortical connections from other regions of the cortex to motor action, for instance inputs from regions concerned with transmitting relevant visual inputs needed for visuomotor grasp.

1.2 The cortico-cortical visuomotor grasp circuit

Based on work in non-human primates, the sensorimotor transformation required for visuomotor grasp is believed to arise from cortico-cortical pathways (Jeannerod *et al.*, 1995). The circuit comprises the anterior intraparietal region (AIP), ventral premotor cortex (area F5) and M1 (Figure 1.3, blue). In AIP, the first stage of this circuit, the shape, orientation and size of the object is processed. The hand shape required to interact with the object is then coded in F5 and the grasp executed by M1. This circuit sits within a framework of multiple parallel fronto-parietal circuits coding for different motor actions (Rizzolatti *et al.*, 1998). For instance, the transmission of visual information from the ventral intraparietal region (VIP) to F4 of the ventral premotor cortex (Luppino *et al.*, 1999) and then to M1 (Figure 1.3, red) is thought to be involved in encoding peripersonal space and object location, while a dorsal premotor circuit that transmits visual and somatosensory information from the medial intraparietal region (MIP) to area F2 of the dorsal premotor cortex is concerned with planning and controlling arm movements during reach (Figure 1.3, green) (Rizzolatti *et al.*, 1998).

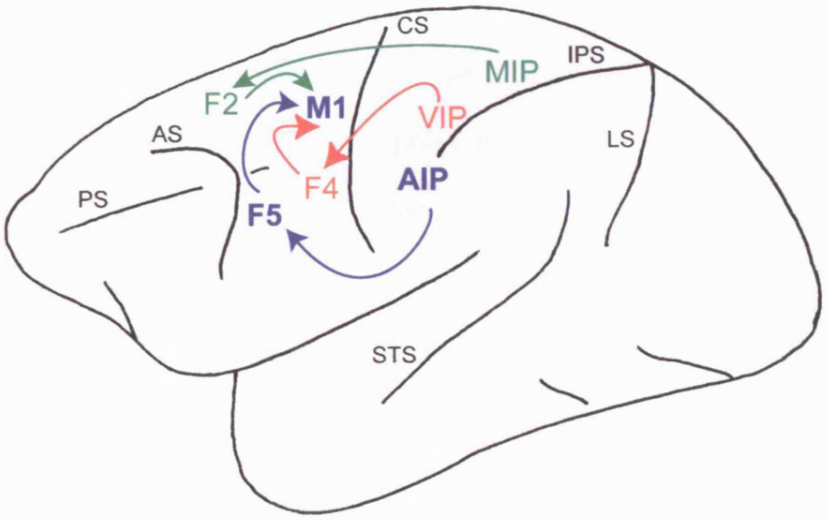

Figure 1.3 Diagrammatic representation the visuomotor grasp and reach circuits of the macaque monkey. Areas in grey represent regions close to the fundus of the intraparietal sulcus, such as the anterior intraparietal region (AIP, which lies in on the lateral bank of the intraparietal sulcus), ventral intraparietal region (VIP) and medial intraparietal region (MIP). The cortico-cortical visuomotor grasp circuit is shown in blue; AIP projects to area F5 which then projects to the primary motor cortex (M1). Two additional fronto-parietal circuits are also shown, one from VIP to F4, of the ventral premotor cortex, to M1 and the other from MIP to F2, of the dorsal premotor cortex, to M1. See text for details. Key: arcuate sulcus (AS), central sulcus (CS), intraparietal sulcus (IPS), lateral sulcus (LS), principal sulcus (PS) and superior temporal sulcus (STS).

1.2.1 Anterior intraparietal region

AIP is located in the lateral bank of the intraparietal sulcus (IPS) (Rizzolatti *et al.*, 1998) as illustrated in Figure 1.3. The IPS divides the parietal cortex into the superior intraparietal (SPL) and inferior intraparietal lobule (IPL). Neurones in the latter, including AIP, show responses to visual stimuli (Rizzolatti and Matelli, 2003; Sakata *et al.*, 1995).

AIP neurones have been categorised according the activity elicited during a grasping task under different visual conditions. Motor dominant neurones were unaffected by the degree of visual information. Visually responsive neurones were categorised as either visual dominant neurones, which required vision of the object, or visual-motor dominant neurones that showed greater firing for grasping in the light than dark (Murata *et al.*, 2000; Sakata *et al.*, 1995; Taira *et al.*, 1990). Within AIP, visually responsive neurones predominated (135/182 vs. 47/182, for visually responsive and motor dominant neurones, respectively (Murata *et al.*, 2000)). 'Object-type' neurones fired on visual presentation, either for a specific object, including those with complex geometrical shapes composed of several or more components (Sakata *et al.*, 1999), or a class of object, e.g., flat shapes (Murata *et al.*, 2000). Visually responsive neurones that did not fire on object presentation, 'non-object' types, were considered, along with the motor dominant neurones, to encode the hand shape required to grasp the objects (Murata *et al.*, 2000; Sakata *et al.*, 1995). In addition to encoding motor aspects such as hand shape, the non-object type neurones, if responding to the sight of the hand, could provide visual feedback on hand position (Murata *et al.*, 2000; Sakata *et al.*, 1995). AIP neurones can also encode orientation and size of an object, parameters concerned with grasp, but not the position of an object in space, an aspect concerned with reach (Taira *et al.*, 1990). Similarly, deficits from reversible lesions of AIP, by injection of the $GABA_A$ agonist muscimol, were consistent with a role in grasping rather than reaching movements (Gallese *et al.*, 1994). These deficits were confied to visuomotor grasp, the monkey could grasp the object after tactile exploration of the object (Gallese *et al.*, 1994).

The visual and motor encoding in AIP has led to the suggestion that here the visual features of an object, such as shape, size and orientation, is matched to the hand movement required for grasp (Sakata *et al.*, 1995; Taira *et al.*, 1990) (see Section 1.2.2 and 1.2.3). As the majority of visually responsive neurones show similar activation patterns for a particular object, or groups of objects, prior to grasp as during object manipulation, the role of AIP has been related to movement preparation (Sakata *et al.*, 1995; Taira *et al.*, 1990). Moreover it is hypothesised that AIP encodes the action representations associated with an object, an object's affordance (Fagg and Arbib, 1998; Jeannerod *et al.*, 1995). For instance actions 'afforded' by a mug would include grasp of its handle, rim and side. AIP could also be involved in visual memory of objects, possibly for delayed grasp, as some AIP neurones responded to visual presentation of an object when no subsequent grasp was required and over an extended delay period (2 s) (Murata *et al.*, 1996; Murata *et al.*, 2000; Sakata *et al.*, 1995).

1.2.2 Ventral premotor cortex

Neural tracing studies have shown strong, selective and reciprocal connections between AIP and F5 (Borra *et al.*, 2007; Luppino *et al.*, 1999). The densest pattern of anterograde labelling from AIP was found on the posterior bank of the arcuate sulcus (F5ab). "Canonical neurones" predominate in this region (see below), while in the convexity of the arcuate sulcus (area F5c) "mirror neurones" were found in greater numbers (Rizzolatti *et al.*, 2002). Both types of F5 neurone show activation for goal-related movements of the hand and mouth, the majority firing for a type of grip and in particular for precision grip (Rizzolatti *et al.*, 1998). The neurones differ in their visual

responses, mirror neurones fire when watching someone performing a goal-directed action (Gallese *et al.*, 1996; Rizzolatti *et al.*, 1996) and canonical neurones during object observation (Murata *et al.*, 1997; Raos *et al.*, 2006). For both mirror and canonical neurones there was congruence between the visual and motor response, so for instance, for canonical neurones congruence between grasp of a sphere and observation of a sphere, while mirror neurones would fire for grasp and observation of someone grasping a sphere. As mirror neurones fire for both self-initiated actions and observation of the same action by another, these neurones have been related to our ability to imitate others and recognise actions of others, so providing a possible cognitive function for area F5 (Gallese *et al.*, 1996; Rizzolatti *et al.*, 1996).

The properties of F5 neurones reflect the intermediate position of F5 in the visuomotor grasp circuit. This is seen in three measures: firstly, the number of neurones showing visual responses; secondly, the period in which F5 neurones fire; and thirdly in the type of motor actions the neurones encode. Similarly to AIP, F5 neurones showed activation during grasping actions and also on visual presentation of an object when no subsequent action was required. There are no visual dominant neurones in F5 (neurones that discharge for only visual presentation of the object), and a greater proportion of motor dominant neurones than in AIP (Murata *et al.*, 2000). Approximately half of F5 neurones responded to visual presentation of the object, without subsequent grasp, the remaining neurones were classified as motor neurones and did not show activation during the movement planning period or fixation (Murata *et al.*, 1997; Raos *et al.*, 2006). In comparison, three quarters of AIP neurones showed increased firing for grasping in

the light, compared to grasping in the dark, and of these more than half responded to object fixation alone (Murata *et al.*, 2000). Secondly, there is the temporal gradient of action segmentation. Typically, in AIP a cell is active from hand shaping to the end of the hold stage, so such cells appear to represent the entire action (Jeannerod, 1997). F5 activation was more phasic, with firing for a particular phase of the movement (for example, the pre-movement phase, or hold phase) (Fagg and Arbib, 1998; Geyer *et al.*, 2000; Jeannerod *et al.*, 1995; Murata *et al.*, 1997). This leads to the third aspect of F5 coding, firing is often specific for categories of action (such as grasp and hold) or type of movement, for instance finger configuration (palm opposition or opposition of all fingers, even though these may subserve the same grip types) (Fagg and Arbib, 1998; Geyer *et al.*, 2000; Jeannerod *et al.*, 1995; Murata *et al.*, 1997). With such phasic neuronal firing, F5 has been described as coding for the 'vocabulary of actions' whereas M1, encoding for the individual movements forming the action, holds the 'vocabulary of movements' (Rizzolatti and Fadiga, 1998). Transmission of the required grasp to M1 is believed to occur via the numerous reciprocal cortico-cortical connections between F5 and M1 (Ghosh *et al.*, 1987; Ghosh and Porter, 1988; Godschalk *et al.*, 1984; Matelli *et al.*, 1986; Muakkassa and Strick, 1979) (see also Section 1.4). Furthermore, F5 is electrically excitable, although to a lesser degree than M1, whereas motor responses cannot be elicited from electrical stimulation of AIP.

The aforementioned differences between AIP and F5 have been related to their roles in the visuomotor grasp. AIP, with greater visual responses, is thought to encode object affordance (Fagg and Arbib, 1998; Rizzolatti and Luppino, 2001). F5 is hypothesised to

encode general motor goals, such as hold or grasp, and also motor prototypes, how an action is to be made, for instance using whole hand prehension or precision grip (Rizzolatti and Luppino, 2001). The presence of a motor prototype, a preformed movement plan, would facilitate motor execution, and matching of object affordance to grasp (Rizzolatti and Luppino, 2001). Object meaning and intention also influences the selection of grasp. For instance a person picking up a mug to drink would use the handle, but to move the mug it is often grasped by the rim. AIP receives cortical connections from the inferior temporal lobe (Borra *et al.*, 2007), so AIP could integrate object meaning with object affordance (Fagg and Arbib, 1998; Rizzolatti and Luppino, 2001). The decision of the action to be carried out would then determine the relevant grasp. F5 receives inputs from regions concerned with working memory (area 46 of the prefrontal cortex), instructional stimuli (F2, supplementary motor area) and movement sequence (F6, pre-supplementary motor area) that would allow F5 to select the correct motor prototype according the current goals of the individual (Fagg and Arbib, 1998). Alternatively, as AIP also receives prefrontal connections, grip selection may occur here (Borra *et al.*, 2007; Rizzolatti and Luppino, 2001); so it is uncertain whether information related to object affordance or the corresponding grasp is sent from AIP to F5.

Along with encoding object affordance AIP may maintain an 'active memory' of the grasp that is going to be or is being executed (Rizzolatti and Luppino, 2001). In a model of visuomotor grasp, F5 neurones are thought to update AIP motor neurones during planning and execution of grasp (Fagg and Arbib, 1998; Jeannerod *et al.*, 1995; Jeannerod, 1997); the motor neurones in AIP reflecting a corollary discharge from F5

that keeps AIP neurones active until the object is released (Sakata *et al.*, 1995; Taira *et al.*, 1990). The similar deficit in visuomotor grasping present in F5 and AIP after muscimol injection in either F5 or AIP (Fogassi *et al.*, 2001; Gallese *et al.*, 1994) may due to the requirement for this continual feedback between F5 and AIP.

The similar cytoarchitectonic characteristics of Brodmann's area 44 (BA44), of the human frontal cortex, to F5 suggests that it is the human homologue of F5 (Petrides, 2005; Picard and Strick, 2001). Imaging experiments have shown increased activation of BA44 when subjects manipulated complex objects (Binkofski *et al.*, 1999), imitated gestures and executed grasp (Grezes *et al.*, 2003), imagined grasp (Grafton *et al.*, 1996a; Rizzolatti *et al.*, 1996) and during observation of objects or object-related actions (Buccino *et al.*, 2001; Grezes *et al.*, 2003; Manthey *et al.*, 2003); activation patterns reminiscent of those recorded from F5 neurones in monkeys. However other imaging studies have failed to show increased activation of BA44, or other inferior frontal areas, in humans when comparing matching, reaching and pointing tasks to grasping tasks (Faillenot *et al.*, 1997; Frey *et al.*, 2005; Grafton *et al.*, 1996b). Furthermore, while F5 neurones are clearly involved in visuomotor grasp (Murata *et al.*, 1997; Raos *et al.*, 2006; Umilta *et al.*, 2007), activation of BA44 has been observed during haptic (Binkofski *et al.*, 1999; Ehrsson *et al.*, 2000) but not always visually-guided grasp (Begliomini *et al.*, 2007). The difference in activation patterns of F5 and BA44 may be due to: intersubject variability in the borders of BA44 reducing the probability of obtaining statistical significance (Binkofski *et al.*, 1999; Picard and Strick, 2001); that some of the tasks were not demanding enough to produce significant changes in

neuronal activity (Binkofski *et al.*, 1999; Grafton *et al.*, 1996b; Picard and Strick, 2001); and interspecies differences (Binkofski *et al.*, 1999; Grafton *et al.*, 1996b; Picard and Strick, 2001).

In grasping tasks humans sometimes show a left hemispheric dominance in BA44 activation (Daprati and Sirigu, 2006; Johnson-Frey *et al.*, 2005), but in non-human primates reversible inactivation of the ventral premotor cortex (Schieber, 2000) and neuronal recordings (Murata *et al.*, 1997; Raos *et al.*, 2006; Umilta *et al.*, 2007) have not shown a hemispheric bias. It has been suggested that in humans the neural structures employed in action towards an object depend upon whether subjects are 'reaching to use' or 'reaching to grasp' (Daprati and Sirigu, 2006). While both types of action require knowledge of the object's size and shape, additional semantic knowledge is required when 'reaching to use'. In such purposeful actions, such as cutting with scissors, premotor and parietal regions had a left prevalence regardless of whether the action is performed by the right or left hand (Daprati and Sirigu, 2006; Frey, 2007; Johnson-Frey *et al.*, 2005). Converging evidence for the importance of the left hemisphere comes from patients with ideomotor apraxia, resulting from a left-sided lesion to the middle frontal gyrus (dorsolateral frontal cortex) and intraparietal sulcus, who are unable to perform goal-related actions such as writing (Haaland *et al.*, 2000).

1.2.3 Primary motor cortex

1.2.3.1 Motor representation in M1

The primary motor cortex is believed to segment actions planned by other motor cortical regions, such as F5, into elementary movements. Inactivation of M1 produces some paresis and hypotonia of the contralateral limb, deterioration in digital manipulation and reduction in the speed of movements (Fogassi *et al.*, 2001; Matsumura *et al.*, 1991). M1 has the largest output of CST fibres of any cortical region (Dum and Strick, 1991) and a large amount of cortex devoted to the hand that was famously caricatured by the motor homunculus (Penfield and Rasmussen, 1950) (Figure 1.4). While the motor homunculus provides an indication of the amount of cortex devoted to the different body parts, it is misleading with respect to the relationship of regions within M1 to the musculature.

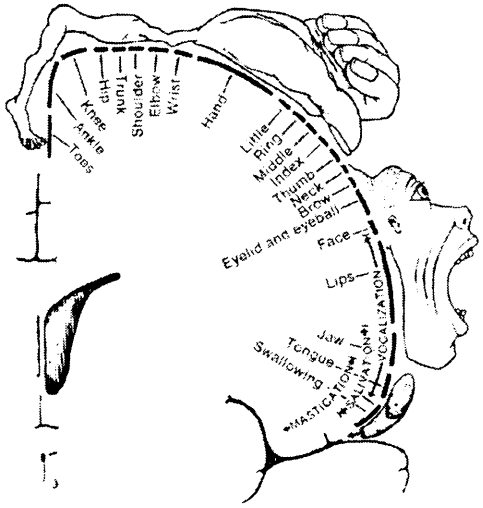

Figure 1.4 Motor homunculus of Penfield and Rasmussen (1950).
The amount of cortex that is presumed to represent each human body part is indicated by the size of the caricature.

The nature of movement representation in M1 was considered by Hughlings Jackson (1870) to consist of overlapping minute representations, rather than the abrupt localisation that is suggested by the motor homunculus caricature (Walshe, 1943). Based on clinical observations, Jackson recognised that all movements required the co-ordinated action of many muscles, not just the prime mover. Even when moving a single digit, stabilisation of the other joints was essential and this would require a movement with all its complexity, rather than individual muscles, to be encoded in M1 (Walshe, 1943). Techniques that were not available to Jackson have since provided strong support for both observations.

Electrical stimulation studies in patients having surgery for the removal of tumours and epileptic foci (Penfield and Boldrey, 1937) (Figure 1.5A, B); functional magnetic resonance imaging (fMRI) of M1 in humans (Indovina and Sanes, 2001); StA of EMG from 24 simultaneously recorded forelimb muscles in non-human primates (Park *et al.*, 2001; Park *et al.*, 2004); and retrograde neuronal transport of herpes virus from muscles to CM cells (Rathelot and Strick, 2006) have provided converging evidence for multiple representations of a single muscle and overlapping representations in M1. Rather than the distinct segregation of body parts suggested by the motor homunculus, these studies support a broad somatotopic organisation with overlapping body parts (compare Figure 1.5A, B to Figure 1.4). Deficits in finger movements in stroke patients with lesions to the hand region of M1 provide further evidence for an intermingled and fractured organisation, with patients showing weakness of all the fingers, regardless of the mediolateral location of the lesion; not the discrete pattern of finger impairment

expected if M1 had abrupt somatotopic organisation (Schieber, 1999). A similar pattern of finger impairment occurred from injection of muscimol into the M1 hand region of non-human primates (Schieber and Poliakov, 1998). Interestingly, when removing food from a small food well, by extension of the index finger, extension of digits not required for the task interfered with the movement of the index finger. This is direct evidence for the 'stabilisation' idea that Jackson first proposed.

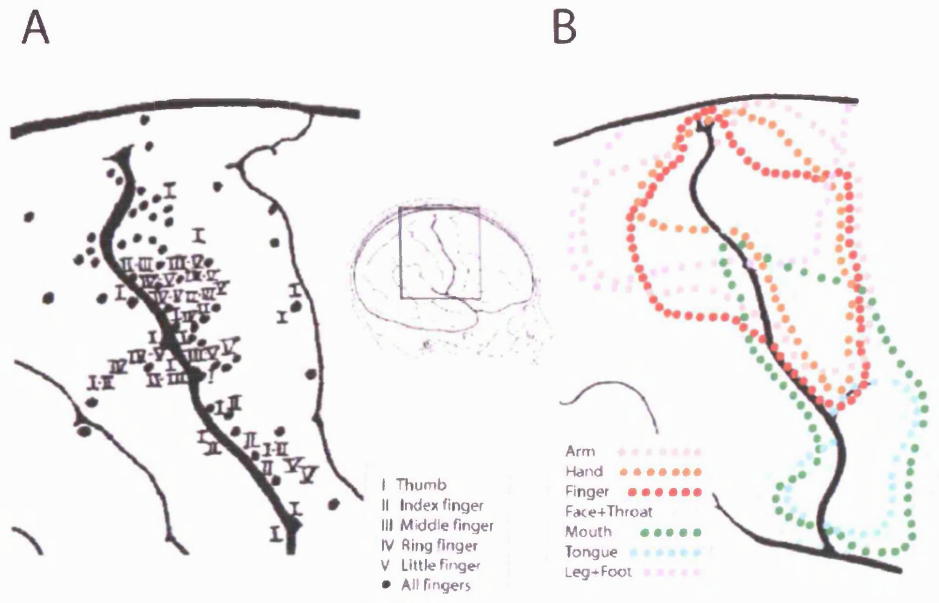

Figure 1.5 Motor responses from electrical stimulation in man.
Localisation of finger movements (A) and body movements (B) elicited from electrical stimulation of the cortex in man. Adapted from Penfield and Boldrey (1937).

There is mounting evidence that, within this broad somatotopic organisation, groups of muscles that are often used together are represented close to each other, with a muscle represented numerous times in M1 (Schieber, 2001). The "constrained somatotopy" of M1 has been suggested to be advantageous in the control of movement, as the distributed organisation, with one muscle represented multiple times, permits connections between a wide range of muscles with small conduction delays (Schieber,

2001). Complex co-ordained movements have been elicited by delivering long trains of high intensity stimulation to M1 (up to 150 μA and at 50-400 Hz lasting 500 ms), which has led to the hypothesis that M1 that contains a map of behaviourally meaningful postures (Graziano *et al.*, 2002b; Graziano *et al.*, 2002a). This stimulation paradigm may be producing physiological spread of current that reflects activation patterns that occur in natural movements. Alternatively, repetitive stimulation is known to have a greater physical spread (see Section 4.4.2) and the movements could be due to a large area of the cortex being excited.

1.2.3.2 Patterns of discharge in M1 neurones

There is evidence for tasked-related organisation of M1 outputs. For instance, 75% of PTNs showed delay period activity (prior to movement onset) that was congruent with the firing pattern in the movement period, for example 'push' neurone firing would decrease after a 'pull' instruction and increase for a 'push' instruction (Tanji and Evarts, 1976). However, PTN firing does not directly relate to amount of activity in the target muscle. The PTN firing rate for the highly controlled act of precision grip was greater than for a power grip, even though the power grip produced higher EMG levels (Muir and Lemon, 1983). Notably these PTNs showed increased firing when the finger muscles were used in a fractionated manner. Similar results have been shown in human subjects, using transcranial magnetic stimulation (TMS) and recording muscle units in 1DI. Task-related movements (rotation, pincer grip) produced a larger response to TMS and the muscle units were more likely to discharge compared to index finger abduction, even though the EMG activity recorded in 1DI was equivalent for all movements

(Flament *et al.*, 1993). These results are reminiscent of Jackson's observation that M1 would need to encode a movement with all its complexity (Walshe, 1943).

The grip chosen to interact with an object is determined by the purpose of the action, for instance, precision grip would be used to hold a pen when writing and power grip when using a hammer to hit a nail (Napier, 1956). Recently, analysis of hand shaping for the same grasp with different end-goals has revealed more subtle distinctions. While the kinematics of the final grip was not significantly different according to whether the object had to be lifted or placed in a tightly or loosely fitting box, the timing of hand pre-shaping varied between experimental conditions (Ansuini *et al.*, 2006). Upstream from M1, the firing rate of single units recorded in IPL were modulated according to the goal of the action, whether the food item was to be placed (for a food reward) or eaten (Fogassi *et al.*, 2005). Connections between the IPL to the ventral premotor cortex and then to M1 (Ghosh *et al.*, 1987; Ghosh and Porter, 1988; Godschalk *et al.*, 1984; Matelli *et al.*, 1986; Muakkassa and Strick, 1979) could provide pathways by which information on end-goal of an action influences M1 activity.

1.2.3.3 Encoding of movement parameters

Aspects of reach and grasp movements, such as direction, grip force and sensory feedback from the movement itself, may also be encoded in M1 firing. Using a wrist extension-flexion task with varying loads, the majority of PTNs recorded from M1 were primarily related to the force rather than the direction of displacement (Evarts, 1981). In precision grip tasks, M1 firing rate was modulated according to the rate of change of

grip force and the grip force required (Baker *et al.*, 2001) although this can be influenced by the sequence and range of force change (Hepp-Reymond *et al.*, 1999). Using a centre-out reaching task, it was shown that populations of M1 neurones encoded the direction of reach (Georgopoulos *et al.*, 1986). M1 neurones also respond to the limb posture used during the movement (Scott and Kalaska, 1995; Scott and Kalaska, 1997) and cutaneous and proprioceptive stimuli during active and passive movements of the hand (Porter and Lemon, 1993). The complexity of hand movement results in multiple parameters that could be encoded by M1, and that can be difficult to dissociate, such as direction, muscle activation, joint rotation, speed and force, and, as mentioned previously, end-goal. It has been noted that the most consistent feature in M1 activity is the diversity of information that could be encoded by the discharge pattern of individual neurones (Scott, 2003).

Lastly for visuomotor object-orientated grasp, extrinsic coding of space, the location of an object independent of body position, would need to be transformed into intrinsic co-ordinates that relate to a body part, a muscle-based frame of reference. The discharge pattern of neurones has been investigated during wrist flexion and extension in different postures (supination, pronation and with the palm facing to the side), to dissociate muscle, joint angle and extrinsic space. While the majority (81%) of ventral premotor neurones showed extrinsic-like firing, so fired according to the movement of the hand in space, regardless of starting posture, a smaller proportion of M1 neurones (24%) showed this firing pattern and 39% had a muscle-based intrinsic frame of reference (Kakei *et al.*, 2003; Kakei *et al.*, 2001; Kakei *et al.*, 1999). The authors suggest that the intracortical

processing between M1 and the ventral premotor cortex could transform the target location, in a visual frame of reference, into direction of action, in a motor frame of reference. Another study using a motor illusion, monkeys saw a 3D representation of their hand rather than the actual hand, this representation could be displaced so the visual feedback to the animal differed from the actual movement (Schwartz *et al.*, 2004). The authors found that cell firing in the ventral premotor cortex matches the visual path whereas that in M1 matches the hand path. Similarly prisms have been used to dissociate visual space from motor space in a reaching task, producing a movement direction that was different from the apparent target location (Kurata and Hoshi, 2002). Here M1 neurones rarely encoded the target location in visual co-ordinates, rather this type of reference frame was almost exclusively observed in the ventral premotor cortex. The mixture of coding within M1 may reflect inputs to M1 from regions such as the ventral premotor cortex that are involved in processing information in an extrinsic co-ordinate reference frame and projections from M1 to spinal structures requiring intrinsic or 'muscle-like' frame of reference (Scott, 2003).

1.3 Dorsal and ventral streams

The visual information used for action is believed to be produced by different brain regions and to have different properties compared with that used for perception. Two quasi-separate pathways are thought to be involved: a ventral pathway subserving visual perception, and a dorsal pathway subserving on-line visual control of action (Milner and Goodale, 1995). The visual information used to assist manipulation of objects within our environment is thought to arise from the dorsal visual processing stream. The ventral stream processes allows us to recognise objects. Initially, the two streams of visual processing were thought to correspond to space versus object perception (Mishkin and Ungerleider, 1982), but this was subsequently redefined as a division between a perception/semantic mode and a pragmatic mode relevant for action (Jeannerod *et al.*, 1995; Milner and Goodale, 1995). The anatomical substrate for the ventral stream is the pathway from the visual cortex centred on V4 to the inferotemporal cortex, whilst the dorsal stream projects from MT/V5 of the visual cortex to the posterior parietal cortex (PPC) (Figure 1.6). The dorsal stream is seen as the evolutionarily more ancient pathway (Milner and Goodale, 1995), requiring objects to be coded in terms of the effectors (egocentric coding) whereas the ventral stream is organised in allocentric co-ordinates enabling us to recognise objects despite differences in size or orientation. The visual information sent to AIP is from V3A, part of the dorsal stream.

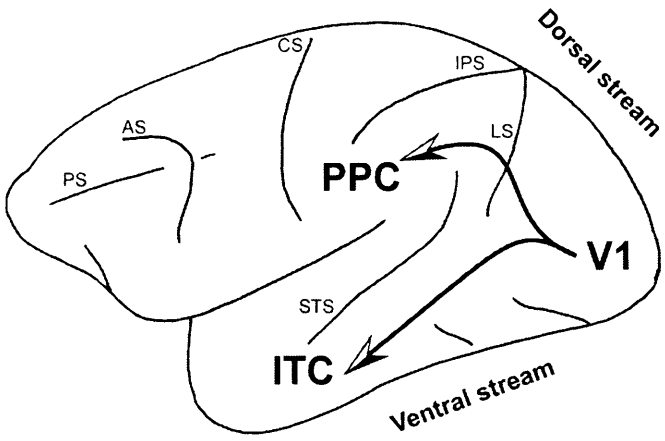

Figure 1.6 Schematic of the dorsal and ventral streams of visual processing.
Illustration of the two visual processing streams on macaque cortex. The ventral stream projects to the inferotemporal cortex (ITC) whilst the dorsal stream to the posterior parietal cortex (PPC). The arcuate sulcus (AS), central sulcus (CS), intraparietal sulcus (IPS), lateral sulcus (LS), principal sulcus (PS) and superior temporal sulcus (STS) are labelled.

The existence of two separate pathways was first suggested by neurophysiological tests that showed a double dissociation between optic ataxic patients, who have damage to the PPC, and the visual-form agnosic patient D.F. (Goodale and Westwood, 2004; Milner and Goodale, 1995). Optic ataxic patients have problems with visually-guided movements towards objects, but are able to describe the orientation and position of the object accurately and, in keeping with damage to the dorsal stream, have preserved recognition of objects. In contrast, patient D.F., with damage to the lateral occipital complex (ventral stream) is able to reach and grasp objects normally, but cannot indicate the size and shape of the object. The dichotomy has been highlighted in experiments using a size contrast illusion and measuring changes of the peak grip aperture (greatest separation between index finger and thumb during the reach to grasp) (Aglioti *et al.*, 1995; Goodale and Westwood, 2004). The peak grip aperture scales with object size and, if dorsal stream processing is being used, it should not be affected by visual

illusions as these require coding in allocentric co-ordinates. The peak grip aperture was not affected by the illusion unless the target was occluded during the action initiation. Such studies propose that dorsal stream is used for immediate action when the object is visible, otherwise ventral stream processing is involved (Milner and Goodale, 1995). So, for rapid 'automatic' processing dorsal stream characteristics emerge, such as insensitivity of visual illusions in the kinematics profiles. If subjects are required to memorise the target (for example when a delay is inserted) then sensitivity to illusions and ventral processing becomes apparent.

Clearly in daily life we often require both ventral and dorsal processing streams, for instance using memory of an object when deciding which one to grasp. It has been suggested that the dorsal stream should be sub-divided into dorsal-dorsal and dorsal-ventral streams (Rizzolatti and Matelli, 2003) to reflect such differences. Injection of WGA-HRP into the IPL showed projections from the superior temporal polysensory area, so providing IPL with information on space and in the temporal lobe possible encoding of action. No such labelling occurred with injection into SPL (Rizzolatti and Matelli, 2003). Additionally, retrograde tracers injected into AIP have shown connections to the inferior temporal cortex (Borra *et al.*, 2007). AIP in the IPL could therefore have access to information processed by the ventral stream.

1.4 Cortical stimulation

The visuomotor transformations carried out by the dorsal processing stream ultimately result in movement commands being sent to the motoneurones of hand and forelimb muscles via descending motor pathways. Of these, the CST, as discussed earlier, is believed to play a dominant role. Electrical stimulation of M1 and activation of M1 by TMS both result in descending volleys in the CST. By changing the stimulus parameters used, different neuronal structures are facilitated, and this is reflected in changes in the descending corticospinal volley and the resulting muscle response.

Electrical stimulation of the cortex was first used in the 19th century to study motor representations of different parts of the body (Phillips and Porter, 1997). In humans, direct stimulation of M1 is only possible in patients during surgery (Penfield and Boldrey, 1937) whilst transcranial electrical stimulation (TES), through electrodes on the scalp, allows the study of healthy volunteers. However, as bone has a high electrical resistance, the large voltage required in TES to penetrate skull causes activation of the pain endings in the scalp (Barker, 2002; di Lazzaro *et al.*, 2004a). TMS, first used by Barker *et al.* (1985), has the advantage over TES in being painless and non-invasive. According to Faraday's laws of electromagnetic induction, a brief rapidly alternating current passed through a coil of wire will generate a strong, transient magnetic field which in turn induces a secondary electrical current in a nearby conducting medium. The magnetic field produced by a TMS coil placed on the subject's scalp passes through the scalp and skull unaffected by their electrical properties, but attenuated by distance

from the coil ($F \propto 1/distance^4$), inducing a current in the underlying brain tissue resulting in depolarisation of the neurones and axons (Barker, 1999).

The response evoked from electrical and magnetic stimuli is affected by characteristics of the stimulation protocol used and the anatomy and physiology of the cortex. For instance, the electrical conductive properties of the cellular structures and the orientation of the neurones result in different structures being depolarised when the current direction to stimulate the cortex is altered. TMS induces an electrical field parallel to the skull, whereas electrical stimulation produces an additional field in the radial direction (Rothwell, 1991; Ruohonen and Ilmoniemi, 2002). As an electrical current preferentially excites cells in a direction parallel to the current flow, only horizontal structures are activated by TMS, where as electrical stimulation is less selective in this respect, exciting vertical and horizontal components of the cortex (Jahanshahi and Rothwell, 2000; Rothwell, 1991). Differences between the electrical fields produced by these stimulation methods result in PTNs in the crown of the precentral gyrus, where the long axis (cell bodies and the apical dendrites) are perpendicular to the skull, being directly activated by electrical stimulation but not TMS. In contrast, PTNs located in the anterior bank of the central sulcus, such as those that project to the motoneurones of distal muscles, where the long axis of the PTNs lies parallel to the skull surface, can be directly stimulated by both methods (Amassian *et al.*, 1987; Rothwell, 1991). This is not to suggest that excitation is restricted to these structures; due to the intricate interconnected nature of the motor system, a large current delivered to the motor cortex will result in indirect activation of multiple components of the motor system. For TMS,

the coil used for cortical stimulation also determines the amount of cortex stimulated. TMS delivered through a figure of eight coil, which has double windings its the centre, results in a point of maximum induced current (at the intersection of the windings) and subthreshold effects under other areas of the coil, whereas a round coil results in a less focal discharge (Barker, 2002; di Lazzaro *et al.*, 2002; Jahanshahi and Rothwell, 2000; Rossini *et al.*, 1994). By using different stimulation paradigms the contribution of different cortical structures to the evoked response and the amount of cortex stimulated can be varied.

Direct electrical stimulation of the cat and monkey motor cortex produces a high frequency repetitive discharge (~600 Hz) lasting 5-20 ms recorded as multiple descending volleys in the CST (Amassian *et al.*, 1987; Patton and Amassian, 1954). The volleys consist of an initial direct (D-) wave followed by subsequent indirect (I-) waves (Amassian *et al.*, 1987; Patton and Amassian, 1954). I-waves occur at intervals of approximately 1.2 ms, and are named according to their latency, so I_1 occurs 1.2 ms after the D-wave and I_2 at 2.4 ms, and so forth. The D-, I_1- and the later I-waves are thought to arise from different mechanisms acting on the corticospinal neurones.

1.4.1 The D-wave

The D-wave is considered to arise from direct (non-synaptic) excitation at or near the axon hillock of the PTN. Evidence for this comes from investigations of non-human primates. The early descending D-volley recorded in the spinal cord, elicited from TMS delivered to M1, was completely collided with a stimulus to the PT verifying its

corticospinal origin (Edgley *et al.*, 1990) and the rapid condition time of D-wave recorded in the bulbar pyramid (0.5-0.8 ms) is indicative of fast PTN axons (Amassian *et al.*, 1987; Patton and Amassian, 1954). D-waves, evoked by TMS are more easily elicited in fast conducting axons suggesting activation at the axon-hillock or nearby regions of the initial segment or nodes of Ranvier, where threshold is inversely related to the axon diameter (Amassian *et al.*, 1987).

The D-wave can have several sites of origin, depending upon the TMS and electrical stimulation protocol employed. Electrical stimulation using an anodal stimulus elicits D-waves at lower thresholds than cathodal stimulation (Amassian *et al.*, 1987; Day *et al.*, 1989a). Cathodal stimulation is thought to hyperpolarise the axons and depolarise the dendrites of vertically orientated PTNs, whilst anodal stimulation depolarises the axon and hyperpolarise the dendrites (Phillips and Porter, 1997). Therefore, in anodal stimulation there is direct stimulation of the PTN whilst cathodal stimulation produces indirect stimulation (Amassian *et al.*, 1987; Day *et al.*, 1989a). Anodal TES can stimulate CST axons deep in the brain, even to the level of the medullary pyramid, with increasing stimulus intensity there are large jumps in latency possibly related to sites of stimulation where the axon bends (Burke *et al.*, 1993; Edgley *et al.*, 1990; Edgley *et al.*, 1997). Consistent with this, the D-wave persists after cortical ablation and can be elicited by direct stimulation of the subcortical white matter (Patton and Amassian, 1954). The D-wave evoked by anodal TES and recorded in the epidural space during scoliosis surgery was not sensitive to anaesthetics whereas that from TMS was; suggesting the former has a site of initiation at the nodes of Ranvier of corticospinal

axons, where it is unaffected by excitation levels of the corticospinal neurone, and the latter is elicited much nearer the cell body, probably at the axon hillock (Burke *et al.*, 1993; Burke *et al.*, 2000). The threshold and amplitude of the D-wave in an individual axon is relatively insensitive to increases in TMS stimulation intensity, compatible with a site of origin close to the soma of the PTN (Edgley *et al.*, 1990). If TMS does elicit the D-wave at the initial segment, then it should be modulated by factors that affect the excitability of the PTN (Baker *et al.*, 1995; Lemon, 2002; Lemon *et al.*, 1995). Task related changes of short-latency TMS responses were observed both in humans and non-human primates during a reach-to-lift and precision grip task, respectively (Baker *et al.*, 1995; Lemon *et al.*, 1995).

With TMS, by manipulating the orientation of the coil, specific populations of cortical neurones can be stimulated directly. In epidural recordings from human subjects, MEPs and single motor unit activity recorded from hand muscles all showed an earlier response (up to 3 ms earlier) when a lateral-medial (LM) TMS current was induced in the cortex, compared to posterior-anterior (PA) induced current (Kaneko *et al.*, 1996; Nakamura *et al.*, 1996; Werhahn *et al.*, 1994). As the components of the corticospinal volley occur at relatively fixed intervals, these results have been explained by the PA direction preferentially producing I-waves whilst the LM direction produces D-waves (Kaneko *et al.*, 1996; Nakamura *et al.*, 1996). Due to the physical principles of electrical stimulation, TMS activates neurones parallel to current flow so the difference in the trajectory of the PTNs may determine the mode of action of the two current directions (Nakamura *et al.*, 1996) (also see above).

1.4.2 I-waves

The lack of temporal dispersion between the D-wave and the subsequent I-waves, suggest both are elicited from fast conducting axons of the CST (Amassian *et al.*, 1987; Baker *et al.*, 1995; Edgley *et al.*, 1990; Patton and Amassian, 1954). However, the I-waves are believed to arise from different neuronal mechanism to the D-wave. Intracortical electrical stimulation of M1 in the macaque monkey produced I-waves to a depth of 2 mm below the cortical surface, whilst D-waves occurred when stimulation was deeper, at 6 mm (Patton and Amassian, 1954). This suggests the D-wave results from direct excitation of the PTN and I-waves through cortical interneurones. In a patient with alcoholic cerebral atrophy, clear D-waves, but not I-waves, could be elicited by TMS, suggestive of I-waves being generated within the cortical grey matter, (di Lazzaro *et al.*, 2004b) and mirroring results from electrical stimulation after cortical injury in the monkey and cat (Patton and Amassian, 1954). Finally, cathodal electrical stimulation, thought to depolarises the cortical dendrites, elicits I-waves at lower thresholds than anodal stimulation, which hyperpolarises the dendrites (Amassian *et al.*, 1987; Day *et al.*, 1989a). I-waves with higher thresholds, latencies and a more labile nature than the D-wave, are considered to represent transsynaptic activation of PTNs (Edgley *et al.*, 1997; Lemon, 2002; Patton and Amassian, 1954; Rothwell, 1991; Terao and Ugawa, 2002). The proposed origins of the D- and I-waves are illustrated in Figure 1.7.

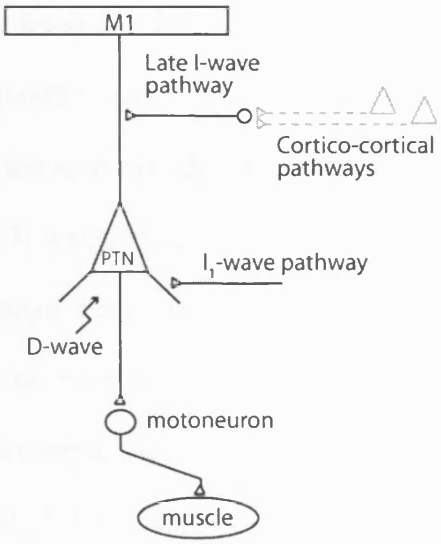

Figure 1.7 Cartoon showing possible origin of the D-waves and I-waves of the corticospinal volley. The D-wave is elicited at the axon-hillock or nearby regions, the I_1- and late I-waves from separate presynaptic pathways. See text for details. Adapted from Shimazu *et al.* (2004).

The different origin of the I_1- and late I-waves shown in Figure 1.7 is supported by TES and TMS data. Epidural recordings in patients show different components of the corticospinal volley facilitated by different TMS paradigms. This is considered to reflect the excitability of differently orientated neuronal elements that produce the I_1 and I_3 components (Sakai *et al.*, 1997; Ziemann and Rothwell, 2000). When current flow was directed forwards across the central sulcus (using medially and anteriorly induced current), the latency of the MEP was 1.5 ms longer than that from anodal TES. With laterally and posteriorly induced currents that flowed backwards across the central sulcus, MEP latency increased 4.5 ms compared to TES (Sakai *et al.*, 1997; Terao *et al.*, 1998b). The peaks of the poststimulus time histograms (PSTHs) from single motor unit recording of the muscles, considered to represent arrivals of successive I-waves (Day *et al.*, 1989a), showed that the I_3-waves are readily produced with AP and medio-lateral (ML) induced currents and I_1-waves by posterior-anterior (PA) and LM induced currents

(Sakai *et al.*, 1997). Additionally, the I_3-wave is easier to suppress and is more susceptible to cortical excitability than I_1 (Ziemann and Rothwell, 2000). Lorazepam, a GABA agonist increasing intracortical inhibition, produced selective suppression of the later I-waves, but not the I_1-wave, elicited from single pulse TMS (di Lazzaro *et al.*, 2000). As would be expected from components elicited from different structures, the order of recruitment of the different I-waves is not sequential, I_1 can be elicited independently of I_3 and vice versa, suggesting the mechanisms that are generating them are independent (Day *et al.*, 1989a; Sakai *et al.*, 1997). The late I_2-I_3 components are thought to result from excitatory afferent inputs to corticospinal neurones (Amassian *et al.*, 1987; Ilic *et al.*, 2002), including activity in cortico-cortical pathways from premotor areas (Amassian *et al.*, 1987). Consistent with cortico-cortical inputs producing the late I-waves, premotor and postcentral stimulation in the macaque monkey and the somatosensory cortex of the cat produce I-waves in M1 corticospinal neurones (Patton and Amassian, 1954).

The interval between successive I-waves (1.5-2 ms) and their time course (up to 10 ms) is consistent across corticospinal neurones with different velocities and across species (Amassian *et al.*, 1987; Lemon, 2002). Why I-waves occur with such periodicity has not been resolved. The duration of excitatory postsynaptic potentials (EPSPs), of 10-15 ms recorded in monkey M1, is too long to account for the ~1 ms periodicity of I-waves (Ghosh and Porter, 1988; Ziemann and Rothwell, 2000). It is possible that I-waves represent a series of EPSPs punctuated by inhibitory postsynaptic potentials (IPSPs) (Ziemann and Rothwell, 2000). In keeping with periodicity due to inhibitory changes, I-

waves are reduced by GABA agonists (Ziemann *et al.*, 1998b). While such sharply tuned synaptic activity has been recorded from rodent auditory cortex (Wehr and Zador, 2003), it has not been shown in corticospinal neurones in cats or monkeys, animals in which I-waves are known to occur. Another hypothesis that this periodic discharge could originate from thalamic synaptic input to the PTNs, is also unlikely as degeneration of the thalamus afferents from the anterior and ventrolateral thalamus, the main thalamic inputs to M1, did not affect I-wave generation (Amassian *et al.*, 1987).

Two other possibilities are that I-waves arise from the intrinsic properties of the neuronal membrane to a large sustained stimulus, or from the precise timing of synaptic inputs to the cell (Lemon, 2002; Ziemann and Rothwell, 2000). Using an intracortical stimulation electrode, later I-waves were recruited as an electrode was moved through the cortex; stimulation of the deeper layers, near laminae V, produced a prominent D-wave, together with I_1-wave, the first I-wave, whereas in the superficial layers later I-waves, such as I_3, were elicited (Amassian *et al.*, 1987; Patton and Amassian, 1954). These experiments led to the hypothesis that I-waves are caused by a vertical chain of interneurones (activation of superficial neurones exciting interneurones deeper in the cortex that then excite PTNs) with fixed temporal characteristics providing periodic bombardment of PTNs (Amassian *et al.*, 1987; Patton and Amassian, 1954). Consistent with this idea, cooling the cortex reduced the I_4 wave (Patton and Amassian, 1954), although this result may be explained by the more labile nature of the late vs. early I-waves (Ziemann and Rothwell, 2000). This model has been adapted to account for the non-sequential order of I-wave recruitment described above. It has been suggested that

I-waves are elicited from independent chains of interneurones, each generating a different I-wave (Day *et al.*, 1989a; Sakai *et al.*, 1997; Ziemann and Rothwell, 2000), with the I_1 response from stimulation of last order synaptic inputs (i.e., no other interneurones involved). Alternatively, the intrinsic properties of the PTN may give rise repetitive discharge after strong depolarisation (Ziemann and Rothwell, 2000) with different parts of the membrane giving rise to different I-waves.

Thus by differentially facilitating components of the corticospinal volley, TMS provides a method for investigating the contribution of different cortical elements to M1 output. However, there is a caveat. Discharge of PTNs at I-wave frequency rarely occur naturally (Amassian *et al.*, 1987; Lemon, 2002). In this way I-waves cannot be taken to reflect normal physiological processes *per se* (Lemon, 2002), but it is argued that they are likely to have functional relevance, with the rhythmic precision possibly reflecting a timing function and acting as a coincidence detector for cortico-cortical or thalmo-cortical inputs (Amassian *et al.*, 1987; Ziemann and Rothwell, 2000). In addition, the different origins of the early (I_1-) and late (I_2-) components may illuminate the properties of cortico-cortical transmission between the premotor cortex and M1.

1.4.3 Cortical stimulation during visuomotor grasp

Paired-pulse TMS can be used to facilitate I-wave components. MEP and epidural recordings in humans have shown that a suprathreshold (130% of resting motor threshold, RMT) followed by a subthreshold (90% of RMT) stimulus, or two threshold stimuli (Tokimura *et al.*, 1996; Ziemann *et al.*, 1998a) interact exclusively at the cortical

level, representing the facilitatory interaction of the I_2- and I_3-waves evoked by the two stimuli (di Lazzaro *et al.*, 1999c; Hanajima *et al.*, 2002). A solely intracortical interaction is thought to underlie this facilitation since replacement of the paired TMS pulses by anodal or cathodal TES, did not produce any facilitation at the first interstimulus interval (ISI) (Tokimura *et al.*, 1996; Ziemann *et al.*, 1998a). The effects of cathodal and particularly anodal TES are though to be less dependent upon cortical excitability than TMS.

Furthermore, epidural recordings using an ISI of 1.2 ms showed specific facilitation of the I_2 and I_3 components of the corticospinal volley (di Lazzaro *et al.*, 1999c). As the second stimulus occurs 1.2 ms after the first stimulus, corticospinal axons will be refractory to the second stimulus, which is further suggested by the absence of facilitation from anodal stimulation (di Lazzaro *et al.*, 1999c). However the first stimulus may have raised the excitability of cell bodies or initial segments of neurones, which are not normally thought to be excited by TMS, to threshold, these then depolarise on delivery of the second stimulus (Amassian *et al.*, 1987; di Lazzaro *et al.*, 1999c). Alternatively, the second stimulus may excite the initial segment of the axon of excitatory interneurones along the late I-wave pathways that are hyperexcitable at the time of the second stimulus having received EPSP from the first stimulus (Ilic *et al.*, 2002). The intracellular recordings of EPSPs in monkey or cat M1 that could distinguish between these last two hypotheses have not yet been carried out.

While paired-pulse TMS is known to test all classes of cortico-cortical interactions, and those arising from within M1, it is expected that if cortico-cortical F5-M1 interactions are mediated by neuronal circuits that produce the late I-waves so facilitation of the I-waves would be expected in visually-guided grasp. Recently, the effect of F5 interactions with M1 have been investigated in anesthetised and sedated macaques (Cerri *et al.*, 2003; Shimazu *et al.*, 2004). Intracortical microstimulation (ICMS) delivered using single pulses to M1 evoked D and I_1, I_2 and I_3 corticospinal volleys, which generated synchronised excitatory responses in hand motoneurones and muscles. ICMS delivered to F5 rarely produced any detectable corticospinal output or overt motor responses. In contrast, these conditioning F5 stimuli markedly enhanced responses to M1 stimulation. Strong facilitation of I_2 and I_3 waves led to larger motor responses in motoneurones and this was particularly marked for motoneurones supplying intrinsic hand muscles. F5-M1 interactions occurred at short intervals (0-1 ms) suggesting a local interaction, and with a periodicity compatible with involvement of the high-frequency I-wave generators in corticospinal neurones.

These results from non-human primates, indicating ventral premotor cortex-M1 interactions can occur via the late I-waves pathways, was the basis of a recent study using paired-pulse TMS over M1 to probe I-wave interactions during preparation to grasp visible objects in human subjects (Cattaneo *et al.*, 2005). The authors found that MEPs elicited several hundred ms prior to movement onset had a pattern of facilitation that predicted subsequent muscle activity when grasping the same object. Thus there was greater facilitation in the 1DI muscle when subjects were preparing to grasp a handle than a disc, and vice-versa for abductor digiti minimi (ADM). Control

experiments involving equivalent hand and digit movements, but without a visible and graspable object, failed to produce MEP interactions. The results suggested that responses to paired-pulse TMS reflect the visuomotor transformations and action preparation that occur during natural grasping behaviour. However, this method cannot provide information about the sources of these cortico-cortical inputs.

1.4.4 Effects of voluntary contraction

Along with the excitation level of the corticospinal neurones, the level of excitation of the motoneurones at the time of the descending volley affects the latency and size of the MEP. For a motoneurone to discharge temporal summation of EPSPs is required. If the muscle is contracted, the spinal motoneurones are already excited and fewer EPSPs are required than in the resting state, as the motoneurone is already close to threshold, resulting in an increase in MEP size and decreased latency (Rothwell, 1991).

Recordings from the cervical cord in patients showed that muscle contraction decreased the threshold and increased the number and amplitude of descending volleys and the size of the resulting EMG response produced by TMS (di Lazzaro *et al.*, 1998). Here using a PA induced current flow, to preferentially facilitate I-waves, the size of the descending volley with maximal contraction could be 50% greater than at rest. In contrast, for both anodal and cathodal TES, the D-waves elicited was not enhanced by maximal voluntary contraction, even though there was a clear increase in the evoked EMG response (di Lazzaro *et al.*, 1999b). Cortical elements involved in the generation of I-waves, but not D-waves, were presumably excited during muscle contraction.

1.5 Rationale for Thesis

The thesis reports a series of experimental studies which investigate how visual representation of objects in F5 before movement influences activity in M1 during grasp. Three aspects were examined: the coding patterns within F5 and M1 from single cell recordings in macaque monkeys; the pathways used for transmission of visuomotor information from F5 to M1, tested by single-pulse ICMS to these regions; and, in humans, the changes in excitability of inputs to M1 prior to visuomotor grasp. This was tested by delivering TMS pulses to M1 and examining changes in hand muscle MEP amplitude.

In the visuomotor grasp circuit, area AIP has been suggested to encode object properties and F5 grasp properties. In keeping with these roles, there is an increased proportion of neurones showing motor responses in F5 compared to AIP. However, previous work has associated each object with a particular grip, so object and grasp were confounded. In the first part of the thesis, the type and evolution of coding patterns observed in F5 and M1 neurones during a visually-guided grasping task was investigated in two macaque monkeys. Two objects were used that could be grasped using a side or hook grasp, in this way object could be dissociated from grasp. To evaluate the similarity of the four grasps, EMG activity was recorded from arm and hand muscles. Each trial was divided into seven periods to identify temporal changes in object and grasp coding, and the relationship to object presentation, reaction time, movement and hold phases was evaluated.

The second part of the non-human primate work investigated the pathways used for transmission of visuomotor information from F5 to M1. Previously, in lightly sedated or anaesthetised animals, the late I-waves of the corticospinal volley were shown to be selectively facilitated when a M1 stimulus was conditioned with a F5 stimulus. The same pathway that modulates late I-waves may be used to transmit visuomotor information in object-orientated grasp. The effect of F5 conditioning stimuli on muscle responses to M1 stimulation was investigated in two awake behaving monkeys trained to carry out a delayed response, visually-guided grasp task. In the first experiment, the timing between F5 and M1 stimuli was varied. As the corticospinal I-waves elicited by M1 stimulation show rhythmic discharges of ~1.2 ms, if F5 stimulation enhances facilitation of muscle responses by I-wave components, EMG facilitation should occur at intervals which coincide with I-wave discharge. In the second experiment, one monkey was trained to grasp different objects. If the F5-M1 stimulation is targeting pathways concerned with visuomotor transformation, object-related facilitation (or suppression) would be expected.

In the last set of experiments, the cortico-cortical inputs to M1 were tested in healthy human volunteers. These experiments are based on the involvement of the late I-wave pathways in visuomotor grasp suggested by the previous studies in non-human primates. Paired-pulse and single-pulse TMS over M1 was used to enhance the late I-wave and I_1 components of the corticospinal volley, respectively. The background to this study is described in Chapter 5. Briefly, MEPs from the paired-pulse paradigm show an object-specific facilitation prior to grasp, whereas the single-pulse MEP shows suppression of

the muscle to be activated in pre-cued reaction time tasks. The differential effects of the early and late I-waves provide a measure of when motor commands are sent downstream to M1. Changes in excitability of M1 inputs were measured during: object observation and preparation to grasp; predictable and random presentation of the 'go' signal; and at different timings from object presentation and the 'go' cue. The importance of visual information for the pattern of MEP facilitation was also considered. Although F5 receives inputs from the somatosensory cortex, when muscimol was used to inactivate F5, monkeys were still able to grasp objects using tactile information, suggesting the AIP-F5-M1 circuit is not involved with transformation of such somatosensory information. In the final experiments the level of visual information available to subjects was manipulated. Firstly, no visual information was given, so subjects had to rely on information gained from haptic exploration of the objects. If the TMS paradigm was facilitating inputs concerned with visuomotor transformation then an object-related facilitation would not be present. Grasping a visible object is generally considered to involve dorsal visual stream processing. If vision is occluded, so that the subject is required to remember the target object, there is evidence of ventral stream visual processing, either due to the absence of visual information or the requirement to initiate grasp from the memory of the target object. The final experiment investigated the importance of the current visual input to dorsal stream visual. Subjects were able to see both objects throughout the experiment, but the visual signal designating the target object, object illumination, was varied. In one block they were required to remember the target object for 1 s, in the other the target was designated throughout the trial.

2. Methods 1: Non-human primates

2.1 Subjects

The data presented here were recorded from three adult purpose-bred macaque monkeys. Two *Macaca mulatta* monkeys (M39 and M40, weights 6.0 kg and 6.3 kg, female and male, respectively) and one *Macaca fascicularis* monkey (CS15, weight 8.5 kg, male). All procedures were carried out in accordance with the UK Animals (Scientific Procedures) Act 1986.

2.2 Experiments

Two studies were carried out, each involving two animals. In the first experiment (Chapter 3) single unit activity from area F5 (M39 and M40) and M1 (M39) were recorded during a visuomotor grasping task. In the second study (Chapter 4), electrodes implanted in area F5 and M1 were used to deliver intracortical microstimulation (ICMS) during reach-to-grasp for a visually presented object (CS15 and M39).

2.3 Behavioural task

2.3.1 Training

Before training on the grasping task, monkeys were taught to voluntarily move from their home cage to a smaller training cage and accept fruit from the experimenters. The complexity of the task was gradually increased from reaching for fruit to touching the

objects and homepads, before starting to use the experimental apparatus itself. At various stages, the monkeys were taught to accept increasing degrees of restraint including a metal neck collar and, for M39 and M40, head fixation. Whenever a new restraint was introduced, diazepam (1-2 mg/kg, APS Ltd) was administered for the first few sessions to minimise stress to the animal. Complete training took around eight months in CS15, 10 months in M39 and 12 months for M40.

2.3.2 Black box task

The apparatus used was based on the "black box" task of Murata *et al.* (1996). The black box consists of two sections, divided by a semi-silvered half mirror (Figure 2.1A). The lower section houses a carousel, capable of holding six objects (Figure 2.1B), and two lights used for object illumination. Objects were mounted on a low friction horizontal shuttle with a weak spring to provide resistance. Object displacement was monitored by Hall-effect sensors. In the upper section a red-orange-green light emitting diode (LED) was positioned so that when illuminated its reflection, from the semi-silvered mirror, was superimposed onto the object. A computer-controlled motor allowed the carousel to rotate allowing different objects to be presented in either a pseudorandom or fixed order. When the box was positioned in front of the monkey, one centrally presented object was visible. Two waist-level homepads were attached to the monkey's training cage, in between the monkey and the black box (Figure 2.1A). These were two small boxes, one for each hand, containing switches which could be closed by the application of gentle downwards pressure from the monkey's hands.

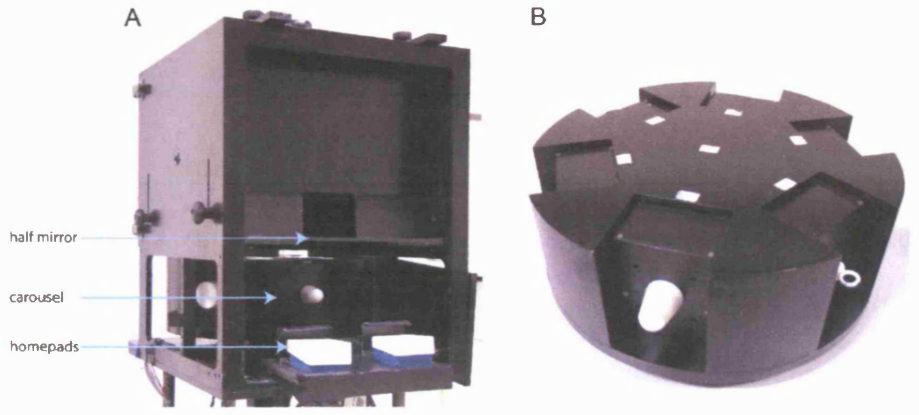

Figure 2.1 Black box task.

A, the black box consisted of two portions, the upper part housing the LED and a lower section that held a carousel on which the objects to be grasped were mounted and two lights for object illumination. The sections were divided by a semi-silvered half mirror. The two homepads, on which the monkey's hands rested, are shown. B, the carousel section of the black box showing the six sections each of which can house one object.

Figure 2.2 summarises the trial sequences used for the three monkeys. The monkey sat in a dimly lit room. At the start of each trial the monkey used both hands to gently press two waist-level homepads. After a fixed period (0.2 s for CS15 and M39; 0.4 s for M40) an object mounted on a shuttle device in front of the monkey was illuminated (the object presentation period). Light from a red/orange LED was reflected onto the object through the half-mirror at the start (M39), or 0.5 s after (M40), object illumination. After a variable object presentation period of 1 ± 0.8 s (M39 and CS15), or a fixed period of 1 s (M40), the monkey was cued, by either the LED switching to green (M39 and M40) or by a tone for CS15 (the monkey did not respond to the visual cue), to reach, grasp, and pull the object into a target displacement zone; correct positioning was indicated by a tone. The monkey had 2 s in which to reach, grasp and displace the object, and the object had to be held for 1 s in the displacement zone (4 to 14 mm from the rest position) requiring a force of between 0.9 and 2.4 N, respectively. A food

reward was given for correct trials, on release of the object, to the non-grasping hand. During the trial itself this hand remained on the homepad. For all animals the inter-trial interval was for 1-2.5 seconds, without object illumination. Monkeys performed the task with the right (CS15 and M40) or left (M39) hand. M39 and M40 were head-restrained throughout the sessions; CS15 was head free, restrained only by a loose-fitting metal neck collar. In each recording session the monkey performed 150-600 trials.

For M39 the object and grasp required was indicated throughout object illumination, when an object could be grasped by a hook or side grip, a red marker on the object signified a side grip was required. In contrast, for M40 object presentation and the cue indicating the type of grasp was dissociated to differentiate object and grasp encoding. For this monkey an LED cued when a hook (red) or side (orange) grip was required, this was illuminated midway through the 1 s object presentation period. Therefore for the first half of object presentation only the object was illuminated, then for the second 500 ms the red/orange LED was also illuminated thus indicating the grasp required.

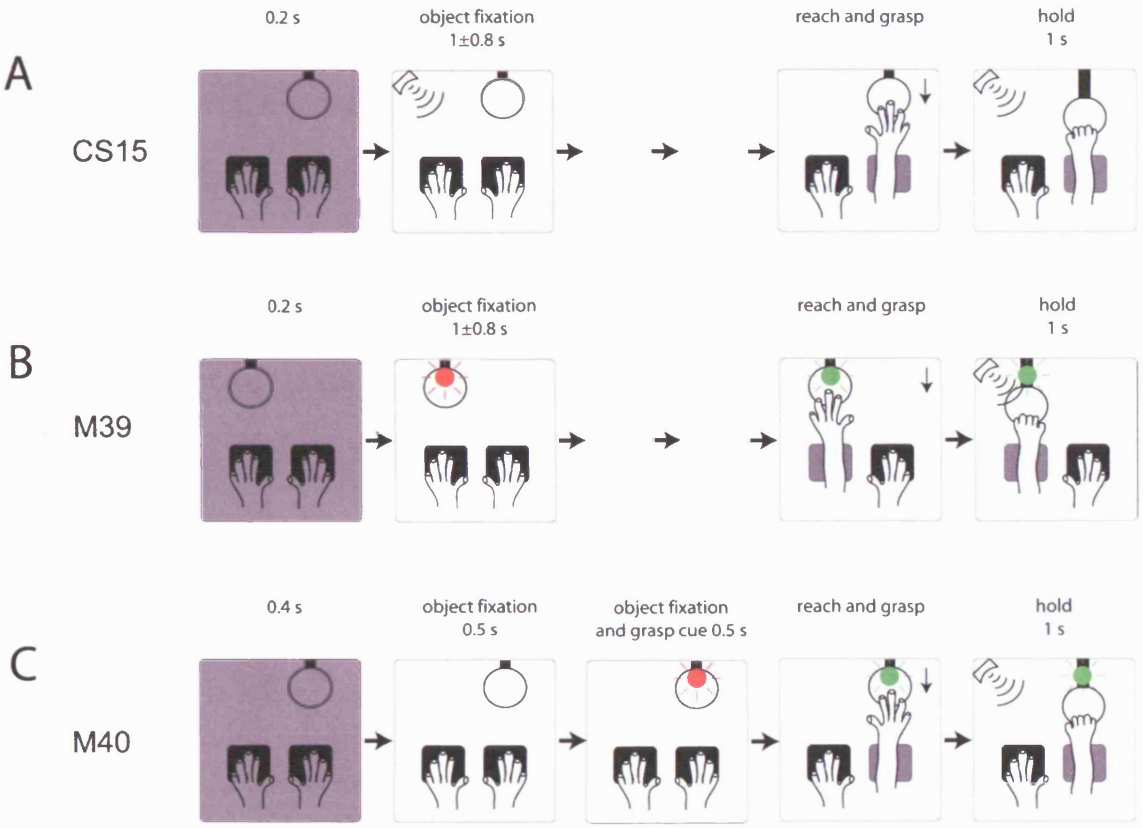

Figure 2.2 Trial sequence for the visuomotor grasping task.

For all three monkeys CS15 (A), M39 (B) and M40 (C) the trial began when both hands were placed on homepads, for either 200 (CS15 and M39) or 400 ms (M40). Object illumination indicated the start of the trial; this was for a variable time of 0.8-1.8 s for two of the monkeys (CS15 and M39) or a fixed period for the other (M40, 1 s). The cue to grasp differed between animals. CS15 was cued by an auditory tone, M39 by light from an LED changing from red (at the start of object illumination) to green. For M40 a red or orange LED (indicating a hook or side grip would be required, respectively), which was illuminated 0.5 s after object illumination, turned green after a further 0.5 s. All three monkeys were required to reach, grasp and pull the object into a displacement zone for 1 s to receive a food reward. CS15 and M40 were trained to use right hand to grasp the objects, M39 the left hand. See text for details.

2.3.3 Objects

Monkeys were trained to use a specific grasp for each object (Figure 2.3). The grasps used by M39 for each object have been previously shown to be consistent across recording sessions (Brochier *et al.*, 2004). M39 was trained to grasp the disc, horizontal plate, cube and ring; CS15 the cone; and M40 the cube and ring. For grasping of the cube and ring M39 and M40 were trained to use either a hook or a side grip (Figure 2.3). For M39 if a side grasp was required there was a red marker on the object, whilst for M40 an orange (rather than red) LED was reflected onto the object. The objects used could vary across sessions.

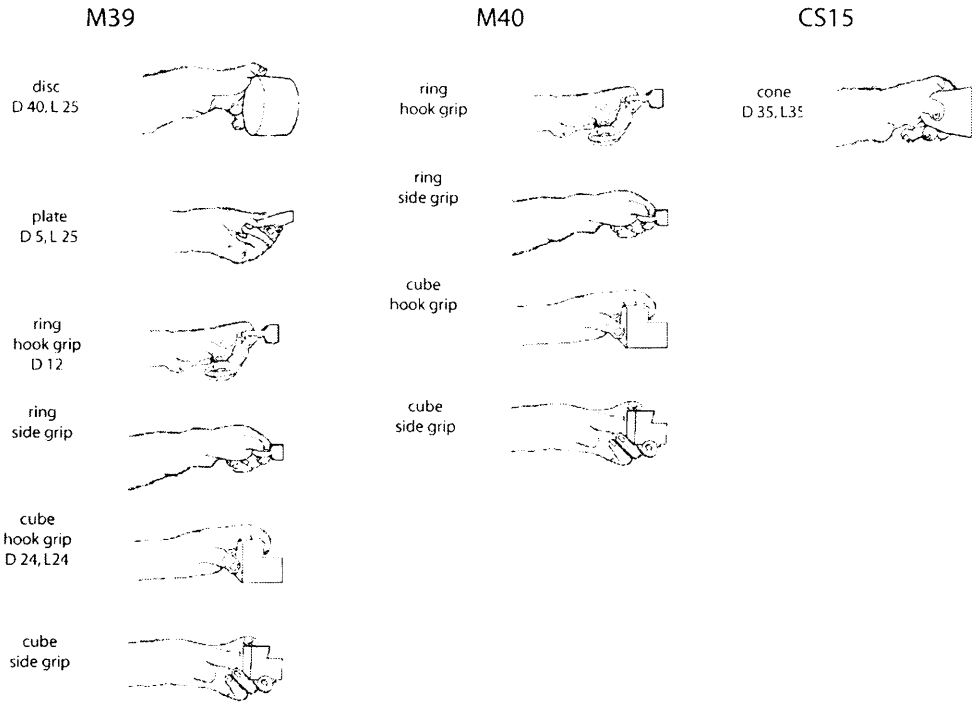

Figure 2.3 The objects and hand shapes used to grasp the objects.
Line diagrams taken from photos of M39 grasping objects with the left hand. For the hook grip of the ring the monkey inserted the index finger in the centre of the ring. For the side grip of the ring, the ring was sandwiched between the thumb (pressing downwards on the upper side of the ring) and the index finger (pressing upwards on the underside of the ring). D=diameter at the widest point, L=length from back to front, dimensions are given in mm.

2.4 Surgical procedures

2.4.1 Anaesthesia and medication

Prior to any surgery involving a craniotomy the animal received glucocorticoid premedication (25 mg/kg i.m., Solu-Medrone, Pharmacia & Upjohn Ltd.) to prevent cerebral oedema. Surgery was performed under deep anaesthesia, induced with ketamine hydrochloride (10 mg/kg i.m., Ketaset, Fort Dodge Ltd.) administered concurrently with atrophine sulphate (20 μg/kg i.m., Atrocare, Animalcare Ltd.) and maintained with 1.5-2.5% isoflurane in 50:50 O_2:N_2O inhaled through an endotracheal tube. Full aseptic procedures were observed. Throughout the surgery 0.9% saline was administered intravenously (10 drops/min) to maintain hydration. Saline infusion rate, body temperature, heart and respiration rate and exhaled pCO_2 were monitored throughout and logged every 15 minutes. Antibiotics (20 mg/kg i.m., Terramycin, Pfizer Ltd) and analgesics (10 μg/kg i.m., Vetergesic, Reckitt & Colman Products Ltd.) were given postoperatively.

Minor procedures such as dura 'stripping' and removal of sutures were performed under sedation with 15 mg/kg i.m. ketamine:medetomidine (Dolmitor, Pfizer Ltd), mixed 80:1 by weight, and reversed by atipamezole hydrochloride (4 mg/kg i.m., Antisedan, Pfizer Ltd.).

2.4.2 MRI and skull mould

Data from the MRI scans of M39 and M40 were used to produce a plastic mould of the skull. These moulds were used to shape the headpiece required to restrain the monkey's head during recordings. In addition, the location and orientation of the recording chambers (CS15, M39 and M40), microwires (CS15 and M39) and PT electrodes (M39) were guided by the structural MRI (Baker *et al.*, 1999).

2.4.3 Chronic implants

In the first surgery M39 and M40 were implanted with headpieces, custom built from the plastic mould produced using data from the MRI scan. The headpiece was either a stainless steel ring (M39) or a hydroxyapatite polyethylene composite ring (HAPEX, supplied by Prof. E Tanner, Dept. of Biomaterials, Queen Mary, University of London) (M40) secured to the skull with four bolts. Three threaded posts protruded from the upper surface of the ring that enabled the head to be fixed during the recordings, an example of the implant is shown in Figure 2.4A.

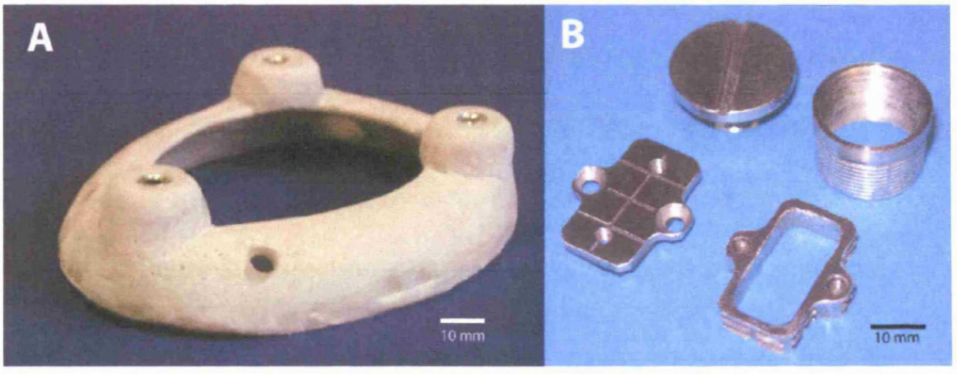

Figure 2.4 Headpiece used for M40 and recording chambers used for all monkeys.
A, shows the HAPEX headpiece that was attached to M40; M39 had a stainless steel headpiece of a similar design. B, illustrates the circular recording chamber and lid used for CS15 and the rectangular chamber and lid used for M39 and M40.

Prior to single unit recording (M39 and M40) and cortical stimulation (CS15), custom designed recording chambers were positioned above a craniotomy that exposed M1 and F5 contralateral to the performing hand. A circular chamber with a diameter of 20 mm (CS15) or a rectangular chamber of 25 x 17 mm (M39 and M40) were fitted (Figure 2.4B). For M39, two varnish insulated tungsten stimulating PT electrodes (impedance ~20kΩ at 1 kHz) were implanted in the medullary pyramid, rostral to the decussion and contralateral to the performing hand (stereotaxic co-ordinates A2.0 L1.5 and P3.0 L1.5) were implanted during the same surgery. The locations of the PT electrodes were confirmed during surgery by recording antidromic field potentials over the M1 following stimulation. The thresholds for these potentials were 50-180 μA. Post-mortem histology confirmed the location of all electrode tips within the pyramids.

In a second (M39 and M40) and third (CS15) surgery, monkeys were implanted with EMG patch electrodes (Microprobe, USA). The patches were sutured onto exposed surfaces of intrinsic and extrinsic digit, hand and arm muscles with the electrode leads running subcutaneously to a miniature D connector on the monkey's back (Brochier *et al.*, 2004; Miller *et al.*, 1993). Muscles implanted in each monkey are shown in Table 2.1. In a terminal experiment, under anaesthesia, the EMG electrode location was verified by muscle twitches evoked by electrical stimulation (~0.5 V) through the back connector. Post-mortem dissection of the arms provided further confirmation of the electrode location (Brochier *et al.*, 2004).

Table 2.1 Muscles implanted in each animal

Muscle	Abbreviation	M39	M40	CS15
Abductor digiti minimi	ADM	Implanted	Implanted	-
Abductor pollicis longus	AbPL	Implanted	Implanted	Implanted
Anterior deltoid	AD	Implanted	-	-
Brachioradialis	BrR	Implanted	-	-
Extensor carpi ulnaris	ECU	-	Implanted	-
Extensor carpi radialis longus	ECRL	-	Implanted	-
Extensor digitorum communis	EDC	Implanted	Implanted	-
Extensor digitorum 4,5	ED 4,5	Implanted	Implanted	Implanted
First dorsal interosseous	1DI	Implanted	Implanted	-
Flexor carpi ulnaris	FCU	Implanted	Implanted	-
Flexor digitorum profundus	FDP	Implanted	Implanted	-
Flexor digitorum superficialis	FDS	Implanted	Implanted	Implanted
Palmaris longus	PL	Implanted	Implanted	-
Thenar	Th	Implanted	Implanted	Implanted

The final surgery for M39 and the second surgery for CS15 was the implantation of intracortical microwires in M1 and F5. Prior to the surgery, the hand representations in areas F5 and M1 contralateral to the trained arm (right hemisphere in M39, left hemisphere in CS15) were mapped using repetitive intracortical microstimulation (rICMS) (M39 and CS15) and single unit recording (M39). This was done under light sedation in CS15 and in the awake state in M39. Subsequently, single planar arrays of four to five low impedance (~20 kΩ) elgiloy microwire electrodes (2-5 mm long, interelectrode distance of 1-1.3 mm) were implanted in M1 and F5 (Figure 2.5) (Cerri *et al.*, 2003; Shimazu *et al.*, 2004). The precise orientation of the implant was guided by

structural MRI (Baker *et al.*, 1999) with the F5 array targeted at the inferior bank of the arcuate sulcus, just lateral to the spur, and M1 to the rostral bank of the central sulcus (see Figure 4.2) and fixed 3-5 mm from the pial surface. The electrodes, once cemented to bone screws in the skull, were connected to a miniature D-connector mounted on the skull. To verify the position of each microwire, in a terminal experiment an electrical current (20 μA d.c., 20 ms, tip positive) was delivered through the head connector to produce a small cortical lesion.

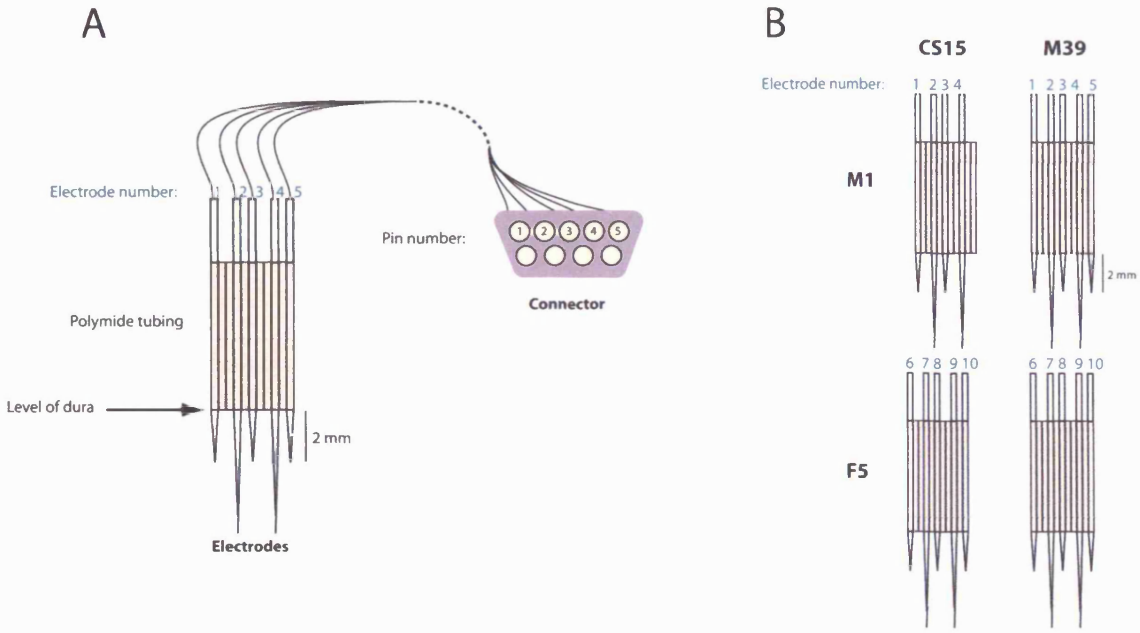

Figure 2.5 Microwire implants for cortical stimulation.
A, five Elgiloy wire electrodes were coated with epoxylite insulation over their shafts. These were inserted into Polymide tubing and connected to a 9 mm connector which was cut to size. Dental cement fixed the connector to the monkey's skull. Electrodes could reach a maximum of 2 or 5 mm into the cortex. B, the microwire numbering for M1 and F5 implants in CS15 and M39.

2.4.4 Care of the dura mater and implants

To prevent the growth of scar tissue over the exposed dura mater, which would prevent electrode penetration, tissue was removed and growth was abated by topical application

of an antimitotic solution. Prior to a recording session the dura was stripped with a corneal hook. If the dura was covered with vascular tissue or a thick layer of tissue, the dura was first covered with local anaesthesia cream for 5 minutes (lignocaine/prilocaine; EMLA, Astra Pharmaceuticals Ltd.). At the end of a recording session the dura was treated with an antimitotic solution (25 mg/ml 5-Fluorouracil, Sigma Chemicals Ltd.) for 5 minutes, then rinsed with a large volume of sterile saline (Baker *et al.*, 1999). Topical antibiotic (0.3 % Gentamicin; Genticin, Roche Products Ltd.) was added to the chambers before sealing with an airtight lid.

To prevent infection, exposed implants and skin edges were cleaned with 3% hydrogen peroxide and coated with neomycin powder (Cicatrin, Wellcome) as necessary. Any incident of infection was treated with topical application of Enroflaxin (Baytril 2.5%, Bayer), and Duphamox LA, (subcutaneous injection, 0.1 ml Kg^{-1}, Fort Dodge).

2.4.5 Post-mortem

At the end of the experimental period M39 and CS15 were deeply sedated and then killed with an overdose of sodium pentobarbitone (50 mg/kg i.p. Sagatal, Rhone Merieux) before perfusion through the heart. Tissue blocks from the brain stem and recording sites were Nissl stained to reveal electrode tracts and verify positioning of the microwires and assess tissue damage. Figure 2.6 shows Nissl staining of the primary motor cortex and Figure 2.7 the right ventral premotor cortex, area F5 (M39). Healthy cells are visible through all layers of the cortex and the position of the M1 and F5 microwires indicated.

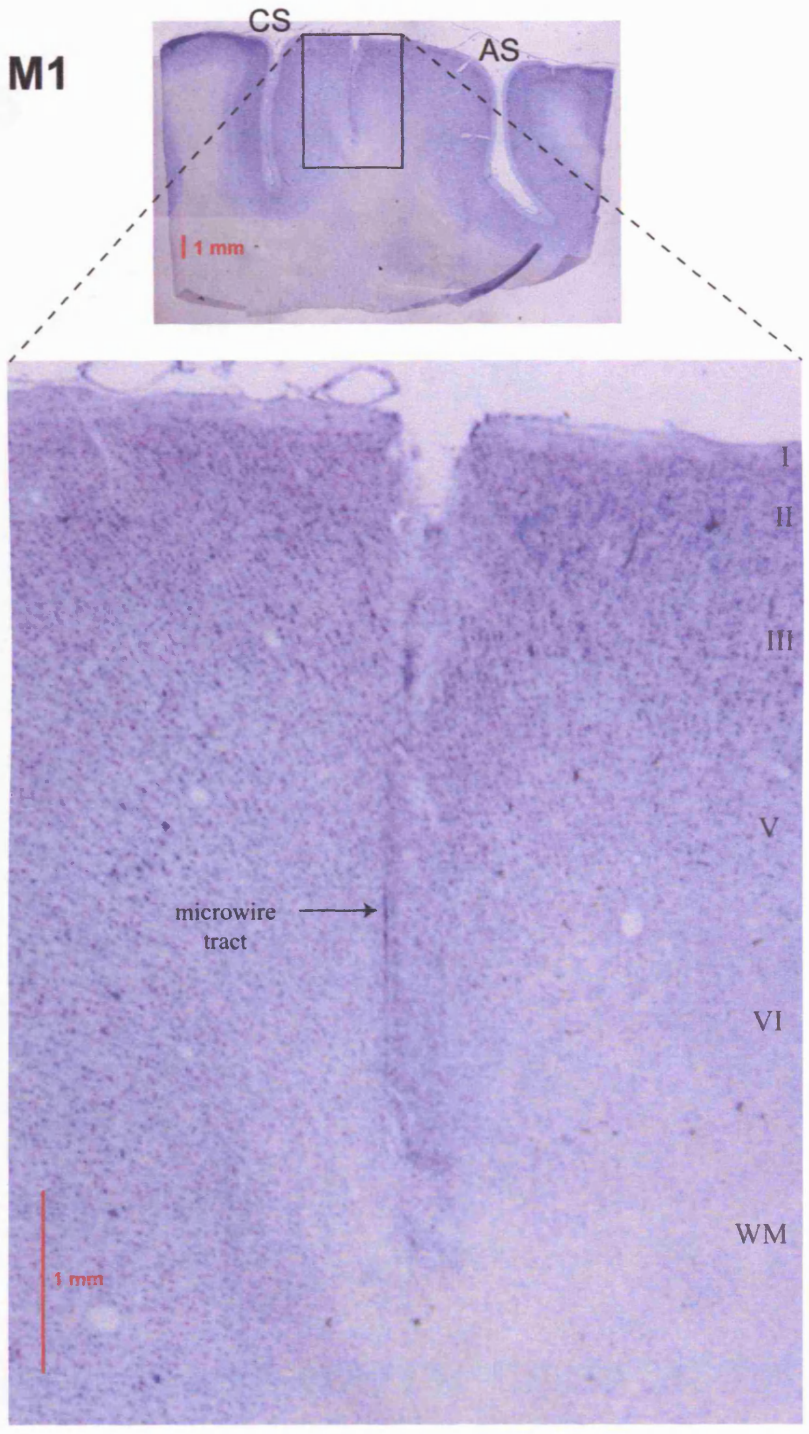

Figure 2.6 Post mortem histology M1 (M39).

Nissl stained transverse section through the convexity of the right precentral gyrus showing the lamination of cells in the primary motor cortex, with lamina (I, II, III, V and VI) and the white matter (WM) labelled. The tract of the cathode used for M1 stimulation (microwire electrode 4) and the central sulcus (CS) and arcuate sulcus (AS) are indicated.

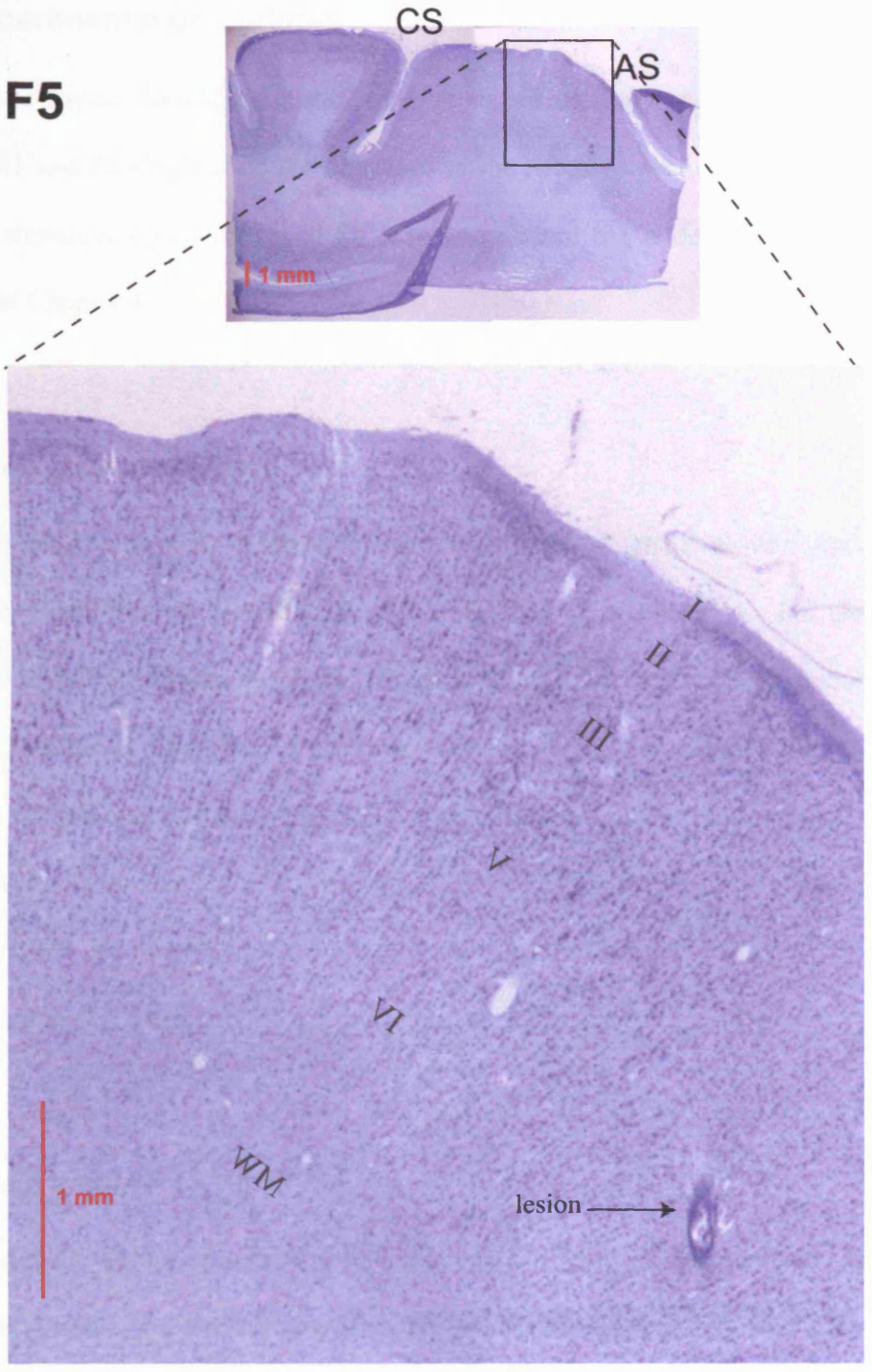

Figure 2.7 Post mortem histology F5 (M39)

Nissl stained transverse section through the convexity of the right precentral gyrus showing the lamination of cells in F5, with lamina (I, II, III, V and VI) and the white matter (WM) labelled. The lesion indicates the position to the tip of the cathode used for F5 stimulation (microwire electrode 7) and the central sulcus (CS) and arcuate sulcus (AS) are indicated.

2.5 Experimental procedures

Electrode drives, electrodes, location of single unit recordings and spike discrimination of the M1 and F5 single units are described in the Methods section of Chapter 3. The cortical stimulation paradigm used for ICMS of F5 and M1 is detailed in the Methods section of Chapter 4.

2.5.1 Cortical stimulation

For the single unit study (Chapter 3) repetitive (r) rICMS mapping was used to elicit motor responses at each electrode location at the end of each session. For the cortical stimulation study (Chapter 4) rICMS effects from each electrode was examined to help identify suitable combination of electrodes for the subsequent experiments. Cathodal unipolar rICMS was delivered through each electrode from a Neurolog NL800 stimulus isolator (Digitimer Ltd, UK). For rICMS a train of 20 0.2 ms biphasic constant current pulses at 300 Hz delivered at a rate of 0.5 Hz with a stimulation intensity of up to 35 μA (single unit experiments) or 125 μA (cortical stimulation study).

2.5.2 Data capture

EMG signals were amplified x 2000, high pass filtered at 30 Hz (Neurolog EMG amplifier, NL824, and isolator amplifier, NL820, Digitimer Ltd, UK) and sampled at 5 kHz using an A-D interface (PCI-6071E, National Instruments). Following amplification of x 20 k, single unit activity was filtered at 0.3-10 kHz. Sampling rates on the A/D interface were 25 kHz per channel.

Behavioural events either analogue (object displacement), obtained from the task computer via a digital to analog (D2A) card (PCL-818L, Advantech), or digital (object illumination onset, LED onset, homepad release and end of the hold period) were recorded along with EMG activity. EMG data were recorded directly to a computer hard disc via two analog to digital (A2D) cards (PCI-6071E, National Instruments).

2.6 Data processing

Analysis of single unit data and the response evoked from single-pulse ICMS are detailed in Chapters 3 and 4, respectively.

2.6.1 Acceptance of trials

Analysis was performed only on data recorded from successful trials. Trials were removed if: the monkey released the homepads prior to the 'go' LED; both homepads were released during the trial; the movement was too slow; the hold was for less than 1 s; the monkey used the incorrect hand to grasp the object; or the animal used an incorrect grasp. For incorrect grasps, the trial was aborted online by the experimenter. For all the other error criteria trials were discarded offline, a custom written program removed the trials where these criteria were not met. For M39 and CS15, typically over 67% of trials were defined as successful, for M40 57%, this aspect of the data, in relation to the single unit activity recorded, is discussed in Section 3.4.1, Chapter 3.

2.6.2 EMG analysis

The pattern of muscle activity during reach and grasp of the different objects (M39 and M40) was examined using normalised EMG values. Analysis was from all 12 muscles for M40, but only 10 muscles from M39 as there were artefacts in 1DI and thenar recordings. For each muscle, EMG activity was rectified, averaged and the baseline activity (average EMG during the visual presentation period) subtracted. The average EMG amplitude at the time window of interest was then normalised by the peak activity for that muscle across objects and all time points (i.e. the start of object illumination to the end of the hold period) with the maximal value for any muscle being one and the minimum zero. Each muscle therefore had the same amplitude scale, allowing the relative level of EMG activity for each object to be compared across muscles. As the movement time (the time from homepad release to object displacement) was different for each object (330 to 420 ms), a normalised time scale, used by Brochier *et al.* (2004), allowed comparison of the EMG activity across objects. The time from homepad release to just before object displacement was divided into nine epochs (epochs 1-9), and the time from object displacement to the end of the hold period into 11 epochs (epochs 10-20) (Figure 2.8).

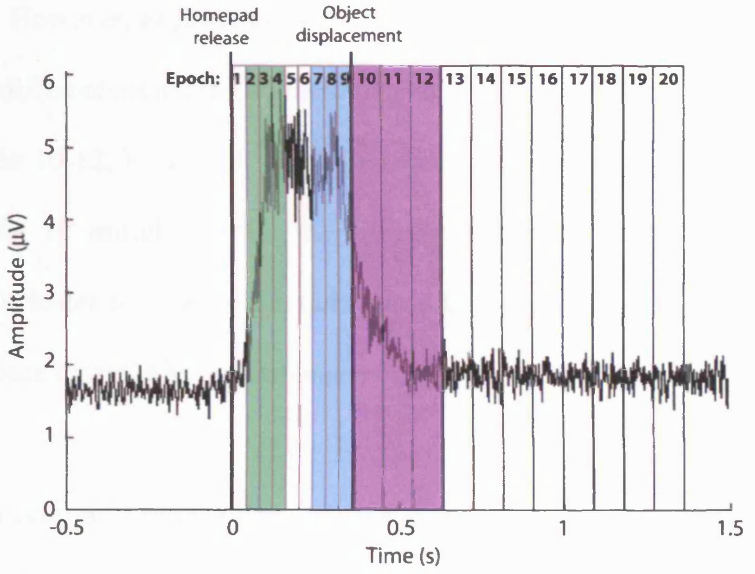

Figure 2.8 Averaged, rectified EMG activity from abductor digiti minimi, recorded during reach to grasp of the disc, illustrating the epochs used for the EMG analysis (n = 81, M39).
The time from homepad release to object displacement was divided into nine epochs and from object displacement to the end of the hold period into 11 epochs. The three time windows used for EMG analysis are illustrated: epochs 2-4 (green), 7-9 (blue) and 10-12 (purple). See text for details.

For the microwire study (Chapter 4) the normalised EMG activity (M39) from three periods were analysed to examine if muscles in which the test response was facilitated by F5 conditioning were more active during grasp or reach phases of the task than muscles that did not have a significant C-T response. Data from one experiment, with no cortical stimulation, was used for this analysis. Previously, M39 has been shown to use consistent grasps for each object across sessions (Brochier *et al.*, 2004). The EMG activity during three stages of movement was examined. Firstly EMG activity was analysed at the time of cortical stimulation (50 ms after homepad release) (epochs 2-4, Figure 2.8 green). Secondly, EMG during hand shaping (epochs 7-9, Figure 2.8 blue), prior to object contact, was examined. During object displacement there is somatosensory feedback from touch of the object and EMG activity related to pulling

the object. However, as EMG during object displacement has previously been shown to have good differentiation across grasps (epoch 10 (Brochier *et al.*, 2004)), activity at this time (epochs 10-12, Figure 2.8 purple) was also investigated. The similarity of activity levels in the 10 muscles across the six object-grasp combinations was assessed by hierarchical cluster analysis on the normalised EMG values for each of the three periods, with Euclidean distance as the distance metric.

A distance matrix (dissimilarity) matrix was constructed as described by Brochier *et al.* (2004). For each time window, object and session, the normalised EMG values from each muscle formed n-dimensional muscle vectors (NDMVs); each muscle representing a dimension. In the single unit study, for M39 there were 10 sessions and four object-grasp combinations, producing 40 NDMVs, for M40 there were five sessions so 20 NDMVs. In the cortical stimulation study there were five sessions and six object-grasp combinations, therefore 30 NDMVs. A hierarchical cluster analysis calculated the shortest Euclidean distance linking pairs of NDMVs within and between sessions for each study. This was used to construct between-sessions distance matrices at the time of hand shaping (epochs 7-9). Figure 2.9 illustrates the construction of the NDMVs and the between and within session comparisons carried out using dummy data for two sessions.

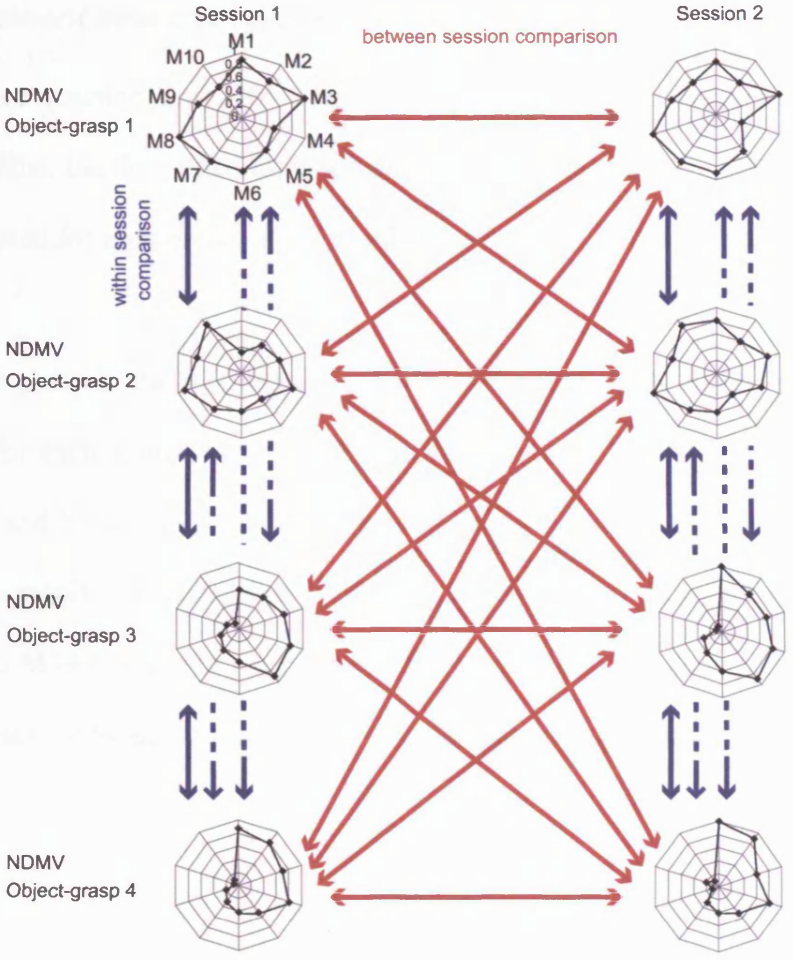

Figure 2.9 Illustration of the n-dimensional vector (NDMV) pairings used for the construction of the distance matrix.

Each polar plot represents a NDMV for a particular object-grasp and session, giving a total of eight NDMVs in this illustration. Within each NDMV are the average normalised EMG amplitudes from 10 muscles (M1 to M10), these 10 values represent the 10 dimensions of the NDMV. To construct a distance matrix the differences between pairs of NDMVs are calculated. The larger the difference the greater the Euclidean distance between a NDMV pair, which represents dissimilarities between the two NDMVs. The distance is calculated both within session (represented by the blue arrows) and between sessions (represented by the red arrows), so here comparison is between 28 pairs of NDMVs. Dummy data were used for the construction of the NDMVs in this diagram.

2.6.3 Movement time and reaction times

The average reaction time, the time from the GO signal to homepad release, and movement time, the time taken from homepad release to the start of object displacement, were calculated for each object in 14 recording sessions for both M39 and M40.

For the single unit study (Chapter 3) a repeated measures ANOVA was performed separately for each animal for the within-subject factors of object (ring and cube) and grasp (side and hook grips). In the microwire study (Chapter 4), a one-way ANOVA tested for a significant difference of reaction or movement times for the six objects presented to M39 (cube side grasp, cube hook grasp, ring side grasp, ring hook grasp, plate and disc). Subsequent t-tests (Bonferroni corrected) were performed as necessary.

3. Single unit activity during visuomotor grasp in macaque monkeys

3.1 Introduction

A cortico-cortical 'grasping circuit' is believed to perform the sensorimotor transformation required to grasp a visible object, whereby visual information about an object's size, shape and orientation is used to form the hand shape appropriate for grasp of that object (Jeannerod *et al.*, 1995). The 3-dimentional features of an object are encoded in the activity of neurones in the anterior intraparietal region (AIP), while the suitable motor plan for grasp is selected in area F5 of the ventral premotor cortex and the execution of grasp is controlled by the primary motor cortex (M1). Evidence for these different processes has come from neuronal recordings in non-human primates. AIP neurones respond during object fixation and grasping (Murata *et al.*, 1996; Sakata *et al.*, 1995). The visual responses of AIP neurones show selectivity for object orientation, size, shape and common geometric features, for instance flat vs. round shapes (Murata *et al.*, 2000). Neurones in F5 also show motor and visuomotor responses. However, the firing patterns of F5 neurones have been related to specific actions, such as precision grip and whole hand prehension (Rizzolatti *et al.*, 1988). Differences in the proportion of neurons with visual and motor properties in these two regions have led to the hypothesis that AIP encodes object affordance whilst F5 encodes hand shaping (Fagg and Arbib, 1998) (see also Sections 1.2.1 and 1.2.2, Introduction). A sub-type of F5 neurones, called 'canonical neurones', show responses to object presentation in a manner congruent with the subsequent grasp (Murata *et al.*, 1997). For instance, a

canonical neurone firing for grasping a sphere would also respond to visual presentation of a sphere, even when grasp was not required. This has led to the proposal that F5 neurones not only code for the motor prototype, but also the 'potential action', a movement that may or may not be executed (Murata *et al.*, 1997; Rizzolatti and Luppino, 2001). There is however an alternative explanation for these visuomotor responses that, during object presentation these F5 neurones encode the object presented rather than grasp being prepared. In this interpretation, the encoding shown by F5 neurones may depend upon the current requirements of the task, with neurones showing object-related coding during object observation and grasp-related coding during movement execution. Previous studies have associated each object with a particular grip, and it has therefore not been possible to disambiguate discharge related to the object from that related to the grasp.

The aim of this Chapter was to identify any object- or grasp-specific changes in the discharge of F5 neurones, and to investigate whether such changes indicate that visuomotor transformation can occur within this same population of neurones. In a 2x2 factorial design, two macaque monkeys were trained to grasp two different objects, a cube and a ring, using two different types of grip (side or hook grip). The grip required was specified by a visual cue. EMG activity from 10-12 hand and arm muscles was recorded to confirm that the monkey was generating similar patterns of EMG activity to make the side grips of ring and cube and a different pattern for the hook grips. Single unit activity was recorded from area F5 and compared to that recorded from M1 during

visual presentation of the object and in the subsequent grasp phase, which followed after a delay period.

3.2 Methods

Single unit activity was recorded in two purpose bred M. mulatta monkeys (case M39, female, and M40, male) from area F5 (M39, M40) and M1 (M39). For M39 cortical recordings were from the right hemisphere and the monkey grasped the object with the left hand, for M40 cortical recordings were from the left hemisphere and the monkey grasped the objects with the right hand. The cortical and muscle implants used, and the recording and analysis of EMG activity are detailed in Methods 1.

3.2.1 Cortical recording

M1 data was recorded using a 16 channel 'Eckhorn' multiple electrode drive (Thomas Recording Ltd., Marburg, Germany) and F5 data from a seven channel Eckhorn drive (Figure 3.1A-C). The Eckhorn system allows glass-insulated platinum electrodes (impedance 1-3 MΩ, interelectrode spacing 300 μm, shank diameter 80 μm) to be independently lowered into the cortex to search for cells. The guide tubes of the 16 channel drive forms a 4x4 grid (Figure 3.1B), whilst the seven channel a concentric array (Figure 3.1C). The system is described in detail by Baker *et al.* (1999). Some of the sessions from M39 involved simultaneous recordings from M1 and F5 (Figure 3.1D).

The location of microelectrode penetration was calculated by reference to triangulation points on the lid of the chamber. As the stereotaxic location of the chambers had previously been measured during the surgery, the position of the electrode penetration site could then be calculated in stereotaxic co-ordinates. The locations of the electrodes were logged for each recording session. At the end of each session cathodal rICMS (13 pulses at 333 Hz, intensity up to 35 μA) was delivered through each recording electrode by a Neurolog NL800 (Digitimer, UK) isolated stimulator and any movements elicited noted.

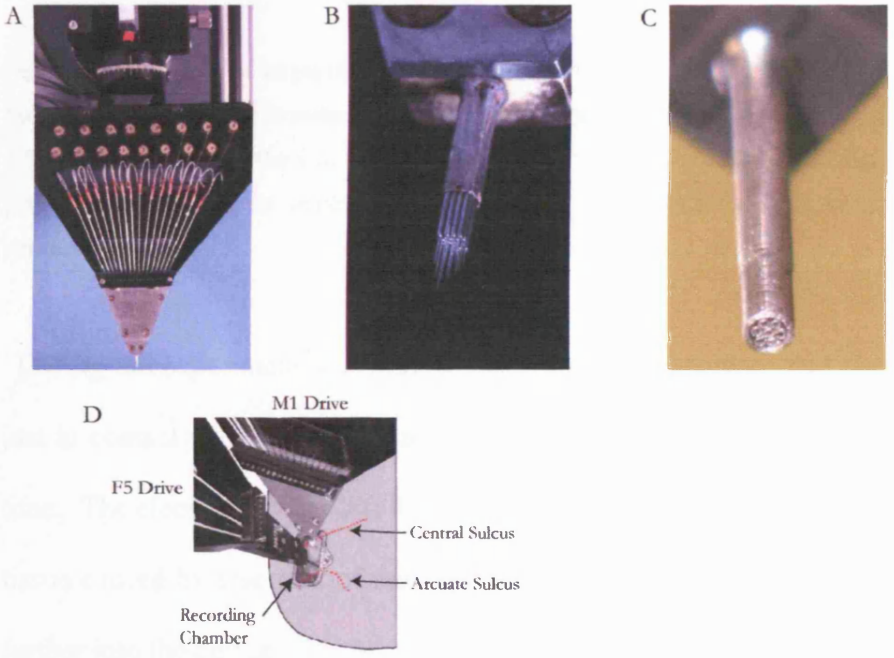

Figure 3.1 Thomas multiple recording system.
The arrangement of the electrodes and motors (A) guide tubes (B) in the 16 channel drive and the guide tubes of the seven channel array (C). D, the configuration of the two drives used for simultaneous recording in one chamber.

The locations of recordings for M39 are shown in Figure 3.2. Measurements of the sulci and fundi were taken post-mortem. M40 is still alive. The recordings from area F5

were centred on the inferior bank of the arcuate sulcus, just lateral to the spur and that from M1 on the rostral bank of the central sulcus.

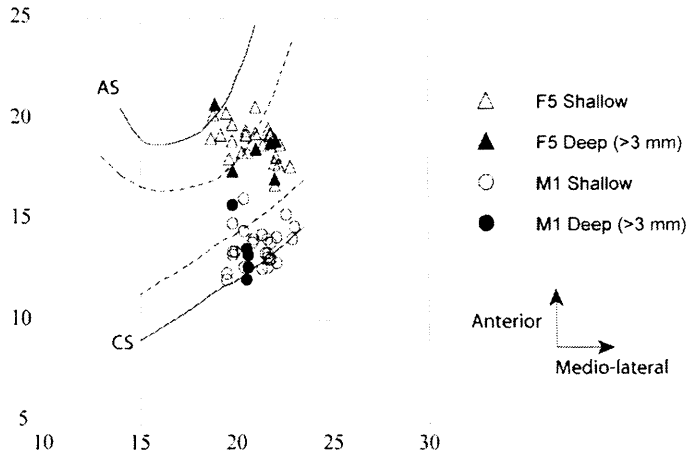

Figure 3.2 Locations of single unit recordings in M39.
Solid lines represent the arcuate sulcus (AS) and central sulcus (CS), dotted lines the caudal bank of the AS and rostral bank of the CS. Triangles represent the locations of F5 recordings, circles of M1, deep penetrations (>3 mm) are indicated by filled shapes. Figure adapted from Umilta *et al.* (2007), with permission.

During the experiment, each drive was positioned in turn so that the guide tubes were just in contact with the dura. Each electrode was then driven through the dura one at a time. The electrodes were left for 10 minutes to allow any mechanical depression of the tissue caused by insertion of the electrodes to subside before electrodes were advanced further into the cortex.

A network of computers was used to allow up to four people to simultaneously control the electrodes; 3-8 electrodes were used in each session. Spike activity at each recording electrode was amplified (x 20 k) and filtered (1-10 kHz). Cells were discriminated on-line using a double amplitude time window algorithm allowing the interspike interval (ISI) histograms to be compiled in real time. Due to the refractory period following

spike firing, a single neuron cannot produce two spikes in less than 2 ms. Therefore, an ISI shorter than 2 ms was a sign of poor discrimination and required a change in the electrode position to increase the signal-to-noise ratio. All subsequent analysis was performed on spike activity discriminated off-line with Get Spike, a custom-made software package (Dr S Baker, Newcastle University).

3.2.2 PT stimulation

For M39, PTNs were identified using antidromic activation from PT electrodes and collision tests (Baker *et al.*, 1999). The mean (SD) antidromic latency was 1.4±0.7 ms and threshold was 194±79 μA using a single biphasic constant current pulses (each phase 0.2 ms duration) between the PT electrodes (M39), as reported in Umilta *et al.* (2007). Post-mortem histology confirmed the location of electrode tips within the pyramids.

3.2.3 Spike discrimination

Analysis was performed on spikes discriminated off-line using Get Spike software. First, spike events crossing a suitable threshold were extracted. The spike shapes were parameterised by height, width and the weighting of the first three principal components (Nicolelis *et al.*, 1997). This resulted in spikes with similar parameters forming clusters. To separate spikes from different cells, an ellipse, generated by the program, was positioned around a spike cluster (Eggermont, 1990) (Figure 3.3A). Successful discrimination of single units was verified by inspection of the ISI histograms (Figure

3.3B) and the consistency of waveforms sampled throughout the recording (Figure 3.3C). The quality of the discrimination was confirmed by showing that the interspike interval histogram did not contain counts in the first 1–2 ms. However such short interspike intervals could not be entirely avoided in some of the neurones recorded from F5 where the activity was more unstable.

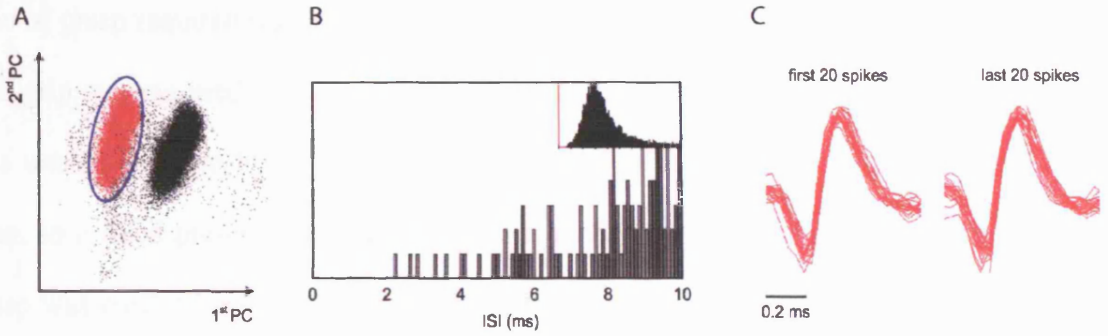

Figure 3.3 Spike discrimination by principal component analysis

A, the two clusters in the scatter plot of the two principal components of the spike wave forms, suggest that there are two cells in this recording. One set of spikes within the ellipse (shown in red, n=1253) is further analysed. B, the interspike histogram for the selected spike waveform shows no spikes at short intervals (<2 ms), which is as expected if only one unit has been discriminated. C, the stability of the waveform is shown by the consistency of the waveform of the first 20 spikes compared to the last 20 spikes of the recording.

3.2.4 Spike analysis

Each trial was divided into seven periods (Figure 3.4) and the firing rate calculated for each period. The visual presentation phase was divided into thirds (VP_1, VP_2, VP_3), to allow any gradation of coding from initial presentation of the object to anticipation of the 'go' signal to be observed. The reaction time (RT) period was the time taken from the 'go' signal to homepad release (HPR), and the movement period (Mv), the time from HPR to object displacement (OD). The hold phase was divided into two equal periods

(H_1, H_2). For each neurone the number of spikes per second in each period was calculated.

The presentation period and the grasp cue were different for the two monkeys (Figure 3.4). For M39, there was a variable visual presentation time (1±0.8 s). Additionally, the type of grasp required was indicated on object illumination by the presence, indicating a side grip was required, or absence, for a hook grip, of a red marker on the object. M40 was unable to grasp the object at the correct time with a variable visual presentation time, so a fixed presentation period (1 s) was used. In addition, for M40, the required grasp was cued midway through visual presentation by illumination of an orange (side grip) or red (hook grip) LED that was reflected onto the object; thereby dissociating object presentation from the cue for the required grasp. See Section 2.3, Methods 1, for further description of the task.

Analysis was performed on 401 neurones, from two monkeys, that showed activity for 10 or more trials for an object. To test for task-related activity, a repeated measures ANOVA was performed on each neurone using the within-subject factors of period (period 1 to 7), object (ring vs. cube) and grasp (hook vs. side grip) (ANOVA 1). If the neurone showed a significant effect of period ($p \leq 0.05$), a repeated measures ANOVA with the within-subject factors of grasp and object was performed for each of the seven periods (ANOVA 2). The results from ANOVA 2 were used to classify neurones as either early-selective or late-selective, according to whether they showed a significant ($p \leq 0.05$) main effect of object and/or grasp during visual presentation. Early-selective

neurones showed a main effect during visual presentation, but also could show a main effect in the RT, Mv and hold phases. Late-selective neurones *only* showed a main effect in the RT, Mv and hold phases. Thus characterisation was based only on whether there was significant modulation in the visual presentation phase of the task.

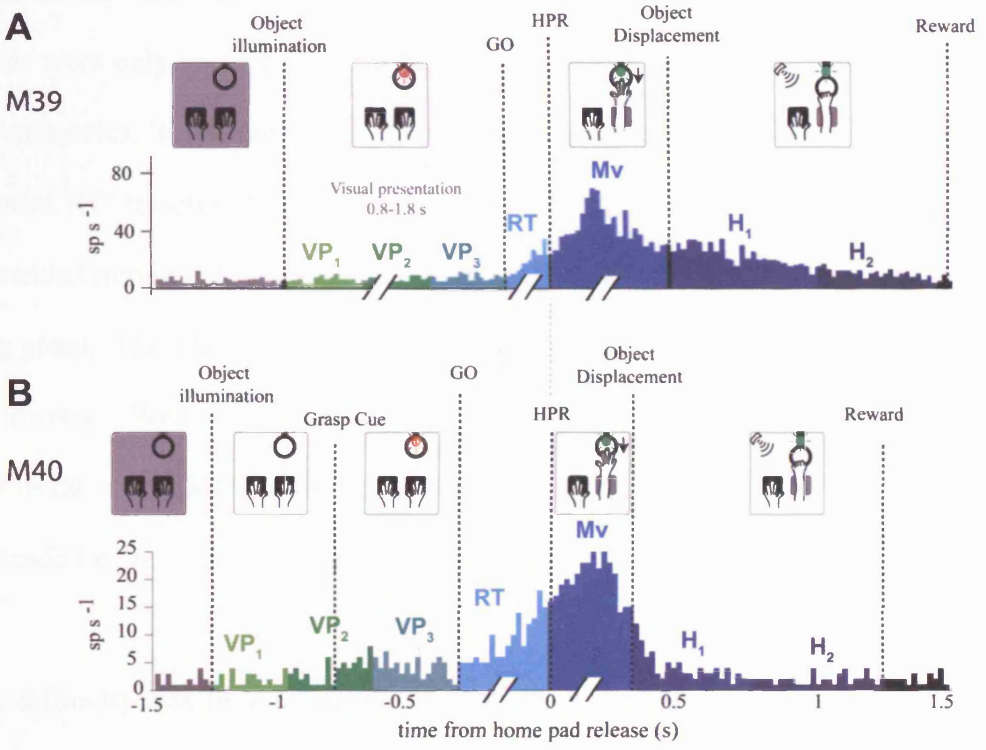

Figure 3.4 Examples of spike activity from the two monkeys illustrating the task sequence and seven periods used for spike analysis.

Timing of object presentation and the cue specifying whether a hook or side grasp was required was different for the two monkeys. For M39 (A) there was a variable visual presentation period and the grasp required was cued by the presence (side grip) or absence (hook grip) of a red marker on the object, visible on object illumination. For M40 the visual presentation period was fixed and the grasp required was indicated half way through object presentation by a red (hook grip) or orange (side grip) LED that was reflected onto the object. At the start of the trial both monkeys sat in darkness. After exerting downward pressure on the homepads for 200 ms (M39) or 400 ms (M40) the object was illuminated. The cue to grasp was the LED light reflected onto the object turning green and the monkey was required to reach out, and grasp the object and hold it for 1 s. Spike activity during visual presentation was divided into three periods (VP_1, VP_2 and VP_3). The remaining portions of the trial were divided into reaction time (RT) (the time taken from the 'go' signal to homepad release), the movement time to displace the object (Mv) and the two hold periods of equal duration (H_1, H_2). Spike activity illustrated is centred on HPR.

3. 3 Results

3.3.1 Performance

The number of successful trials was strikingly different for the two monkeys. M39 performed the task with a 67% success rate, M40 with a 57% success rate. Food rewards were only given for successful trials. The error trials were broken down into three categories: 'early movement', due to the monkey releasing the homepad too early; 'extended RT' (reaction time>1 s); and 'incomplete movement', which could be due to an extended movement time (>1 s), a short hold period (<1 s), or the monkey using the wrong grasp. Trials when the monkey used the wrong grasp were aborted on line by the experimenter. While these trials were not distinguishable off-line from the other two errors in the incomplete movement category, it was noted during the experiments that M40 made frequent incorrect grasps and M39 always used the correct grip.

Task difficulty may be a factor in the error rates observed for the two monkeys. The monkey for which the 'go' signal occurred at a fixed time after visual presentation (M40) made fewer early movement errors compared to M39 where the 'go' signal occurred randomly in a 1 s window (18.5 and 35%, respectively). The number of errors due to extended RT and incomplete movement were negligible for M39 (0.2 and 0.8%, respectively), whereas M40 showed a greater number of RT errors (2.3%) and most of M40's errors were due to incomplete movements (21%). Incomplete movement errors included incorrect grasps, which were often performed by M40 and noted during the session. For M40 the cue indicating the type of grasp required was a LED that was illuminated in VP_2, while for M39 it was a marker on the object that was visible at the

start of visual presentation (see Section 2.3.2, Methods 1). These differences in the timing and type of grasp cue used may have resulted in the presence (M40) and absence (M39) of incorrect grasp errors. The effect of behavioural performance on the single unit activity recorded is discussed in Section 3.4.1.

The average times taken for M39 and M40 to reach and grasp the four objects are summarised in Table 3.1. The values represent the average movement time from 14 sessions. A repeated measures ANOVA showed a significant effect main effect of object ($p<0.05$ and $p<0.001$, for M39 and M40 respectively) representing an overall increased movement time for the cube (M39) and the ring (M40). There was also a significant interaction of object and grasp ($p<0.001$, both monkeys). Subsequent paired t-tests (bonferonni corrected) on the movement times for M39 showed there was a significant difference between the movement times for the two side grasps and also for the hook and side grasp of the ring (both, $p<0.001$). For M40 movement times for the two grasps of the ring ($p<0.001$), cube ($p<0.01$) and for the hook grips ($p<0.001$) were significantly different. For both monkeys there were no significant main effects or interactions in the reaction times.

Table 3.1 Average movement times for M39 and M40 for each of the four object-grasps.

Object-grasp	**Movement times (ms)**	
	M39	**M40**
Cube side grip	355 (±23)	294 (±35)
Ring side grip	330 (±24)	297 (±39)
Cube hook grip	347 (±27)	274 (±41)
Ring hook grip	349 (±23)	323 (±53)

The average (±SD) movement time from homepad release to the start of object displacement. Data taken from 14 sessions for each monkey.

3.3.2 Similarity of muscle and grip type

To investigate the relationship between grasps and objects, EMG activity was recorded from 10-12 arm, hand and digit muscles during the reach-to-grasp movement. The polar plots in Figure 3.5A illustrate the average EMG responses and the hand postures used by M39 during hand shaping (epochs 7-9, see Section 2.6.2, Methods 1). For the hook grip of the ring and cube the general shape of the hand is similar and when comparing the levels of muscle activation, as seen in the pattern in the polar plots (lower plots in Figure 3.5A), only EDC shows a clear difference in the level of EMG between the two hook grips. The side grip of the ring vs. the cube differed in the degree of pronation of the hand and the EMG patterns shown in the polar plots, although having points of similarity, were not as alike as those for the two hook grips. In contrast, there were striking differences in muscle activation across grip types. The polar plots demonstrate much greater activation of FDP, ED 4,5, BrR, ADM and FCU for the side grips compared to the hook grips.

The separation of the two grasp types by EMG activity is clearly identifiable in the distance matrix (Figure 3.5B) comparing the Euclidean distance between pairs of NDMVs (see Section 2.6.2, Methods 1) recorded over 10 different sessions during hand shaping. A blue square represents highly similar grasps, conversely a red square dissimilar grasps. The dark blue diagonal line is the comparison of each NDMV to itself, representing identical grasps. For the side grasps, the shortest distance for NDMVs corresponds to the same grasp in different sessions, suggesting high level of consistency of grasp between sessions. As in the polar plots, the two side grasps do

show some differences, but are closer to each other than to either hook grip. For the hook grips, there is a continuous block of blue encompassing grasp of both cube and ring, signifying that the hook grip of the two objects was highly similar.

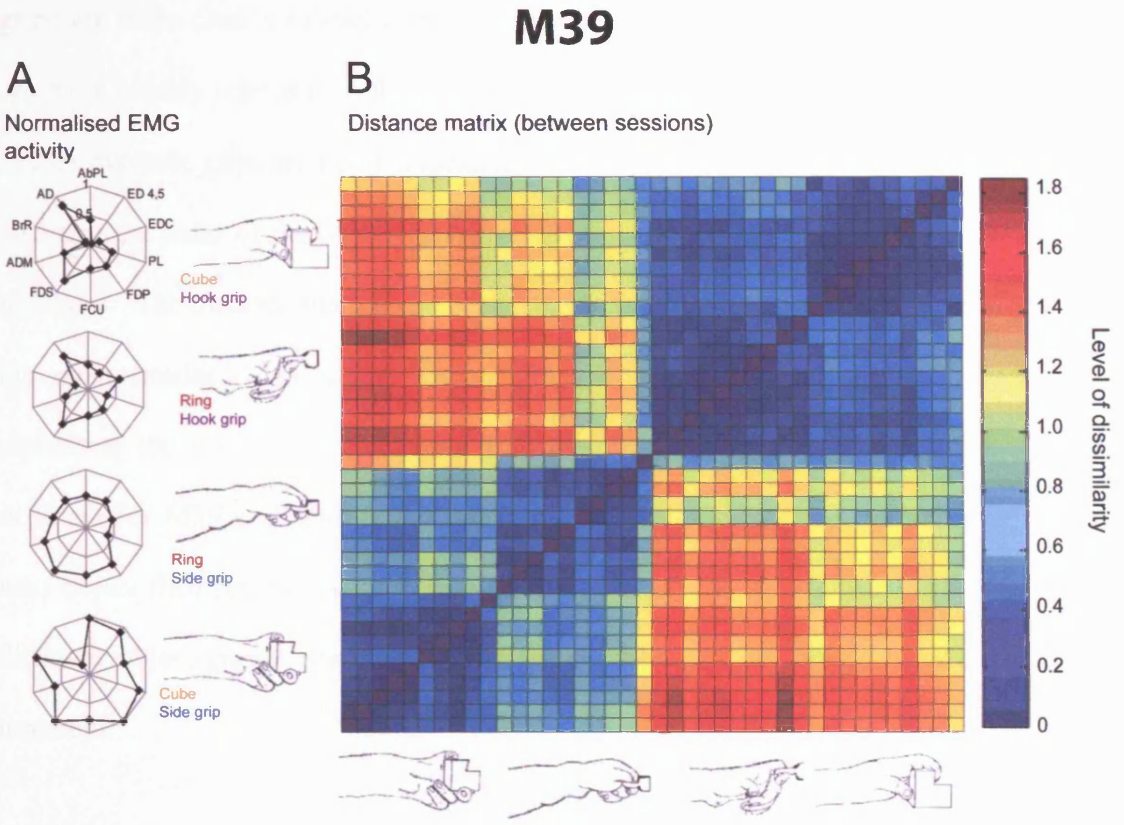

Figure 3.5 Polar plots illustrating the rectified mean normalised muscle activity during hand shaping and a distance matrix (between sessions) based upon n-dimensional muscle vectors (NDMV) (M39).
A, average amplitude of rectified EMG activity taken at the time of hand shaping (epochs 7-9) for the four conditions (60 trials per object). Activity from abductor pollicis longus (AbPL), extensor digitorum 4,5 (ED 4,5), extensor digitorum communis (EDC), palmaris longus (PL), flexor digitorum profundus (FDP), flexor carpi ulnaris (FCU), flexor digitorum superficialis (FDS), abductor digiti minimi (ADM), brachial radialis (BrR) and anterior deltoid (AD) muscles are shown. B, NDMVs calculated from the average amplitude of rectified EMG activity at hand shaping were used to produce a between sessions distance matrix (10 sessions) indicating the Euclidian distance between every NDMV pair (see Section 2.6.2, Methods 1). Blue indicates high degree of similarity (lowest values), red little similarity (highest values). The matrix is symmetrical so the dark blue diagonal line is the comparison of each NDMV to itself (null distance). The object-grasp order is different to that in Figure 3.6 for M40 (see text for details).

Figure 3.6 illustrates the EMG activity during grasp from M40. The pattern of muscle activity for the object-grasp combinations is different to that observed for M39, but again there are similarities between grip types rather than between objects. The hook grips are more clearly related to each other than the side grips, similarly the side grips are more closely related than the hook grips. This is highlighted in the distance matrix. In fact two side grips are not distinguishable on the basis of the distance matrix. Notice also that the order of the object-grasps in the distance matrix were different for the two monkeys. The distance matrix was produced by first finding the two NMDVs that were the most similar. The object-grasp at the bottom left hand corner of the matrix represents the object-grasp with the shortest distance between NDMVs, which was different for M39 and M40 (cube side grasp and ring hook grasp, respectively). The next object then represents the object-grasp closest to this first object. Therefore, the different object-grasp order reflects differences between the grasps used by the two monkeys.

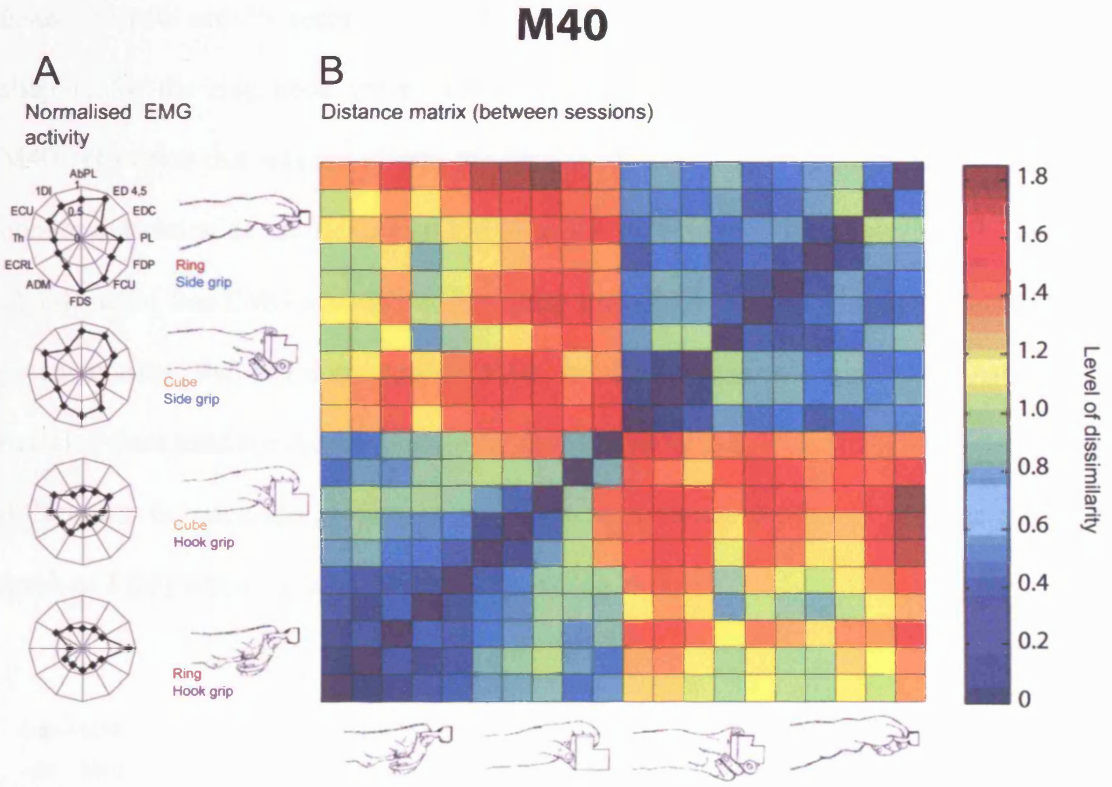

Figure 3.6 Polar plots illustrating the rectified mean normalised muscle activity during hand shaping and a distance matrix (between sessions) based upon n-dimensional muscle vectors (NDMV) (M40).
A, average amplitude of rectified EMG activity taken at the time of hand shaping (epochs 7-9) for the four conditions (57 trials per object). Activity from abductor pollicis longus (AbPL), extensor digitorum 4,5 (ED 4,5), extensor digitorum communis (EDC), palmaris longus (PL), flexor digitorum profundus (FDP), flexor carpi ulnaris (FCU), flexor digitorum superficialis (FDS), abductor digiti minimi (ADM), extensor carpi radialis longus (ECRL), thenar (Th), extensor carpi ulnaris (ECU) and first dorsal interosseous (1DI) muscles is shown. B, NDMVs calculated from the average amplitude of rectified EMG activity at hand shaping were used to produce a between sessions distance matrix (5 sessions) indicating the Euclidian distance between every NDMV pair (see Section 2.6.2, Methods 1). Blue indicates high degree of similarity (lowest values), red little similarity (highest values). The matrix is symmetrical so the dark blue diagonal line is the comparison of each NDMV to itself (null distance). The object-grasp order is different to that in Figure 3.5 for M39 (see text for details).

Comparing the eight muscles that were implanted in both M39 and M40, there were similarities in the pattern of EMG activation between the two monkeys (Figure 3.7). EMG activity from certain muscles are superimposed on the nodes of the polar plots, for

instance EMG activity recorded from AbPL, ED 4,5, FDP, FCU and ADM during hand shaping for the ring hook grasp, representing similar EMG levels for both M39 and M40. However this was not always the case, for the hook grip of the cube M39 showed greater activation of the flexors and M40 of the extensors. Previously, Brochier *et al.* (2004) noted that EMG activity used to grasp the objects while highly reproducible in a given monkey was not consistent between monkeys; rather different combinations of muscles were used for the same grasp by different monkeys. The authors suggested that differences in electrode placement may also be a factor, especially in large muscles (such as FDP) where functional sub-divisions can exist.

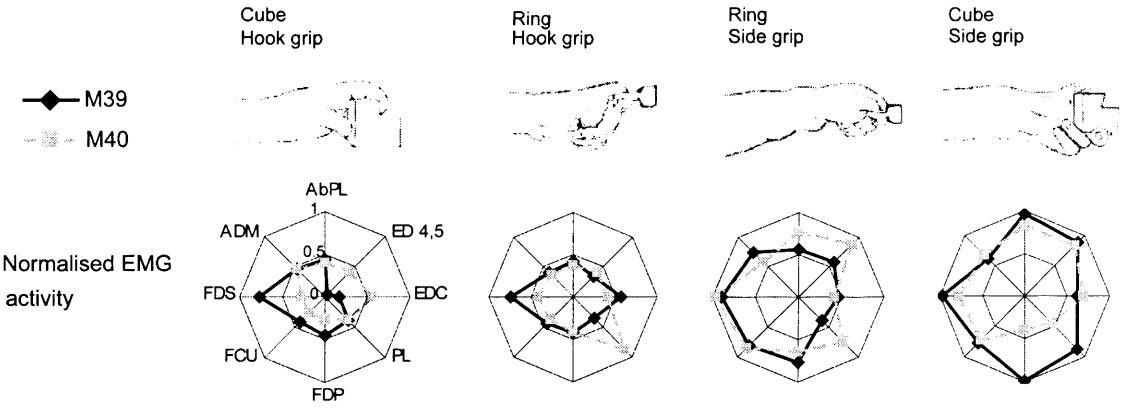

Figure 3.7 Polar plots comparing the rectified mean normalised muscle activity during hand shaping from M39 and M40.

Average amplitude of rectified EMG activity was taken at the time of hand shaping (epochs 7-9) for the four conditions from the two monkeys. Data is from one session from each monkey, 60 and 57 trials per object for M39 and M40, respectively. Key: abductor pollicis longus (AbPL), extensor digitorum 4,5 (ED 4,5), extensor digitorum communis (EDC), palmaris longus (PL), flexor digitorum profundus (FDP), flexor carpi ulnaris (FCU) and flexor digitorum superficialis (FDS) and abductor digiti minimi (ADM).

3.3.3 Object- and grasp-related activity in early- and late-selective F5 neurones

Single unit recordings from F5 were collected from two monkeys. For M39, 67 units were discriminated from a total of 23 recording sessions. Eleven neurones were excluded as there was no main effect of period (ANOVA 1) or no main effect of either grasp or object in any period (ANOVA 2). A further two neurones were excluded as there were less than 10 trials per object. For the remaining 54 neurones, there was on average 38 trials per object. Neurones were then classified as either 'early-selective' or 'late-selective'. Early-selective neurones showed a main effect of either object and/or grasp ($p \leq 0.05$) during visual presentation, whereas late selective neurones *only* showed a main effect of object or grasp during movement phase (RT, Mv, H_1 and H_2). As classification was based on the presence of a main effect during the visual presentation phase, an early-selective neurone could show a main effect of object or grasp during the movement phase, but a late-selective neurone could not show a main effect of object or grasp during the visual presentation phase. Twenty-three neurones were classified as early-selective and 31 as late-selective. For M40, 197 units were recorded over 18 sessions. One neurone was excluded as it had less than 10 trials per object and 93 neurones did not show either a main effect of period (ANOVA 1) or a main effect of grasp/object in at least one period (ANOVA 2). Of the remaining 103 neurones (on average 55 trials per object), 70 were classified as early-selective neurones and 33 as late-selective.

Single units recorded from M39 will be described first. As illustrated in Figure 3.8, in both early- and late-selective categories there were examples of object- and grasp-related activity. An example of object-related firing, prior to movement, is illustrated in Figure 3.8A. This neurone showed an increase in firing rate for all three visual presentation periods for the cube, regardless of whether a side or hook grip was required, and this increased level of discharge was not seen when the ring was presented. The specific increase after presentation of the cube is unlikely to be related to the preparation of the upcoming grasp (which was cued by the 'go' signal), because, as illustrated by the EMG activity (Figure 3.5), the monkey was preparing quite different grasps. During the Mv period there was increased firing for the side grasp, which returned to a main effect of object, for the cube, in the hold period. Another early-selective neurone (Figure 3.8B) showed increased firing during VP_3, when a side grasp of the cube or ring was required, a selectivity that was maintained during the movement phase and early hold period. Thus this neurone exhibited activity that previous studies have shown to be characteristic of F5 visuomotor neurones, congruent grasp-related selectivity during the visual presentation and movement periods (Murata *et al.*, 1997; Raos *et al.*, 2006). The late-selective neurone in Figure 3.8C showed object-related activity at homepad release, with greater activation for the cube than the ring, and particularly pronounced activity for hook grip of the cube. Notably, the increased firing for the cube continued into the hold stage of the trial. Clear preference for the side grasp of the ring or cube is shown by the neurone illustrated in Figure 3.8D. This activity is characteristic of 'motor' neurones in F5 (Murata *et al.*, 1997; Raos *et al.*, 2006), with little or no modulation during visual presentation, but pronounced grasp-related activation during movement.

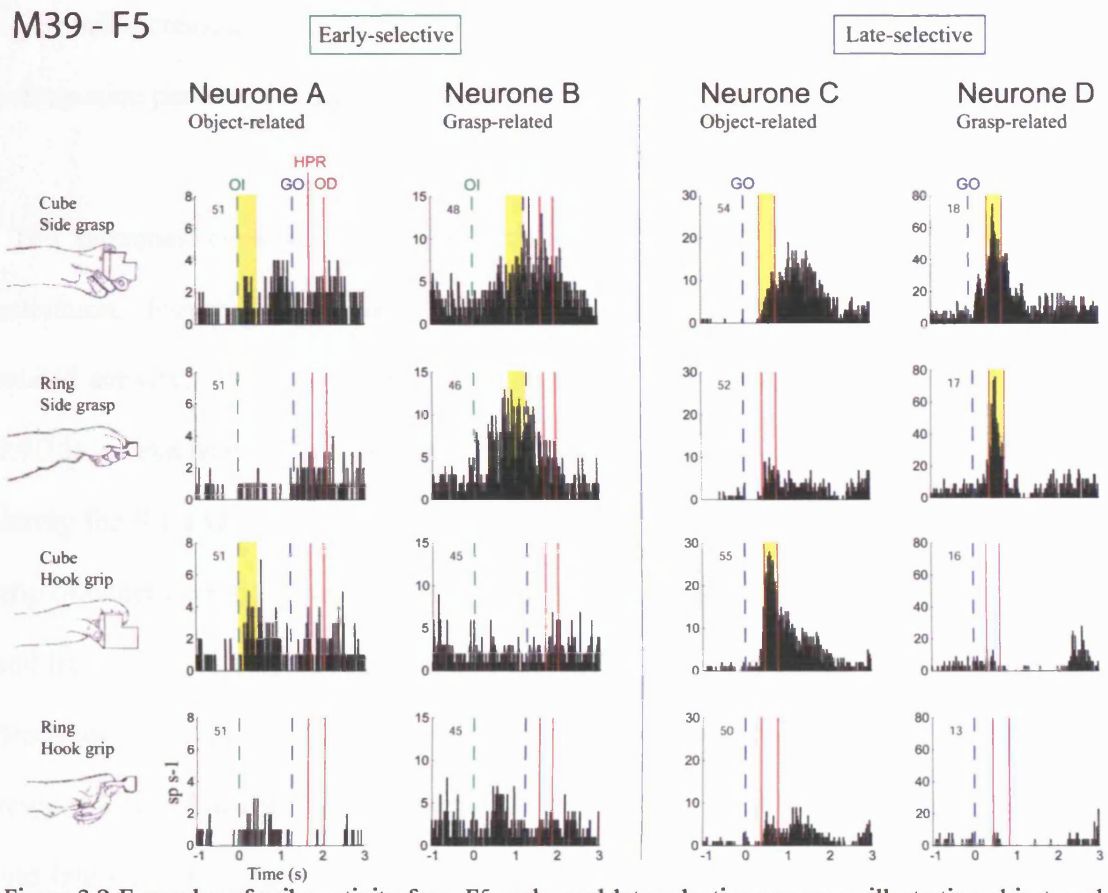

Figure 3.8 Examples of spike activity from F5 early- and late-selective neurones, illustrating object- and grasp-related activation (M39).

Object-related (A) and grasp-related (B) activity from early-selective neurones is centred on the object illumination (OI), 0 s. The subsequent blue and red vertical lines indicate the average time of the GO signal, homepad release (HPR) and object displacement (OD). For the late-selective neurones object- and grasp-related activity (C and D, respectively) is centred on the GO signal (0 ms). The number of sweeps contributing to the spike activity is indicated on the top left hand corner of each histogram. Yellow bars indicate an epoch showing a significant main effect of object or grasp ($p \leq 0.05$).

The units recorded from M40 had a similar pattern to that observed for M39. Figure 3.9A illustrates an object-related activity recorded from an early-selective neurone, with increased firing during VP_3 for the ring, this significant main effect of object was also present during the RT, Mv and H_2 periods. The second early-selective neurone (Figure

3.9B) had increased activation when there was an upcoming side grasp in all three visual presentation periods, this was maintained during the RT, Mv and hold periods.

The neurones classified as late-selective, also showed object- and grasp-related activation. Figure 3.9C shows an example of a late-selective neurone that had object-related activity, with a clear peak of firing for the ring during the Mv period. Figure 3.9D is an example of a neurone with grasp-related activation, with far greater activity during the RT and Mv periods for the side grip of the cube and ring than for the hook grip of either object. As noted for the F5 recordings from M39, the activity of the early- and late-selective grasp-related neurones from M40 were reminiscent of the F5 neurones described by Murata *et al.* (1997) and Raos *et al.* (2006) as 'motor' and 'visuomotor', respectively. However in the present study, in addition to F5 neurones showing early- and late-selectively for grasp, there was also significant modulation of the firing rate corresponding to the object to be grasped. Furthermore, this object-specific increase in firing could not be explained on the basis of EMG activity during grasp. As illustrated Figure 3.6, M40 had clearly different EMG patterns for the side grip of the cube and the hook of the cube and grip types were clearly separated in the distance matrix, reflecting the lack of similarity between these two grasps.

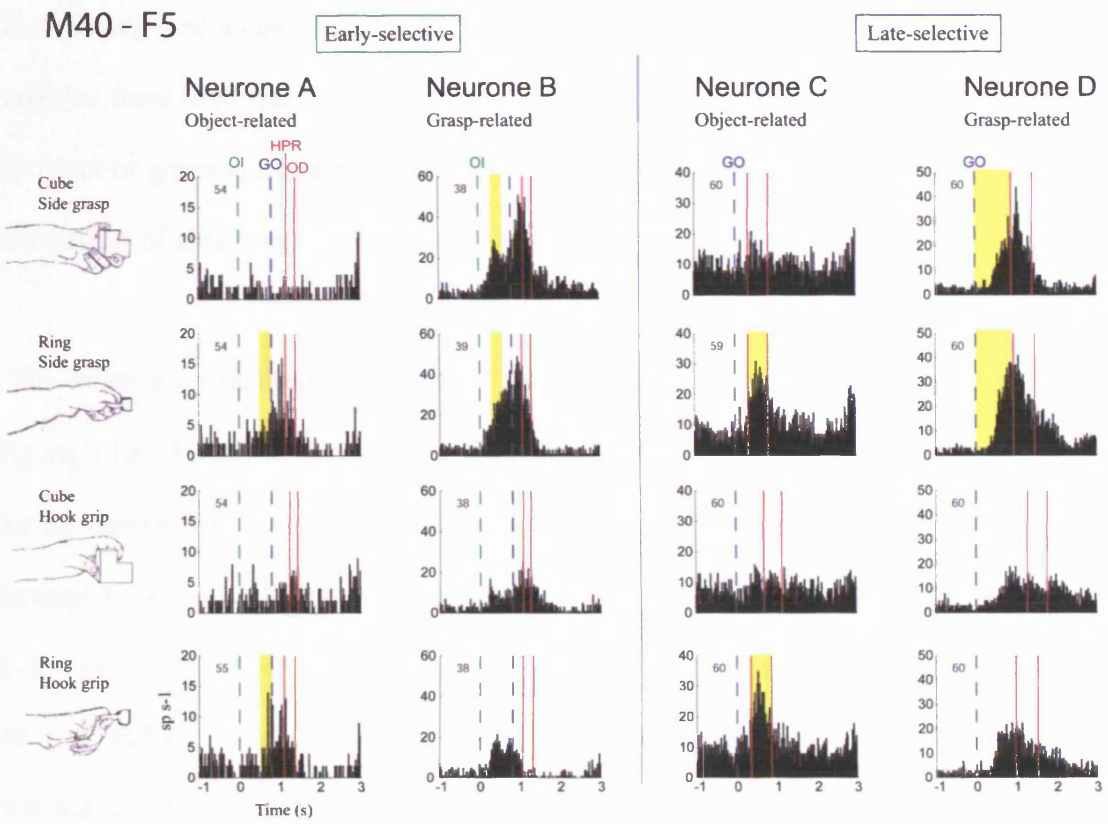

Figure 3.9 Examples of spike activity from F5 early- and late-selective neurones, illustrating object- and grasp-related activation (M40).

Object-related (A) and grasp-related (B) activity from early-selective neurones is centred on the object illumination (OI), 0 s. The subsequent blue and red vertical lines indicate the average time of the GO signal, homepad release (HPR) and object displacement (OD). For the late-selective neurones object- and grasp-related activity (C and D, respectively) is centred on the GO signal (0 ms). The number of sweeps contributing to the spike activity is indicated on the top left hand corner of each histogram. Yellow bars indicate an epoch showing a significant main effect of object or grasp ($p \leq 0.05$).

3.3.4 Temporal changes in population coding in F5

Overall, both early- and late-selective neurones showed a change in object and grasp preference ($p \leq 0.05$) as the trial evolved. For M39, only 8/54 neurones showed a significant main effect of object or grasp in just one period (ANOVA 2). For the remaining neurones, which showed a significant effect in more than one period, only 5

neurones showed a consistent main effect for one type of grasp or object. F5 neurones recorded from M40 had a similar pattern, 15/103 neurones has a significant main effect of object or grasp in just one period (ANOVA 2) and only 16 neurones had a consistent main effect of either object or grasp.

The average normalised firing rate of these task-related F5 neurones is illustrated in Figure 3.10. For both monkeys the firing rate of the F5 population was at its highest during movement. During this period neurones recorded from M39 showed a clear increase in firing for the two side grasps. However if the population activity is equally distributed across type of object or grasp, no mean differences will be detected as both the ring and the cube are grasped using the hook and the side grasp. In the visual presentation periods, for both monkeys, similar firing rates were observed for the four object-grasps, so it is uncertain whether there was a preference for object or grasp. The pattern of object and grasp main effects suggest that, for M39, there could be increased object-related firing during visual presentation (Table 3.2). The percentage of neurones showing main effects of object during VP_1-VP_3 was approximately or more than double that observed for grasp. For M40, the percentage of neurones showing object and grasp main effects was remarkably similar during visual presentation, differing on average by less than 1% (Table 3.2). Object main effects were not restricted to the presentation phase, in fact during movement the number of object and grasp main effects increased. For M40, the same proportion of neurones (25.2%) showed a main effect of object or grasp, whereas for M39 the percentage of neurones with a main effect of grasp was nearly double that for object (20.4% and 11.1% respectively). Some neurones showed a

main effect of both object and grasp, not shown in Table 3.2, and these also reached a peak at Mv (M39, 46.3%; M40, 25.2%). The number of neurones showing a main effect during movement (Table 3.2) and the increased firing rate at this time (Figure 3.10), compared to that during visual presentation, highlight the importance of F5 during movement execution. The object main effects during movement may represent object selectivity being maintained over this movement period.

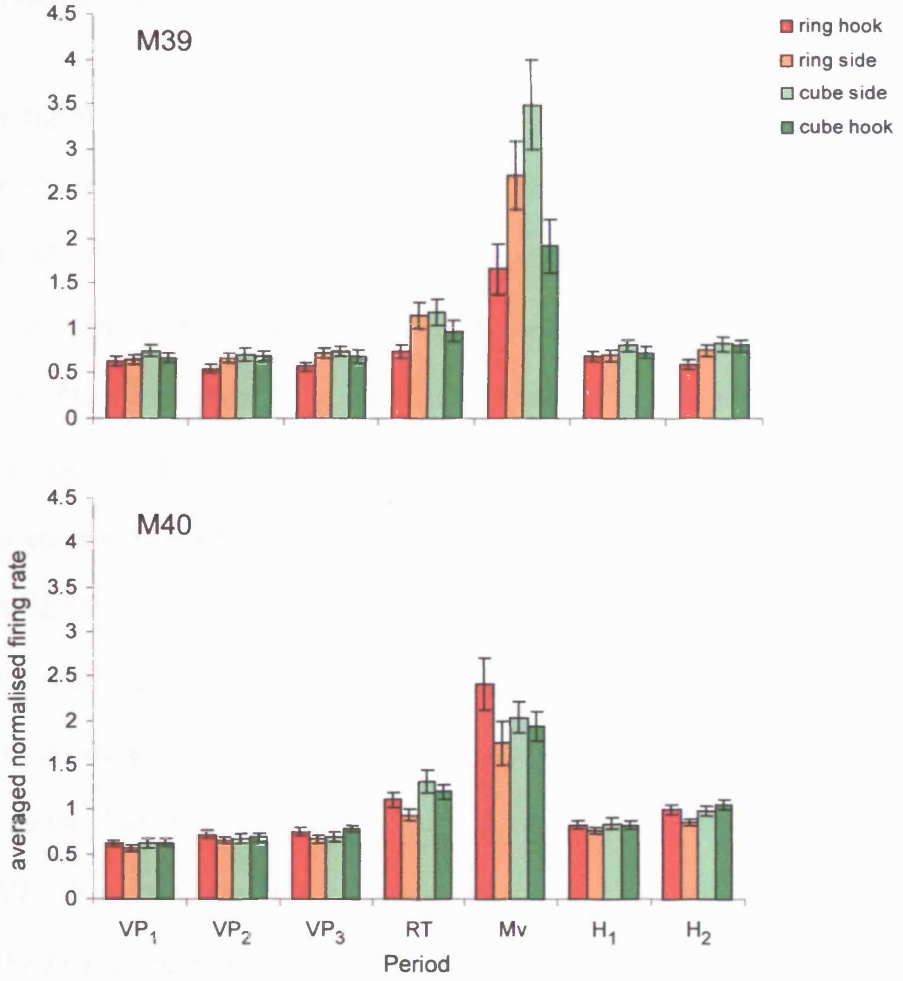

Figure 3.10 Averaged normalised firing rate of F5 neurones recorded from the two monkeys.
The histograms show the average normalised firing rate (±SE) of the F5 population for M39 (top) and M40 (bottom). The firing rate for each neurone, object-grasp and period was normalised by the mean firing rate (across periods and object-grasps) for that neurone.

Table 3.2 The percentage of neurones showing a main effect of object and grasp.

Case	Region	Percentage of neurones showing a main effect of object and grasp for the seven periods of the task						
		VP1	VP2	VP3	RT	Mv	H1	H2
M40	F5	7.8/6.8	14.6/15.5	19.4/19.4	17.5/15.5	25.2/25.2	9.7/11.6	24.3/16.5
M39	F5	11.1/1.8	12.9/7.4	9.3/5.5	22.2/22.2	11.1/20.4	14.8/5.5	14.8/14.8
M39	M1	3.3/8.3	3.3/3.3	13.3/8.3	15/18.3	16.7/21.7	3.3/5	11.7/8.3
M39	PTN	11.4/7.1	4.3/8.6	7.1/7.1	17.1/14.3	21.4/22.8	7.1/5.7	12.9/11.4

For each of the seven periods the first figure indicates the percentage of neurones with a main effect of object and the second a main effect of grasp.

To investigate object- and grasp-related firing of the F5 neurones a population analysis was carried out on the ranked firing rate. The early- and late-selective classification, based on ANOVA 2, was used to group the neurones. For each single unit and each period, the average firing rate for each of the four object-grasp conditions was calculated. The two highest firing rates for each period categorised the neurone at that time as having object (either cube or ring), grasp (side or hook grips) or mixed coding (all other combinations) (Figure 3.11A). For instance, a neurone showing the highest firing rate in VP_1 for side grip of the *cube* and hook grip of the *cube* was considered as coding for *object* in VP_1, if in the Mv period the highest firing rates were for the *hook grip* of the cube and *hook grip* of the ring then it was *grasp*-related in Mv. In this way a neurone could change category during the trial, showing object-related coding for the cube in VP_1, then show grasp-related activity for the hook grip during reach-to-grasp and so on. The final group was mixed coding; this consisted of neurones that did not fit into the other two groups. For instance, combinations such as highest firing for side grip of the cube and hook grip of the ring, or if the firing rate for three, or all four, object-grasp

conditions was the same. Therefore by chance alone a neurone is more likely to fall in the mixed group.

In the ranked population analysis any change in firing rate, regardless of magnitude, would be considered meaningful. This analysis assumes that neurones with high and low firing rates are equally important in the visuomotor grasp circuit. All neurones included in this analysis had already been shown to have task-related firing (a significant effect for ANOVA 1 and ANOVA 2). Therefore a small increase in firing rate would have the same impact on the ranked population analysis as an increase that was significant as defined by ANOVA 2. Additionally, a neurone with no relationship to object or grasp in any one period would still fall into one of three categories. If it is taken that there is an equal chance for a neurone to fall into any of the three categories by chance alone, then 30% of neurones would be object-related, 30% grasp-related and 30% would have mixed coding. For the results described below, only when over half of the neurones showed an increase in object- or grasp-related firing was the ranked data considered meaningful.

For the early-selective neurones recorded from M39, there was initially a greater proportion of neurones showing increased firing for object, which decreased as the trial progressed, reaching a minimum at the time of movement onset (Figure 3.11B, top graph, light green line). At the end of the trial, at the hold phase, there was also a rise in the number of early-selective neurones exhibiting object-related activity, which may reflect confirmation of grasp or the upcoming release of the object. Concurrent with the decrease observed in the proportion of neurones showing object-related firing in the

visual presentation phase, the number of neurones showing grasp-related activity increased during visual presentation and reached a peak at the time of movement initiation and then decreased once more (Figure 3.11B, top grasp, dark green line). Over 50% of early-selective neurones showed object-related increases in their firing rate during VP_1-VP_3 and H_2 periods, which switched to over 50% showing grasp-related activation during the RT and Mv periods of the trial. The late-selective neurones (Figure 3.11B, bottom graph), showed a similar peak in the proportion of grasp-related coding at movement onset (dark blue line) as observed for the early-selective population. Just over half of the late-selective neurones recorded from M39 had grasp-related firing during Mv. The proportion of late-selective neurones with object-related firing remained at a constant rate (~35%) throughout the trial (light blue line).

For M40 although there was greater proportion of neurones showing object-related, compared to grasp-related, activity during the visual presentation periods for the early-selective neurones (Figure 3.11C, light and dark green traces, respectively), the difference between these two populations was not as marked as that observed for M39 (Figure 3.11B). Additionally, for M40, the proportion of neurones with object- or grasp-related activity in the early-selective population (Figure 3.11C) was undifferentiated across the seven periods of the trial. For the late-selective neurones the proportion of neurones with object- or grasp-related activity remained below 50% for all seven epochs, so while the number of neurones with grasp-related activity reached a peak during Mv, this was still only 45% of this population (Figure 3.11C, dark blue trace). The proportion neurones showing object-related activity for the late-selective population

(Figure 3.11C, light blue trace) was higher during the movement periods than that from M39.

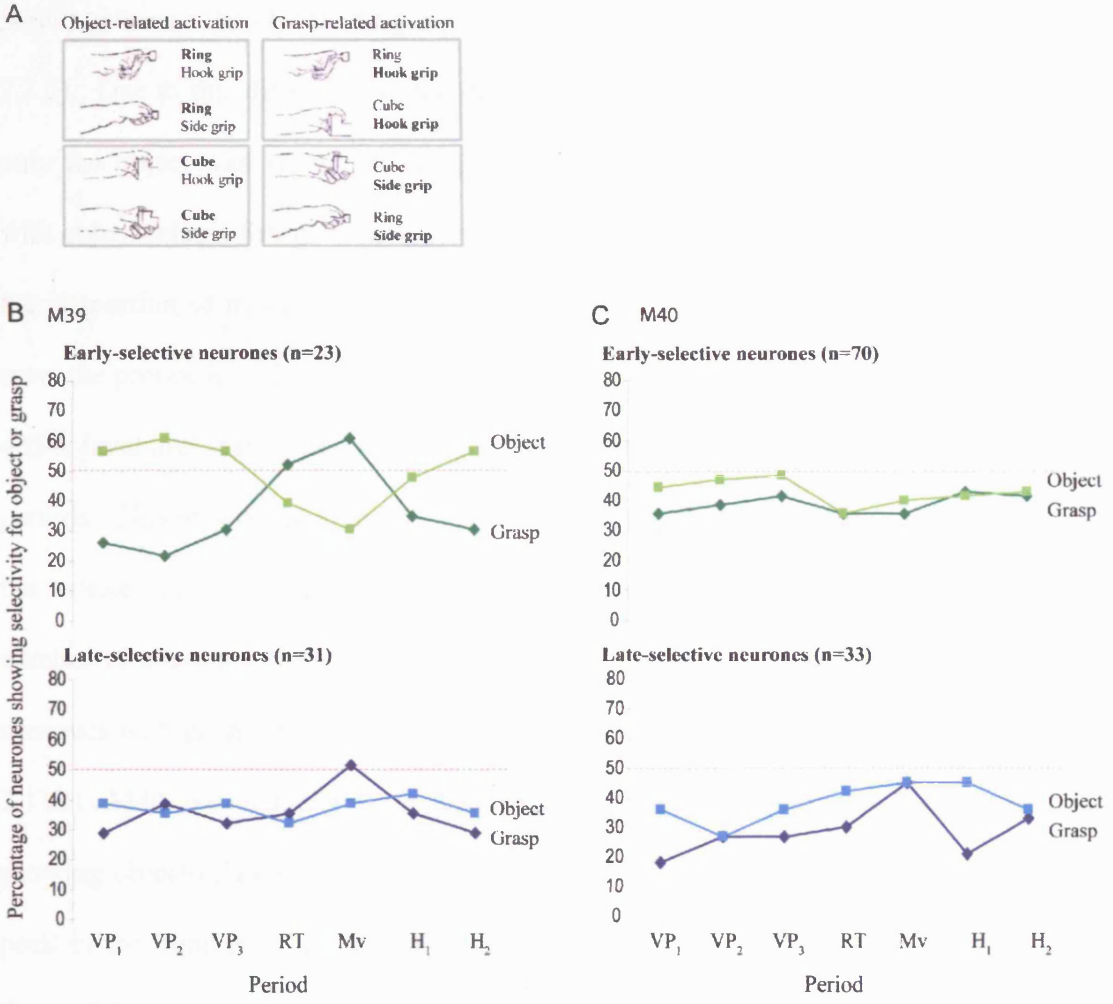

Figure 3.11 Ranked data showing object- and grasp-related firing in F5.

A, illustration of the object and grasp classification categories used for early- and late-selective neurones (see text for details). The numbers of neurones showing the highest firing rates for object (squares, light shading) or grasp (diamonds, dark shading) are plotted for the early (top, green) and late (bottom, blue) populations for each period for M39 (B) and M40 (C). During the first three visual presentation periods (VP_1, VP_2, VP_3) the monkey observed the object, the reaction time (RT) was the time from the 'go' cue to homepad release, movement time (Mv) the time taken to displace the object, and the hold period was divided into two equal portions (H_1, H_2). The red line indicates the 50% level. As there were three groupings for the ranked data (object-related, grasp-related and mixed coding), the number of neurones showing object- and grasp-related activity in a given epoch does not sum to 100%.

The pattern of object and grasp-related firing observed for M40 was unexpected. For M40 the type of grasp required was cued in the second half of the visual presentation period, whereas the object and grasp was cued in VP_1 for M39 (see Methods 1, Section 2.3.2). Due to this difference in the structure of the task it was expected that in VP_1, as only the object was known to M40, there would be increased proportion of neurones with object-related firing. Conversely in VP_3, after M40 was cued on the grasp required, the proportion of neurones with grasp-related firing would increase. This was not the case, the proportion of early-selective neurones with grasp-related firing remained at the ~35% level and that of object-related at ~45% throughout the three visual presentation periods. This may relate to the M40's performance of the task (see Section 3.3.1). M39, the monkey that did not make any incorrect grasps, had a systematic increase in the number of neurones with object-related firing during the observation of the object, and neurones with grasp-related activity that peaked in the Mv period (Table 3.2 and Figure 3.11B). M40, who made errors in grasp, had a slight increase in the number of neurones showing object-related activity during the object observation stages and no build-up or peak in the number of grasp-related neurones at any stage of the task (Table 3.2 and Figure 3.11C). So even though clear object- and grasp-related single unit activation was recorded in both M39 and M40 (Figure 3.8 and Figure 3.9, respectively) the population data showed a poorly differentiated temporal pattern in the number of neurones with object- and grasp-related firing from M40 (Table 3.2 and Figure 3.11). The importance of the task and behaviour of the animal to the temporal pattern of the population data in early- and late-selective F5 populations is considered in Section 3.4.1 of the Discussion.

3.3.5 Object- and grasp-related activity in the primary motor cortex

Single units were recorded from neurones in the primary motor cortex of one monkey (M39) of which some were identified as PTNs. For simplicity, neurones that were not identified as PTNs are termed M1 neurones. In total 140 single units were recorded in 25 sessions, of these 72 were PTNs and the remaining 68 M1 neurones. Of these, two PTNs and eight M1 neurones were excluded as there was either no main effect of period (ANOVA 1) or no main effect of object or grasp in any of the seven periods (ANOVA 2). For the remaining neurones, the average number of trials per object for the PTNs and M1 neurones were 51 and 63, respectively. Twenty-eight PTNs were classified as early-selective and 42 as late-selective, for the M1 neurones the respective number of neurones were 27 and 33.

The same proportions of early-selective neurones were present in M1 as previously observed from area F5. For M39, 43% of neurones were classified as early-selective F5 neurones, the equivalent percentages for M1 neurones and PTNs were 47% and 39%. However, for the early-selective M1 neurones the object- and grasp-related activity in the single unit histograms show a small increases in spike frequency that is difficult to discern by eye. Figure 3.12A is an example of an early-selective M1 neurone showing greater activation for the ring in VP_3 that was maintained during RT and Mv periods; the increased firing for object was subtle, especially when compared with that observed in F5 (Figure 3.8A). Therefore while the classification used for F5 and M1 activity was the same (based on ANOVA 2) the activity of the individual units was, visually, dramatically different. This was not due to the examples of units used to illustrate M1

activity, as the units shown are the best examples of early-selective object- and grasp-related activity.

Figure 3.12B shows a typical example of grasp-related firing from a M1 early-selective neurone. The increase in firing of the early-selective M1 neurone for the hook grip, although significant, was again not easily discernable, once more this is highlighted by comparison to the grasp-related modulation present in the early-selective F5 neurone (Figure 3.8B). In contrast the late-selective neurones showed definite peaks of firing during the movement phases. Figure 3.12C illustrates a late-selective neurone that showed increased firing for the ring during RT and Mv periods, regardless to whether a side or hook grip was used to grasp the object. Conversely, a clear peak of activity during RT and Mv periods when using a side grasp is shown by the late-selective neurone in Figure 3.12D.

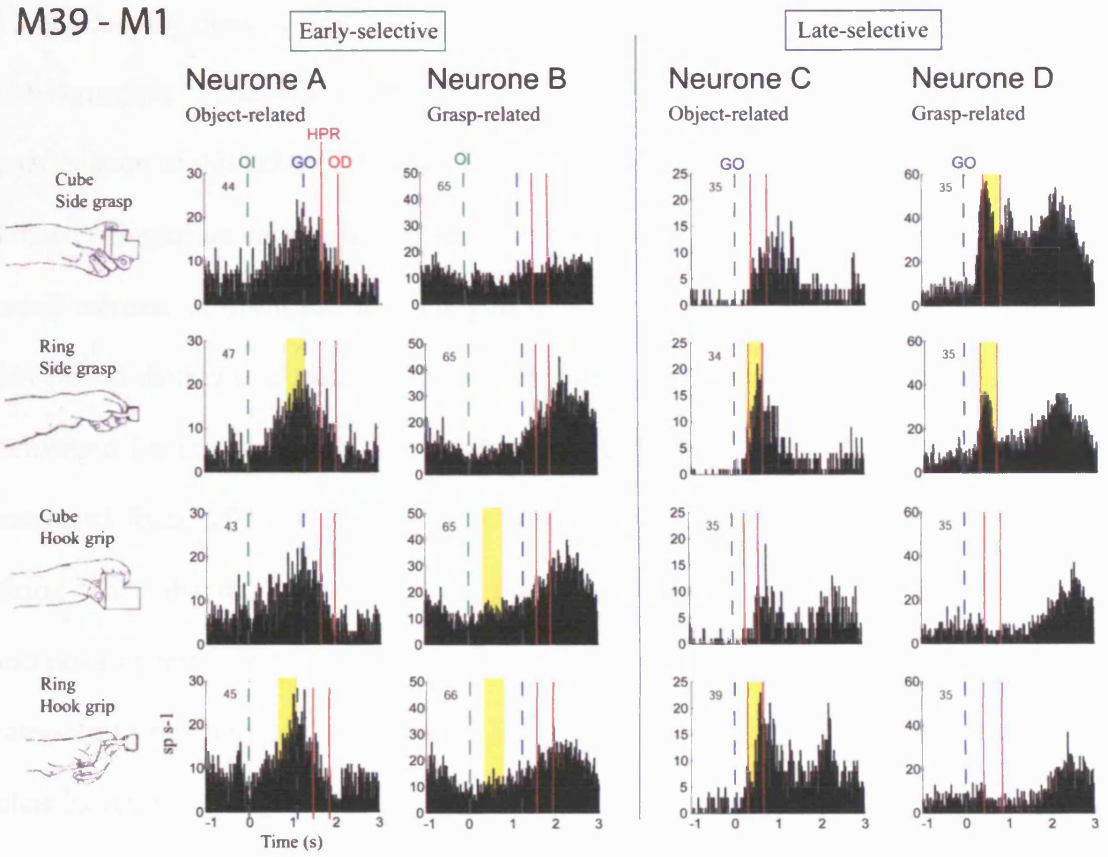

Figure 3.12 Examples of spike activity from M1early- and late-selective neurones, illustrating object- and grasp-related activation (M39).

Object-related (A) and grasp-related (B) activity from early-selective neurones is centred on the object illumination (OI), 0 s. The subsequent blue and red vertical lines indicate the average time of the GO signal, homepad release (HPR) and object displacement (OD). For the late-selective neurones object- and grasp-related activity (C and D, respectively) is centred on the GO signal (0 ms). The number of sweeps contributing to the spike activity is indicated on the top left hand corner of each histogram. Yellow bars indicate an epoch showing a significant main effect of object or grasp ($p \leq 0.05$).

PTNs recorded from M39 had a similar pattern of activation as observed from the M1 neurones. Early-selective neurones had increases in object- or grasp-related firing that were difficult to distinguish when looking at the spike histograms. Figure 3.13A illustrates increase in firing for the ring on object illumination by an early-selective neurone. Interestingly, in the 200 ms prior to object illumination there is excitation for

all object-grasp combinations, this corresponds to the time when the monkey is pressing the homepads. The significant effect of object present during VP_1 appears to be a continuation of this activity that then rises when the object presented is the ring. Grasp-related firing of an early-selective neurone is shown in Figure 3.13B. Here there was a small increase in firing for the hook grip in the first visual presentation period. In the Mv period there was a main effect for of both object and grasp, representing increased activation for the hook grip and for the ring. Once again for this neurone there was increased firing 200 ms prior to object illumination, suggesting this neurone is also firing when the monkey presses the homepads. Much like the M1 neurones, the increases in firing rate for the object- (Figure 3.13C) and grasp-related (Figure 3.13D) late-selective neurones is more marked than that for the early-selective neurones, with a clear increase in firing for the ring and hook grasp, respectively.

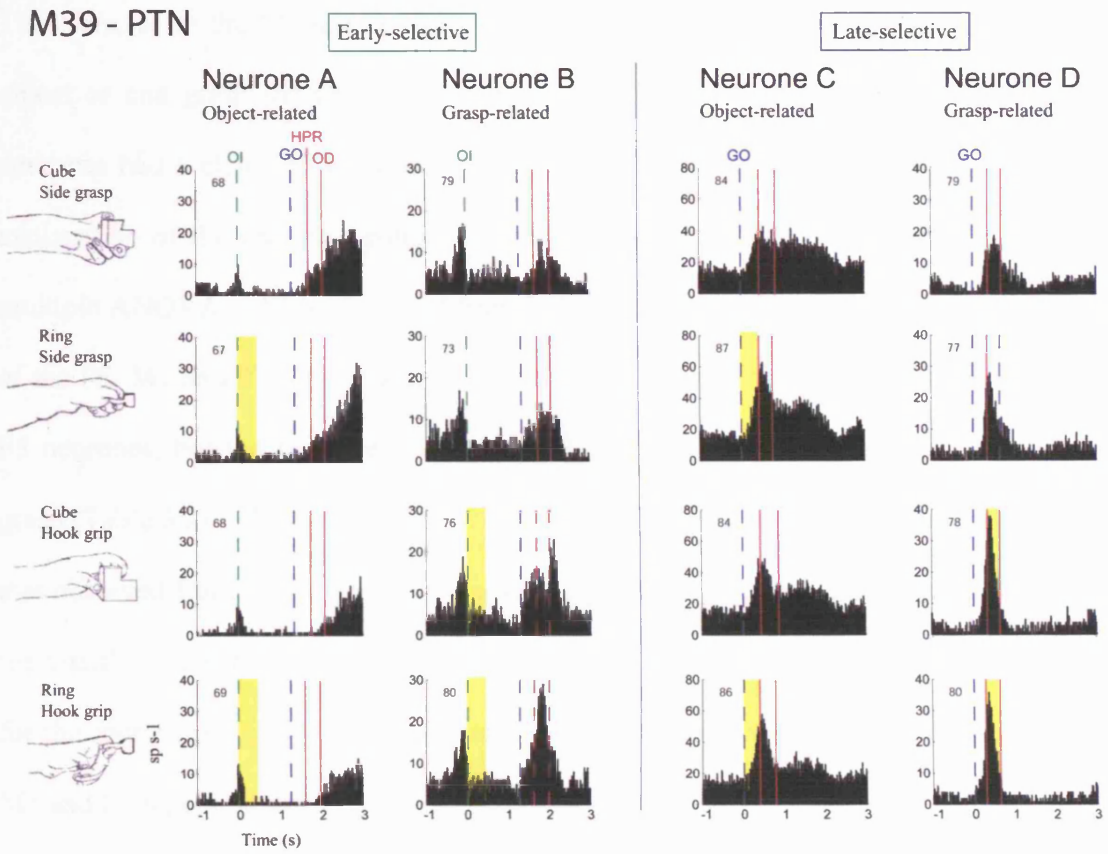

Figure 3.13 Examples of spike activity from early- and late-selective PTNs, illustrating object- and grasp-related activation (M39).

Object-related (A) and grasp-related (B) activity from early-selective neurones is centred on the object illumination (OI), 0 s. The subsequent blue and red vertical lines indicate the average time of the GO signal, homepad release (HPR) and object displacement (OD), respectively. For the late-selective neurones object- and grasp-related activity (C and D) is centred on the GO signal (0 ms). The number of sweeps contributing to the spike activity is indicated on the top left hand corner of each histogram. Yellow bars indicate an epoch showing a significant main effect of object or grasp ($p \leq 0.05$).

3.3.6 Temporal changes in population coding in M1

The proportion of neurones that showed a main effect of object or grasp (ANOVA 2) in only one period was 13/70 for PTNs and 13/60 for M1 neurones. The remaining neurones had a significant main effect of either object or grasp in more than one period, of these 4 PTNs and 7 M1 neurones showed a consistent effect for just object or grasp.

Therefore, as in the F5 data, a small proportion of neurones consistently fired for one object or one grasp throughout the trial. Rather, the majority of PTNs, F5 and M1 neurones had a changing preference for object and grasp as the trial progressed. One explanation of the changing pattern of encoding is familywise errors from performing multiple ANOVAs. However, as expected, the pattern of object and grasp main effects of the F5, M1 and PTN populations differed in the visual presentation phase with more F5 neurones, but not those recorded from M1, showing a main effect for object than grasp (Table 3.2). The average firing rate of the M1 and PTN populations was similar to that observed from F5 (Figure 3.14), with the greatest firing rate during movement. In the visual presentation periods, all three populations showed similar levels of activation for the four object-grasps. Whether there was an increase of grasp-related firing in the M1 and PTN populations was investigated using the ranked firing rate analysis.

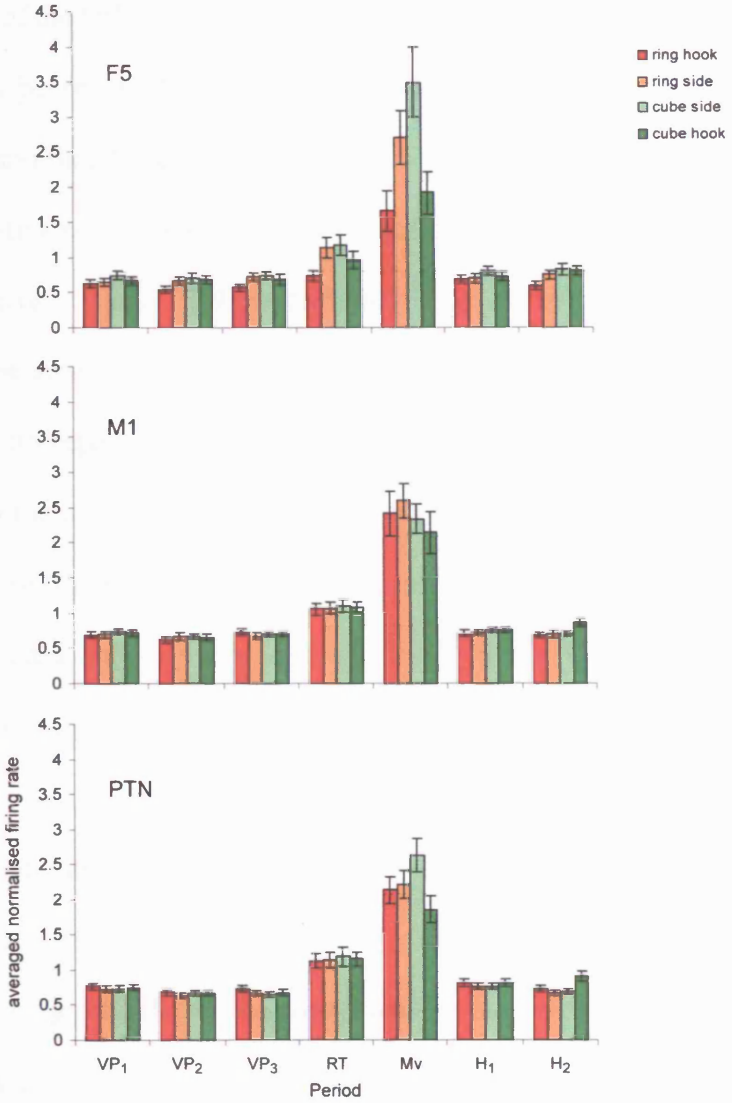

Figure 3.14 Averaged normalised firing rate of F5, PTN and M1 neurones recorded from M39.
The histograms show the average normalised firing rate (±SE). The firing rate for each object-grasp and period was normalised by the mean firing rate (across periods and object-grasps) for that neurone.

M1 and PTN firing was ranked into object-related, grasp-related (Figure 3.15A) and mixed categories (see Section 3.3.3). The number of early- and late-selective M1 neurones and PTNs with object-related activity (Figure 3.15B and C, respectively), was fairly constant across the seven period of the task and always below 50%. In contrast, over 50% of early-selective M1 neurones showed grasp-related firing during the reach-

to-grasp phase of the task. In VP_1, when the monkey first sees the object (and knows the grasp that will be required) approximately 50% of early-selective M1 neurones and PTNs had grasp-related activation. This early increase in the proportion of neurones showing grasp-related activation was not observed in F5 (Figure 3.11B), nor in the late-selective M1 neurones and PTN populations (Figure 3.15B and C, respectively). It is possible that the activation of these neurones reflect movements of the hand when first placed on the homepad. However, during the experiment no hand preshaping was observed when the monkey's hand rested on the homepads and visual inspection of the EMG activity confirmed there was no anticipatory activity in the 10 recorded muscles. Therefore neurones showing grasp-related firing during VP_1 are unlikely to reflect ongoing hand movements, but rather the upcoming grasp.

The number of late-selective M1 neurones showing grasp-related activity peaked during the RT and Mv periods (Figure 3.15B, dark blue trace) and there was also a rise in the number of grasp-related neurones from the late-selective PTNs (Figure 3.15C, dark blue trace), but this remained below the 50% level even during the Mv period. Overall, the ranked population data is consistent with PTN and M1 populations encoding grasp.

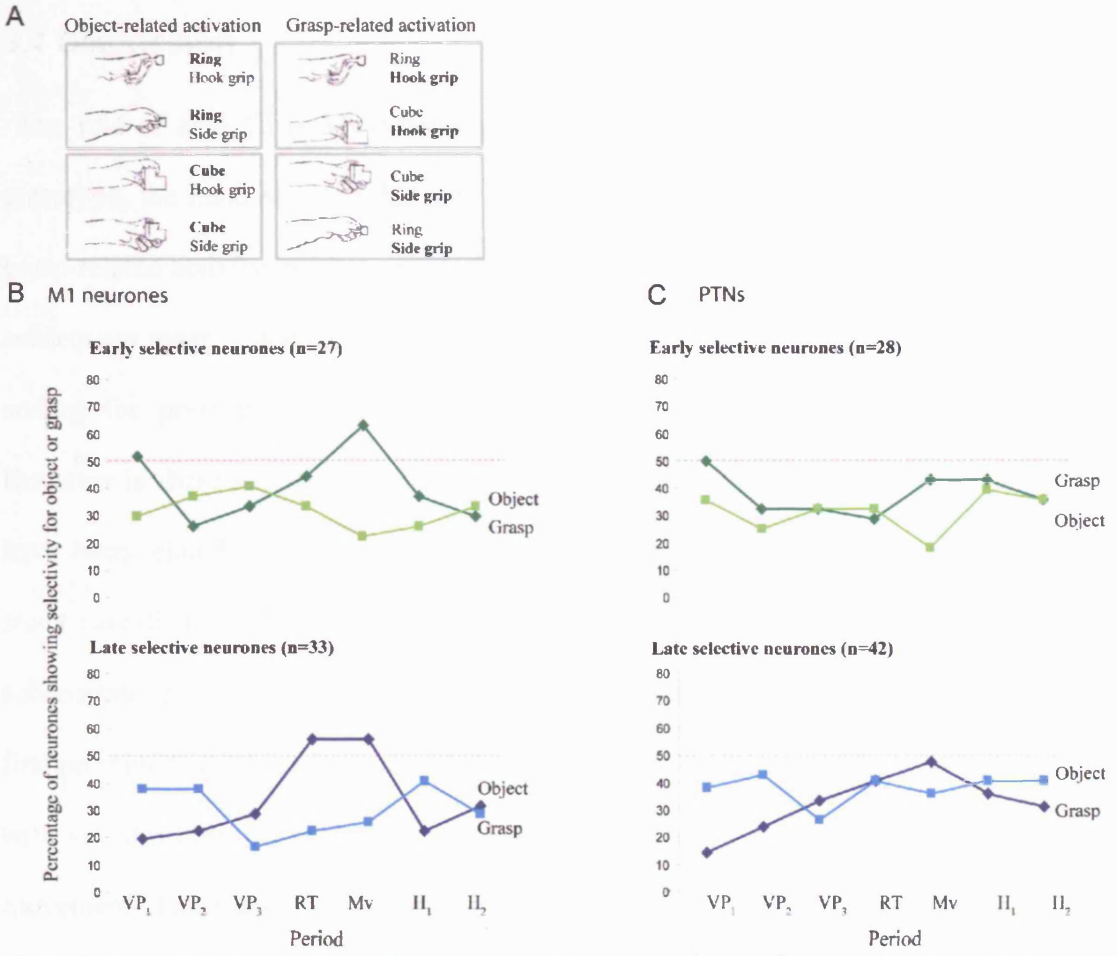

Figure 3.15 Ranked data showing object- and grasp-related firing in the primary motor cortex (M39). A, illustration of the object and grasp classification categories used for early- and late-selective neurones (see text for details). The numbers of neurones showing the highest firing rates for object (squares, light shading) or grasp (diamonds, dark shading) are plotted for the early (top, green) and late (bottom, blue) populations for each period for unidentified M1 neurones (B) and PTNs (C). During the first three visual presentation periods (VP_1, VP_2, VP_3) the monkey observed the object, the reaction time (RT) was the time from the 'go' cue to homepad release, movement time (Mv) the time taken to displace the object, and the hold period was divided into two equal portions (H_1, H_2). The red line indicates the 50% level. As there were three groupings for the ranked data (object-related, grasp-related and mixed coding), the number of neurones showing object- and grasp-related activity in a given epoch does not sum to 100%.

3.4 Discussion

The role of area F5 in visuomotor grasp has been described as encoding the motor prototype, the hand shape to be used for grasp (Jeannerod *et al.*, 1995). Findings of grasp-related activity in F5 neurones during the presentation phase of a task, even when subsequent grasp was not required (Murata *et al.*, 1997), has expanded the role of F5 to coding for potential action (Murata *et al.*, 1997; Rizzolatti and Luppino, 2001). However in these studies each object elicited a different grasp, therefore F5 firing may have been related to object presentation rather than the grasp prototype. The present study investigated whether F5 activation during object observation was related to the subsequent grasp or to the object itself. The results here suggest that when an object is first presented, a sub-population of F5 neurones, early-selective neurones, are concerned with visual processing of the physical properties of the objects rather than planning the movement. Later, after receiving the cue to initiate grasp and the subsequent movement phases of the trial, firing of both early- and late-selective neurones (the latter only fire during movement) corresponded to the required grasp, rather than object. In this way the coding of populations of neurones within F5 reflects the visuomotor transformation, with both object and grasp represented according to the demands of the task at that time. Behavioural performance affected this temporal relationship. The ranked F5 activity from a monkey that performed incorrect grasps showed object- and grasp-related firing that was poorly differentiated across observation and movement phases of the trial. In the primary motor cortex, activation of M1 neurones and PTNs was consistent with the representation of grasp during movement.

3.4.1 The relationship between F5 activity and task performance

There were clear differences in the temporal pattern of object- and grasp-related F5 activity from the two monkeys. For M39, during object observation the number of neurones with a main effect of object was greater than that with a main effect of grasp, whilst following homepad release more neurones showed a main effect for grasp (Table 3.2). In contrast, for M40, the number of neurones showing object and grasp activity was not differentiated over these periods (Table 3.2). A similar pattern emerged when the firing rates of the neurones were ranked. A clear task-related pattern in the proportion of neurones that were firing for object or grasp was observed for M39 but little modulation was present in the number of neurones recorded from M40 (Figure 3.11B and C, respectively). The low proportion of neurones with grasp-related activity during movement was not due to M40 using a similar pattern of grasps for the four object-grasp combinations. Both M39 and M40 had different EMG patterns for the side grips compared the hook grips that were particularly evident in the distance matrices (Figure 3.5 and Figure 3.6, respectively). In fact, while for M39 each of the four object-grasp combinations can be clearly observed in the distance matrix, for M40 the two hook grips were difficult to dissociate. Furthermore while the population data for the two monkeys differed, single units from both monkeys showed clear object- and grasp-related activity (Figure 3.8 and Figure 3.9, for M39 and M40 respectively).

The disparity in the population data from the two monkeys may reflect differences in the tasks or differences in behavioural performance. For M40 an LED was used to cue the required grasp, while a visual marker on the object was used for M39; the timing of

the visual presentation period had a variable duration of 1±0.8 s for M39, but was fixed at 1 s for M40; and the grasp was cued at the start of the visual presentation period for M39, but mid-way for M40. These differences prevent a clear comparison between the data collected from the two monkeys.

However, for two reasons it seems unlikely that these task differences resulted in the poor differentiation of object- and grasp-related activation from M40. Firstly, the cue informing M40 of the required grasp occurred midway through visual presentation. If this affected the number of neurones showing object- or grasp-related firing, then in VP_1 when the monkey only knew the object to be grasped, there should be more object-realted firing and VP_3 when the object and grasp required was known, there should be more grasp-related firing. However, the same proportion of neurones (less than 50%) with object- and grasp-related firing was observed for all three visual presentation periods (Figure 3.11). Secondly, as the visual presentation period for M40 was fixed (1 s) whilst that for M39 varied (1±0.8 s), there was a greater chance of M40 anticipating the 'go' signal, however only F5 activity recorded from M39 showed increasing grasp-related activity from period VP_3.

Difference in behaviour could account for the undifferentiated temporal pattern of the population data from M40. It is striking that monkey M39, that consistently used the correct grasp, had systematic task-related changes in the number of neurones showing object- and grasp-related neuronal activity, whereas the monkey that sometimes used the incorrect grasp (M40) had undifferentiated object- and grasp-related firing across the

seven periods of the trial. Changes in neuronal activity related to poor overall task performance have been reported for M1 local field potential recordings (Roux *et al.*, 2006). The importance of task performance to the quality of F5 activity recorded is also indicated in the present study.

3.4.2 Classification of F5 activity

Neuronal activity from M39 had a clear relationship to the different stages of the visuomotor grasping task; however the activity observed did not correspond to the traditional classification of F5 neurones. Previously F5 neurones have been divided into visuomotor and motor categories, according to whether or not they showed activation during visual fixation without subsequent grasp and if they fired during grasping in the dark (Murata *et al.*, 1997; Raos *et al.*, 2006). In the present study the terms visuomotor and motor neurones have been avoided, as the late-selective neurones, i.e. those which would have been called motor neurones (neurones showing activity only during the movement phases of the task) often had object-related activation. As the EMG activity during grasp shows a different pattern of muscle activation for the two grasps within object (Figure 3.5), object-related activity is more closely related to the visual input than the motor output.

Within the early- and late-selective populations, individual F5 neurones showed varying object- and grasp-related activity. Typically a single neurone did not have increased firing for just one object or one grasp, but showed a significant effect for object and grasp. Figure 3.8A illustrates a neurone that had increased firing for the cube

during the visual presentation period and increased firing for the side grip during the Mv period. Here the firing pattern reflects both object and grip according the task demands. At the population level a similar pattern emerges, with object-related activity during visual presentation and grasp-related activity on movement execution (Figure 3.11B). Thus, when more than one grasp is associated an object, the firing rate of F5 neurones reflects this more complex relationship between object and grasp.

3.4.3 The role of area F5 in the cortico-cortical visuomotor grasp circuit

These results expand our understanding of the role of F5 neurones in visuomotor grasp. Previously the separate roles of the three regions that comprise the cortico-cortical visuomotor grasp circuit has been emphasised, with AIP encoding object affordance, F5 hand shape and M1 execution of the grasp (Fagg and Arbib, 1998; Jeannerod *et al.*, 1995). In particular, the model proposed by Fagg and Arbib (1998) predicted that object distinction would no longer be present at F5; rather F5 selects a grasp and manages its execution (although other regions would also be involved in grasp execution, such as the dorsal premotor cortex (Davare *et al.*, 2006)). Yet, here the majority F5 neurones showed significant main effects of object and grasp, suggesting that the division between these areas may be more graded. It is possible that the object-related firing of the F5 neurones represents encoding of all the affordances for an object rather than visual physical properties of the object *per se*. The authors also hypothesised that when an object can be grasped in two ways F5 will correspond to both possibilities (Fagg and Arbib, 1998). If this is the case then the 'grasp-related' firing represents activation for a

particular grip and 'object-related' firing represents firing for all the grips that can be used to interact with that object.

Notably only when motor action was expected, or when hand shaping was being carried out, did the number of F5 neurones with grasp-related firing increase. During object presentation and the hold period there was a low level of neurones that had grasp-related firing. The number of neurones with object-related activity in the early-selective population decreased at these timings. It may be that the 'default' activity pattern of the F5 early-selective neurones is encoding object, only when grasp is required does the activity pattern of the population 'switch' to encoding grasp.

While object- and grasp-related firing was present in F5 neurones recorded in the present study, in a recent paper F5 neuronal firing has been suggested to reflect grip posture rather than object shape (Raos *et al.*, 2006). The authors approached the analysis of F5 coding by presenting the monkey with different shaped objects and the same object in different sizes or orientations. During object presentation, prior to grasp, cluster analysis of the discharge from visuomotor neurones showed high similarity between the large and small ring. The small sphere, cylinder in container, sphere in container were in the same cluster and the large sphere by itself. The authors argue the rings were differentiated, because, unlike the other objects, they do not require opposition of the thumb to be grasped. Similarly the separation of the large sphere was due to the thumb's role as a reinforcing agent for this object, compared to its role in the opposition grip for the other objects. The same division of clusters were present from

visuomotor neurones during movement and from F5 motor neurones, again suggestive of the firing in the presentation phase encoding grasp. For three reasons these results do not preclude the object-related firing seen here. Firstly, there were differences in the clustering of objects according to task. When the monkey was required to just fixate on the object there was clustering reflecting the object's shape: the two rings formed one cluster, the three spheres another cluster and the cylinder alone. These results fit well with our hypothesis that the visuomotor responses of F5 neurones depend upon the task demands. Secondly, comparison was between different shaped objects or differently sized objects of the same shape; so the visual input was not constant. AIP is strongly connected to F5 (Luppino *et al.*, 1999), AIP neurones show selectivity for the size and orientation of an object (Murata *et al.*, 2000), which may be reflected in F5. Indeed, Raos *et al.* (2006) show the discharge rate of F5 neurones can be modulated by changes in orientation. Whether these neurones are also modulated by object size was not directly tested. Finally, kinematic or muscle activity was not recorded so the changes in hand posture with object had not been quantified.

3.4.4 Object and grasp-related activity in the primary motor cortex

Early-selective neurones were recorded in the primary motor cortex in similar numbers to that found in F5. Comparing the data from F5 and M1, 43% of the task-related neurones in the ventral premotor cortex were classified as early-selective, 47% of M1 neurones and 39% of PTNs. However, while the proportion of early-selective neurones are the same, the temporal pattern of the population data and the spike histograms, clearly indicate differences between neurones recorded in F5 and M1. Even in the first

stage for the population analysis (Table 3.2) the greater number of neurones with a significant main effect for object in F5 during visual presentation can be clearly seen, whilst the numbers of neurones with main effect for grasp and object from M1 is similar. Notably for M1 neurones and PTNs, while individual neurones showed a significant main effect for object, in the population analysis the number of neurones that showed increased firing for object remained below 50% for all periods of the task (Figure 3.15B and C). Increases in grasp-related firing occurred in VP_1 in the early-selective PTN and M1 populations, but not for F5 neurones (compare Figure 3.15B and C to Figure 3.11B). This difference between the number of neurones with object- and grasp-related firing in the first visual presentation period may reflect F5 neurones encoding of object or the affordance of the object and M1 encoding the actual grasp required. As expected, the number of M1 neurones showing grasp-related firing also increased during the movement phases of the task (Figure 3.15B).

In another study using the same visuomotor task, F5 neurones showed greater differentiation of object-grasp during the visual presentation periods than M1 neurones or PTNs (Umilta *et al.*, 2007). Here the authors calculated the discharge rate for each object. The results from the present study suggest that the differentiation observed may reflect encoding of the object in F5; such encoding is present to a far lesser extent in the primary motor cortex, in agreement with Umilta *et al.* (2007). In the movement phases of the task the differentiation seen in both cortical regions would reflect grasp-related activity.

The early M1 and PTN object main effects in this study seem inconsistent with the motor output function of the primary motor cortex. However, similar findings have been reported previously. Delay period activity has been recorded prior to visuomotor reaching (Shen and Alexander, 1997) and in response to an LED signalling whether a handle was to be pulled or pushed (Tanji and Evarts, 1976). Visual responses have also been recorded in some studies of M1 (Wannier *et al.*, 1989). Alternatively, the classification of neurones used here may not have been appropriate to classify M1 neurones and PTNs. M1 has been described as encoding the vocabulary of movements, representing the individual movements forming the action, whilst F5 the vocabulary of actions (Rizzolatti and Fadiga, 1998). The firing of M1 may relate to movements being performed for the grasp at different times in the movement rather than the movement as a whole. In the present study there is evidence for such fragmentary encoding, with the early-selective PTNs (Figure 3.13A, B) showing a peak of activity when the monkey first presses the homepads.

3.4.5 Summary

The results suggest that there are two populations of F5 neurones, early- and late-selective, which are differentially modulated during the visual presentation phase of visuomotor grasp. Although neurones within both populations can show object-related activation, only the early-selective population had a large increase in the number of neurones with object-related activity during visual presentation. For both populations the number of neurones showing grasp-related firing increased with the approaching 'go' signal and peaked at movement onset. These results confirm the grasp-related coding of F5 neurones and expand the role of F5 neurones to include object-related activation. The results are compatible with visuomotor transformation for grasp occurring within area F5. Activity recorded from the primary motor cortex showed the number of neurones with grasp-related activation peak during the movement phase of the task, in keeping with the known role of M1 in movement execution.

4. Interactions between ventral premotor cortex and primary motor cortex outputs in macaque monkeys

4.1 Introduction

In Chapter 3, modulation of F5 spike activity was shown to be compatible with F5 neurones encoding both the presented object and the grip required during grasp. This Chapter, the second part of the study, examines how these representations within F5 are transformed into motor commands that allow M1 to shape the hand appropriately for grasp. Two aspects were considered. Firstly, the pathways by which F5 could influence M1 output. Secondly, whether F5-M1 interactions reflected muscle activity during visuomotor grasp.

Recently, intracortical microstimulation (ICMS) of F5 and M1 in anaesthetised and sedated macaques was used to investigate interactions between these two cortical areas (Cerri *et al.*, 2003; Shimazu *et al.*, 2004). A single test (T) stimulus delivered to M1 evoked direct (D) and indirect (I_1, I_2 and I_3) corticospinal volleys, which generated synchronised excitatory responses in hand motoneurones and muscles. Single conditioning (C) stimuli delivered to F5 rarely produced any detectable corticospinal output or overt motor responses. In contrast, when these same F5 stimuli were delivered with a test stimulus (C-T) the responses to M1 stimulation were markedly enhanced. Strong facilitation of the later I_2- and I_3-waves resulted in larger motor responses in motoneurones, particularly those supplying intrinsic hand muscles. This ICMS

technique provides a method for examining the influence of F5 input to M1 output during visuomotor grasp.

The first part of the present study aimed to replicate the C-T facilitation observed in the sedated and anesthetised monkey (Cerri *et al.*, 2003; Shimazu *et al.*, 2004) in two awake behaving animals performing a visuomotor grasping task. An object was presented visually to the monkey, and after a variable delay, the monkey was cued to reach, grasp, displace and hold the object (Section 2.3.2, Methods 1). During reach-to-grasp, single stimuli were delivered to areas F5 and M1 through chronically implanted microwire arrays (Sections 2.3.3, Methods 1). Motor responses were recorded from 4-10 EMG electrodes implanted in digit, hand and arm muscles. If the I-wave pathways mediate the F5 conditioning effect, then the peaks of facilitation should occur at intervals compatible with the inherent periodicity of corticospinal neurones to produce I-waves. This work had been published in abstract form (Prabhu *et al.*, 2005).

Secondly, if the C-T response represents transmission of visuomotor information required for visuomotor grasp, the F5 conditioning effect should vary with object or grasp. One monkey was trained to grasp a set of four objects, two of which, the ring and the cube, could be grasped with a hook or side grip, allowing object and grasp to be dissociated (Methods 1, Section 2.3.3). Lastly, if the ventral premotor cortex is involved in sending the grasp prototype to M1, then F5 conditioning would be expected to occur in muscles preferentially activated during a particular grasp. The EMG activity during hand shaping and hold for the different object-grasp combinations was examined to

investigate if muscles that showed C-T facilitation were more active during grasp than those muscles that did not show C-T facilitation.

4.2 Methods

The study was undertaken in two adult purpose-bred monkeys (*M. fascicularis*, case CS15; *M. mulatta*; case M39). For M39 cortical stimulation was from the right hemisphere and the monkey grasped the objects with the left hand, for CS15 cortical stimulation was from the left hemisphere and the monkey grasped the object with the right hand. Identification of hand representation regions in F5 and M1, surgical procedures and implants, the visuomotor grasping task and analysis of EMG activity during reach-to-grasp without cortical stimulation are described in Methods 1.

4.2.1 Cortical stimulation

To investigate the effect of F5 conditioning of a M1 stimulus, single monophasic stimuli (0.2 ms in duration, of 150-275 μA) were delivered to pairs of microwires in M1 and F5 from a Neurolog NL800 stimulus isolator. A test (T) stimulus to M1, conditioning (C) stimulus to F5, or combined conditioning-test stimuli (C-T) were delivered in an interleaved fashion to counteract any slow changes in excitability during the course of the recording session, with one stimulation condition (T, C or C-T) being delivered in a given trial. Stimuli were delivered at 25 ms, 50 ms, 100 ms and 150 ms (M39) or 100 ms (CS15) after homepad release. Examples of average EMG activity when grasping the disc (M39, 67 sweeps) and the cone (CS15, 215 sweeps) are shown in

Figure 4.1. In these averages the time of stimulation after homepad release used subsequently (50 ms, M39; 100 ms CS15) is shown by the red arrows. The intensity of M1 stimulation was selected so that when given alone, it evoked a clear EMG response in the test muscle on the majority of trials. For F5, the stimulus was just subthreshold for a motor response (see Section 4.3.2).

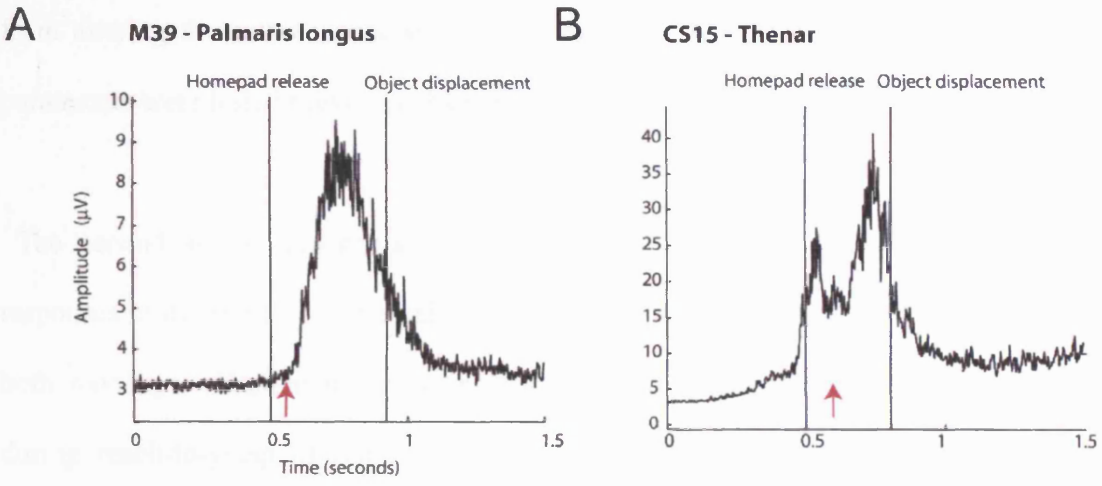

Figure 4.1 Muscle activity during reach and grasp of the disc and cone.
A, the average rectified EMG for palmaris longus during reach and grasp of the disc (M39, 67 sweeps) and (B) for thenar (CS15, 215 sweeps) during reach and grasp of the cone. The trials shown were without cortical stimulation, the time of stimulation used subsequently for M39 (50 ms after homepad release) and CS15 (100 ms after homepad release) is indicated by the red arrows.

EMG was monitored online with a custom-designed system which rectified and averaged the muscle activity during each stimulus type (F5 alone, M1 alone and M1 conditioned by F5); this allowed the correct thresholds to be set and the pairs of stimulating electrodes to be chosen. All subsequent analysis was performed with data rectified and averaged off-line.

4.2.2 Experimental outline

The first set of experiments examined the stimulation parameters (selection of electrodes in areas F5 and M1, current intensity and the time of stimulation from homepad release) that produced a C-T response greater or less than that evoked by a test stimulus to M1 alone (Section 4.3.2). Changes in the C, T and C-T evoked responses from altering these three parameters are detailed for M39; for CS15 the stimulation parameters were tested previously by G Cerri and H Shimazu (unpublished data).

The second set of experiments investigated F5 facilitation of M1 evoked EMG responses at different C-T intervals (Sections 4.3.3 to 4.3.7). Data are presented from both monkeys. Each monkey grasped one object. Data from CS15 were recorded during reach-to-grasp of the cone. M39 grasped the disc, as previously this had produced clear EMG activity for all 10 implanted muscles of the digits, hand and arm (Brochier *et al.*, 2004).

In the last experiment, M39 grasped one of four objects: a plate, disc, cube or ring. The last two objects could be grasped with either a hook or side grasp, to examine whether the C-T evoked response was modulated by either object or grasp (Section 4.3.8).

4.2.3 Location of microwires

Microwire location was verified by post-mortem histological analysis, using frozen sections cut in the sagital plane (Figure 4.2). The F5 microwire array was positioned in the inferior bank of the arcuate sulcus, just lateral to the arcuate spur. The tips of the

effective F5 cathodes were in laminae III and V, for CS15 and M39, respectively. In both animals M1 electrodes were located in the anterior bank of the central sulcus with the effective cathodes in laminae V and VI border for CS15 and M39, respectively. Nissl stained transverse sections through the precentral gyrus show the electrode tracts of the cathodes in M1 (Figure 2.6) and F5 (Figure 2.7).

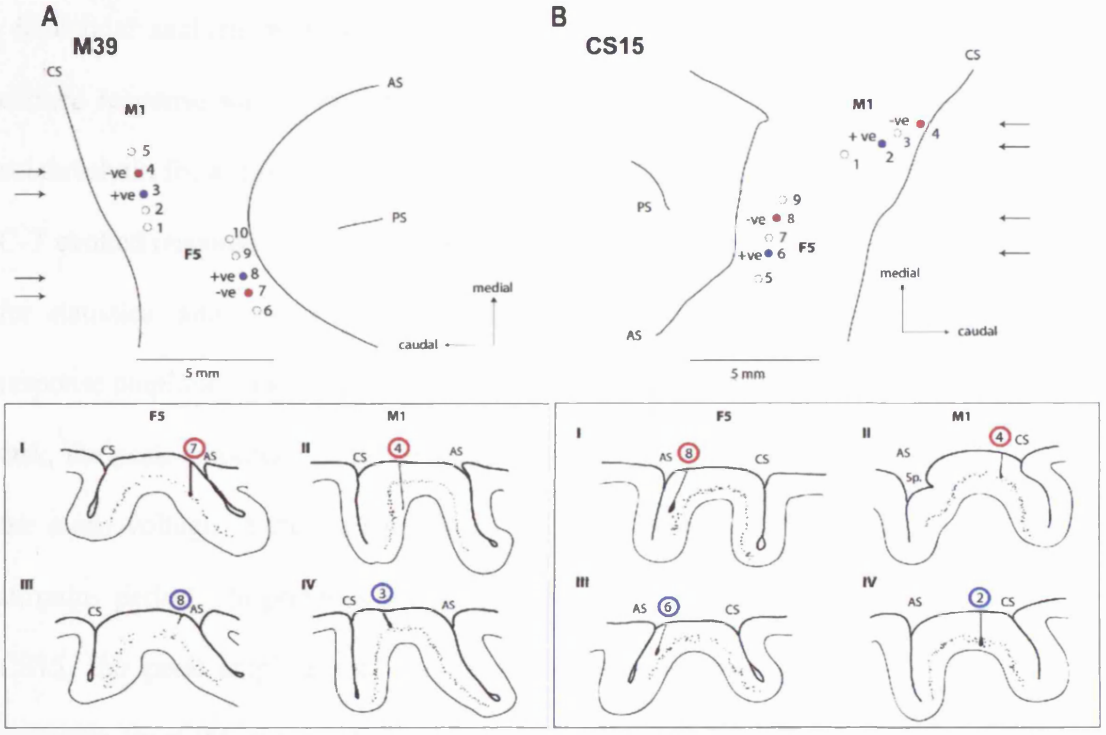

Figure 4.2 Locations of microwire implants in M39 (A) and CS15 (B).
Surface diagrams are shown in the upper section. The arcuate sulcus (AS), central sulcus (CS) and principal sulcus (PS) are shown. The cathode (red circle) and anode (blue circle) used for stimulation in M1 and F5 are indicated. Boxed drawings are of parasaggital histological sections indicating the position of the cathode (I and II, red) and anode (III and IV, blue) for these microwires in areas F5 (I and III) and M1 (II and IV) for M39 (left box) and CS15 (right box).

4.2.4 Analysis

EMG activity from each muscle was rectified and averaged with respect to stimulus delivery, according to stimulus condition (C, T, C-T), with averages comprising data from 25-121 trials per condition.

Statistical analysis was only undertaken if a facilitation or suppression of the C-T evoked response was visible on the average traces. As, by design, F5 stimulation was subthreshold for a motor response in the muscles that were analysed (Section 4.3.2), the C-T evoked response had to be visibly larger or smaller than that from M1 alone in order for statistical analysis to be performed. To control for the trial-by-trial variation in response amplitude and background EMG activity during the reach-to-grasp phase of the task, the peak amplitude of the response in each trial was normalised by dividing it by the mean voltage of the background EMG activity that was present in an 18 ms pre-stimulus period. In previous studies (Cerri *et al.*, 2003), and the data recorded from CS15, the peak amplitude of response for each trial was measured at the latency predicted from the average C-T response. For M39, the peak amplitude of responses recorded in each trial was measured in a 1 ms window centred on the latency predicted from the C-T average to allow for slight variations between the peak response for the C-T and T response (Figure 4.3).

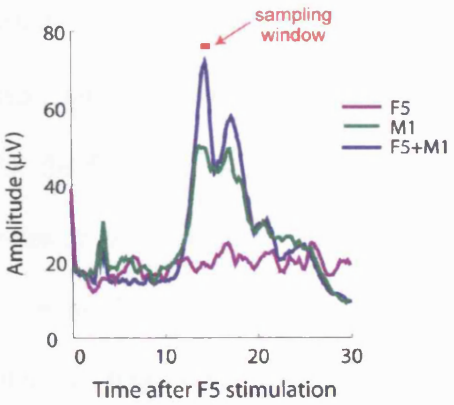

Figure 4.3 Sampling window for measuring the evoked response in the arm, hand and digit muscles to cortical stimulation (M39).

The response to the conditioning stimulus to F5 (magenta), the test stimulus to M1 (green) and the response to C-T (blue) stimulation at C-T= 3.5 ms recording in palmaris longus during reach-to-grasp of the disc. The horizontal red bar indicates the window in which the peak activity was calculated.

The modulation of the test M1 response by the conditioning F5 stimulus was measured for each C-T interval, by calculating the ratio of the normalised responses i.e. [conditioned (C+T) response/background]/[test stimulus (T) response/background]. A Kruskal-Wallis test was then performed for each muscle on the ratio of the normalised response from data pooled across session, with the factor of C-T interval or object. If this was significant Wilcoxon signed-rank tests were performed separately on each C-T interval or object comparing the T and C-T response in each session or data pooled across sessions.

For the second set of experiments, manipulating the C-T interval, statistical analysis was undertaken for AbPL, FDS and PL muscles. Statistical analysis was undertaken on FDS, even though no clear facilitation or suppression of the C-T response was visible, to compare changes in the C-T evoked response with those in AbPL and PL. The data

from CS15 had been collected previously and had 10% outliers removed. For the third experiment, the object-grasp study, evoked responses from AbPL, BrR, EDC, and PL muscles were analysed. For the final experiment, a Kruskal-Wallis test was performed for EDC, BrR and PL muscles on the ratio of the normalised response from data pooled across session, with the factor of object. If this was significant Wilcoxon signed-rank test were performed separately for each object comparing the T and C-T response pooled across sessions.

For all statistical tests the significance level was taken as $p \leq 0.05$, so a p-value of >0.05 was non-significant.

4.3 Results

4.3.1 rICMS effects and location of electrodes

The position of the microwire implants was guided by data from MRI scans (CS15 and M39) and single unit recordings (M39). Electrode positions were verified post mortem. For both monkeys, histological analysis revealed M1 electrodes were located in the anterior bank of the central sulcus and F5 electrodes in the inferior bank of the arcuate sulcus, just lateral to the arcuate spur (Figure 4.2). The laminae containing the electrode tips are documented in Table 4.1. Adjacent electrodes were separated by a horizontal distance of 1-1.3 mm and a vertical inter-electrode distance of 3 mm (see Figure 2.5, Methods 1), so the tips of adjacent electrodes were in different laminae.

Motor effects evoked from the implanted electrodes were tested using two different forms of repetitive (r) rICMS. First, movements were elicited by monopolar cathodal rICMS, and confirmed that the microwires were positioned in the hand representations of area F5 and M1. Cathodal stimulation produces prolonged intracortical activity by depolarising neurones in the superficial layers of the cortex which synapse onto PTNs; this transsynaptic effect is intensified by using rICMS, while anodal stimulation, which depolarises axons in the deep cortical layers, requires higher stimulation intensities to elicit excitation (Jankowska *et al.*, 1975; Lemon, 1984; Phillips and Porter, 1997; Ranck, 1981; Stoney *et al.*, 1968). Cathodal stimulation of M1 electrodes evoked movements of the arm, hand, digits or face (22-80 μA), regardless of the laminae in which the electrode tip was located (Table 4.1). Stimulation through adjacent electrodes always elicited different movements. In one instance when the electrodes tips were in the same

laminae, similar movements were elicited (electrodes 2 and 4 in laminae VI, inter-electrode distance approximately 2.3 mm, M39).

Table 4.1 Electrode location and movements elicited from monopolar rICMS stimulation (CS15 and M39)

	CS15 (M. fascicularis)			M39 (M. mulatta)		
	Electrode number	**Laminae**	**Effect of rICMS and threshold**	**Electrode number**	**Laminae**	**Effect of rICMS and threshold**
M1	1	III	Face mvt. (50 μA)	1	Not seen	Finger flex. (65 μA)
	2 •	V/VI	Finger flex. (80 μA)	2	VI	Thumb mvt. (22 μA)
	3	Upper V	Shoulder mvt. (80	3 •	III	Index abd. (50 μA)
	4 •	V	μA)	4 •	VI/WM	Thumb ext. (35 μA)
			Finger ext (80 μA)	5	V	Ulnar digit ext. (55 μA)
F5	5	III	Nil (80 μA)	6	II	Nil (125 μA)
	6 •	III	Elbow flex. (80 μA)	7 •	V	Thumb abd. (90 μA)
	7	II/III	Nil (80 μA)	8 •	II	Nil (125 μA)
	8 •	III	Thumb ext. (50 μA)	9	V	Wrist radial dev. (125 μA)
	9	Not seen	Nil (80 μA)	10	II/III	Nil (125 μA)

Circles indicate anode (•) and cathode (•) used for the subsequent studies in which bipolar stimulation was used; abd.=abduction, dev=deviation, ext.=extension, flex.=flexion, mvt.=movement, WM=white matter.

For the electrodes in F5, only those with their tips located in laminae III and V produced movements of the thumb, hand and arm (Table 4.1). Furthermore, the intensities required to elicit movements were on average higher for F5 than M1 (86±31 and 58±21 (SD) μA, respectively). This result is compatible with previous findings of fewer responses and higher intensities required to elicit motor responses from F5 (Cerri *et al.*, 2003; Godschalk *et al.*, 1995; Umilta *et al.*, 2007; Weinrich and Wise, 1982), although with only 4-5 penetrations in each cortical region the sample is very small.

It is clear that the current thresholds for rICMS for chronically implanted electrodes (22-80 μA in M1 and 50-125 μA in F5) are much higher than would be expected for sharp electrodes introduced acutely through the dura (typically 5-20 μA for M1 and 20-

40 μA for F5, R. Lemon unpublished observations). This was probably due to a number of factors, including low electrode impedance and gliosis and other tissue changes around the electrode tips.

We also tested rICMS using bipolar stimulation delivered to pairs of M1 and F5 electrodes. The bipolar electrode configuration, although having more complex stimulation effects than monopolar stimulation, results in the least amount of current spread (Lemon, 1984). Additionally, while both monopolar and bipolar stimulation activate CM cells indirectly, via the I-wave pathways, bipolar stimulation is thought to produce a more focal, direct activation of PTNs then monopolar stimulation (Jankowska *et al.*, 1975; Lemon *et al.*, 1987; Maier *et al.*, 2002; Porter and Lemon, 1993). Furthermore, by using monophasic stimulation, the relative effects of cathodal versus anodal stimulation through a given electrode could be identified. This can be observed in the effects from M1 stimulation presented in Table 4.2 bipolar rICMS produced different movements by changing the cathode whilst keeping the anode constant, but the opposite configuration, changing the anode whilst keeping the cathode the same, generally had little effect.

Table 4.2 Movements elicited from rICMS bipolar monophasic stimulation of M1 (M39).

Date	Electrodes	Effect of rICMS and threshold
29/10/03	2(-ve), 3(+ve)	Thumb flexion/abduction 30 μA
	1(-ve), 3(+ve)	Finger extension 60 μA
	4(-ve), 3(+ve) •	Radial deviation of the wrist 40 μA
	5(-ve), 3(+ve)	Wrist extension 40 μA
26/02/04	4(-ve), 2(+ve)	Wrist extension 60 μA
	4(-ve), 1(+ve)	Wrist extension 80 μA
	2(-ve), 1(+ve)	Finger flexion 150 μA

The polarity of electrodes tested in parenthesis (-ve/+ve), • indicates electrode combination used in the subsequent studies.

Single bipolar monopolar stimulation was used for all the F5-M1 interaction studies described below.

4.3.2 Selection of electrodes, stimulation intensity and the timing of stimulation.

There were five factors that could affect the amplitude of the F5 conditioned response evoked by M1 stimulation. Firstly, the location of the anode and cathode electrode pair used in area F5 and M1. Secondly, the current intensity used; the stimulus intensity to M1 should be such as to produce a clear evoked response that was sub-maximal, to allow any facilitatory or suppression effect of F5 conditioning to be observed. Ideally, F5 stimulation would be sub-threshold for any motor response, so that any facilitation or suppression induced by the conditioning (C) stimulus could be attributed entirely to the M1 test (T) response rather than the algebraic sum of the C and T evoked response. Thirdly, the responses being monitored do not necessarily have the same thresholds in different muscles; that is a stimulus that is subthreshold for one muscle can be suprathreshold in another. Fourthly, the level of ongoing EMG affects the amplitude of the response to cortical stimulation (Bennett and Lemon, 1994; Devanne *et al.*, 1997; Kischka *et al.*, 1993). Ongoing EMG is often required to reveal an evoked response from cortical stimulation (Cerri *et al.*, 2003; Shimazu *et al.*, 2004). However, a high and variable level of ongoing EMG increases the variability and magnitude of the evoked response from cortical stimulation, making it difficult to identify evoked responses as opposed to spontaneous activity. Therefore a constant low-level pre-stimulus EMG is preferable. Experimental variables relating to the EMG level are the time of stimulation

after homepad release and the object to be grasped. The final factor is the C-T interval. In lightly sedated and anesthetised macaque monkeys, a significant facilitatory C-T response was only observed at specific C-T intervals that were multiples of the I-wave interval (~1.2 ms) (Cerri *et al.*, 2003; Shimazu *et al.*, 2004).

The approach used was first to select suitable electrode combinations and stimulation intensities and times. Then, once these parameters had been set, the central questions of this Chapter, as to whether the F5-M1 evoked response was modulated by the C-T interval and the upcoming grasp were investigated.

In eight sessions (M39) different electrode combinations, stimulation intensities and times of stimulation were tested during reach-to-grasp of the disc. The short centre electrode was selected for the M1 and F5 anode (electrode 3 and 8, respectively) so there would be minimal current spread for all cathode combinations. A superficially positioned anode and a deep cathode had an additional advantage for M1 stimulation, as this has been found to be the most effective configuration for directly stimulating corticospinal neurones (Maier *et al.*, 2002). Finally, for the first few sessions, a C-T interval of 0 ms was used as this was known to be effective in producing a facilitatory C-T response (Cerri *et al.*, 2003; Shimazu *et al.*, 2004). The effects of C, T and C-T stimulation was assessed by visual inspection of the evoked response; unless a clear consistent conditioning response was evident, no statistical analysis was undertaken.

Table 4.3 summarises the C, T and C-T evoked responses elicited using various electrode combinations, stimulation intensities, C-T intervals and stimulation times after homepad release. The large number of variables meant it was difficult to repeat the same set of parameters often. In the first three sessions the effect of stimulation intensity delivered to different M1 electrodes (1, 2, 4 and 5) was investigated, using stimulus intensities of 100-200 μA. The timing of stimulation was initially fixed at 100 ms after homepad release. There was a clear evoked response from a 100 μA test stimulus delivered to electrode 4 for all muscles, while responses from electrodes 1, 2 and 5 were at threshold. Subsequently, when the M1 stimulation intensity was increased to 200 μA, electrode 2 produced clear test responses in all muscles. For the later experiments, examining the effect of C-T interval and object-grasp combinations, the C-T evoked response was investigated using M1 4(-ve) 3(+ve) electrode pairing, which showed the lowest threshold for eliciting a test response (100 μA).

The evoked response to F5 stimulation was more variable than that observed from M1 stimulation. F5 stimulation through electrode 7 elicited an evoked response in two muscles during session seven, but only one muscle in session eight even though all other parameters were held constant (Table 4.3). Within session seven stimulation using electrode 9 elicited a response from four muscles at 175 μA, but only two muscles when the intensity was 150 or 200 μA. Notably, unlike the response from M1 that produced either a threshold or suprathreshold response in all the recorded muscles, the F5 stimulus only evoked a response in a sub-set of muscles.

The effects of combined F5-M1 stimulation produced both facilitation and suppression of the M1 evoked response (Table 4.3). The F5 conditioning of the M1 stimulus evoked from electrode 9 was not consistent across sessions. In session six, 50 ms after homepad release, AbPL, EDC and BrR muscles all had facilitatory effects but in session seven the C-T responses were no longer facilitated. This inconsistency may have been due to the stimulation intensity chosen for this pairing or the position of the electrodes. For the subsequent studies electrode 7 was used as the F5 cathode using a stimulus intensity of 200 μA to produce a more consistent response.

Table 4.3 The effect of different cathodes, stimulation intensities, ISIs and times from homepad release in the evoked responses from cortical stimulation in 10 arm, hand and digit muscles (M39).

Session (trials per condition)	Electrode (stimulation intensity)		Time from homepad release	C-T interval	Evoked response		
	M1	F5			Test stimulus to M1	Conditioning stimulus to F5	Condition-Test stimuli to M1-F5
1	4 (100 μA)	6 (100 μA)	100 ms	0 ms	Suprathreshold	Nil	Nil
(n=150)	4 (100 μA)	10 (100 μA)	100 ms	0 ms	Suprathreshold	Nil	Nil
2	2 (100 μA)	10 (100 μA)	100 ms	0 ms	Threshold	Nil	Nil
(n=50)	1 (150 μA)	10 (100 μA)	100 ms	0 ms	Threshold	Nil	Nil
	5 (150 μA)	10 (100 μA)	100 ms	0 ms	Threshold	Nil	Nil
3	2 (200 μA)	7 (200 μA)	100 ms	0 ms	Suprathreshold	All muscles, except FDP.	Fac: FDP.
(n=30)							
4	4 (100 μA)	7 (150 μA)	100 ms	0 ms	Suprathreshold	Nil	Nil
(n=25)	4 (100 μA)	7 (175 μA)	100 ms	0 ms	Suprathreshold	Nil	Nil
	4 (100 μA)	7 (175 μA)	100 ms	3.5 ms	Suprathreshold	Nil	Nil
	4 (100 μA)	9 (175 μA)	100 ms	3.5 ms	Suprathreshold	Nil	Nil
5	4 (150 μA)	9 (175 μA)	100 ms	3.5 ms	Suprathreshold	Nil	Nil.
(n=86-109)	4 (125 μA)	9 (200 μA)	100 ms	3.5 ms	Suprathreshold	Nil	Sup: AbPL, Th, PL, FDP.
	4 (150 μA)	9 (175 μA)	100 ms	0 ms	Suprathreshold	Nil	Nil.
	4 (150 μA)	9 (175 μA)	100 ms	1 ms	Suprathreshold	Nil	Fac: ED 4,5, BrR.
	4 (150 μA)	9 (175 μA)	100 ms	2 ms	Suprathreshold	Nil	Sup: AbPL, EDC, PL, BrR.
6	4 (150 μA)	9 (175 μA)	50 ms	3.5 ms	Suprathreshold	Nil	Fac: AbPL, EDC, PL, BrR.
(n=31)	4 (150 μA)	9 (175 μA)	50 ms	0 ms	Suprathreshold	Nil	Fac: AbPL, PL, BrR.
	4 (150 μA)	9 (175 μA)	25 ms	3.5 ms	Suprathreshold	Nil	Fac: PL.
7	4 (150 μA)	9 (175 μA)	50 ms	3.5 ms	Suprathreshold	FDP, ED45, BrR, AD.	Nil.
(n=90)	4 (150 μA)	7 (175 μA)	50 ms	3.5 ms	Suprathreshold	ED45, BrR.	Fac: PL, BrR.
	4 (150 μA)	6 (175 μA)	50 ms	3.5 ms	Suprathreshold	Nil.	Fac: ED 4,5; Sup: AbPL, PL.
	4 (150 μA)	9 (200 μA)	50 ms	3.5 ms	Suprathreshold	ED45.	Fac: PL, BrR.
	4 (150 μA)	9 (150 μA)	50 ms	3.5 ms	Suprathreshold	ED45.	
8	4 (150 μA)	7 (175 μA)	50 ms	3.5 ms	Suprathreshold	BrR	Fac: EDC; Sup: AbPL.
(n=30)	4 (150 μA)	7 (150 μA)	50 ms	3.5 ms	Suprathreshold	Nil.	Nil.
	4 (150 μA)	7 (200 μA)	50 ms	3.5 ms	Suprathreshold	BrR	Fac: AbPL, PL.

Data from eight sessions recorded over 13 days. Electrode 3 and 8 were the M1 and F5 anode, respectively. Muscles recorded: abductor digiti minimi (ADM), abductor pollicis longus (AbPL), anterior deltoid (AD), brachioradialis (BrR), extensor digitorum communis (EDC), extensor digitorum 4,5 (ED 4,5), flexor carpi ulnaris (FCU), flexor digitorum profundus (FDP), flexor digitorum superficialis (FDS) and palmaris longus (PL). For M1 stimulation all muscles showed either suprathreshold or threshold responses according to the parameters used. Compared to test (T) responses, conditioned (C-T) responses showed either facilitation (Fac) or suppression (Sup).

The electrode pairing chosen for the subsequent experiments was, for M39, electrodes 4(-ve) 3(+ve) in M1, and 7(-ve) 8(+ve) for F5. When tested with rICMS these pairs produced radial deviation of the wrist (40 μA) and thumb abduction (90 μA), respectively.

For CS15 the bipolar pairing used was 4(-ve), 2(+ve) in M1, which produced extension of the digits (threshold 80 μA), and for F5, 8(-ve), 6(+ve) producing extension of the thumb (threshold 50 μA); only this F5-M1 pairing produced clear C-T facilitation and suppression.

In both animals the tip of the effective M1 electrode was in lamina V or VI. In F5 the cathode was in lamina III or V. Electrodes in these laminae were previously shown to be effective in producing C-T facilitation anaesthetised and lightly sedated animals (Cerri *et al.*, 2003; Shimazu *et al.*, 2004). In the current experiment, in the awake behaving monkey, stimulation was at either 50 ms after homepad release (M39) or 100 ms (CS15).

4.3.3 Facilitation by F5 stimulation of EMG responses evoked from M1

Figure 4.4 illustrates F5 facilitation of M1 evoked EMG responses in the two monkeys when grasping the disc (M39) and the cone (CS15). The difference in the amplitude of the response in the three stimulus conditions is evident in single sweeps of rectified EMG responses from PL in M39 (Figure 4.4A). F5 stimulation (single 200 μA shock), given alone, evoked no consistent responses (Figure 4.4A, top graph). M1 stimulation

alone (single 150 μA shock) evoked clear responses at a latency of 8 ms of variable amplitude on some trials (Figure 4.4A, middle graph). When both stimuli were given together (C-T=0 ms), larger more consistent responses were evoked (Figure 4.4A, last graph). The conduction time from the ventral premotor cortex to M1 is short, 1-4 ms, (Ghosh and Porter, 1988; Godschalk *et al.*, 1984; Tokuno and Nambu, 2000). In a previous study, the evoked response observed in the thenar motoneurones was compatible with discharge after the arrival of the I_2 wave (Cerri *et al.*, 2003). With a C-T interval of 0 ms, this would give enough time (at least 2 ms) in which F5 stimulation could facilitate the interneuronal circuits that generate the late I-waves when using simultaneous F5-M1 stimulation. The averaged responses in Figure 4.4B, from three different sessions in M39, confirm that while F5 alone produced no effect, when it conditioned the M1 stimulus, the amplitude of the response was significantly enhanced (arrows). Wilcoxon signed-ranks test showed significance ($p<0.05$) for all the facilitatory responses shown (asterisks in Figure 4.4B). The average facilitation was calculated by dividing the F5-M1 conditioned response by the test response evoked from M1 stimulation alone, therefore a value of one indicates no effect, whilst a value of greater than one indicated facilitation and a value of less than one suppression. For M39, the average facilitation (± SE) of the M1 evoked response in PL by F5 conditioning at C-T=0 ms was 2.31 ± 0.17 (n=105 sweeps per condition, recorded in three sessions over an eight day period, 10% outliers removed); therefore on average F5 conditioning more than doubled the response to the M1 test stimulus, with no evoked response from F5 stimulation alone. AbPL also showed no effect for F5 stimulation alone but a F5 conditioning effect (Figure 4.4C), the average facilitation at C-T=0 ms

was 1.96 ± 0.17 (n=105 sweeps per condition), that is close to double the response of that by M1 stimulation alone.

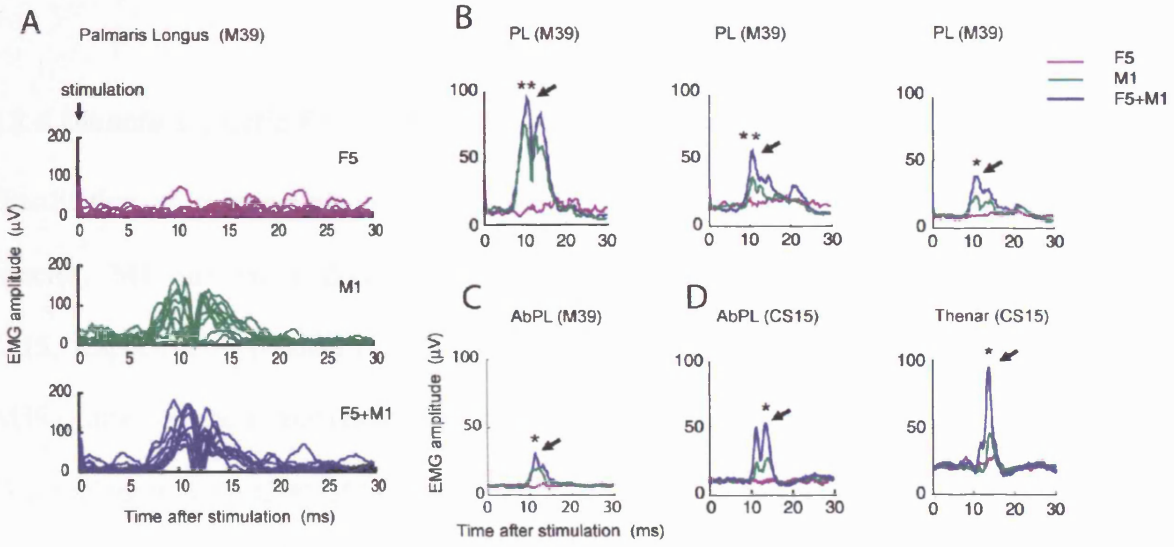

Figure 4.4 Rectified EMG evoked responses from the three stimulation conditions during reach-to-grasp. A, shows 10 single superimposed sweeps for each condition: F5 conditioning (200 μA), magenta; M1 test (150 μA), green; and F5+M1 (C-T) blue, from palmaris longus (PL) in M39. B, the average EMG response in PL (M39) on 3 subsequent days (25, 40, 40 sweeps per condition respectively). C, the response from abductor pollicis longus (AbPL) in M39 (40 sweeps per condition). D, the response from AbPL and thenar in CS15 (25-30 sweeps per condition). The F5 and M1 stimuli were 110 μA and 180 μA, respectively. Arrows indicate significant facilitatory peaks. For all graphs and all conditions stimulation was at time zero, C-T=0 ms. For M39, stimulation was 50 ms after homepad release during reach-to-grasp for the disc, for CS15, at 100 ms for the cone. Wilcoxon signed-rank,*=$p<0.05$, **=<0.01. All figures are with 10% outliers removed.

Figure 4.4D show similar facilitatory effects in AbPL and thenar muscles in the second monkey (CS15). Single shocks of 180-200 μA were used for M1 and 100-150 μA for F5 stimulation. The average facilitation (±SE) of the M1 evoked response in AbPL by F5 conditioning at C-T=0 ms was 3.25 ± 0.39 (n=121 sweeps per condition from two sessions over two days, 10% of outliers removed). For thenar EMG, the average

facilitation at C-T=0 ms was 2.07 ± 0.17 (n=95 sweeps per condition from two sessions).

4.3.4 Muscle specific F5 conditioning effects

Facilitation or suppression by F5 conditioning was confined to responses in a few muscles. M1 stimulation alone at the intensities used (150 μA and 180 μA, M39 and CS15, respectively) produced an evoked response in every muscle apart from FCU (M39), although the responses in FDP, FDS and ADM recorded from M39 were small. F5 stimulation alone (200 μA) produced a response in the extensors EDC, ED 4, 5 and BrR in M39 (Figure 4.5) but was sub-threshold for all other muscles in M39 and for all four muscles in CS15. F5 stimulation was at threshold for certain muscles, but for others the stimulation intensity was slightly above threshold producing an evoked response in most sessions for BrR and ED 4,5 (M39). Therefore with the stimulation parameters used here, evoked responses from these muscles were not further analysed. In the only proximal muscle recorded, the anterior deltoid (M39), there was suppression of the EMG activity from a test stimulus, no effect from stimulation to F5 alone, and the C-T response was the same as that evoked from the T stimulus. F5 is thought to have a much larger representation of the distal rather than the proximal muscles (Rizzolatti *et al.*, 1988). The lack of a conditioning effect from the F5 stimulus supports this hypothesis.

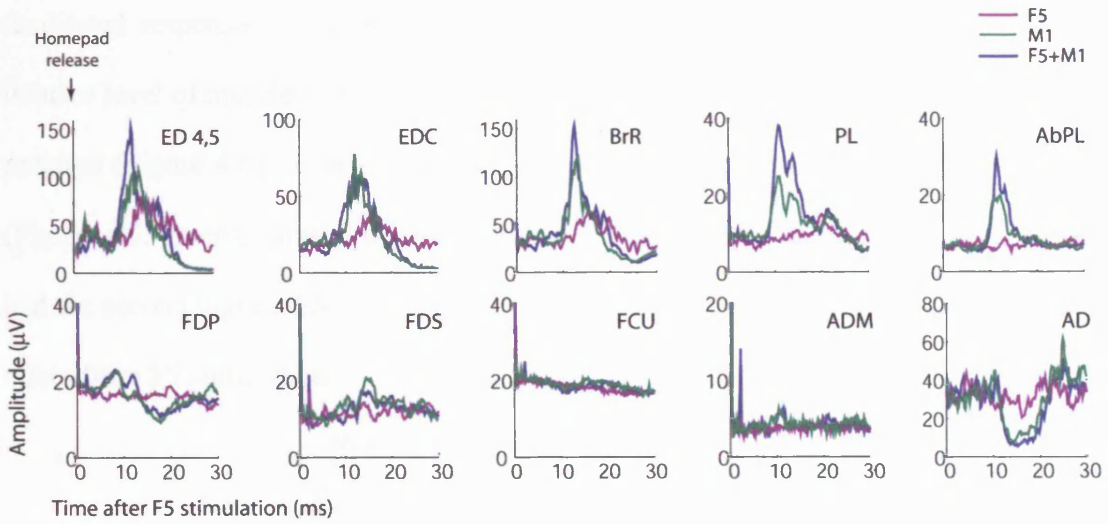

Figure 4.5 Different effects of F5 and M1 stimulation in simultaneously recorded muscles (M39).
The effects of the stimulation paradigms in the 10 muscles: extensor digitorum 4,5 (ED 4,5), extensor digitorum communis (EDC), brachioradialis (BrR), palmaris longus (PL), abductor pollicis longus (AbPL), flexor digitorum profundus (FDP), flexor digitorum superficialis (FDS), flexor carpi ulnaris (FCU), abductor digiti minimi (ADM) and anterior deltoid (AD). Data shown is from 40 trials per stimulus condition (10% outliers having been removed) in one session at C-T 0=ms, stimulation was 50 ms after homepad release. The effect of F5 stimulation (200 μA) is shown in the magenta trace, M1 stimulation (150 μA) in green and F5+M1 in blue.

4.3.5. Selectivity of task-related EMG activity

The polar plots in Figure 4.6 illustrate the muscle activity at the time of F5 stimulation (green trace, average EMG in a 41-126 ms window after homepad release) and at hand shaping (blue trace, average in EMG 294-379 ms window after homepad release). The activity was normalised to the peak EMG activity across objects and trial duration, within each muscle; so allowed comparison of relative EMG levels across muscles (see Section 2.6.2, Methods 1). At the time of cortical stimulation the muscles which showed C-T facilitation or a response to a C stimulus when given alone, are not necessarily those with the greatest EMG activity. In fact AbPL and BrR, which showed both a C-T

facilitated response and a response to F5 alone (Figure 4.5, green), had the lowest relative level of muscle activation at the time of C-T stimulation when comparing the 10 muscles (Figure 4.6). Conversely, AD, which had the highest EMG level at this time (Figure 4.5, green), showed suppression from the T stimulus (Figure 4.6). FDP which had the second highest EMG activity during F5 stimulation also showed no conditioning effect from F5 stimulation.

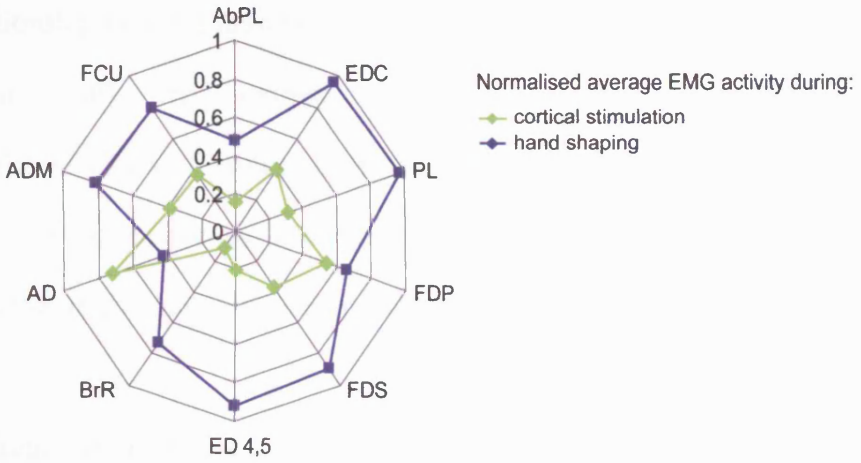

Figure 4.6 Polar plots of normalised muscle activity during reach and grasp of the disc (M39).
Average EMG activity at the time of cortical stimulation (green, epochs 2-4) and during hand shaping (blue, epochs 7-9) is illustrated from one session (180 trials). To assess the EMG levels, no stimulation was given during these trials and to compare EMG activity across muscles EMG activity was normalised within muscles. See Section 2.6.2, Methods 1 for details. Key: abductor pollicis longus (AbPL), extensor digitorum communis (EDC), palmaris longus (PL), flexor digitorum profundus (FDP), flexor digitorum superficialis (FDS), extensor digitorum 4,5 (ED 4,5), brachioradialis (BrR), anterior deltoid (AD), abductor digiti minimi (ADM) and flexor carpi ulnaris (FCU).

While the ongoing EMG activity is an important factor in determining the amplitude of the evoked response (Bennett and Lemon, 1994; Devanne *et al.*, 1997; Kischka *et al.*, 1993; Lemon *et al.*, 1987), the hypothesis behind the design of the cortical stimulation experiments was that conditioning effects of F5 stimulation would be enhanced because of cortical activity encoding visuomotor grasp (Cattaneo *et al.*, 2005) (see also Chapters

6 and 7). If the facilitation from F5 conditioning represents a functional role, there should be a relationship between the evoked responses and the upcoming muscle activity. At the time of hand shaping AD shows the lowest level of EMG of the 10 muscles. As already mentioned, F5 has a greater representation of the distal musculature of the forelimb (Rizzolatti *et al.*, 1988), and therefore F5 stimulation was not expected to produce a conditioning effect in AD. However, in the distal muscles, there was also no clear relationship between the amount of EMG activity during hand shaping and the C-T facilitation. AbPL, which showed a C-T facilitation and FDP, which did not, have similar relative levels of muscle activity during hand shaping. The F5 conditioning effect therefore does not occur exclusively in the muscles which show the highest EMG activity at the time of hand shaping or at the time of cortical stimulation.

Normalisation of the EMG allows for comparison between muscles, but it is possible that the muscles showing C-T facilitation were those which had the greatest EMG activity for grasping the disc compared to the other five object-grasp combinations. In other words, rather than comparing responses across muscles, the comparison should be within a given muscle for a range of different object-grasp combinations. How the level of muscle activity and C-T facilitation changes with the object grasped is examined in Section 4.3.7 and 4.3.8.

4.3.6 Influence of C-T interval on F5-evoked facilitation

Figure 4.7A shows the modulation in the normalised EMG responses in PL (M39) when the C-T interval was altered over a range from -0.8 ms (M1 stimulation 0.8 ms

before F5 stimulation) to 3.5 ms (F5 3.5 ms before M1). The intervals chosen were based on previous investigations of I-wave facilitation (Shimazu *et al.*, 2004). Tests of six intervals were repeated in different sessions (0.8, 1 and 1.2 ms in two sessions and 0, 1.8 and 3.5 ms in three sessions). A Kruskal-Wallis test confirmed a significant relationship between C-T interval and the amount of facilitation ($p<0.001$). Wilcoxon signed-ranks test showed significant facilitatory effects ($p\leq0.01$) at C-T intervals of 0 ms (ratio = 2.31), 1 ms (ratio = 2.04) and 3.5 ms (ratio = 2.73). The two early significant peaks in Figure 4.7A were 1 ms apart (arrows) compatible with I-wave generation (Shimazu *et al.*, 2004). Significant facilitation of the AbPL response (Kruskal-Wallis, $p<0.001$; Wilcoxon signed-ranks, $p<0.05$) was seen at the same C-T intervals (Fig. 3B): at 0 ms (ratio=1.96), 1 ms (ratio=2) and 3.5 ms (ratio=1.94). The C-T facilitation for the flexor FDS is shown for comparison over the 17 C-T intervals; there was no significant effect from F5 conditioning for this muscle (Kruskal-Wallis, $p>0.05$).

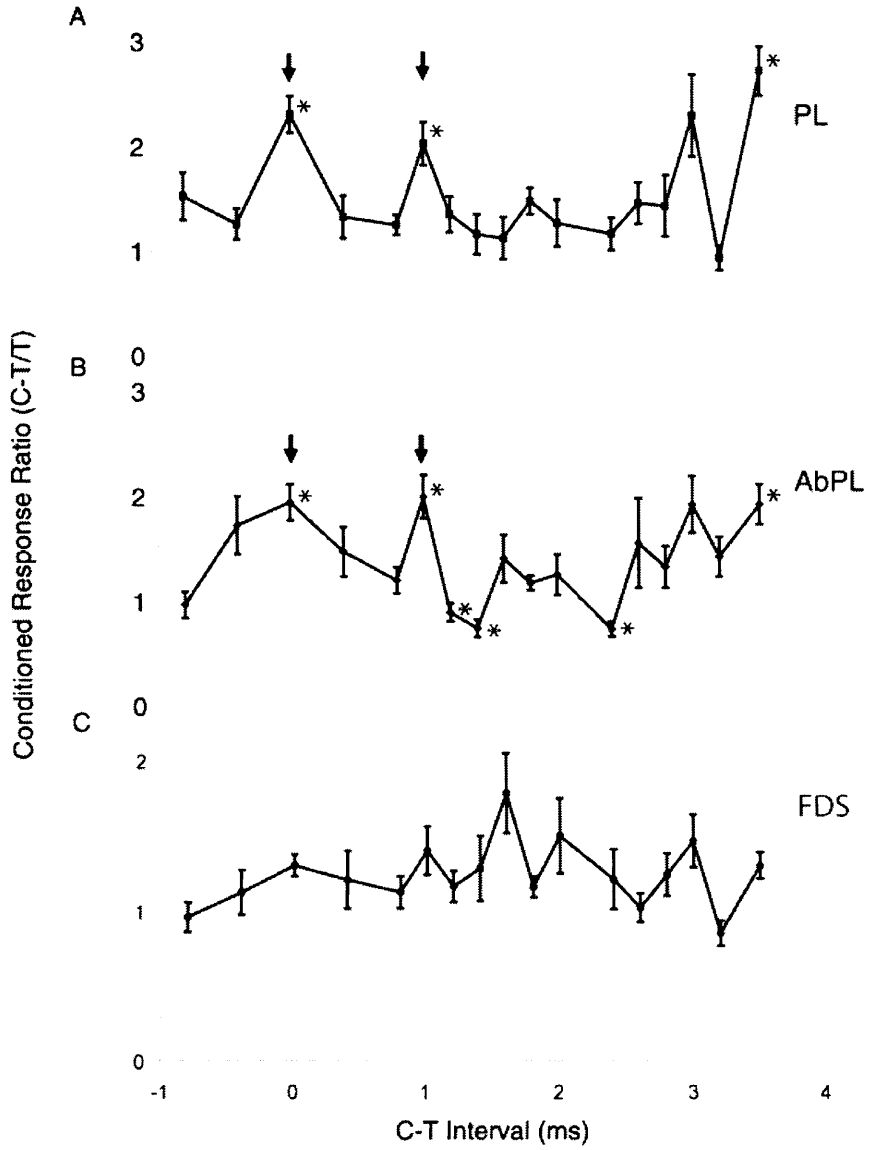

Figure 4.7. Time course of the F5 conditioning effect in three muscles.

The effect of changing the C-T interval on the F5-M1 interaction in the three muscles recorded in case M39. The conditioning response ratio was calculated by dividing the response from stimulation of both F5 (200 μA) and M1 (150 μA) (C-T) by that of M1 alone (T). The ratio is shown for palmaris longus (PL), abductor pollicis longus (AbPL) and flexor digitorum profundus (FDS) over 17 C-T intervals from -0.8 ms (F5 0.8 ms later M1 stimulation) to 3.5 ms (M1 stimulation 3.5 ms after F5). Six C-T intervals are pooled over 2-3 sessions (0 ms, 0.8 ms, 1 ms, 1.2 ms, 1.8 ms and 3.5 ms). In PL and AbPL two significant peaks of facilitation were seen at short intervals, (arrows) compatible the natural frequency of I-wave generation. A late peak at 3.5 ms was also present in both these muscles. FDS showed no effects at any of the intervals tested. Significant suppression effects were seen in AbPL at 1.2 and 1.4 ms. *Wilcoxon signed-rank=$p<0.05$. The mean values are plotted after 10% outliers were removed.

4.3.7 Suppression of M1 responses from F5

In some instances the response to M1 stimulation was suppressed by conditioning F5 stimulation. Examples from the two monkeys are shown in Figure 4.8. In each case the response evoked by combined F5 and M1 stimulation was *smaller* than the test M1 response (arrowed). In M39 this was significant in AbPL ($p<0.05$) at C-T intervals of 1.2 ms (F5-M1/M1 ratio (±SE): 0.9 ± 0.09), 1.4 ms (0.75 ± 0.08) and 2.4 ms (0.74 ± 0.07). In CS15 suppression was significant ($p<0.05$) in AbPL at 6 ms (0.62 ± 0.08). The same electrode pairings that in CS15 and M39 that produced facilitation at very early C-T intervals could also produce suppression at later C-T intervals. These suppression effects only occurred in AbPL in both monkeys, and at four C-T intervals, so suppression was not as frequently observed as the facilitatory effects.

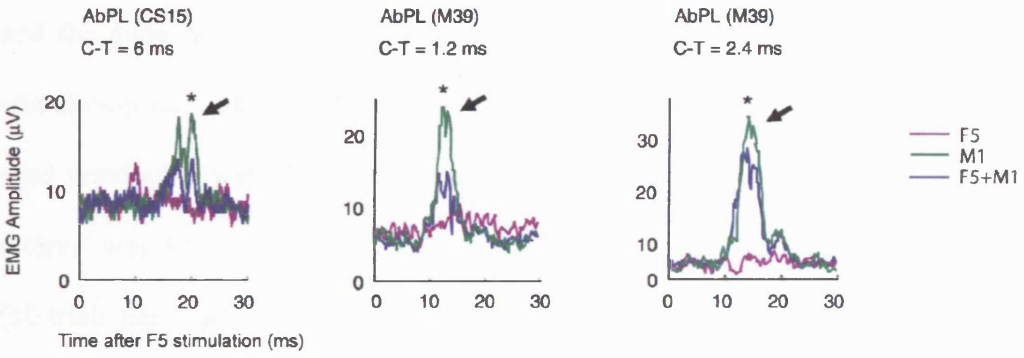

Figure 4.8. Average traces showing suppression from F5 conditioning during reach-to-grasp.
At C-T intervals of 6 ms (abductor pollicis longus, AbPL, CS15) and at 1.2 and 2.4 ms (AbPL, M39) suppression effects from F5 conditioning of a M1 test stimulus were evident. Average, rectified responses from the conditioning, C stimulus to F5 (magenta), the test, T stimulus to M1 (green) and C-T stimuli (blue) are shown. *Wilcoxon signed-rank=$p<0.05$. All figures are with 10% outliers removed (25 sweeps per condition).

4.3.8 Changes in F5 conditioning with object to be grasped

In the second part of the study one monkey (M39) grasped one of four objects: a ring, cube, disc or plate. As in the single unit study (Chapter 3) the ring and cube could be grasped by a side or hook grip, to allow any effect of object to be differentiated from that of grasp (see Section 2.2.3, Methods 1). While the experiment was designed so there was no involvement of the thumb for the hook grips, the monkey did use the thumb to stabilise the grasp for the hook grip of the cube (as seen in the grasp postures in Figure 4.9).

The C-T response was investigated during the reach-to-grasp phase (50 ms after homepad release) for six objects in four sessions over seven days. The cube side grip was performed in each of the four sessions, the disc in three sessions, the plate twice, and the cube hook grip, and both grips of the ring were performed once. The M1 stimulation intensity was 150 μA and F5 stimulation was 175 μA, a lower level than used previously was chosen so as to be sub-threshold for the extensors, and the C-T interval was 3.5 ms. Three objects for the first session were presented in blocks of 150 (50 trials per condition) so the same number of C, T and C-T stimuli were delivered for each object. To counteract any order effects, for subsequent sessions three objects were presented in pseudorandom order (27-77 trials per condition). No change in the C-T response was noted by changing the design from block to pseudorandom.

A facilitatory C-T response was present in BrR, EDC and PL muscles when performing both side grips and grasping the disc, but a significant effect was only present for PL and BrR (Kruskal-Wallis, $p<0.01$, $p<0.05$, respectively). Wilcoxon signed-ranks test on the

pooled values for each object for PL and BrR, isolated the C-T facilitation to side grasp of the ring (both muscle, $p<0.01$) and the cube (both muscles, $p<0.001$); the large disc (both muscles, $p<0.001$); and the hook grip for the cube ($p<0.05$ and $p=0.001$, PL and BrR respectively). There was no significant effect on either muscle for the hook grip of the ring or for grasping the plate. Therefore the C-T response was restricted to specific muscles and during specific grasps.

The degree of C-T facilitation observed in BrR and PL between objects was comparable, with clear facilitation for the side grasps and grasp of the disc in both muscles, and a lower, though still significant, effect for the hook grip of the cube (Table 4.4). Although the side grasp for the cube showed a significant effect in the pooled data from four sessions, in one session for PL and two sessions for BrR the C-T facilitation did not reach significance ($p>0.05$). In contrast, for the grasp of the disc (three sessions), there was always a significant C-T facilitation for both muscles ($p<0.05$). The side grip of the ring and the hook grip of the cube were only performed in one session. The facilitation ratio from BrR prior to grasping the ring using the hook grip was also large but had a large standard error, 2.48 (±0.46), so failed to reach significance.

Table 4.4 C-T facilitation ratio for palmaris longus and extensor carpi ulnaris for the six objects

Muscle	**Object**					
	Disc	**Cube (side)**	**Ring (side)**	**Cube (hook)**	**Ring (hook)**	**Plate**
BrR	2.3 (±0.14)***	2.15 (±0.15)***	3.23 (±0.41)***	1.79 (±0.13)**	2.48 (±0.46)	1.69 (±0.18)
PL	1.9 (±0.09)***	1.64 (±0.08)***	2.14 (±0.27)**	1.51 (±0.18)*	1.32 (±0.15)	1.32 (±0.09)

The mean C-T ratio (with 10% outliers removed) for palmaris longus (PL) and brachioradialis (BrR) with standard error in parenthesis. Significance level (from pooled data) indicated by the asterisks, *= $p<0.05$, **=$p<0.01$, ***=$p<0.001$.

Figure 4.9 shows examples of the evoked responses from the C, T and C-T conditions for BrR and PL. The F5 conditioning of the test response was smaller than those shown in Table 4-4. This may be due to the analysis used to compare the C-T and T evoked responses being designed for paired data (to allow for changes in cortical excitability). However, in the current experiment objects were not always presented in blocks, so there could be several trials between C-T and T stimuli for any given object. Therefore a second statistic was performed. A Kruskal-Wallis test compared the C-T ratio for the six object/grasp combinations (with 10% outliers removed) but, unlike the previous analysis, the C-T evoked responses were normalised to the average evoked response from M1 stimulation for that object and within session. For both BrR and PL there was a significant difference in the amplitude of the evoked response across objects (both, $p<0.001$). However, these new C-T facilitation ratios were lower than previously. During reach-to-grasp for the ring (side grip) the new C-T facilitation ratio for BrR was 2.73 ± 0.24 (SE), for the disc 1.86 ± 0.07, the hook grip of the cube 1.70 ± 0.07 and the side grasp of the cube $1.52\ \pm0.07$. These are the same reach-to-grasp combinations that produced a significant effect previously (Table 4.4). For the hook grip of the ring and grasp of the plate the C-T ratio represented an increase from F5 conditioning of less than 50 % of the response from M1 stimulation alone (both, C-T facilitation ratio<1.50). For PL the C-T facilitation was above 1.50 during reach-to-grasp for the disc and the side grasp of the ring (1.66 (±0.06) and 1.66 (±0.10), respectively). Here the side grasp of the cube, which had clear C-T facilitation in three of the four sessions, has a C-T ratio of 1.31 ± 0.07 (SE) for PL.

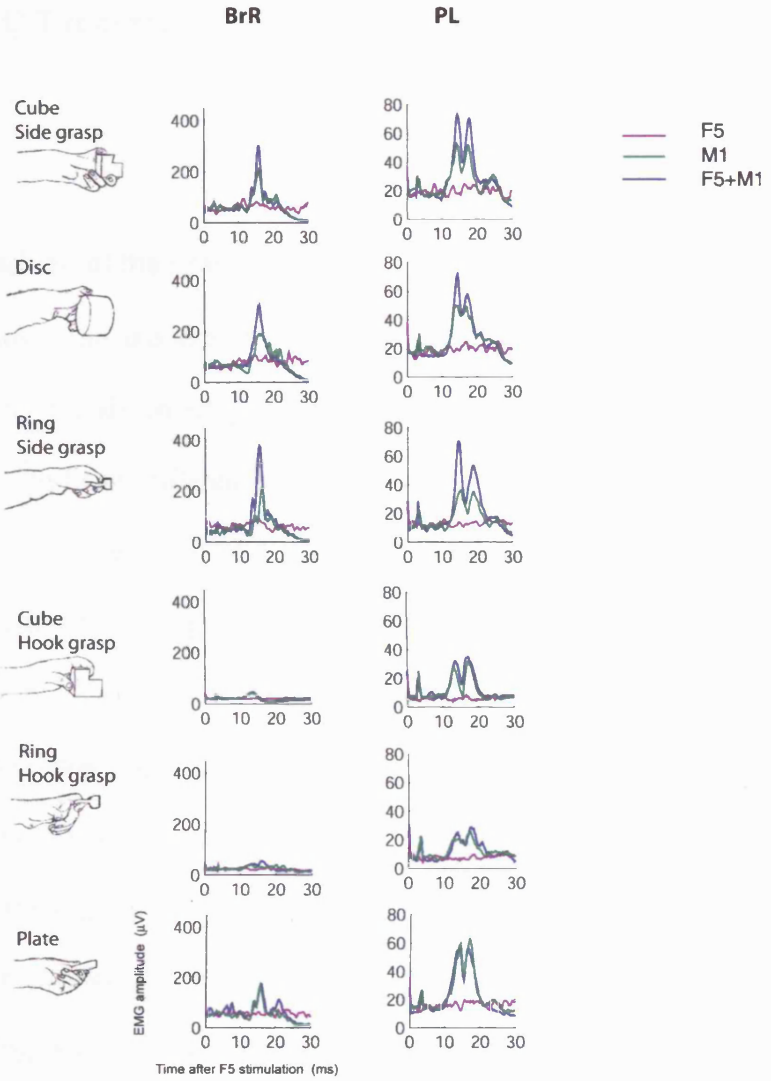

Figure 4.9 Evoked responses from brachioradialis (BrR) and palmaris longus (PL) during the three stimulation conditions during grasp for all six object-grasp combinations.

The response elicited from a test stimulus to M1 alone (green, 150 μA), to F5 alone (magenta, 175 μA) and to both F5 and M1 (blue) at C-T=3.5 ms is illustrated. Stimuli to F5 were deliver 50 ms after homepad release. 10 % outliers removed.

A central question of this Chapter was whether these C-T facilitatory responses corresponded with the muscle activity used to grasp the objects. This was examined by investigating the similarity of the EMG activity during the different grasps and

comparing the C-T responses with the level of EMG during grasp and at the time of F5 stimulation.

4.3.8.1 Comparison of the grasps

Table 4.5 shows the movement times (the time from homepad release to object displacement) for the six object-grasp combinations. Data was taken from 14 sessions and showed a significant difference in the movement times ($p<0.001$). As the time of cortical stimulation was fixed at 50 ms after homepad release this would result in cortical stimulation occurring at different stages of the reach-to-grasp movement for each object-grasp. Therefore the absence of a significant C-T facilitation for grasp of the plate or ring (hook grip) may be due to cortical stimulation being delivered too early or too late in the reach-to-grasp movement, rather than the F5 conditioning effect being specific to certain grasps. Reach-to-grasp for the plate indeed had the slowest movement time (cortical stimulation at 11 % of movement time), but all other object-grasps, including hook grip of the ring, fell between the movement times for the ring side grasp (cortical stimulation at 16 % of movement time) and the grasp of the disc (cortical stimulation at 13 % of movement time), both of which had significant C-T responses. Therefore there appears to be a grasp-specific facilitation from F5 conditioning, although the timing of cortical stimulation may account for the absence of a significant F5 conditioning effect during grasp of the plate. There was no significant effect in the reaction time.

Table 4.5 Mean movement times for the six object-grasps

Ring side	Cube hook	Ring hook	Cube side	Disc	Plate
330±0.02	347±0.03	349±0.02	355±0.02	379±0.02	419±0.04

Mean movement times (from homepad release to the start of object displacement) and standard deviation from 14 sessions.

Normalised EMG activity recorded from the 10 digit, hand and arm muscles during hand shaping for grasp were used to produce a distance (dissimilarity) matrix (Figure 4.10). The normalised EMG values took into account the different movement times for the different objects (epochs 7-9, see Section 2.6.2, Methods 1). The dark blue diagonal line through the centre of the matrix indicates an identical grasp, when each grasp was compared to itself, with a distance of zero. Blue squares represent grasps for which the overall EMG activity was similar. From the distance matrix there is a clear separation of the plate from the other object-grasps. Notably there was no C-T facilitation during reach-to-grasp for the plate, in fact a tendency for suppression in PL (Figure 4.9). The side grasps of the cube and disc were related, and for both these grasps there was a significant facilitation, though a more consistent response for the disc than for the side grasp of the cube in BrR and PL. There is a striking similarity for the two hook grips, however while the hook grip of the cube showed a significant C-T facilitation that of the ring did not. It should also be noted that in this matrix the side grip of the ring is more clearly grouped with the hook grip of the ring and rather than the side grip of the cube, as observed previously (Figure 3.5B). This is due to the addition of the plate and the disc to the normalisation process. As the peak activity for each muscle is divided by the peak activity for that muscles across all objects (see Section 2.6.2, Methods 1), and since for most of the muscles the activity is much larger for grasping the plate or the disc, the

relative difference between the ring side and the ring insertion grips becomes relatively smaller when the plate and disc are included in the matrix.

While the distance matrix possibly provides an explanation of why the side grasps and grip of the disc all showed a significant C-T facilitation, it also highlights the differences in overall muscle activity between these grasps and that of the cube hook grip, which also produced a significant C-T facilitation. Even when using the ratios from the second analysis, the grip types that showed clear increases in the C-T response, the side grasps of the ring and disc, did not show marked similarity in the distance matrix. As the distance matrix was constructed using data from all the muscles and as only BrR and PL showed significant effects, the changes in EMG activity that result from cortical stimulation may have been masked by the effects of the other muscles.

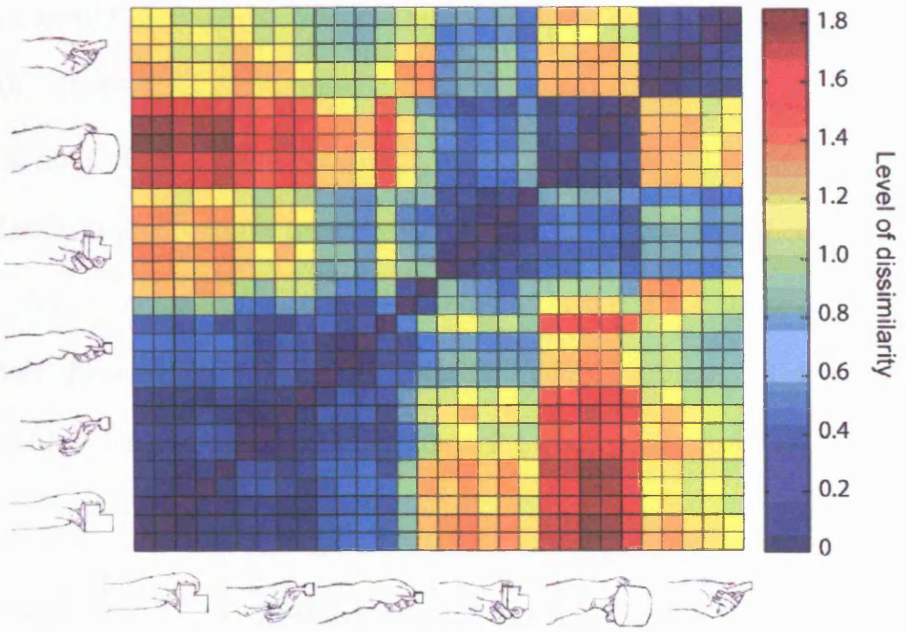

Figure 4.10 Between sessions distance matrix for the six object-grasps, using EMG data recorded from 10 muscles.

NDMVs calculated from the average amplitude of rectified EMG activity at hand shaping (epochs 7-9) were used to produce a between sessions distance matrix indicating the Euclidian distance between every NDMV pair (see Section 2.6.2, Methods 1). Blue indicates high degree of similarity (lowest values), red little similarity (highest values). The matrix is symmetrical so the dark blue diagonal line is the comparison of each NDMV to self (null distance). Data is from five sessions.

4.3.8.2 C-T facilitation and EMG activity during grasp

C-T facilitation could correspond to the level of EMG required to grasp the objects within BrR and PL. Figure 4.11A illustrates the normalised EMG activity for each muscle for the six object-grasp combinations. For BrR during hand shaping, the three objects for which the highest EMG activity was recorded also showed a clear facilitatory C-T response: the side grasp of the ring, side grasp of the cube and grasp of the disc. However, lowest level of muscle activity for all six object-grasps was produced when grasping the cube with a hook grip, yet this grasp yielding a significant C-T response;

although a small C-T response from the second analysis (a C-T facilitation ratio of less than 1.50). If the level of PL muscle activity during hand shaping was the basis of whether or not C-T facilitation occurred, a significant effect would have been observed for the plate as it produced the third highest level of EMG activity, whereas there was a tendency for suppression in the C-T response from PL during reach-to-grasp. Furthermore the side grasp of the ring, which produced a clear C-T facilitation, had EMG activity of less than half that observed during grasp of the plate.

4.3.8.3 C-T facilitation and EMG activity during object displacement

When the EMG activity during the object displacement (epochs 10-12) was analysed a similar pattern to that at hand shaping emerged. PL still had greater activation for the plate and BrR had the lowest activity for the hook grip of the cube (Figure 4.12). However, EMG levels were generally lower and differences between muscles during grasp of an object less differentiated.

A Normalised EMG during hand shaping

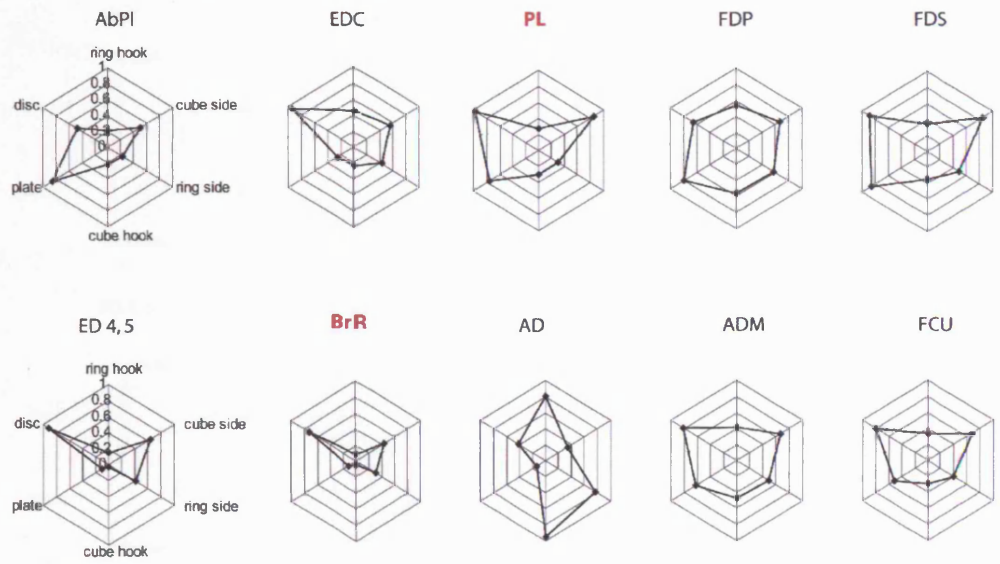

B Hierarchical cluster analysis during hand shaping

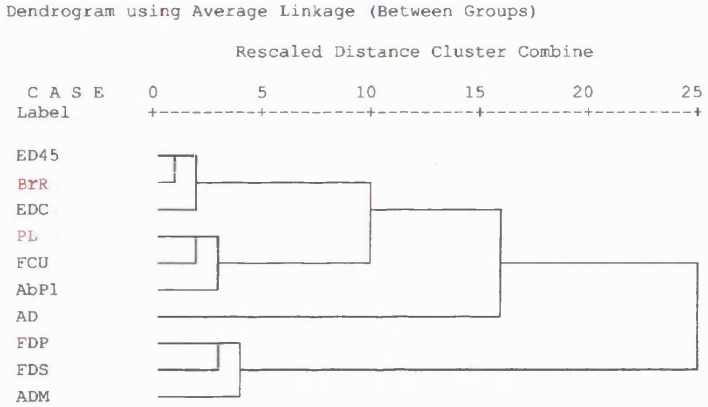

Figure 4.11 Polar plots illustrating rectified normalised average EMG activity from 10 muscles of the arm, hand and digits during hand shaping (epochs 7-9) in the six object-grasp conditions (M39).

A, EMG activity from one session was normalised across objects and the duration of trial and within muscles to allow comparison between muscles and objects. B, dendrogram from hierarchical cluster analysis of the EMG data. Key: abductor pollicis longus (AbPL), extensor digitorum communis (EDC), palmaris longus (PL), flexor digitorum profundus (FDP), flexor digitorum superficialis (FDS), extensor digitorum 4,5 (ED 4,5), brachioradialis (BrR), anterior deltoid (AD), abductor digiti minimi (ADM) and flexor carpi ulnaris (FCU). Only PL and BrR (red) showed a significant C-T facilitation, this was for the side grasp of the cube, side grasp of the ring, hook grip of the cube and grasp of the disc. Data are from 180 trials in one session.

A **Normalised EMG during object displacement**

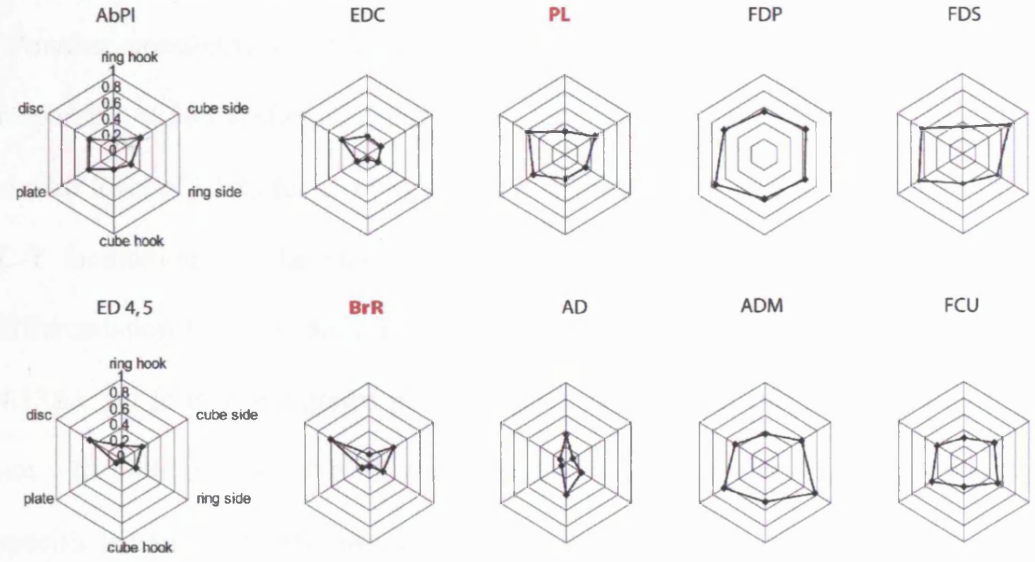

B **Hierarchical cluster analysis during object displacement**

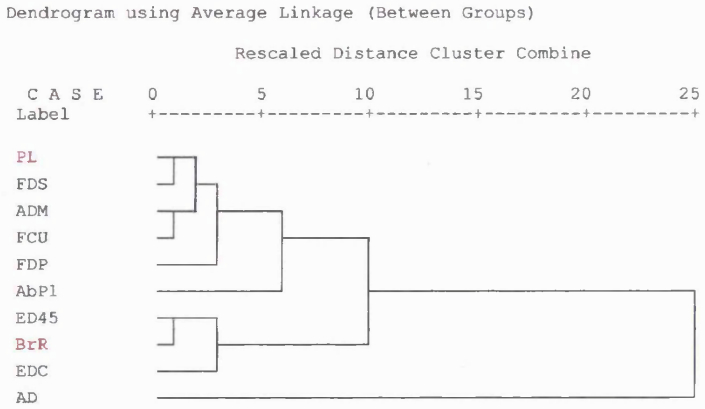

Figure 4.12 Polar plots illustrating rectified averaged normalised EMG activity from 10 muscles of the arm, hand and digits during object displacement (epochs 10-12) in the six object-grasp conditions (M39). A, EMG activity from one session was normalised across objects and the duration of trial and within muscles to allow comparison between muscles and objects. B, dendrogram from hierarchical cluster analysis of the EMG data. Key: abductor pollicis longus (AbPL), extensor digitorum communis (EDC), palmaris longus (PL), flexor digitorum profundus (FDP), flexor digitorum superficialis (FDS), extensor digitorum 4,5 (ED 4,5), brachioradialis (BrR), anterior deltoid (AD), abductor digiti minimi (ADM) and flexor carpi ulnaris (FCU). Only PL and BrR (red) showed a significant C-T facilitation, this was for the side grasp of the cube, side grasp of the ring, hook grip of the cube and grasp of the disc. Data are from 180 trials in one session.

4.3.8.4 C-T facilitation and EMG activity during cortical stimulation

Another possibility is EMG activity at the time of stimulation determines the C-T response. At 50 ms after homepad release, at the time of cortical stimulation, BrR had a similar level of EMG for all object-grasp combinations (Figure 4.13A), but there was no C-T facilitation for the plate or ring hook grip. Similarly, for PL there was no differentiation between the muscle activity for the six different object-grasps (Figure 4.13A), yet four object-grasps produced a significant C-T effect and the other two did not. In both muscles, the F5 conditioning effect elicited during reach-to-grasp was specific to certain object-grasp combinations but the EMG during reach was not. Thus it appears the C-T response does not correlate in any simple way to the pattern of EMG activity at the time of stimulation or during hand shaping or object displacement.

A **Normalised EMG during cortical stimulation**

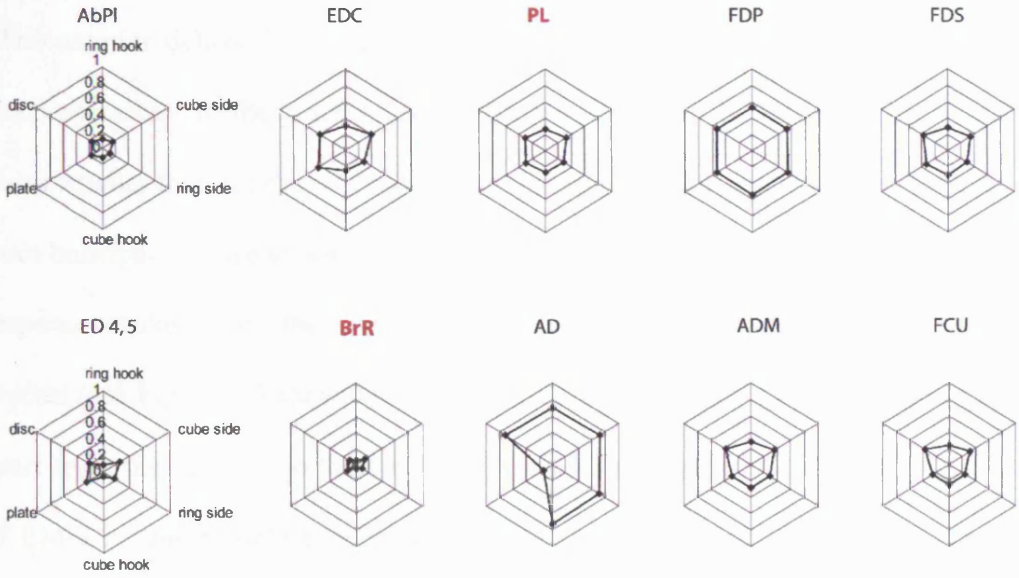

B **Hierarchical cluster analysis during cortical stimulation**

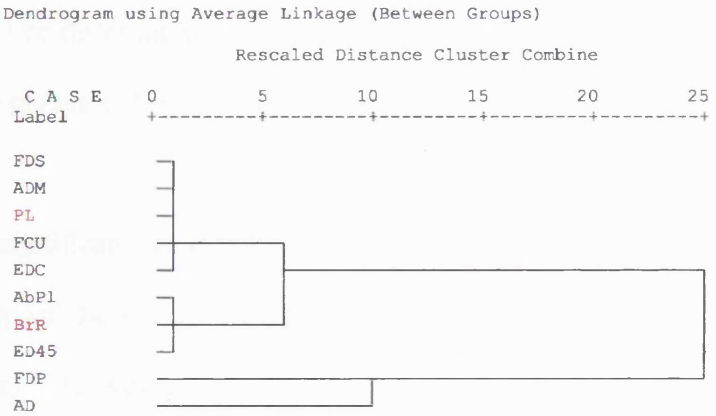

Figure 4.13 Polar plots illustrating rectified normalised EMG activity from 10 muscles of the arm, hand and digits during F5 stimulation (epochs 2-4) in the six object-grasp conditions (M39).

A, EMG activity from one session was normalised across objects and the duration of trial and within muscles to allow comparison between muscles and objects. B, dendrogram from hierarchical cluster analysis of the EMG data. Key: abductor pollicis longus (AbPL), extensor digitorum communis (EDC), palmaris longus (PL), flexor digitorum profundus (FDP), flexor digitorum superficialis (FDS), extensor digitorum 4,5 (ED 4,5), brachioradialis (BrR), anterior deltoid (AD), abductor digiti minimi (ADM) and flexor carpi ulnaris (FCU). Only PL and BrR (red) showed a significant C-T facilitation, this was for the side grasp of the cube, side grasp of the ring, hook grip of the cube and grasp of the disc. Data are from 180 trials in one session.

4.3.8.4 The pattern of EMG activity for the grasps

The anterior deltoid had a different pattern of EMG activation compared to the nine distal muscles. In the reach phase, EMG from AD for the plate (Figure 4.13A) was much smaller than for the other five object-grasp combinations. Notably, the time taken from homepad release to object displacement was greatest for the plate (Table 4.5). The response evoked from the test stimulus during reach was one of suppression for all objects (see Figure 4.5 showing the evoked responses during reach-to-grasp of the disc) apart from the plate when there was no T response; most likely reflecting the low level of EMG in this muscle at the time of stimulation. During hand shaping and object displacement, AD had increased EMG activity for the two hook grips and the range of muscle activity (from ~0.2-1) had the same range as the distal muscles. Therefore there must be differences in the reach for the hook grips and that of the plate compared to the side grasps and when grasping the disc.

A significant facilitatory C-T response in PL and BrR was observed during reach-to-grasp of the same object-grasps (the disc, the side grasps and the hook grasp of the cube). However, the relative pattern of muscle activation differed between these muscles. During hand shaping the extensors and BrR showed a similar shape in the polar plots (compare ED 4,5, BrR and EDC) as did the remaining flexors (FDP, FDS and FCU) and the anterior deltoid was strikingly different to the other muscle patterns (Figure 4.11A). Hierarchical cluster analysis of the normalised EMG activity, used in the polar plots, confirmed these groupings. At hand shaping the dendrogram shows four clear groups, ED 4,5, BrR, EDC, and the second group, PL, FCU, AbPL, and the third

FDP, FDS, and ADM with AD by itself. When pulling the object, there was less differentiation with three clear groups, with the extensors and BrR still forming one group and AD by itself (Figure 4.12B).

In contrast to this differentiated muscle pattern at hand shaping and when pulling the object, 50 ms after homepad release (Figure 4.13B) all muscles, apart from the AD, have a similar shape, so did not differentiate between object/grasps. Cluster analysis showed that at the time of cortical stimulation there were two main muscle groups FDS ADM, PL, FCU and EDC forming one group, while AbPL BrR and ED 4,5 formed the second group, with FDP and AD each forming a cluster of one. Therefore, for the times examined in the 10 muscles recorded, BrR and PL, the two muscles showing a significant facilitatory effect from F5 conditioning, do not show a similar pattern of muscle activity for the object-grasp combinations used in this experiment. Notably, the EMG activity does not divide into flexor or extensor groups. EMG amplitude during hand shaping may contribute to the C-T facilitation observed, but it is certainly not the only factor.

While the C-T facilitation did not fully relate to the amount or pattern of EMG produced for the six object-grasps during stimulation or hand shaping, certain grasps tended to be associated with facilitation. Grasp of objects that did not produce C-T facilitation may be distinguished by the postures and digits required for grasp. The plate was the only object with complete supination of the hand and where just the index finger and thumb were used during grasp. The hook grip of the ring required only the index

finger to pull the ring, while C-T facilitation was present for the side grasps the hook grip of the cube, all of which have some involvement of the thumb. Kinematic data would help in the understanding of whether or not these differences were related to the degree of C-T facilitation.

4.4 Discussion

During the hand transport and pre-shaping stages of a visuomotor grasping task, a single conditioning stimulus to area F5, whilst not evoking a significant EMG response alone, can produce robust modulation of EMG responses evoked in hand and digit muscles by a test stimulus to M1. The demonstration of these effects in the awake, behaving monkey performing a visually-guided grasping task lends further support to the role of F5 in shaping of the hand appropriately for grasp. The effects observed were specific to particular muscles, objects and electrode combinations. The general characteristics of this modulation were similar to that previously reported in anaesthetised and sedated monkeys (Cerri *et al.*, 2003; Shimazu *et al.*, 2004). The facilitatory effects from F5 conditioning were large, reproducible and significant, with a doubling of the test M1 response. The results seen were identical in two species of monkey performing a visuomotor grasping task.

4.4.1 Location of electrodes

The tips of the effective M1 cathodes were in lamina V or VI in the anterior bank of the central sulcus. rICMS confirmed the electrodes were in the hand area of M1. This positioning of the electrodes, in the deep cortical layers (V/VI) of the M1 hand area, was the same as previously used in sedated and anaesthetised macaque monkeys to produce an M1 evoked response that was facilitated by F5 stimulation (Cerri *et al.*, 2003; Shimazu *et al.*, 2004). The spread of current from cathodal stimulation and the projections of neurones within these laminae (Jones and Wise, 1977; Ranck, 1981),

would result in ICMS targeting corticospinal neurones that project to hand motoneurones.

Low M1 thresholds were found in lamina V or VI with motor responses also evoked from lamina III. Low threshold responses from the deep laminae and the tendency to evoke motor responses in lamina III, V and VI have been observed in the monkey (Kwan *et al.*, 1978) and baboon (Andersen *et al.*, 1975). This has been related to the rich axonal systems that arise from and are received by these laminae (Kwan *et al.*, 1978; Stoney *et al.*, 1968). In contrast, electrical stimulation of the more superficial laminae sometimes (Kwan *et al.*, 1978) but not always (Andersen *et al.*, 1975) produced a motor response. These may also reflect excitation of PTN cell apical dendrites and axon collaterals, as these ramify extensively in the superficial cortical layers, producing antidromic excitation of the cell soma (Asanuma, 1981; Kwan *et al.*, 1978).

F5 microwires were located in the inferior bank of the arcuate sulcus just lateral to the spur (Figure 4.2). In this region, canonical neurones have been recorded that have grasp-specific patterns of discharge that is generally present prior to movement onset (Murata *et al.*, 1997; Raos *et al.*, 2006; Umilta *et al.*, 2007). Electrical stimulation of this region often produces movements of the hand, digits and mouth (Cerri *et al.*, 2003; Godschalk *et al.*, 1995; Rizzolatti *et al.*, 1988). In keeping with this, thumb movements were elicited from the effective cathodal electrodes. As in previous reports (Cerri *et al.*, 2003; Shimazu *et al.*, 2004), the most effective site for the cathode, used to elicit a C-T response, was in laminae III or V. Neuronal tracing studies have shown extensive

cortico-cortical input to M1 from F5 arising from lamina III (Godschalk *et al.*, 1984; Muakkassa and Strick, 1979), therefore the F5-M1 interaction could occur in M1 (see Section 4.4.4). F5 corticospinal projections originate from lamina V (Dum and Strick, 1991; He *et al.*, 1993) and provide an alternative route for the EMG responses evoked from F5 (see Section 4.4.6.). Notably, in the first experiment, the largest C-T responses were observed (over 3 times the T response) in CS15, where the F5 cathode was located in lamina III; the optimal position for stimulating cortico-cortical pathways from F5 to M1.

4.4.2 Current spread

The specificity of the C-T facilitation/suppression to certain electrodes is suggestive of limited current spread. Studies investigating stimulus spread suggest that at the intensities used here (110-200 μA), the physical spread of cathodal monopolar current is in the order of 1 mm (Lemon, 1984; Ranck, 1981), and bipolar stimulation would then have a similar or smaller spread (Lemon, 1984). Another study expressed the spread of excitation as within a wide range, with cathodal monopolar stimulation at 90 μA affecting an region of 0.17-0.6 mm in baboon M1 (Andersen *et al.*, 1975). According to these estimates, since the distance between pairs of electrodes within arrays was 1-1.3 mm, the electrode combinations used should have stimulated different clusters of neurones. There is certainly no question that there was spread of T stimulation to F5 or C stimulation to M1.

In addition to physical spread of current, one has to consider physiological spread, i.e. synaptic effects on other connected neurones. This would produce inhibitory as well as excitatory actions (Andersen *et al.*, 1975). ICMS can indirectly activate PTNs through transsynaptic activation of the cortical interneurones and their axons (Andersen *et al.*, 1975; Asanuma, 1981; Cheney and Fetz, 1985; Jankowska *et al.*, 1975; Stoney *et al.*, 1968). This is believed to be the main route of excitation produced by single-pulse ICMS, and to an even greater extent when using rICMS (Andersen *et al.*, 1975; Jankowska *et al.*, 1975; Ranck, 1981). By measuring the conduction time from the cortex to the pyramid, Lemon *et al.* (1987) showed that the latency of the earliest neuronal response to single-pulse ICMS (10-20 μA) was consistent with indirect stimulation of PTNs. The physiological spread of current from horizontal connections, determined by investigations on firing probability in M1 (Baker *et al.*, 1998) and using single ICMS pulses of 20 μA (Cheney and Fetz, 1985), was thought to activate neurones 1-2 mm away from the cathode. The effective ICMS currents for chronically implanted implants used here (110-200 μA), is higher compared with sharp electrodes used for acute penetration (range for M1 typically 5-20 μA). This may be due to oedema and gliosis that follows the implant of the chronic electrode, and to a significant decrease in electrode tip impedance.

The motor responses evoked are also dependent on the organisation of F5 and M1. Both regions show a somatotopic structure. In M1 there is strong evidence for multiple overlapping motor representations of the arm, hand and digits (Indovina and Sanes, 2001; Park *et al.*, 2001; Park *et al.*, 2004; Penfield and Boldrey, 1937; Schieber, 2001).

Within such a motor representation, a 'colony' of PTNs are thought to represent a functional group projecting to a given motoneurone pool. Aggregation of 'colonies' project to overlapping pools (Andersen *et al.*, 1975), and single cells also diverge to project to different pools (Buys *et al.*, 1986; Fetz and Cheney, 1980). Because of the intermingling of motor outputs, ICMS at a single site is likely to affect CM cells with different muscle fields.

The ventral premotor cortex has an overall somatotopic representation which is broadly similar to M1 with a medial (face) to lateral (arm and hand) representation (Godschalk *et al.*, 1995; Kurata and Tanji, 1986; Muakkassa and Strick, 1979). Neuronal recordings and stimulation studies have shown the lateral portion of the post arcuate region contains representations of the face and mouth, those of the genus of the arcuate sulcus relating to the distal forelimb and posterior medial region concerned with the proximal arm (Godschalk *et al.*, 1984; Godschalk *et al.*, 1995; Kurata and Tanji, 1986; Muakkassa and Strick, 1979; Rizzolatti *et al.*, 1988). The projections between F5 and M1 show a topographical organisation with the lateral part of the post arcuate region projecting to the lateral part of M1 (Godschalk *et al.*, 1984). Discrete regions of M1 make reciprocal back projections to multiple regions of the premotor cortex, but this is likely to reflect the more diffuse representations in the premotor cortex, with greater overlap between forelimb and face representations (Godschalk *et al.*, 1984; Godschalk *et al.*, 1995; Muakkassa and Strick, 1979). Nevertheless, it has been suggested by Cerri *et al.* (2003) that F5-M1 interactions are specific since only certain electrodes produced interactions; these may have activated specific somatotopic relationships between F5 and M1. The

C-T facilitation may have been confined to a few electrode combinations because there is diffuse mosaic-like representation within F5.

4.4.3 Muscle specific facilitation

The modulation of M1 responses by F5 stimulation is unlikely to be solely due to the general increase in excitability that occurs during the reach-to-grasp movement. The conditioning effect of F5 stimulation was limited to a few of the tested muscles. In the C-T interval study these were PL, a flexor of the wrist, and extrinsic (AbPL) and intrinsic (thenar) muscles acting on the thumb; these muscles all show grasp-specific changes in activity during reach-to-grasp of a range of different objects (Brochier *et al.*, 2004). If F5 modulated M1 output, then the pattern of muscles showing C-T facilitation should relate to the muscle activity required for the task. Alternatively, the effects may not be influenced by the type of grasp used.

The effect of cortical stimulation during reach-to-grasp was investigated by presenting four objects, two of which (the ring and cube) could be grasped by either a side or hook grip. The C-T response could reflect the pattern of EMG activity at the time of stimulation. The motor responses evoked by corticospinal volleys elicited by cortical stimulation is modulated by the level of excitability of the target motoneurones (Bennett and Lemon, 1994; Devanne *et al.*, 1997; Kischka *et al.*, 1993; Lemon *et al.*, 1987). Though this was a factor, it was not the major influence. The muscles which showed a significant C-T response, BrR and PL, did so for certain grasps, the side grasps for the ring and cube, the hook grip of the cube and when grasping the disc. The EMG activity

at 50 ms after homepad release, when the cortical stimulus was delivered, showed little differentiation between the six object-grasp combinations. If the C-T response reflected the motoneuronal excitability at the time of stimulation, then the evoked C-T response, on the basis of the EMG activity, should have been similar for all object-grasp combinations.

If the conditioning effects of F5 stimulation were influencing by grasp-related inputs from F5, the C-T facilitation pattern should relate to EMG levels during subsequent hand shaping rather than EMG during reach. BrR showed a C-T response for the two side grips and for the disc, which was associated with the high EMG activity compared to the other object-grasp combinations at this time (Figure 4.11). However, it is unlikely that the F5 condition simply reflects the subsequent EMG activity during hand shaping. PL also had a highly significant C-T response for these grasps ($p<0.01$), but unlike BrR grasp of the plate produced the high EMG activity during hand shaping. Additionally, the relative level of EMG activity shown by BrR for the six object-grasp combinations was different to that from PL. Hierarchical cluster analysis of EMG activity from the 10 muscles produced four groups, with AD forming a group of its own and PL and BrR in separate groups (Figure 4.11B). Nor was there a clear relationship when the pattern of C-T facilitation was compared to EMG during cortical stimulation (Figure 4.13A) or object displacement (Figure 4.12A).

The EMG activity during cortical stimulation (epochs 2-4), hand shaping (epochs 7-9) or object displacement (epochs 10-12) were not the primary influence on the degree of

C-T facilitation. However, the possibility cannot be excluded that the C-T facilitation correlates to EMG levels at an untested time point during the reach-to-grasp movement.

Alternatively, the orientation of the hand and the digits used in the grasp may determine whether a conditioning response is observed. In a recent paper Raos *et al.* (2006) found the common factor in the modulation of the F5 neurones during grasp of different objects was whether or not the thumb was involved in the grasp. In the hook grip of the ring, only the index finger was used to grasp and pull the object, and there was no involvement of the thumb and neither BrR or PL showed a significant C-T response. For the hook grasp of the cube, the thumb had a more active role, touching the object (grips are illustrated in Figure 4.9). For both the side grips and when gripping the disc, the thumb was required. The side grasps and that of the disc showed greater facilitation of the C-T response than seen for the hook grip of the cube (Figure 4.9). Finally, grasping of the plate required the thumb, yet there was no C-T facilitation. Orientation selectivity has been observed in F5 neurones, with horizontal but not vertical presentation of a ring evoking spike activity (Raos *et al.*, 2006). Only for grasping the plate was complete supination of the hand required, the rotation of the wrist and hand could have affected the F5 inputs being facilitated. It may be by recording EMG activity from a small selection of hand and digit muscles the complexity of the movement is not being adequately described and therefore the relationship of the F5 conditioning effect to the grasp not clear.

4.4.4 Timing of the F5 conditioning effect

It is possible that the facilitation observed here involved the same cortico-cortical pathway from F5 to M1 proposed to explain the modulation of M1 outputs observed in previous studies (Cerri *et al.*, 2003; Shimazu *et al.*, 2004). These authors showed that late I-waves from M1 corticospinal neurons were particularly enhanced by conditioning stimuli delivered to F5, and these late I-waves gave rise to enhanced motor responses. Late I-waves are thought to arise from interneuronal circuits within M1 (Edgley *et al.*, 1997; Lemon, 2002; Patton and Amassian, 1954; Rothwell, 1991; Terao and Ugawa, 2002) (see also Section 1.4.2, Introduction). In a terminal experiment on one of the monkeys in this study (CS15) the sites that facilitated EMG responses also strongly facilitated I_2 and I_3 waves (H. Shimazu, unpublished observations). The extensive cortico-cortical input to M1 from F5 (Godschalk *et al.*, 1984; Muakkassa and Strick, 1979) could provide one mechanism of boosting late I-wave discharge. The facilitation of EMG responses observed here in both AbPL and PL at short C-T intervals (0 and 1 ms) (Figure 4.7), was similar to that observed in the sedated monkey (Cerri *et al.*, 2003) and is consistent with F5 inputs acting via a late I-wave pathway (Shimazu *et al.*, 2004). The latency of EMG responses from M1 stimulation (for AbPL, around 8.0 ms in M39 and 10 ms in the larger CS15) probably corresponds with the earliest discharge of motoneurones in relation to the I_1- or I_2-wave (Cerri *et al.*, 2003).

The conditioning effects seen in this study were smaller than those previously recorded (Cerri *et al.*, 2003; Shimazu *et al.*, 2004). Interestingly, a similar effect was reported in human subjects. Suppression from premotor-M1 double pulse TMS observed at rest was

not present during the active state (Civardi *et al.*, 2001). In the awake monkey there are differences compared to the sedated animal that could account for the smaller conditioning effect observed, such as in the level of background EMG and motivation levels. The location of the microwires, individual differences between monkeys and cortical suppression could also be factors.

4.4.5 Suppression

In the previous studies of sedated and anaesthetised macaques (Cerri *et al.*, 2003; Shimazu *et al.*, 2004), there was no suppression of M1 effects from F5 conditioning of a M1 stimulus. This may be due to the affect of the anaesthetic (α-chloralose) and sedation (ketamine) used in these studies. In the alert monkey Tokuno and Nambu (2000) showed that the dominant effect of ventral premotor stimulation was inhibition of M1 PTNs and other neurones and in the present study clear signs of suppression were observed, with the conditioned response being significantly smaller than the test M1 response (Figure 4.8). Thus in the awake behaving monkey, it would appear that the selective modulation of M1 outputs by F5 involves both inhibitory and excitatory processes. TMS studies of premotor-M1 cortex interactions in humans have highlighted suppression effects (Civardi *et al.*, 2001; Gerschlager *et al.*, 2001; Munchau *et al.*, 2002). Much like the effects here, these were isolated to certain C-T intervals and required specific stimulus intensities. F5 could provide gain modulation the motor outputs in a similar fashion as the frontal pursuit area of the frontal cortex in the oculomotor system (Tanaka and Lisberger, 2001). This could reflect a common

mechanism, with F5 of the premotor cortex providing gain modulation in the skeletomotor system (Cerri *et al.*, 2003).

4.4.6 Site of F5-M1 interaction

Alternatively, there are several lines of evidence which point to the F5-M1 interaction occurring in M1. Shimazu *et al.* (2004) suggested that M1 was the site of interaction with F5, because local microinjection of the $GABA_A$ agonist muscimol in M1 abolished both the late corticospinal volleys and their postsynaptic responses. Secondly, M1 PTNs can be activated by stimulation of the ventral premotor cortex at latencies of 1-4 ms (Ghosh and Porter, 1988; Godschalk *et al.*, 1984; Tokuno and Nambu, 2000) and this conduction time would provide ample time for F5 inputs to modulate the circuits generating the later I-waves even at the short C-T intervals (<1.0 ms) (Cerri *et al.*, 2003; Shimazu *et al.*, 2004). However the findings discussed here are also compatible with a sub-cortical site of interaction.

Alternatively, F5 outputs could bypass M1 and modulate motoneurone responses through its own corticospinal projections (Godschalk *et al.*, 1984; He *et al.*, 1993; Muakkassa and Strick, 1979). The effects seen from F5 conditioning were from F5 cathodes located in laminae III (CS15) and V (M39). Laminae III in the rostral portion of the ventral premotor cortex, has cortico-cortical projections to M1, and in lamina V corticospinal connections (Dum and Strick, 1991; He *et al.*, 1993). Single cell recordings (Gentilucci *et al.*, 1988; Rizzolatti *et al.*, 1981), stimulation studies (Rizzolatti *et al.*, 1981) and the tactile receptive fields of these F5 neurones (Gentilucci

et al., 1988; Rizzolatti *et al.*, 1981) all relate to hand movements. In contrast the caudal region of ventral premotor cortex (F4), with no CST projections, shows activity consistent with neurones encoding shoulder, arm, chest and facial movements (Gentilucci *et al.*, 1988; He *et al.*, 1993; Rizzolatti *et al.*, 1981). But while the F5 CST projections arise from the rostral region, they terminate mostly in the upper cervical segments (C2-C4) (He *et al.*, 1993), above the lower cervical enlargement that controls hand and arm muscles (Kuypers, 1981). Projections from F5 to the lower cervical segments are particularly sparse (Dum and Strick, 2005). The CST fibres may influence the distal musculature through connections with propriospinal neurones in the upper cervical segments. Alternatively, the function of the CST fibres, may relate to the function of neurones in the upper cervical spinal segments in controlling the postural and axial muscles of the neck and shoulder to control head orientation (Wise, 2006). As the ventral premotor cortex has dense projections to the facial nucleus of the brain stem (Morecraft *et al.*, 2001) it has been put forward that the CST originating from F5 controls of head movements required for accurate hand to mouth actions (Wise, 2006). A comparative anatomy study of the terminations from ventral premotor cortex, described as "Region C" showed a correlation to an arboreal lifestyle (Nudo and Masterton, 1990a; Nudo and Masterton, 1990b) the unimanual feeding patterns that this was likely to entail would require hand-mouth co-ordination (Wise, 2006). The function of the corticospinal fibres from F5 may therefore not be concerned with controlling the hand for visuomotor grasp and the termination pattern of these neurones make it unlikely that these mediate the C-T facilitation observed in this study.

4.4.7 Conclusions

F5 can exert robust modulation of M1 outputs to the hand during hand transport and shaping prior to object grasp. These effects are specific to particular muscles and grasps, and therefore are unlikely to reflect a general change in excitability. The peaks of facilitation of the F5 conditioned motor responses are compatible with generation of I-waves, therefore modulation of responses may involve I-wave pathways active during visuomotor transformations underlying object grasp.

Finally, this study opens up a means of studying some important issues: for example, do the effects from F5 follow a precise time course similar to that exhibited by single neurons in F5 and M1 recorded during the same task as observed in Chapter 3? Also, is there a relationship of the C-T facilitation to the kinematics of the task?

5. Methods 2: Transcranial magnetic stimulation

5.1 Subjects

In total, 119 naïve right-handed healthy volunteers participated in the study. Of these, 46 were rejected due to poor compliance, high TMS thresholds (if TMS during the experiment would need to be greater than 70% of stimulator output), excessive background EMG during the preparation period and if TMS was perceived as painful. Data presented are from the remaining 73 subjects (31 male, 42 female, mean age 26.1 years SD±5.3). All subjects gave informed written consent. The study complied with institutional guidelines and was approved by the local ethics committee.

5.2 Experimental set-up

5.2.1 Serial presentation of objects

Subjects were seated with their hands resting pronated, at waist level, on a table in front of two objects, a handle (9 cm high, 5 cm deep) and a disc (12 cm diameter, 2 cm deep), that were individually presented (Figure 5.1). Subjects wore vision occlusion spectacles (PLATO, Translucent Technologies, Toronto, Canada) to prevent vision during the intertrial interval. For all experiments, trials began with goggles opening. Subjects were asked to either observe the object or, on grasp trials, to reach out and grasp the object with their right hand in a self-paced manner and hold the object for ~0.5 s. A custom-made touch-sensitive electronic circuit was used to determine the time of object contact.

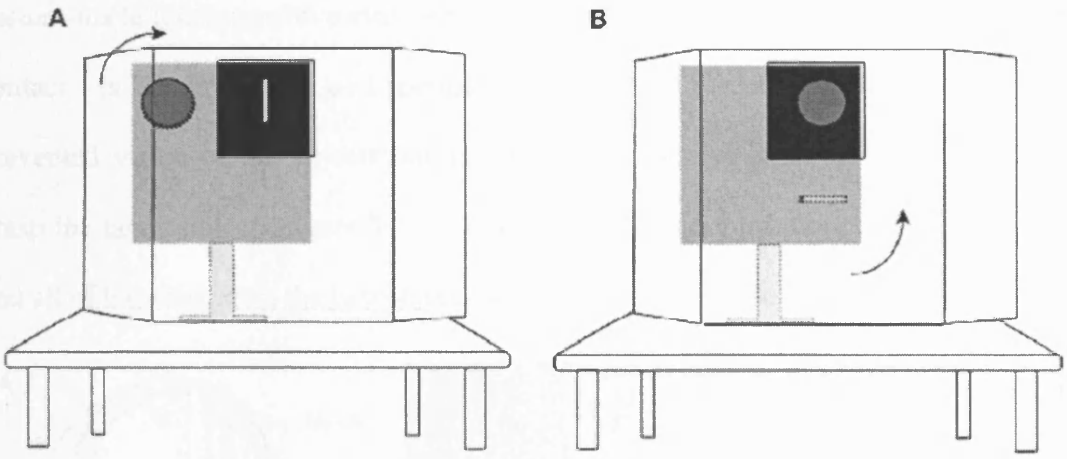

Figure 5.1 Experimental apparatus for serial presentation of objects.
A board with a 20 cm^2 aperture was placed in front of a rotatable device on which a vertically orientated handle (9 cm high, 5 cm deep) and a disc (12 cm diameter, 2 cm deep) were mounted at a viewing distance of 50 cm from the subject. If the board was rotated clockwise (A to B) the disc was visible, and anticlockwise (B to A) the handle was visible. Participants wore computer-controlled visual occlusion spectacles to prevent vision during the intertrial interval.

5.2.2 Simultaneous presentation of objects

Subjects were seated in a dimly lit room in front of two Perspex objects, a handle and a disc, that were simultaneously presented (Figure 5.2A). To ensure the same reach direction the handle was inserted within the ring. Objects were embedded with El Wire (Pacel Electronics Ltd, Poole) so that they could be independently illuminated. The El Wire produced interference with the EMG recording toward the end of Experiment 5 and was replaced with light emitting diodes (LEDs) for Experiment 6 (Figure 5.2B, C). The subject's right hand rested pronated on a custom-made homepad, a switch that was activated by the downward pressure of the hand. This was positioned at waist level, to the right of the body midline. Subjects were asked to reach out and grasp the object with their right hand as soon as they heard the 'go' signal and hold the object for ~0.5 s. A

custom-made touch-sensitive electronic circuit was used to determine the time of object contact. In the first block of Experiment 5 a box was placed over the objects. This prevented vision of the objects but an opening, below eye-level, allowed subjects to grasp the target object (Figure 5.2D). For the second and third blocks of Experiment 5 and all of Experiment 6, the two objects were continually visible (Figure 5.2E).

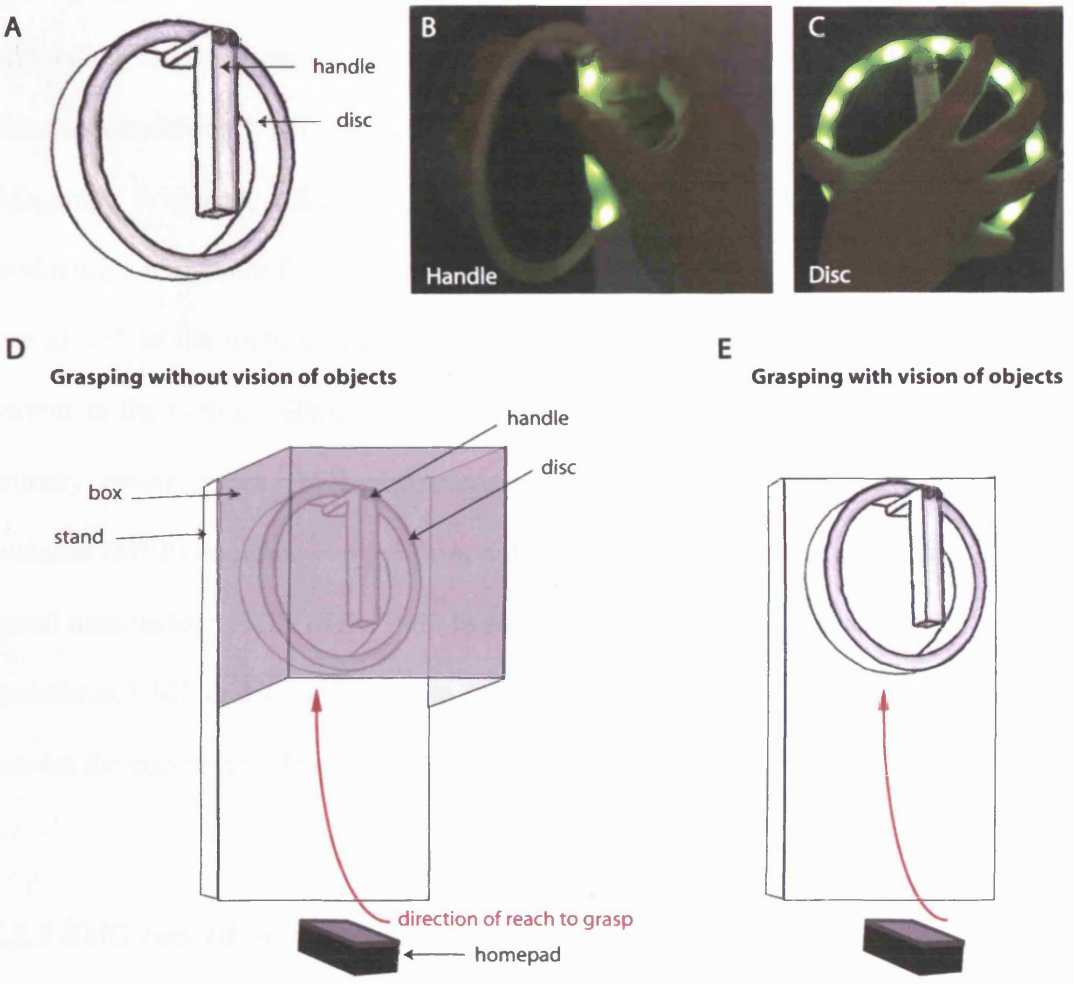

Figure 5.2 Simultaneous presentation of the handle and disc.

A, to ensure the same reach direction a vertically orientated handle (9 cm high, 5 cm deep) was positioned inside a disc (12 cm diameter, 2 cm deep). The handle (B) and disc (C) could be independently illuminated. D, in the first block of Experiment 5 a box prevented vision of the target object. E, for the second and third block of Experiment 5 and for all of Experiment 6, the box was removed so there was vision of both objects for the duration of each block. For all experiments subjects were instructed to rest their right hand on a homepad until the cue to grasp (TMS) was given.

5.3 Experimental procedures

5.3.1 Transcranial magnetic stimulation

TMS pulses were delivered using the same paradigm as that used by Cattaneo *et al.* (2005) with single-pulse (130% resting motor threshold (RMT) (Rossini *et al.*, 1994)) or paired-pulse (130 and 90% RMT for the first and second stimulus, respectively) stimulation at interstimulus intervals (ISIs) of 1.3, 2.5 and 4.1 ms giving four TMS stimulus conditions. TMS pulses were delivered using two Magstim 200 stimulators (Magstim, Whitland, UK) through one figure-of-eight TMS coil (7 cm diameter) producing a maximum field strength from each stimulator of 2.2 Tesla. The coil handle was at 45° to the midline, pointing laterally and backwards with an induced anterior current in the cortex. Stimuli were applied to the "hotspot" on the scalp over the left primary motor cortex (M1) characterised as where a low threshold motor evoked potential (MEP) could be evoked from both the abductor digiti minimi (ADM) and first dorsal interosseous (1DI) of the right hand. For sham TMS, the coil was placed over the contralateral M1 and tilted at 90° to the scalp with both wings touching the head to prevent the cortex from being stimulated (Lisanby *et al.*, 2001).

5.3.2 EMG recording

Electromyographic (EMG) activity was recorded using bipolar (belly-tendon) surface electrodes (Kendall H59P electrodes, Tyco Healthcare Group LP, Mansfield, U.S.A.) over ADM and 1DI muscles.

5.3.3 Object illumination and auditory signals

CED Signal software (Cambridge Electronic Design Ltd, Cambridge) triggered object illumination via the digital output of the 1401 data acquisition interface (Cambridge Electronic Design Ltd, Cambridge). When an auditory tone was required, a sine wave generated by CED Signal software was sent through the computer's speakers.

5.3.4 Data capture

The time of homepad release, object contact time, MEP and EMG activity were recorded using CED Signal software. MEP and EMG activity was amplified at 500x and highpass filtered at 3 Hz (Neurolog EMG amplifier, NL824, and isolator amplifier, NL820, Digitimer Ltd, UK). Data were sampled at 4 kHz via the 1401 data acquisition interface and recorded to the computer's hard disc.

5.4 Experimental protocols

To help subjects maintain attention and to minimise the number of TMS pulses delivered, the experiments were designed to keep sessions brief. Subjects were asked to fixate on the target object and to ignore the TMS pulse if it was not the 'go' signal. Objects and TMS stimulus conditions were presented in pseudorandom order. Blocks were counterbalanced across subjects. There was always at least 6 s between TMS pulses in separate trials.

5.4.1 Protocol 1: Serial presentation of objects

For all experiments objects were presented individually (Figure 5.1). Subjects were asked to grasp the object in a self-paced manner. There were eight trials per object and TMS stimulus conditions. In experiments 1, 2 and 4 all four TMS stimulus conditions were used.

Experiment 1: In two groups of 10 subjects, the object × muscle interaction of the MEP was examined at different times after object presentation. Subjects performed four blocks. In the first two blocks, subjects observed the objects. In one block TMS was delivered at 50 ms, in the other at 100 ms after object presentation (Group A) or at 150 ms and 800 ms (Group B). In two subsequent blocks subjects grasped the objects on delivery of TMS (Figure 5.3A). The time of TMS delivery (50 and 100 ms or 150 and 800 ms) alternated between blocks in a 2x2 factorial design, so each TMS delivery time was represented in an observation and grasp block. TMS timings were counterbalanced within Group.

Experiment 1a (10 subjects): To investigate any behavioural effects of TMS, single-pulse sham TMS at 65% of stimulator output was delivered, in counterbalanced blocks, at 50 and 800 ms after object presentation as the cue to grasp.

Experiment 2 (eight subjects): Examined whether the object × muscle interaction of the MEP represented sustained activation in the 150-800 ms period after object presentation. The cue to grasp was a 100 ms long tone (250 Hz) given at 1200 ms after object presentation. TMS occurred in 75% of trials in counterbalanced blocks at 150 and 800 ms after object presentation. To encourage subjects to prepare throughout the trial, the imperative signal occurred at 250 or 2000 ms in 16 trials, during which only single-pulse

TMS was delivered. Eight 'no TMS' trials occurred when the 'go' signal was at 250 or 2000 ms and for 16 trials 'no TMS' trials when the 'go' signal occurred 1200 ms after object presentation (Figure 5.3B).

Experiment 3: To test the effect of unpredictable TMS, eight subjects performed a task where objects and TMS stimulus conditions were presented in random order. Single- and paired-pulse (only ISI 2.5 ms) TMS served as the cue to grasp and occurred once per object and TMS stimulation condition at 90 ms intervals in a 150-780 ms window after object presentation (Figure 5.3C). To increase the unpredictability of the imperative cue, there was no TMS in two additional trials.

Experiment 4 (12 subjects, seven were naïve, five subjects had previously taken part in Experiment 2 or 3): investigated whether the object × muscle interaction of the MEP occurred with stimulation of ipsilateral M1. TMS delivered at 1200 ms after object presentation, to the right motor cortex, was the cue to grasp with the right hand (Figure 5.3D).

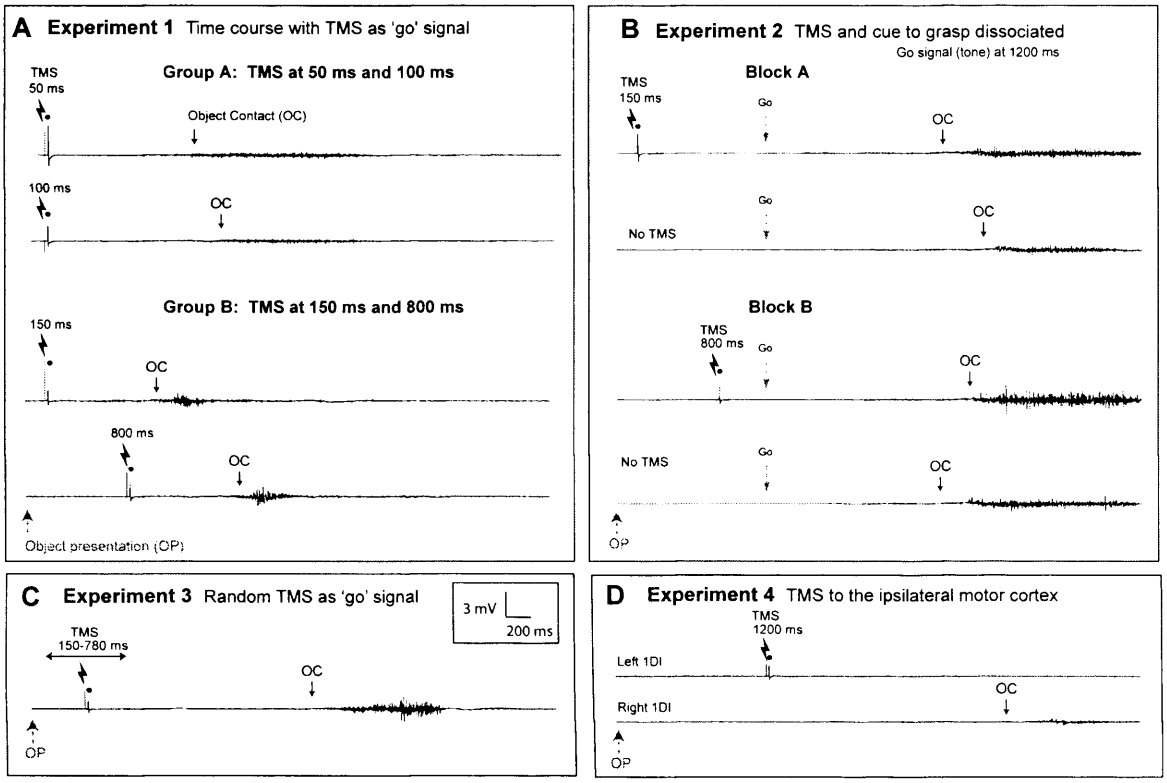

Figure 5.3 Muscle activity (single trial) recorded from the first dorsal interosseous (1DI) of the right hand during grasp of the handle, illustrating Experiments 1 to 4.

A, Experiment 1. In two groups of 10 subjects MEPs (•) were evoked first during object observation (two blocks), and then grasp (two blocks) with TMS delivery being the cue to grasp. TMS was delivered in two counterbalanced blocks of 50 and 100 ms (Group A) and 150 and 800 ms (Group B) after visual presentation of the object (OP). B, Experiment 2. Eight subjects in two counterbalanced blocks (TMS at 150 ms and 800 ms after object presentation), grasped the objects on hearing a 100 ms tone which could occur randomly at 1200 ms (80 of trials), 250 ms (8 trials) and 2000 ms (8 trials). For 25% of trials there was no TMS. C, in Experiment 3 (eight subjects) TMS (as the cue to grasp) was delivered randomly at one of eight time points within a window 150-780 ms after object presentation. Trials without TMS occurred once per object. D, Experiment 4 (12 subjects). TMS delivered 1200 ms after visual presentation to the right motor cortex was the cue to grasp with the right hand. Note, as these were not reaction time studies there was considerable variation in the interval between object presentation and object contact (OC) time.

5.4.2 Protocol 2: Simultaneous presentation of objects

Subjects were asked to grasp the object as soon as they heard the 'go' signal. There were two TMS stimulus conditions (single-pulse and paired-pulse TMS at ISI 2.5 ms) with 10 trials per object and TMS stimulus condition. Prior to the experimental blocks, a training block was run during which subjects were given feedback on pre-movement EMG levels. To avoid the subject being given unnecessary TMS pulses, for the training block single-pulse sham TMS at 130% RMT was used instead of real TMS. Training was repeated until subjects could perform the task satisfactorily.

Experiment 5 (eight subjects): Investigated whether the object-specific modulation of the paired-pulse MEP was specific to the visual modality. Initially, subjects were not allowed to see the objects. A box placed over the objects prevented vision but allowed subjects to easily grasp the target object through an opening at its base (Figure 5.2D). Prior to the training block, subjects explored the objects haptically and learnt which shape was designated by the two different 200 ms tones (a high (500 Hz) or low tone (200 Hz)). A training block of 14 trials (seven per object) was then carried out to ensure subjects understood the task. In the first experimental block, a 200 ms tone at the start of the trial indicated which object to grasp; there was still no vision of the object. For the subsequent two blocks, the box was removed allowing subjects to see the objects (Figure 5.2E). For one block the target object was designated by a 200 ms tone, for the other a 200 ms illumination at the start of the trial indicated the target object. For all blocks the cue to grasp was TMS delivered 1200 ms from the start of the trial (Figure

5.4A). The object specified by each tone was counterbalanced across subjects, as were the final two blocks.

Experiment 6 (12 subjects): This examined the importance of current visual input to the object-specific modulation of the MEP. Trials started with object illumination, either for 200 ms, in one block, or 5 s, for the other block. Blocks were counterbalanced across subjects. TMS delivered 1200 ms after object illumination was the cue to reach out and grasp the object that was still or had been illuminated. Therefore, for the 200 ms block, subjects were required to remember the target object for 1 s (memory-cued) but not for the 5 s block (visually-driven condition) (Figure 5.4B). In the training block (12 trials) the target object altered between the two objects at random and was designated in the same manner as the first experimental block for that subject.

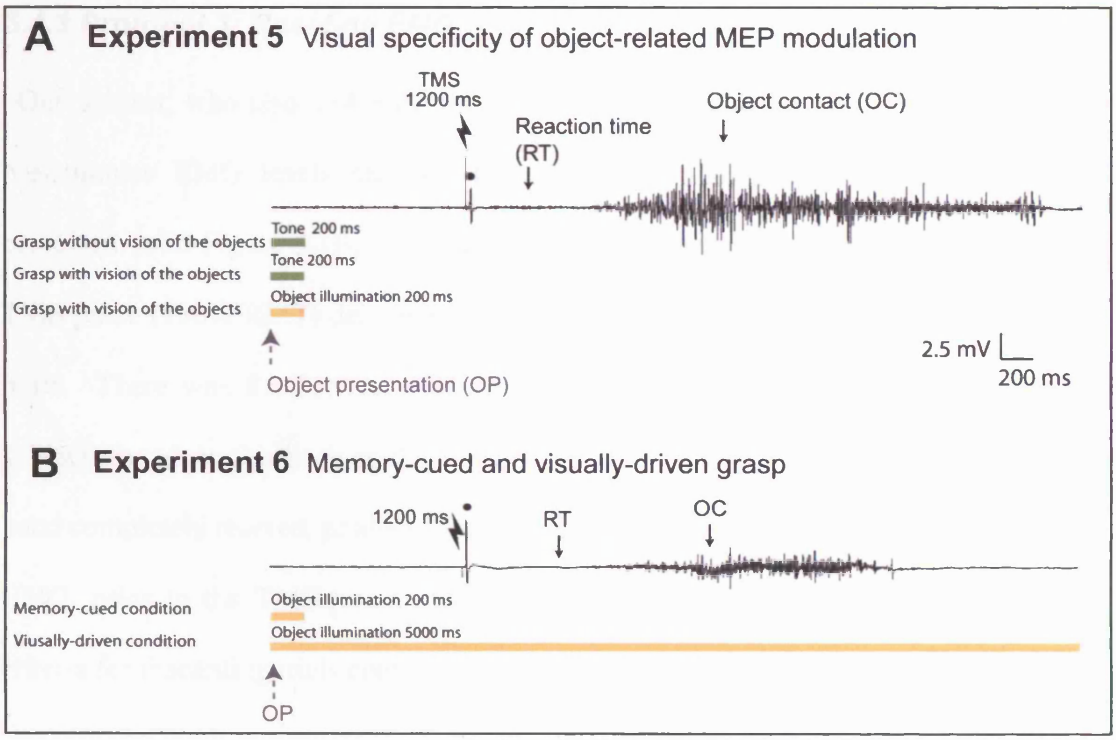

Figure 5.4 Muscle activity (single trial) recorded from the abductor digiti minimi (ADM) of the right hand during grasp of the disc illustrating Experiments 5 and 6.

A, initially subjects were not allowed to see the objects (see Section 5.2.2.) instead prior to the experimental blocks, they haptically explored the objects they would then have to grasp. In the first block the target object was designated by a 200 ms tone at the start of the trial, there was no vision of the object. In the subsequent two counterbalanced blocks subjects could see both objects and the target object was either designated by a 200 ms tone or 200 ms object illumination. For all three blocks TMS delivered at 1200 ms was the cue to grasp. B, at the start of the trial the target object would illuminate either briefly (200 ms) in the memory-cued block, or remain illuminated throughout the trial (5 s) in the visually-driven block. TMS at 1200 ms was the cue to grasp. Blocks were counterbalanced across subjects. MEPs indicated by ●.

5.4.3 Protocol 3: Baseline EMG

One subject, who also took part in Experiment 6, was used to assess the effect of the pre-stimulus EMG levels on the MEP amplitude. The subject grasped the disc, presented as in Figure 5.1B, with the right hand. The cue to grasp was a single-pulse TMS pulse (130% RMT) delivered to the left motor cortex. The subject performed 64 trials. There was 8 s between TMS pulses. Throughout the experimental block the subject was given feedback on the required EMG levels and was asked to keep the right hand completely relaxed, produce a moderate amount of EMG or produce a high level of EMG, prior to the TMS pulse. Data from this subject were then used to guide the criteria for discarding trials contaminated by ongoing EMG activity (Section 5.5.5).

5.5 Data analysis

For all statistical tests the significance level was taken as $p \leq 0.05$, so a p-value of >0.05 was non-significant.

5.5.1 MEPs

The peak-to-peak amplitude of MEPs was measured off-line using custom made software NuCusor (supplied by Prof J Rothwell, UCL). CED Signal software was used to measure and visually assess pre-stimulus EMG levels. To avoid the MEP size being influenced by any ongoing EMG activity, trials with EMG activity in the 150 ms preceding the TMS pulse were discarded (see also Section 5.5.5). Additionally MEPs

from Protocol 1 were discarded if electrical artefacts from the visual occlusion spectacles overlay the MEP. Overall, 6% of trials were not used in subsequent analysis.

Statistical analysis was performed on a MEP 'facilitation ratio' (paired-pulse MEP/single-pulse MEP). This was calculated within-subjects and blocks for each muscle, object and paired-pulse (ISI 1.3, 2.5 and 4.1 ms) condition. If significant, an object-specificity index was calculated to assess the relative changes in single- and paired-pulse MEP within the MEP facilitation ratio, as detailed below.

Experiment 1: A four-way repeated measures ANOVA was performed using within-subject factors of grasp (grasp vs. observation), ISI (1.3 ms vs. 2.5 ms vs. 4.1 ms), object (handle vs. disc) and muscle (ADM vs. 1DI) for each TMS delivery condition (50 ms, 100 ms, 150 ms and 800 ms). Three follow-up ANOVAs were performed to identify the key object × muscle interactions in specific grasp, ISI and TMS delivery conditions. First, a three-way within-subjects ANOVA investigated observation and grasp conditions when TMS was delivered at 150 and 800 ms using the within-subject factors of ISI, object and muscle. A second ANOVA examined each ISI interval for TMS at 150 and 800 ms in the grasp condition using the within-subject factors of object and muscle. The differential effect of long (150 and 800 ms) and short (50 and 100 ms) TMS delivery times at ISI 2.5 ms was then compared in the third ANOVA, with factors of TMS delivery, object, muscle and the between-subjects factor of interval (long vs. short). Lastly, percentage MEP facilitation values were used to illustrate the contributions of single- and paired-pulse TMS (ISI 2.5 ms) to the MEP facilitation ratio.

To provide a measure of object-specificity, each subject's average MEP for each object was divided by the sum of the average MEP for both objects and expressed as a percentage. Therefore an object-specificity index of 50% would indicate no difference in MEP amplitude between the handle and disc, a null, zero-specificity value. The object-specificity index was calculated separately for each muscle and TMS pulse type (single- and paired-pulse). As the percentage contribution for the disc was dependent on the percentage contribution for the handle, a significant effect on the t-test for the handle was equivalent to an object × TMS pulse type interaction for that muscle.

Experiments 2, 3, and 5: Repeated measures ANOVAs were performed, within block, on the MEP facilitation ratios for the within-subject factors of object and muscle. For Experiment 2 this was performed for each ISI interval. In Experiment 3 (random TMS), data from the different time bins were first pooled according to TMS stimulus condition, giving eight trials per single- and paired-pulse TMS condition.

Experiment 4: A repeated measures ANOVA was performed on the MEP facilitation ratios for the within-subjects factors of ISI, object and muscle. The effect of stimulation of ipsilateral and contralateral sides, when TMS was delivered 1200 ms after object presentation, was compared. The data from contralateral TMS at 1200 ms after object presentation was previously recorded by Cattaneo *et al.* (2005). A repeated measures ANOVA was performed on the MEP facilitation ratio at ISI 2.5 ms for the within-subject factors of object and muscle and the between-subject factors of hemisphere (ipsilateral vs. contralateral).

Experiment 6: A repeated measures ANOVA was performed on the MEP facilitation ratios for the within-subjects factors of visual condition (visually-driven vs. memory-cued), object and muscle. The object-specificity index was calculated within-subjects for each muscle, visual condition and TMS pulse type (single- and paired-pulse). A three-way within-subject repeated measures ANOVA was performed on the object-specificity index for the factors of muscle, visual condition and TMS pulse type. To isolate the significant effect, for each muscle, two-way within-subject ANOVAs were performed for the factors of visual condition and TMS pulse type. If significant, a paired t-test was performed within muscle and TMS pulse type for visual condition (visually-driven vs. memory-cued).

5.5.2 EMG

EMG activity from each grasp trial was high-pass filtered (40 Hz) and rectified using CED Signal software. A custom-made MATLAB (Mathworks, Massachusetts) program was used to calculate the integrated EMG activity for the hand pre-shaping phase, the 300 ms preceding object contact. EMG activity for each trial was normalised to that subject's average EMG in that muscle across grasp of both objects. EMG levels were normalised across conditions for each subject to remove individual differences in mean EMG level and highlight differences between conditions. Normalising relative to the pooled-object EMG in this way meant that EMG values for the handle were no longer independent from EMG values for the disc. Therefore, to test for specific involvement of each muscle in grasping each object, paired t-tests were performed on each block comparing ADM (handle) and 1DI (handle). To test whether there was a differential

effect of object within a muscle, paired t-tests were performed between grasp of handle and disc for that muscle. When several such tests were performed Bonferroni correction was used, and the corrected probability values reported. The rectified and integrated EMG activity was calculated from 10-20 trials per object and subject. Statistical analysis of EMG data for TMS at 100 and 150 ms (Experiment 1) was from nine subjects and from 11 subjects for the ipsilateral TMS study (Experiment 4), due to poorly defined object contact artefact in three subjects. In Experiment 4, five trials per object were used in two subjects due to technical difficulties with object contact. Due to problems of electrical interference of the El Wire, EMG analysis was not performed on one subject from Experiment 5.

5.5.3 Object contact

Initially, for Experiments 1, 1a and 2, a within-subject repeated measures ANOVA was performed for the factors of object (handle vs. disc) and TMS delivery time (50 vs. 100 ms, 150 vs. 800 ms, 50 vs. 800 ms). Subsequent analyses were then performed:

Experiment 1: Data from TMS delivery time was divided into short (50 and 100 ms) and long (150 and 800 ms) intervals. A repeated measures ANOVA was performed with the additional between-subject factor of interval (short vs. long). The effect of single- and paired-pulse (ISI 2.5 ms) TMS on object contact times was examined in Experiment 1 when TMS was delivered at 50 ms. A repeated measures two-way ANOVA was performed for the within-subject factors of object and TMS condition (single- vs. paired-pulse).

Experiments 1 and 1a: A repeated measures ANOVA was performed with the additional between-subject factor TMS (TMS vs. no TMS) for TMS at 50 and 800 ms after object presentation.

For Experiment 4, a paired t-test was performed comparing object contact times for the handle and disc. Data from Experiment 5 were analysed using a within-subject repeated measures two-way ANOVA with the factors of object and block type (no vision tone vs. vision tone vs. vision illumination).

Paired and independent t-tests were performed, as necessary. Statistical analysis of object contact time for TMS at 100 and 150 ms (Experiment 1) was from nine subjects and from 11 subjects for ipsilateral TMS study (Experiment 4) due to poorly defined object contact artefact in three subjects.

5.5.4 Reaction time

For Experiments 1 and 3 the timing of the first EMG activity after the 'go' signal was used as a measure of reaction time (RT). In Experiment 1 the mean RT, using pooled data from TMS at 150 and 800 ms, was calculated for each subject. An independent t-test compared RT in random and blocked conditions. In Experiments 5 and 6 homepad release was used to measure RT. A repeated measures two-way ANOVA with the within-subject factors of object and either block type (no vision tone vs. vision tone vs. vision illumination) for Experiment 5, or visual condition (visually-driven vs. memory-cued) for Experiment 6, was performed.

5.5.5 Discarded trials

The pre-stimulus EMG level was assessed by eye for all Experiments (Method 1). To examine whether this produced any bias in the trials discarded, a cut-off value was also calculated using data collected from Protocol 3 (Section, 5.4.3). CED Signal software was used to high-pass filter (40 Hz), rectify and measure the pre-stimulus EMG activity. The maximum amplitude of EMG activity in the 150 ms prior to the TMS pulse was calculated for each trial. Trials were then grouped according to the level of pre-stimulus EMG: absent, slight (0.02-0.04 mV), or clear (>0.05 mV). To determine which level of pre-stimulus EMG produced a significant increase in MEP amplitude, independent t-tests compared the MEP amplitude between absent vs. slight EMG conditions and absent vs. clear EMG conditions. This was used to establish a cut-off value, if pre-stimulus EMG 150 ms prior to the TMS pulse was greater than this value the trial would be discarded (Method 2). The difference in MEP amplitude using the two methods was examined by comparing the MEP facilitation ratio at ISI 2.5 in the grasping condition of Experiment 1 for each of the four blocks. A three-way repeated measures ANOVA using the within-subject factors of object, muscle and method (method 1 vs. method 2) was performed separately for each block.

6. Excitability of human motor cortex outputs prior to grasp

6.1 Introduction

Previous studies using electrical stimulation of the cortex in lightly sedated and anesthetised non-human primates have shown that when an F5 stimulus conditioned an M1 test stimulus there was specific enhancement of the late I-wave (I_2, I_3) components of the corticospinal volley (Shimazu *et al.*, 2004) and of the resulting EMG response (Cerri *et al.*, 2003). In Chapter 4 the task-related nature of this enhancement was investigated in Macaque monkeys performing visuomotor grasp. In this Chapter, TMS is used to facilitate the late I-wave pathways prior to object-orientated grasp in normal human volunteers.

Paired-pulse TMS over M1, suprathreshold (130% of RMT) followed by a subthreshold (90% of RMT) stimulus (Ziemann *et al.*, 1998a), enhances the late I-waves of the corticospinal volley in humans (di Lazzaro *et al.*, 1999c). In non-human primates enhancement of the late I-waves was produced by electrical stimulation to F5-M1 (Cerri *et al.*, 2003; Shimazu *et al.*, 2004) and it has been suggested that the late I-waves elicited from TMS to M1 may arise from cortico-cortical pathways that include inputs from the premotor cortex (Amassian *et al.*, 1987; di Lazzaro *et al.*, 1999c; Hanajima *et al.*, 2002; Ziemann *et al.*, 1998a). However, any comparison of the human and non-human primate work must be made with caution as there are differences between the human ventral premotor cortex and F5 of the macaque monkey (see Section 1.2.2, Introduction)

and furthermore, different stimulation paradigms were used to produce an enhancement of the late I-waves in the two species. Additionally, while the inputs facilitated by TMS may include the ventral premotor cortex, it is likely that cortico-cortical pathways from other regions are also facilitated. Importantly these other cortical regions may also have a role in visuomotor grasp, for instance there is evidence for the involvement of the dorsal premotor cortex when lifting an object (Davare *et al.*, 2006).

A recent study investigated whether the paired-pulse MEP, from TMS over M1, was modulated by the upcoming grasp (Cattaneo *et al.*, 2005). TMS 1200 ms after presentation of either a handle or a disc was the 'go' signal. The resultant MEPs, elicited 600 ms prior to movement onset, predicted the subsequent EMG pattern used to shape the hand for grasp. Prior to grasping the disc, there was facilitation of the paired-pulse MEP in ADM, relative to the MEP prior to grasping the handle, while in 1DI the amplitude of the MEP evoked prior to grasp of the handle was greater compared to that for the disc. Control experiments involving equivalent hand and digit movements, but without a visible and graspable object, failed to produce MEP interactions, as did object observation without subsequent grasp. This suggests that the inputs to M1 facilitated by paired-pulse TMS were concerned with object-orientated grasp. In contrast, single-pulse TMS, which enhances the I_1-wave (Sakai *et al.*, 1997), showed the opposite pattern. In pre-cued reaction time (RT) tasks there was suppression of the single-pulse MEP elicited in the preparation period, that is the time between the warning signal and response signal (Hasbroucq *et al.*, 1997; Hasbroucq *et al.*, 1999; Touge *et al.*, 1998), but such suppression has not so far been shown during grasp. Here paired-pulse and single-pulse

TMS was used to investigate the time course of object-related excitability of cortico-cortical inputs to M1 and the importance of visual inputs for the object-specific modulation of MEPs, reported by Cattaneo *et al.* (2005).

In the first set of experiments, using serially presented objects, the precise temporal resolution of TMS was used to examine the time course of the object-specific MEP modulation and to test whether this excitability of inputs to M1 was confined to the contralateral motor cortex. In Experiment 1, the question of when the object-specific facilitation first occurs and the contribution of the single-pulse and paired-pulse MEP to the object-related facilitation were investigated. TMS was delivered in blocks at 50, 100, 150 and 800 ms after object presentation. If the inputs to M1 that were facilitated by paired-pulse TMS are concerned with transmitting visuomotor information, the object-related facilitation should not occur at the early intervals as previous studies have shown it takes approximately 100 ms for visual cues to reach frontal areas (Schluter *et al.*, 1998; Terao *et al.*, 1998a), therefore there would not be enough time for the transmission of visual information from visual to motor areas.

Experiments 2 and 3 addressed whether the inputs to M1 reflected sustained activation or if the motor commands were sent to M1 immediately prior to the execution of grasp. This question arises from recordings during delayed response experiments in monkeys that have shown two distinct neuronal firing patterns in the dorsal and ventral premotor cortex that could modulate M1 excitability. Firstly, there is tonic, set-related firing of neurones that is sustained or builds up from the instruction cue to the approaching 'go'

signal (Crammond and Kalaska, 2000; Murata *et al.*, 1997; Wise and Mauritz, 1985). Secondly neurones can show phasic activation, with excitation on object presentation and/or movement initiation (Rizzolatti and Luppino, 2001; Weinrich and Wise, 1982). Either of these excitation patterns could be present in M1 inputs prior to grasp. The results from Experiment 1-3 have been previously published (Prabhu *et al.*, 2007b).

The final experiment in this set examined whether object-specific modulation could be elicited from the hemisphere ipsilateral to the grasping hand. Interhemispheric inhibition (IHI) has been shown using a conditioning TMS pulse over the ipsilateral hemisphere which reduces the MEP amplitude to a test stimulus over the contralateral hemisphere at ISIs of 6-50 ms (Chen *et al.*, 2003; Duque *et al.*, 2007; Ferbert *et al.*, 1992; Gerloff *et al.*, 1998; Hanajima *et al.*, 2001). Callosal efferents connecting contralateral M1 to the homologous area in the ipsilateral cortex (Jones and Wise, 1977) provide possible pathways for IHI. The lack of such inhibition with electrical test stimuli supports a callosal mechanism, operating at the cortical level, for this inhibition (di Lazzaro *et al.*, 1999a; Ferbert *et al.*, 1992), although a sub-cortical mechanism cannot be entirely ruled out (Gerloff *et al.*, 1998). As well as changes in ipsilateral motor cortex excitability during rest, simple finger movements have also produced changes in MEP amplitude. For instance, when subjects made unilateral movements of a digit, the single-pulse MEPs of the resting homologous muscle were reduced (Duque *et al.*, 2005; Leocani *et al.*, 2000; van den Hurk *et al.*, 2007). Here changes during a more complex task of visuomotor grasp were assessed. In Experiment 4, changes to corticospinal excitability were examined in left 1DI and ADM muscles when single- and

paired-pulse TMS delivered to the right motor cortex was the 'go' signal to grasp with the right hand. A reversal of the object-muscle interaction prior to grasp would indicate inhibition of the ipsilateral hemisphere.

The second set of experiments, with simultaneously presented objects, examined the importance of visual signals in producing the differential MEP modulation in the two muscles. While there is strong evidence for visual information about an object being transformed into the correct motor prototype by the cortico-cortical grasp circuit (Binkofski *et al.*, 1999; Fogassi *et al.*, 2001; Gallese *et al.*, 1994; Murata *et al.*, 1997; Murata *et al.*, 2000; Raos *et al.*, 2006; Rizzolatti and Luppino, 2001; Umilta *et al.*, 2007), it is uncertain whether somatosensory information gained from haptic exploration of objects can be used by this circuit to produce a motor prototype. In the macaque monkey the ventral premotor cortex receives visual inputs via the posterior parietal cortex and has anatomical connections with the primary and secondary somatosensory regions (Matelli *et al.*, 1986; Tanne-Gariepy *et al.*, 2002). Accordingly, F5 neurones show responses to tactile stimulation (Graziano *et al.*, 1997; Rizzolatti *et al.*, 1988), but these could be used for feedback once the object is grasped. In a similar manner, the object-related facilitation of the paired-pulse MEP may either represent a mechanism concerned solely with visuomotor transformations or, alternatively, one which is more general, concerned with the transformation of geometric properties of objects into hand shapes. Experiment 5 attempted to resolve this question by investigating whether haptic exploration, without any vision of the objects, could produce object-specific modulations of the paired-pulse MEP.

In the final experiment visual information was modulated so the target object was either briefly illuminated (200 ms) at the start of the trial, so subjects were required to remember the target object for 1 s (memory-cued), or the target object was illuminated throughout the trial and therefore present during movement initiation (visually-driven). These two conditions should affect the ventral and dorsal visual processing streams differentially (Milner and Goodale, 1995). The dorsal stream is concerned with vision for action and involves different cortical structures to the ventral stream which processes vision for perception. Westwood and Goodale (2003) showed that, when memory of a target object is required, for example when the object was no longer visible, action patterns had characteristics normally associated with the ventral stream, such as sensitivity to illusions. This could reflect the absence of on-line visual information or different processes that are required to remember the target. In Experiment 6 both objects were continually visible, so that memory of the target object could be dissociated from visual presentation of the objects allowing the importance of these two factors to dorsal stream processing to be disentangled. The results from this experiment has been published (Prabhu *et al.*, 2007a).

6.2 MEPs excluded from analysis

To avoid the MEP being influenced by ongoing EMG activity, MEPs in trials with EMG activity in the 150 ms preceding the TMS pulse were excluded. For Experiment 1, trials were excluded by assessing the EMG activity by eye (Method 1). To investigate whether this was biasing the results, the MEP facilitation ratios (paired-pulse MEP/single-pulse MEP) from Experiment 1 obtained using Method 1 were compared to those using a cut-off value (Method 2). The cut-off value was obtained using data collected from one subject who grasped the disc, with TMS every 8 s as the cue to grasp (Protocol 3, Section 5.4.3, Methods 2). The subject was asked to either keep the right hand relaxed prior to the TMS pulse or to contract the muscles to varying degrees. In this way the effect of pre-stimulus EMG on MEP amplitude could be examined.

Figure 6.1 illustrates the mean MEP amplitude for the different pre-stimulus EMG levels in 1DI from Protocol 3. Only activity from 1DI was used as, unlike ADM, the EMG levels from this muscle could easily be divided into suitable groups. The pre-stimulus EMG was categorised as absent, slight (0.03-0.04 mV) or clear (0.05-0.26 mV). As shown below there was little change in MEP amplitude when there was slight EMG activity (Figure 6.1, light grey bar) to when there was no EMG activity (Figure 6.1, white bar). An independent t-test confirmed there was no significant difference ($p>0.05$) in MEP amplitude when there was slight pre-stimulus EMG compared to when the pre-stimulus EMG was absent. In contrast when the EMG activity was 0.05 mV or greater (Figure 6.1, dark grey bar), there was a significant increase in the amplitude of the MEP (clear EMG vs. no EMG, $p<0.05$) and the MEP amplitude showed more variability. The

larger range of pre-stimulus EMG values in the 'clear EMG' time bin could explain the large increase in MEP amplitude, however if only the 0.06-0.07 mV range (n=6) was included, the mean MEP amplitude was still 5.4 mV. Nevertheless, the smaller sample size for the 'clear EMG' condition compared to the 'slight' and 'no EMG' conditions (9, 29, and 25, respectively) may account for the larger standard error.

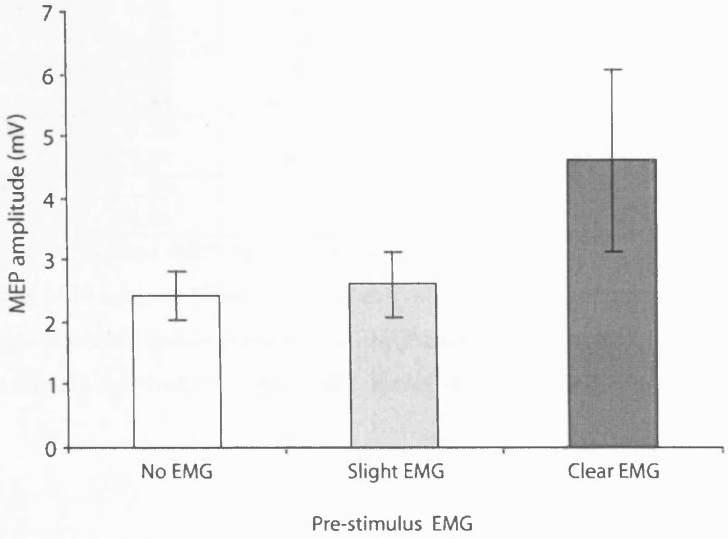

Figure 6.1 The effect of pre-stimulus EMG levels on MEP amplitude.
The average MEP amplitude (with standard error bars) from Protocol 3 for the three pre-stimulus EMG levels: absent (white bar), slight (light grey bar, 0.03-0.04 mV) or clear (dark grey bar, 0.05-0.26 mV).

As the MEP amplitude showed the largest increase when the pre-stimulus EMG level was >0.04 mV, this was the cut-off value chosen for Method 2. The paired-pulse MEP facilitation ratio (paired-pulse ISI 2.5 ms/single-pulse) in the grasp condition from Experiment 1, with TMS at 50, 100, 150 and 800 ms after object presentation, was then examined using Methods 1 and 2, these are shown in Table 6.1 along with a set of data containing all MEPs, regardless of EMG activity prior to the TMS pulse. A three-way within-subjects repeated measures ANOVA comparing Methods 1 and 2 (method × object × muscle) showed neither a significant main effect of Method nor any interaction

with Method. As Method 1 did not appear to be biasing the results, it was used for the subsequent experiments.

Table 6.1 Average MEP facilitation ratio for grasp trials in Experiment 1.

Time of TMS delivery	Object	ADM			1DI		
		Method 1	Method 2	All trials	Method 1	Method 2	All trials
50 ms	Handle	1.72	1.86	1.82	1.38	1.50	1.53
	Disc	1.60	1.69	1.74	1.39	1.49	1.54
100 ms	Handle	2.29	2.30	2.29	1.59	1.73	1.61
	Disc	1.84	2.11	2.09	1.52	1.68	1.55
150 ms	Handle	1.56	1.55	1.56	1.53	1.52	1.52
	Disc	1.88	1.88	1.81	1.48	1.44	1.43
800 ms	Handle	1.79	1.72	1.77	1.86	1.78	1.82
	Disc	2.04	2.10	1.96	1.64	1.64	1.58

The table illustrates the average MEP facilitation ratios (paired-pulse TMS at ISI 2.5 ms/single-pulse TMS) for two groups of 10 subjects (Group A, TMS delivered at 50 and 100 ms; Group B, at 150 and 800 ms) when trials were discarded due to pre-stimulus EMG determined by either visual inspection (Method 1) or an arbitrary cut-off (Method 2). 'All trials' shows the MEP facilitation ratio if no trials were excluded.

6.3 EMG activity during the task

Figure 6.2B illustrates the characteristic activation pattern produced when shaping the hand to grasp the two different objects in Experiment 1. In the 300 ms before object contact, abductor digiti minimi (ADM), which abducts and flexes the little finger, was more strongly activated for grasping the disc, and showed minimal activity for the handle (Experiment 1, all four TMS delivery times, paired t-test, $p \leq 0.05$, Bonferroni corrected). This differential activation of ADM was present for all six experiments. However, 1DI showed less clear and non-significant modulation. Overall, the crossed pattern of activation produced a significant object × muscle interaction in the 300 ms pre-contact period. This is clearly illustrated in Experiment 1 (Figure 6.2B: 50 ms: $p<0.05$; 100, 150 and 800 ms: $p<0.01$, Bonferroni corrected) and is present in all subsequent experiments.

6.4 Experiment 1: Time course of excitability of human motor cortex inputs

6.4.1 Overall MEP facilitation pattern

M1 excitability was investigated during object observation alone and prior to grasp with single- and paired-pulse (ISI 1.3, 2.5 and 4.1 ms) TMS at different times after object presentation. A repeated measures ANOVA was used to test whether manipulation of these factors resulted in an object × muscle interaction of the MEP facilitation ratio at the different TMS delivery times. At the earlier 50 and 100 ms intervals there was no significant object × muscle interaction for all combinations of grasp, ISI and object. For later TMS delivery at 150 and 800 ms there was a significant grasp × object × muscle interaction (both, $p<0.05$). How the pattern of MEP facilitation relates to these factors and to the ongoing muscle activity recorded during grasp, will be discussed.

6.4.2 Object observation vs. Preparation to grasp

Prior to the grasping task, subjects were instructed to just observe the object (Expt. 1, Section 5.4.1, Methods 2). For the later intervals, the significant object × muscle interaction of the MEP facilitation ratio ($p<0.01$) was not present during object observation alone, but was present prior to grasp (Figure 6.2A, E). The results suggest that the mechanism underpinning the interaction seen with TMS at 150 and 800 ms is preparation for active grasp of a visible object. As already noted, the early intervals did not show a significant effect.

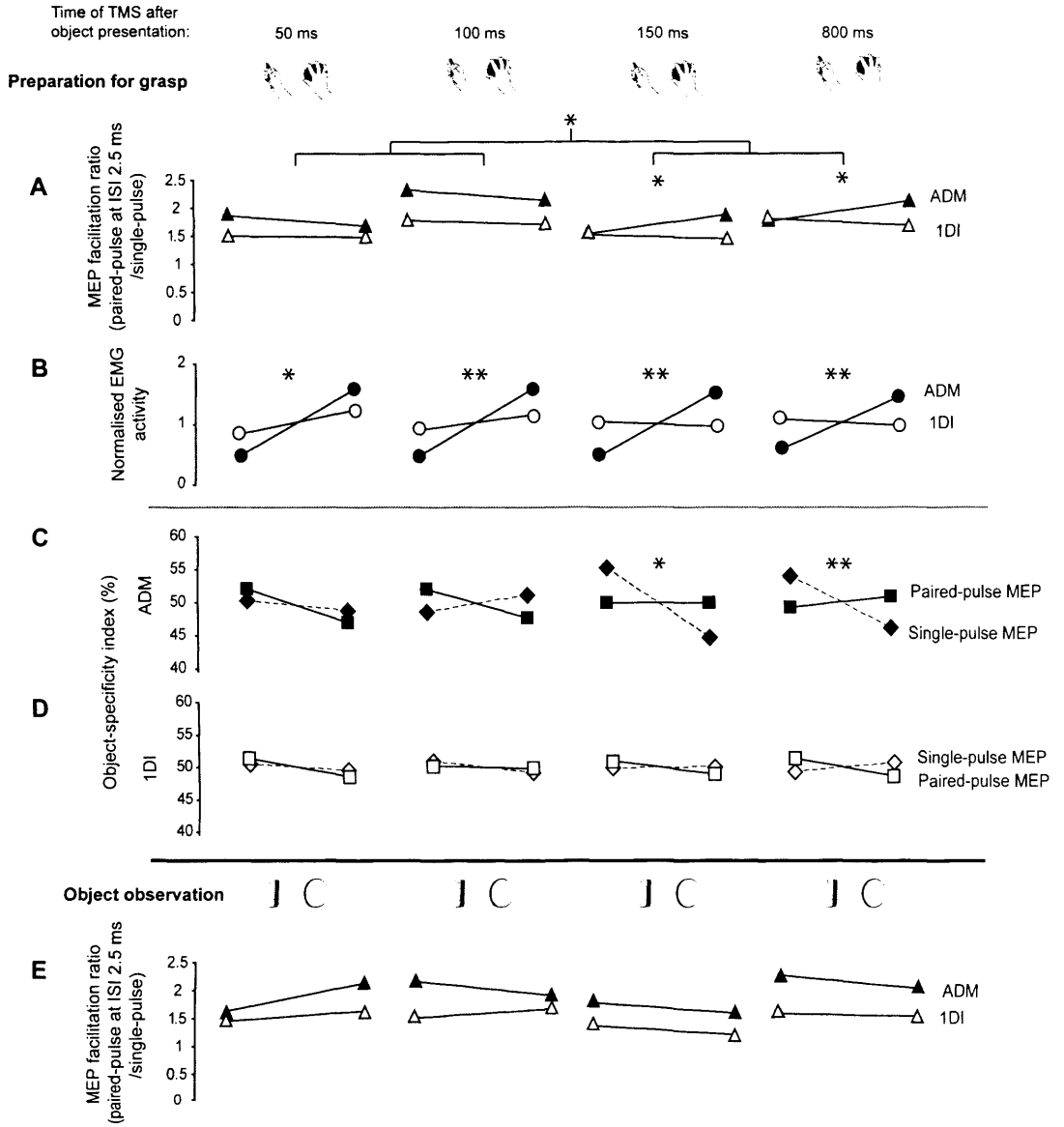

Figure 6.2 MEP facilitation (A, C, D and E) and normalised average EMG activity (B) for TMS delivery at four fixed time intervals after object presentation.

Row A represents the average MEP facilitation ratio (paired-pulse MEP at ISI 2.5 ms/single-pulse MEP) prior to grasp (n=10). B, shows the normalised integral of rectified EMG activity during the 300 ms preceding object contact (n=9-10). The object-specificity index prior to grasping the handle (average MEP for handle/(average MEP for the handle+average MEP for the disc)) and disc (average MEP for disc/(average MEP for the handle+average MEP for the disc)) for single- (dashed line, diamond symbols) and paired-pulse (solid line, squares) TMS is illustrated for ADM (C) and 1DI (D). These indices must sum to 100%, and the hypothesis for no object-specificity predicts a flat line at the 50% value. Row E shows the average MEP facilitation ratio during object observation alone (n=10). Throughout, filled symbols indicate activity recorded from ADM and open shapes from 1DI. * = $p < 0.05$, ** = $p < 0.01$.

6.4.3 The effect of interstimulus interval

Prior to grasp, for TMS at 150 and 800 ms, a significant object × muscle interaction occurred at ISI 2.5 ms (both, $p<0.05$) but not at ISI 1.3 or 4.1 ms. Figure 6.3 illustrates the changes in excitability evoked by paired-pulse TMS at different ISI intervals when TMS was delivered at 800 ms. At ISI 2.5 ms the modulation was more than double that of ISI 1.3 and 4.1 ms, which suggests a specific temporal interaction. This may reflect the selectivity of paired-pulse TMS at ISI 2.5 ms in enhancing the late I-waves of corticospinal activity (Cattaneo *et al.*, 2005; Shimazu *et al.*, 2004).

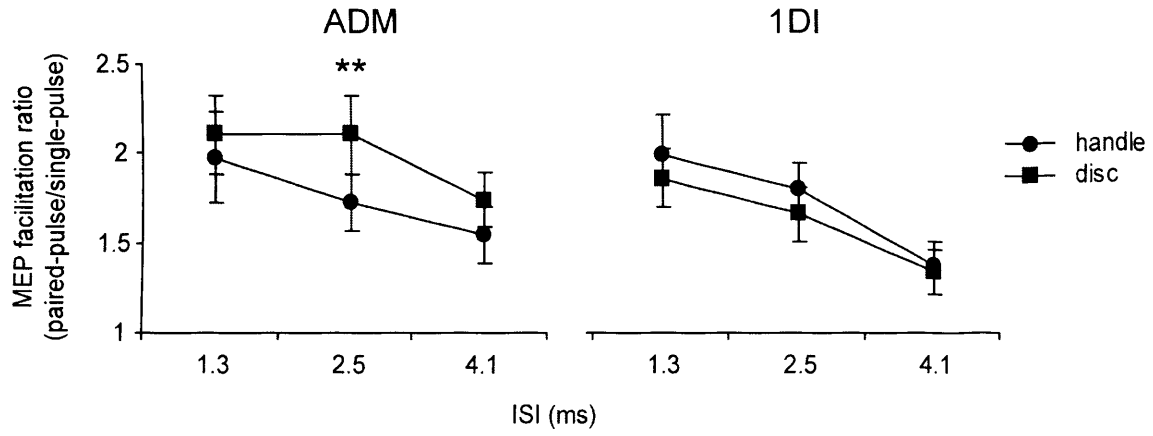

Figure 6.3 The MEP facilitation ratio at different interstimulus intervals (ISIs).
The average MEP facilitation ratio (paired-pulse MEP/single-pulse MEP) in 1DI and ADM prior to grasping the handle (circle) and disc (square) when paired-pulse TMS at ISI 1.3, 2.5 and 4.1 ms was delivered 800 ms after object presentation (n=10) with standard error bars. **= $p \leq 0.01$.

6.4.4 Time course of facilitation of MEPs during preparation to grasp

MEPs elicited prior to grasp showed a pattern which reflected three factors. These were: first, the muscle activity subsequently used by the subject to grasp the object, second, the TMS pulse type (single- or paired-pulse) and finally, the time of TMS delivery from object presentation.

The MEPs elicited by paired-pulse TMS (ISI 2.5 ms) delivered 800 ms after object presentation will be described first. To isolate the effect of the paired-pulse MEP (ISI 2.5 ms) from that of the single-pulse, an object-specificity index was calculated for each combination of TMS pulse type and muscle. The average MEP for each object was divided by the average MEP for both objects and expressed as a percentage. Notice that these indices must sum to 100% and the hypothesis of no object-specificity predicts an index value of 50%. Since the index values for the disc and handle are perfectly inversely correlated, ANOVA analysis was performed on the object-specificity indices for the handle (Section 5.5.1, Methods 2). The paired-pulse MEP, elicited 260-657 ms before movement onset, showed clear facilitation of the muscle that was preferentially activated during subsequent grasp of the object. Thus the MEPs were larger in ADM for the disc than the handle (Figure 6.2C, far right column). The single-pulse MEP showed the reverse pattern, indicating suppression of the muscle that was more highly activated during grasp of the object (Figure 6.2C). A significant paired t-test ($p=0.005$) comparing the single- and paired-pulse object-specificity indices represents an interaction of TMS pulse type × object for ADM. 1DI, which showed less differential

EMG activity for grasp of the two objects, did not show a significant effect (Figure 6.2D, 800 ms).

The timing of TMS delivery was important. There was a clear evolution of the object × TMS pulse type interaction of the object-specificity index in ADM in the period following object presentation. The interaction was absent at 50 and 100 ms, reaching significance at 150 ms ($p<0.05$) and still stronger significance at 800 ms ($p<0.01$; see above). For 1DI, there was no clear modulation of MEPs evoked by either single- and or paired-pulse TMS at any timing (Figure 6.2D). The contrasting effect of early and late TMS delivery on MEP modulation was confirmed by statistical analysis on the facilitation ratio: there was a significant interval (800 and 150 ms vs. 100 and 50 ms) × object × muscle interaction ($p<0.05$), reflecting the suppression by single-pulse TMS and facilitation by paired-pulse TMS at late but not at early delivery of TMS after object presentation, in ADM but not 1DI.

6.4.5 Effect of TMS on timing of grasp and EMG activity

When subjects were preparing to grasp the object, delivery of single- and paired-pulse TMS immediately after visual presentation (50 and 100 ms) appeared to have a disruptive effect on their grasping behaviour. This was not seen at later timings of TMS delivery (150 and 800 ms). The effects were observed in two behavioural measures. Firstly, while EMG activity in ADM and 1DI showed a reciprocal pattern for disc vs. handle for later TMS delivery (see Figure 6.2B, 150 and 800 ms), for TMS at 50 and 100 ms, both muscles showed greater activation for the disc (Figure 6.2B, left columns).

Secondly, the time of grasp onset (the time between the 'go' signal (TMS delivery) and object contact) was longer for early vs. late TMS (Figure 6.4, filled symbols). The EMG activity illustrating the TMS protocols (Figure 5.3) highlights the difference in object contact time in the four TMS delivery conditions when grasping the handle. This increase in object contact time with early TMS was even more marked when grasping the disc (Figure 6.4). The difference in object contact time for the handle and disc with early TMS was confirmed in a within-subjects repeated measures ANOVA with a significant main effect of object ($p<0.05$). Subsequent paired t-tests showed that this was significant at both 50 and 100 ms ($p=0.05$ and $p<0.05$, respectively). In contrast, for later TMS intervals (150 and 800 ms), there was neither a significant main effect of object nor a significant interaction of TMS time and object. A repeated measures ANOVA with the between-subject factor of interval (long (150 and 800 ms) vs. short (50 and 100 ms)) showed a main effect of object ($p<0.05$) but no significant main effect of or interaction with interval.

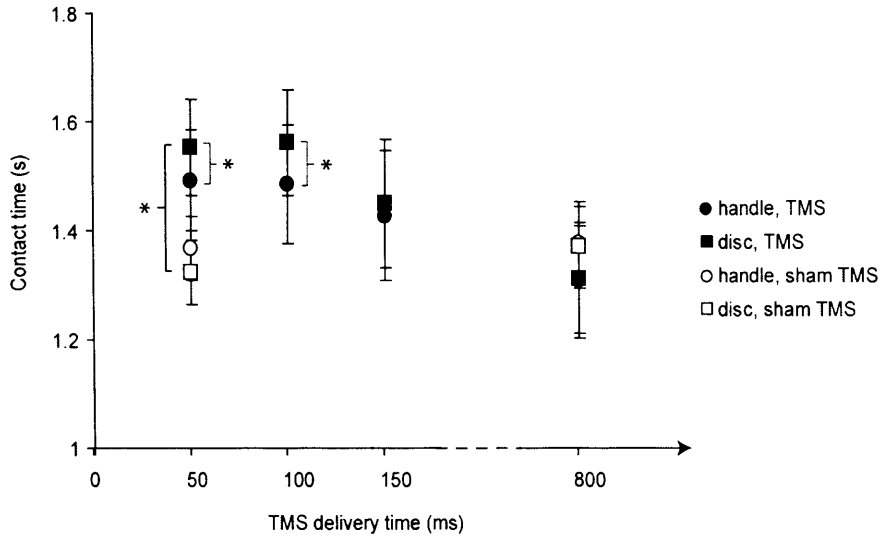

Figure 6.4 Object contact times for Experiments 1 and 1a.
Graph showing the mean time in seconds (with standard error bars) to grasp the handle (circle) and disc (square) after a 'go' signal (TMS delivery) at different times after object presentation. In Experiment 1, TMS was delivered in blocks to two groups of 10 naive subjects at 50 and 100 ms (Group A) and at 150 and 800 ms (Group B) after object presentation, (filled symbols; averages of all TMS conditions). In Experiment 1a, sham TMS (n=10) was delivered in two blocks, at 50 and 800 ms after object presentation (open symbols). n=9-10, * = $p \leq 0.05$.

As the changes in behaviour with early TMS could be related to the early timing of the 'go' signal rather than the delivery of TMS itself, the effect of sham TMS on subjects' performance was examined (Expt. 1a, Section 5.4.1, Methods 2). Sham TMS was delivered at 50 or 800 ms after object presentation (Figure 6.4; open symbols). There was no significant main effect on object contact times of object or sham TMS delivery time (50 vs. 800 ms), nor was there an object × sham TMS delivery time interaction. Between subjects analysis with data collected from Experiment 1a revealed a significant object × TMS (TMS vs. sham TMS) interaction at 50 ms ($p<0.05$) but not at 800 ms. Independent t-tests isolated this effect to increased object contact time for the disc with real TMS compared to sham (mean=1.55 s, SD$\pm$0.28 vs. 1.32$\pm$0.25 s, respectively,

$p<0.05$). The modulation of EMG according to the object grasped was significant for grasps after both real (paired t-test, $p<0.005$) and sham TMS (paired t-test, $p<0.001$), but only with real TMS at 50 ms was there increased EMG activity during grasp for the disc in both ADM and 1DI. These data all indicate that the disturbed pattern of EMG and object contact were due to TMS delivery rather than the requirement for subjects to reach and grasp almost immediately after object presentation.

The disruption at early TMS intervals may have been due to the increased sensitivity to paired-pulse stimulation. The effect of TMS condition (single- vs. paired-pulse) on object contact time was compared when TMS delivered 50 ms after object presentation. A repeated measures ANOVA showed a main effect of object ($p<0.05$) but no main effect of TMS condition and no interaction of object and TMS condition, suggesting the TMS paradigms did not differentially affect the movement times.

6.5 Experiment 2: Pattern of modulation of M1 inputs during the object presentation period

The second part of the study investigated whether modulation of M1 inputs was sustained throughout the period after visual presentation until the 'go' signal was given, or whether modulation occurred for only a brief period just prior to grasp. To distinguish between these two possibilities, the cue to grasp was dissociated from the delivery of TMS (Figure 5.3B, Expt. 2, Methods 2). An auditory cue, 1200 ms after object presentation, was now given as the 'go' signal and TMS was delivered in blocks at either 150 or 800 ms after object presentation; that is either 1050 or 400 ms before the auditory cue to grasp. For both timings, and in both ADM and 1DI, when TMS was dissociated from the cue to grasp, the object × muscle interaction of the MEP facilitation ratio evoked by paired-pulse TMS at ISI 2.5 ms was abolished (Expt. 2, Figure 6.5A). This was also true for the other ISI intervals (not shown in Figure 6.5). EMG activity during grasp, as previously, showed a significant object × muscle interaction (Figure 6.5B; 150 ms: $p<0.01$, 800 ms: $p<0.01$, Bonferroni corrected).

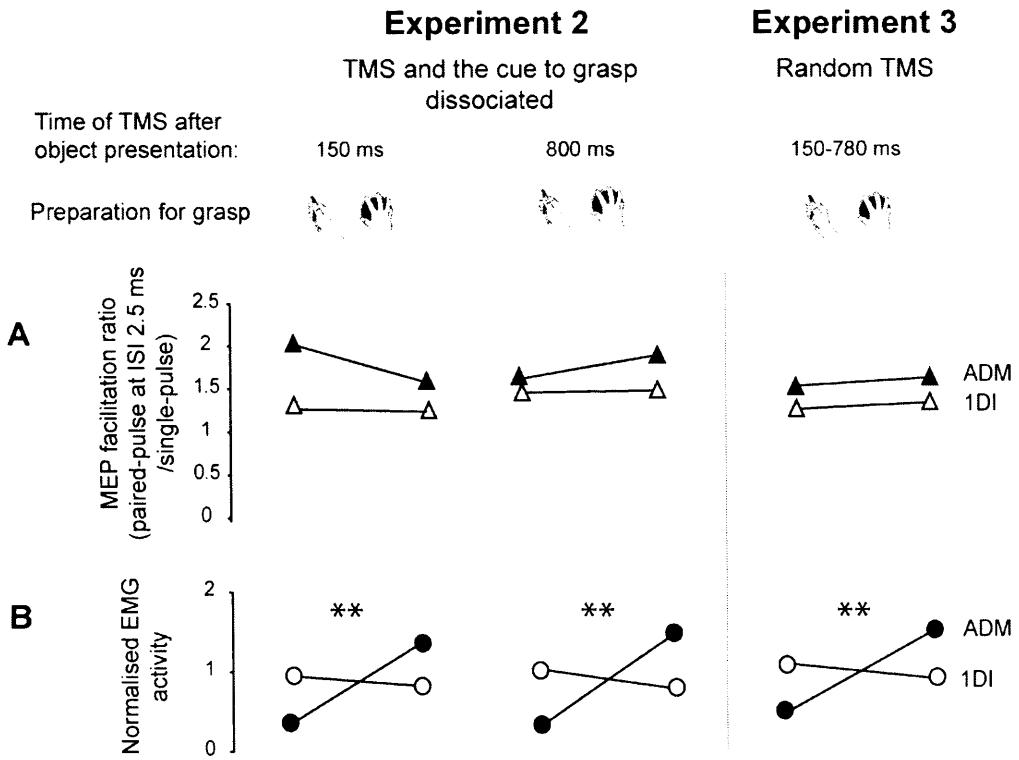

Figure 6.5 Average MEP facilitation ratio (A) and normalised average EMG activity (B) recorded during Experiments 2 and 3.

In Experiment 2, TMS was delivered in blocks at either 150 or 800 ms after object presentation, and subjects were cued to grasp by a tone at 1200 ms. In Experiment 3 random TMS delivered 150-780 ms after object presentation was the cue to grasp. Row A represents the average MEP facilitation ratio (paired-pulse MEP at ISI 2.5 ms/single-pulse MEP) prior to grasp. B shows the normalised integral of rectified EMG activity during the 300 ms preceding object contact. n=8, ** = $p < 0.01$.

6.6 Experiment 3: TMS delivered at random intervals after object presentation

These results suggest that in Experiment 1, the predictability of the 'go' signal somehow gave rise to the changes probed by TMS. Since in Experiment 2, dissociating the 'go' signal from TMS delivery abolished the MEP changes seen at late delivery (compare 800 ms data in Figure 6.2A with Figure 6.5A), it can be hypothesised that in Experiment 1, when subjects were able to predict the timing of the 'go' signal, TMS delivery occurred when subjects were about to execute the grasping action. TMS would then probe late changes in corticospinal excitability related to the upcoming movement, rather than a state of sustained preparation for action. Therefore, in a further experiment, the predictability of TMS delivery as the 'go' signal was removed. Instead TMS was delivered at random intervals between 150 and 780 ms after object presentation (see Expt. 3, Methods 2 and Figure 5.3C). The object × muscle interaction of the MEP facilitation ratio evoked by paired-pulse TMS (ISI 2.5 ms) was abolished for random TMS delivery (Figure 6.5A, right column). This was evidence in favour of phasic activation just prior to movement, rather than the set-related model. As before, the EMG activity in the hand pre-shaping period showed the same differential muscle activity (Figure 6.5B, right column), giving a significant object × muscle interaction ($p<0.001$).

If there was increased preparedness, subjects performing the blocked trials (Experiment 1) should reach and grasp faster than those tested in the random condition (Experiment 3). RT data for TMS (as the cue to grasp) at 150 and 800 ms in the blocked trials was

compared to that from the random TMS experiment. The RTs were indeed faster for TMS at 150 and 800 ms in the blocked condition compared with the random condition (Figure 6.6; 460 and 470 ms vs. 520 ms, respectively). However, this was not significant, perhaps because subjects were not instructed to perform under any particular time constraint, leading to considerable individual differences in RT.

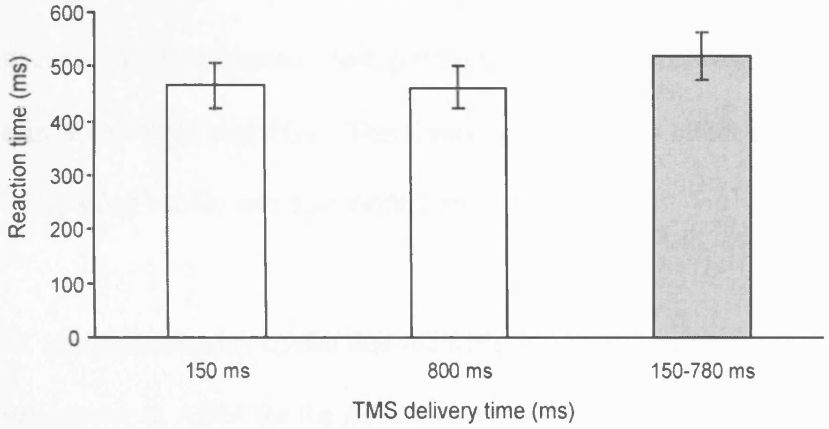

Figure 6.6 Mean reaction times from Experiments 1 and 3.

Mean RT (ms) ± standard error from Experiment 1, where TMS was delivered in blocks at 150 and 800 ms after object presentation (white bars) and RT from Experiment 3, where TMS was delivered randomly at 150-780 ms (grey bar); n=8-10.

6.7 Experiment 4: Effect of TMS ipsilateral to the grasping hand

In Experiment 4 single- and paired-pulse TMS was delivered to the hemisphere ipsilateral to the hand performing the task, with TMS delivery 1200 ms after object presentation as the 'go' signal. Task performance was unaffected by ipsilateral TMS, the EMG activity (Figure 6.7B) again showed a crossed pattern, giving a significant object × muscle interaction (paired t-test, $p=0.01$), although there was greater activation for the disc in both ADM and 1DI. There was no significant effect of object contact time when comparing handle and disc, both 1.36 s $\pm$0.3 (SD).

Figure 6.7A (second column) shows that the MEP facilitation ratio evoked with an ISI of 2.5 ms was greater in ADM for the *handle* compared to the *disc*. This is in contrast to the object-muscle activation observed in the subsequent EMG activity (Figure 6.7B) and the MEPs (ISI 2.5 ms) elicited from contralateral TMS at 800 ms (Figure 6.2A) and 1200 ms (Figure 6.7A, fourth column, taken from Cattaneo *et al.*, 2005) from object presentation, all of which showed greater activation in ADM for the *disc* compared to the *handle*. The reversed MEP pattern from ipsilateral stimulation was present for all three ISI intervals (Figure 6.7A), but failed to reach significance (object × muscle and ISI × object × muscle interactions). The MEP facilitation ratio from ipsilateral stimulation at ISI 2.5 ms, in the present study, and that from Cattaneo *et al.* (2005), where the same paradigm was used with contralateral stimulation (Figure 6.7A second and fourth column, respectively), produced a significant object × muscle × hemisphere interaction ($p<0.01$).

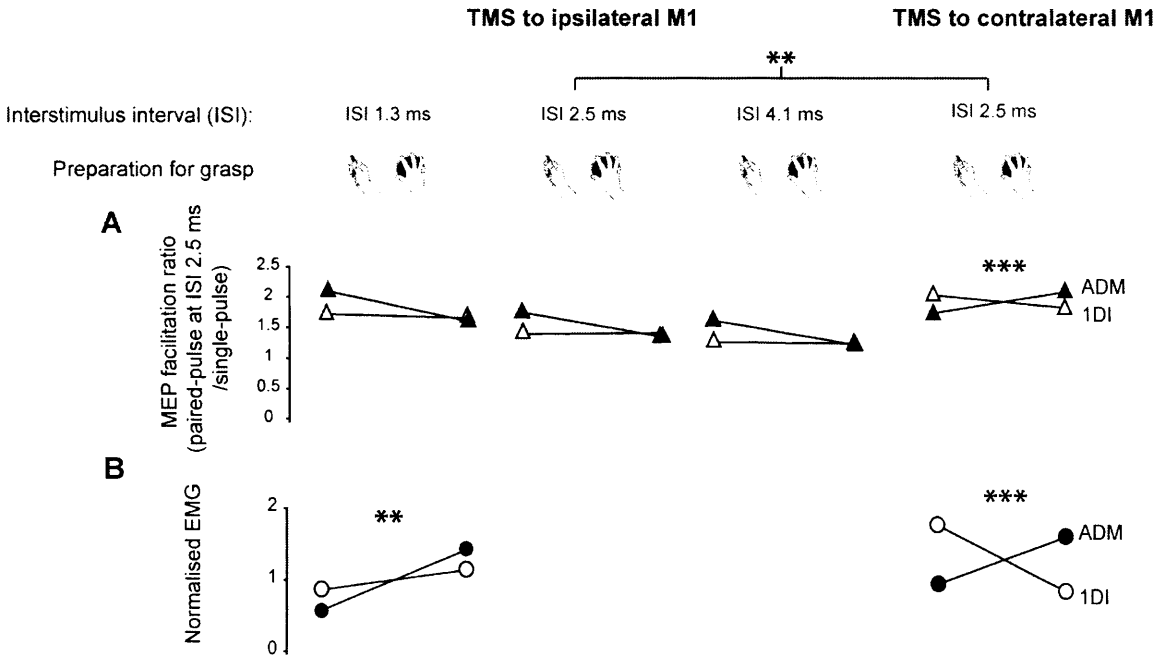

Figure 6.7 MEP facilitation (A) and normalised average EMG activity (B) recorded during ipsilateral TMS and contralateral stimulation of M1.

Row A represents the average MEP facilitation ratio (paired-pulse MEP/single-pulse MEP) prior to grasp. The three ISIs for ipsilateral stimulation (n=12) are shown (1.3, 2.5 and 4.1 ms), the far right column illustrates the average MEP elicited at ISI 2.5 ms with contralateral TMS, taken from Cattaneo *et al.* (2005) (n=10). B shows the normalised integral of rectified EMG activity during the 300 ms preceding object contact (n=11). **p<0.01, ***p<0.001.

The reversal of the MEP facilitation ratio from TMS to the ipsilateral hemisphere was not due to suppression of the paired-pulse MEP. MEPs in ADM and 1DI elicited from paired-pulse TMS had an object-specificity index of 51% for the disc (Figure 6.8, filled symbols); as an object-specificity index of 50% indicates no difference between objects, this object-related facilitation of ipsilateral paired-pulse TMS was negligible. The effect of paired-pulse TMS to the object-specific facilitation of the MEP was therefore restricted to the contralateral hemisphere.

The object-specificity index revealed facilitation from ipsilateral single-pulse TMS for the disc in ADM (57%) (Figure 6.8, left) and using contralateral stimulation (Expt. 1), suppression of the single-pulse MEP in ADM for the disc (Figure 6.2C). Previous studies have shown suppression of the single-pulse MEP, during the movement preparation and the RT period, when TMS was delivered to the ipsilateral hemisphere and facilitation when single-pulse TMS was delivered to the contralateral hemisphere (Duque *et al.*, 2005; Leocani *et al.*, 2000; van den Hurk *et al.*, 2007). The opposite effect elicited from ipsilateral stimulation observed here suggests that the effects of single-pulse TMS in this self-paced movement paradigm are different to the inhibitory effects observed in RT tasks (Duque *et al.*, 2005; Leocani *et al.*, 2000; van den Hurk *et al.*, 2007). There was little change in the object-specificity value for 1DI (Figure 6.8, right), in keeping with smaller degree of modulation observed in the EMG.

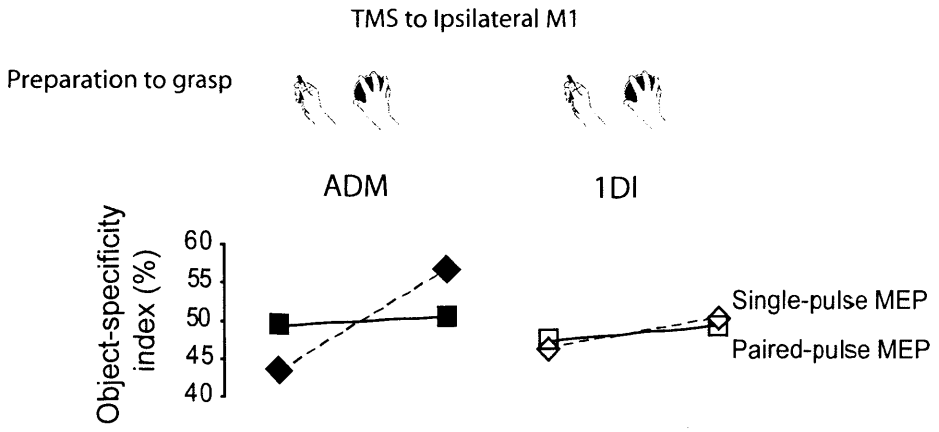

Figure 6.8 Object-specificity indices of MEPs from ipsilateral TMS to M1.
The object-specificity index prior to grasping the handle (average MEP for handle/(average MEP for the handle+average MEP for the disc)) and disc (average MEP for disc/(average MEP for the handle+average MEP for the disc)) for single- (dashed line, diamond symbols) and paired-pulse (solid line, squares) TMS is illustrated for ADM and 1DI, n=12.

6.8 Experiment 5: Visual-specificity of the object-related MEP modulation

Previously Cattaneo *et al.* (2005) showed object-specific facilitation of the paired-pulse MEP prior to visuomotor object-orientated grasp. In Experiment 5 the importance of vision of the object to the MEP interaction was investigated.

Grasping in the absence of visual information was examined first. The objects were placed behind a box, which prevented subjects from seeing the target object but allowed the object to be grasped easily (see Figure 5.2D, Methods 2). The only information subjects had about the objects was from haptic exploration prior to the experimental block. Each object/grasp was associated with a 200 ms auditory tone, which sounded at the start of the trial, TMS 1 s after the tone was the cue to grasp (Section 5.4.2, Methods 2). This timing had previously produced an object-specific modulation of the MEP (Figure 6.7A, last column, taken from Cattaneo *et al.* 2005). The lack of visual information during grasp did not affect the EMG activity during hand pre-shaping. The same significant crossed EMG pattern was seen as in previous experiments (Figure 6.9B, first column; $p<0.01$, Bonferroni corrected). However, with no visual information about the object, there was no object-specific facilitation of the MEP (Figure 6.9A, first column).

Whether the absence of an MEP interaction in the present experiment was due to the paired-pulse paradigm selectively facilitating pathways concerned with visual information was examined in a subsequent block of the experiment. Here the target

object was still designated by a 200 ms tone but both objects were visible (Section 5.4.2, Methods 2 and Figure 5.2E). Once again there was a significant crossed pattern of the EMG activity (Figure 6.9B, second column; $p<0.01$, Bonferroni corrected) but no such pattern of facilitation of the MEP (Figure 6.9A, second column).

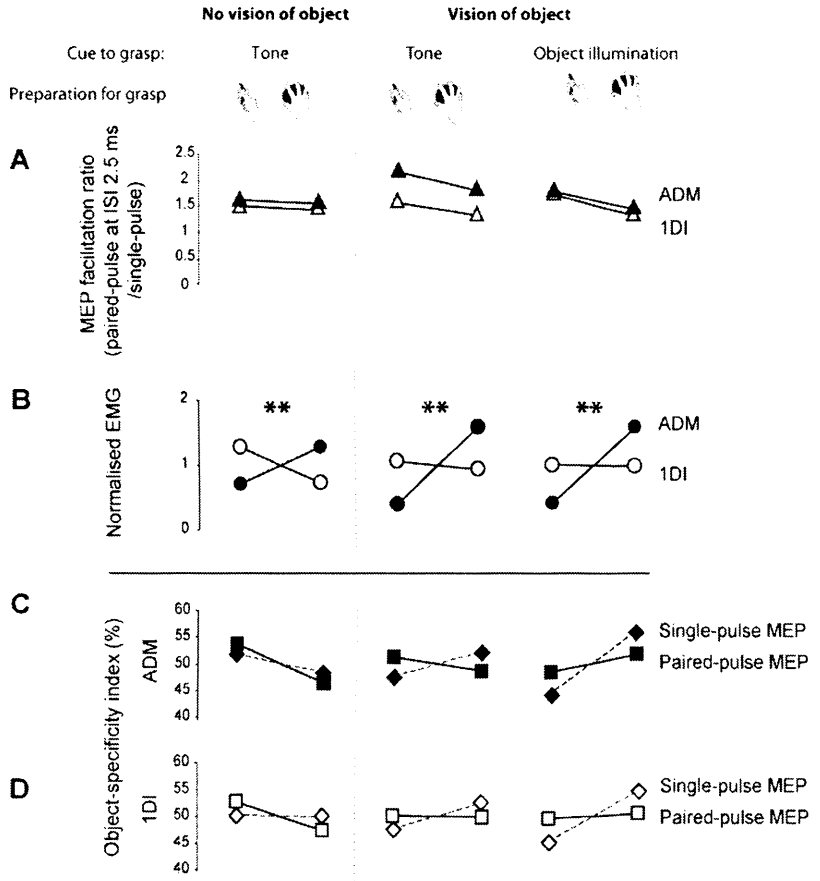

Figure 6.9 Visual specificity of the object-related MEP facilitation.

A, the first column shows the MEP facilitation ratio (paired-pulse MEP at ISI 2.5 ms/single-pulse MEP) (n=8) when subjects grasped the object without vision (the objects were hidden by a box, see Section 5.4.2, Methods 2 for details). The second column shows the MEP pattern with vision of the objects. For both these conditions the target object was identified by a 200 ms tone at the start of the trial. The last column shows the MEP facilitation ratio when the target object was illuminated for 200 ms at the start of the trial. B, the normalised integral of rectified EMG activity during the 300 ms preceding object contact (n=7). In the last two rows the object-specificity index prior to grasping the handle (average MEP for handle/(average MEP for the handle+average MEP for the disc)) and disc (average MEP for disc/(average MEP for the handle+average MEP for the disc)) for single- (dashed line, diamond symbols) and paired-pulse (solid line, squares) TMS are illustrated for ADM (C) and 1DI (D) (n=8). **$p<0.01$.

The absence of the MEP interaction may be due to subjects having to associate an arbitrary tone with each object. In the final block, rather than an auditory cue, the target object was illuminated for the first 200 ms following the start of the trial. As shown in Figure 6.9A, third column, there was still no object × muscle interaction of the MEP. The EMG activity during hand pre-shaping, as previously, showed a significant interaction (Figure 6.9B, third column; $p<0.01$, Bonferroni corrected).

Although the amount of visual information available to the subject and the designation of target objects varied between blocks, the resultant MEP and behavioural data were remarkably similar in all three conditions. Firstly, there was the absence of a significant object × muscle interaction of the MEP facilitation ratio (Figure 6.9A). Secondly for all conditions, a similar crossed pattern in the object-specificity indices for the single- and paired-pulse MEPs in ADM and 1DI was observed (Figure 6.9C, D). For both muscles and all three conditions, the object-specificity index of the paired-pulse MEP showed increased activation for the handle compared to the single-pulse MEP. Whereas prior to grasping the disc, the object-specificity index from the single-pulse MEP was greater than the paired-pulse MEP. The behavioural data showed subjects took longer to grasp the disc in all three bocks. A repeated measures ANOVA on the RT (Figure 6.10A) did not show a significant main effect of block type (no vision tone vs. vision tone vs. vision illumination) nor an interaction with or main effect of object. For the movement times, the time from homepad release to object contact, the main effect of object reached significance ($p<0.05$).

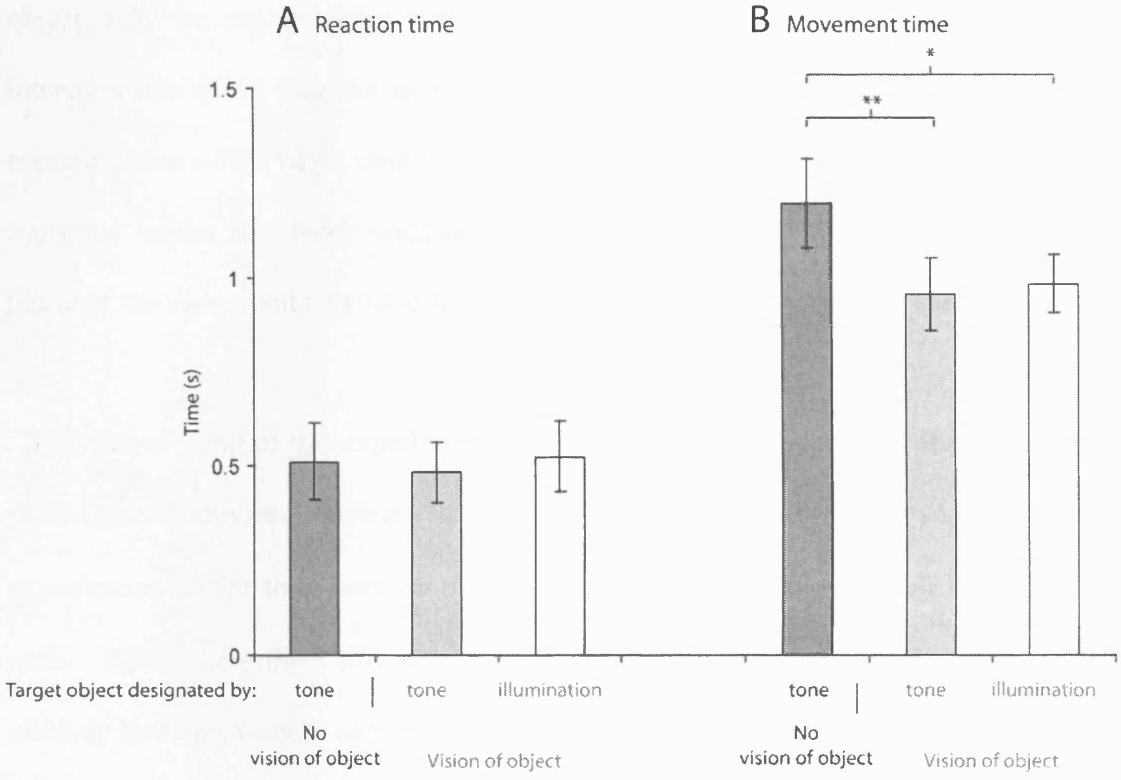

Figure 6.10 Reaction and movement times from Experiment 5.

The mean reaction and movement times, the time from homepad release to object contact, (± standard error) in seconds are shown in A and B, respectively. The dark grey columns illustrate the timings when subjects grasped the objects without vision, with the target object designated by a 200 ms auditory cue. The light grey bars, are for grasping with vision using the auditory cue, and the white bars with vision using 200 ms object illumination to designate the target object. **p=0.01, *p<0.05 (paired t-tests), n=8.

When there was no visual information about the target object available to the subjects, movement time was significantly increased (Figure 6.10B). A repeated measures ANOVA on the movement time showed a main effect of block ($p<0.05$). Subsequent paired t-tests confirmed this was due to increased movement time in the first condition (grasping without vision vs. grasping with vision (visual or auditory cue), both $p<0.05$; grasping with vision: auditory cue vs. object illumination, $p>0.05$). The longer movement time for the first block, when subjects were grasping without vision of the

object, may be explained by two, not incompatible, hypothesises. Firstly, that of increased movement time during the reach phase. The box placed over the objects, to prevent vision of the target object, may have resulted in subjects using a different reach trajectory in the first block compared to subsequent blocks. Alternatively, the grasp phase of the movement may have slowed due to subjects being unable to see the objects.

The central result of this experiment is the absence of object-specific MEP facilitation in all three conditions. There are two differences when comparing this study to previous experiments where there was an object × muscle interaction of the MEP facilitation ratio. Firstly, here there was simultaneous presentation of the two objects. It seems unlikely that the presence of both objects interfered with the planning of the grasp of the target object such that the MEP interaction was abolished. In everyday life we are surrounded by multiple objects. We have no problem in selecting one object amidst a multitude of other objects, for example grasping a spoon from a drawer full of kitchen utensils. The second explanation is that for all three conditions subjects had to remember, for 1 s, which object they would need to grasp. The target object was defined at the start of each block by a 200 ms tone or 200 ms illumination. When an object × muscle interaction of the MEP was present (Expt. 1 and Cattaneo *et al.* (2005)), only the target object was visible, and no memory of the target object was required.

6.9 Experiment 6: On line control of grasping actions

The question addressed in the final study was whether the target object needs to be designated at the time of the 'go' signal to produce object-related facilitation of the MEP. Throughout the experiment both the handle and disc were visible (see Figure 5.2E, Methods 2). In the memory-cued condition, the target object was illuminated for 200 ms at the start of the trial. Subjects had to remember the target object during the pre-movement delay, and prepare to grasp it following a 'go' signal 1200 ms later. In the visually-driven condition, the target object was illuminated throughout the trial. Thus, in this condition, subjects had current visual input designating the target object at the time of the 1200 ms 'go' signal.

As in previous experiments muscle activity during pre-shaping of the hand clearly differed when grasping the handle compared to the disc (both conditions, $p<0.001$) (Figure 6.11B). Muscle activity did not differ between visually-driven and memory-cued conditions (all, $p>0.05$). Analysis of RT using a within-subjects repeated measures ANOVA with factors of visual condition and object showed no significant main effects or interaction. The mean RT in the visually-driven condition was 386 ± 0.02 (SE) ms compared to 373 ± 0.04 ms for memory-cued condition. There were also very similar object contact times, 1.25 ± 0.26 (SD) s compared to 1.22 ± 0.25 s.

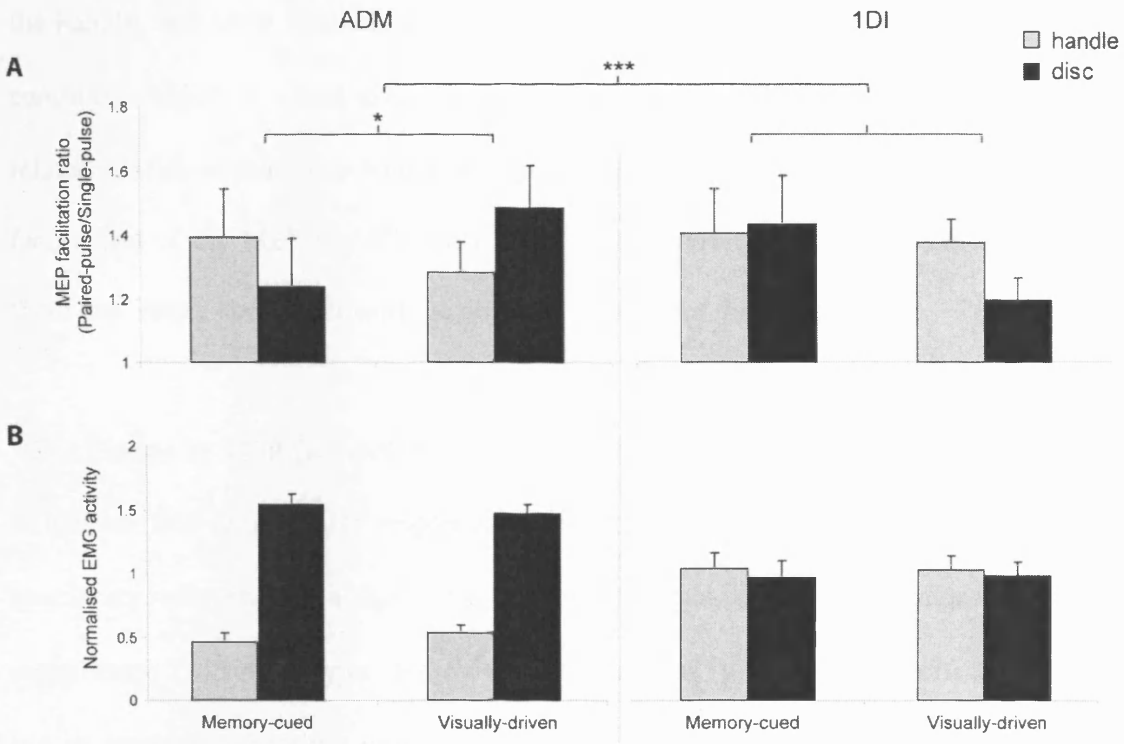

Figure 6.11 Average MEP facilitation (A) and normalised average EMG activity (B) in memory-cued and visually-driven conditions.

A, paired-pulse (ISI 2.5 ms)/single-pulse MEP facilitation ratio for both muscles in memory-cued and visually-driven conditions. B, integrated rectified EMG activity during hand pre-shaping during the 300 ms preceding object contact. n=12, *=$p<0.05$, ***=$p<0.001$.

MEP facilitation at the time of the 'go' signal, 200-640 ms prior to grasp, predicted the subsequent muscle activation pattern in the visually-driven condition, but not in the memory-cued condition (object × muscle × visual condition interaction, $p<0.001$). Thus, in the visually-driven condition, ADM showed an increase of the paired-pulse/single-pulse MEP facilitation ratio prior to grasping the disc compared to the handle (object × visual condition interaction, $p<0.05$) (Figure 6.11A). In contrast, facilitation of the ADM MEP was reduced when grasping the disc compared with the handle for the memory-cued condition. 1DI EMG activity was comparable when grasping the disc and

the handle, and MEP facilitation ratios did not vary significantly with object and visual condition (object × visual condition interaction, $p>0.05$). Thus although the grasp-related muscle activity was similar in visually-driven and memory-cued conditions, the facilitation of the MEP in ADM only reflected the subsequent muscle activation when there was visual specification of the object at the time of the cue to grasp.

This change in MEP facilitation ratio prior to grasping arose from a contrasting pattern of paired- and single-pulse responses in the visually-driven condition. The object-specificity index showed a significant three-way interaction ($p<0.01$) of muscle × visual condition × TMS pulse type. Follow up two-way ANOVA showed no effects for 1DI, but an interaction between visual condition and pulse-type for ADM ($p=0.001$). This arose because in the visually-driven condition only, paired-pulse MEPs in ADM showed significant object-specificity in the direction of the subsequent grasp-related EMG activity, with MEPs being greater for the disc than for the handle ($p<0.05$) (Figure 6.12). Single-pulse MEPs did not show a significant effect. The object-specific MEP facilitation was restricted to paired-pulse TMS stimulation of ADM when the target object was visually designated throughout the period prior to grasping.

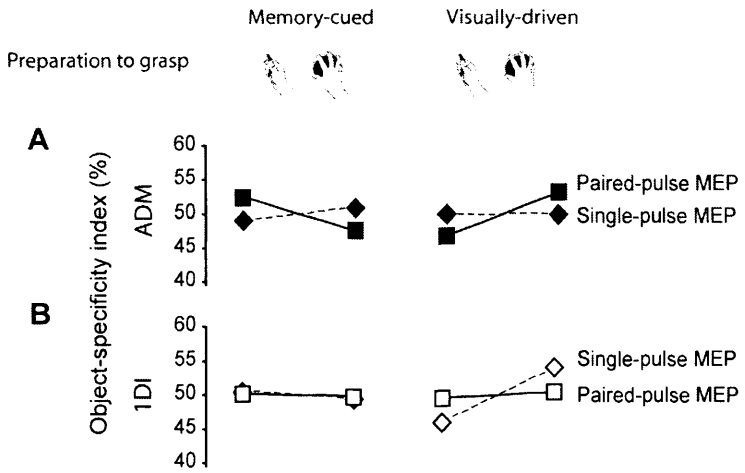

Figure 6.12 Object-specificity of MEPs prior to memory-cued and visually-driven grasp.
The object-specificity index prior to grasping the handle (average MEP for handle/(average MEP for the handle+average MEP for the disc)) and disc (average MEP for disc/(average MEP for the handle+average MEP for the disc)) for single- (dashed line, diamond symbols) and paired-pulse (solid line, squares) TMS is illustrated for ADM (A) and 1DI (B), n=12.

To summarise, these results show that the modulation from paired-pulse TMS occurs only if the target object is specified by current visual input at the moment of grasp initiation. In contrast, when subjects have to remember the target object, even for only 1 s, these results suggest a different neural network is employed. These effects were seen in the MEPs from ADM, which also showed a highly object-specific EMG pattern. The modulation of excitability is revealed as a facilitation of the MEP to paired-pulse TMS.

6.10 Discussion

The aim of the study was to investigate how the visual presentation of graspable objects influences M1 excitability prior to grasp. By manipulating the time of TMS delivery from object presentation or the cue to grasp, the question of when specific information about visible graspable objects influences M1 motor outputs controlling hand muscles was examined, and whether this influence is sustained throughout the presentation period or is only present just before grasp onset. The results confirm that the object-specific modulation of M1 activity associated with the upcoming pattern of voluntary muscle activation is reflected in the responses of hand muscles to single- and paired-pulse TMS. These specific changes were not seen when the delivery of TMS was dissociated from the cue to grasp or if the onset of grasp was unpredictable. The specificity of the object-related facilitation was further confirmed with ipsilateral TMS producing no significant effect.

For the last two studies the degree of visual information available to subjects regarding the target objects was manipulated. The object-specific facilitation of the MEP was not present if subjects were given no visual information about the objects, and were reliant on haptic information (Expt. 5). If both objects were visible but subjects still had to remember which one was the target object, again there was no object-specific facilitation of the MEP (Expts. 5 and 6). Only when the target object was illuminated throughout the trial, providing visual designation at the time of grasp initiation, was the object-related pattern of the MEPs present (Expt. 6).

6.10.1 Facilitation and suppression of MEPs during preparation for grasp

When TMS was delivered 800 ms after visual presentation of an object it evoked either suppression or facilitation of the MEP, depending on whether single- or paired-pulse TMS was used, respectively. Paired-pulse stimulation elicited a larger amplitude MEP in ADM when grasping the disc, whilst single-pulse TMS evoked suppression, and vice versa for the handle (Figure 6.2C).

These MEPs were elicited 260-657 ms before movement onset yet clearly reflected the subsequent grasp-related muscle activity. In ADM, which was much more active during hand shaping for grasping the disc than for the handle (Figure 6.2B), the MEPs also revealed a strong differential activation for the two objects (Figure 6.2C). 1DI showed somewhat more activation for the handle than for the disc, but the differences were far less marked than for ADM (Figure 6.2B). Notably, the differential 1DI activity for grasp of the two objects was not significant and the object-based modulation in the MEP from 1DI was attenuated (Figure 6.2D). Thus the level of differential EMG activity elicited by the grasping task underlies the degree of modulation in the MEP, as shown previously (Cattaneo *et al.*, 2005).

The direction of MEP modulation was determined by the TMS paradigm employed, facilitation with paired-pulse TMS (ISI 2.5 ms) and suppression with single-pulse TMS. MEP suppression could reflect mechanisms operating at both cortical and sub-cortical levels. For example, the spinal H-reflex is reduced in the movement preparation period (Hasbroucq *et al.*, 1999; Touge *et al.*, 1998). Inhibition of motoneurones through spinal

interneurones during delay periods has been directly demonstrated by Prut and Fetz (1999). At the cortical level, local inhibitory inputs to corticospinal neurons can be strongly activated by TMS (Ziemann, 1999), while cortico-cortical inputs from premotor areas can also exert inhibition of corticospinal neurons (Tokuno and Nambu, 2000) and suppression of movement (Sawaguchi *et al.*, 1996; Wise and Kurata, 1989). These pathways may be susceptible to TMS in delay period tasks where subjects are withholding a response until a 'go' signal is given.

In contrast, the characteristic effects evoked by the paired-pulse TMS paradigm are thought to occur largely at the cortical level, through interactions between I-waves evoked by the first (suprathreshold) stimulus and the second (subthreshold) stimulus (di Lazzaro *et al.*, 1999c; Tokimura *et al.*, 1996; Ziemann *et al.*, 1998a). Although both early and late I-waves are thought to arise from pre-synaptic inputs to corticospinal neurons, they show different characteristics. There is evidence that the later I-waves (I_2 and I_3) are particularly sensitive to interactions induced by paired-pulse TMS (Amassian *et al.*, 1987; di Lazzaro *et al.*, 1999c; Hanajima *et al.*, 2002; Shimazu *et al.*, 2004), while the I_1 is much less labile and probably represents a different class of input to the corticospinal neuron distinct from those evoking the later I-waves (Ilic *et al.*, 2002; Ziemann *et al.*, 1998a) (see also Section 1.4.2, Introduction). Importantly the origins of the cortico-cortical inputs facilitated by the paired-pulse TMS paradigm are unknown and are likely to arise from several cortical regions. Furthermore, more than one of these regions may be involved in aspects of object-orientated grasp. For instance in a TMS lesion study, inactivation of the ventral premotor cortex affected finger positioning

on an object whilst TMS delivered to the dorsal premotor cortex disrupted lift of the object (Davare *et al.*, 2006). In the present study, there is a focus upon a *possible* origin of the facilitated cortico-cortical projections being the ventral premotor cortex, but this does not exclude projections from other cortical inputs being facilitated by the paired-pulse paradigm.

6.10.2 Time course of excitation prior to visually guided grasp

The time course of the modulation of the MEP indicates that object-related information that can usefully influence hand shape reaches the motor cortex around 150 ms after object presentation. This is a physiologically plausible timescale. Visual cues for movement reach frontal areas at approximately 100 ms (Schluter *et al.*, 1998; Terao *et al.*, 1998a), and therefore it is unlikely that any effect on MEPs congruent with the pattern of upcoming grasp would be observed for the earliest TMS delivery at 50 ms, and this was indeed the case. Up to 100 ms there was no interaction of either single- or paired-pulse MEPs (50 and 100 ms, Figure 6.2C). Subsequently there is a period, exemplified by the findings at 150 ms, where single-pulse TMS suppressed activity in the muscle being prepared for grasp (150 ms, Figure 6.2C). This suppression was also seen at 800 ms, and at this time point the MEP in this muscle showed significant facilitation with paired-pulse TMS at ISI 2.5 ms (800 ms, Figure 6.2C). A similar significant interaction for paired-pulse TMS delivered at 1200 ms was reported previously (Cattaneo *et al.*, 2005).

6.10.3 Disruptive effects of early TMS

The behavioural results showed disruption when TMS was delivered 50 and 100 ms after object presentation. Object contact time increased when TMS was delivered at very short intervals (Figure 6.4). This suggests that early TMS acts as a virtual lesion, possibly impairing the subsequent transfer of object-related information to M1, thereby explaining the absence of an MEP interaction at these early intervals. The approach here cannot identify the source of the inputs to M1 that are being disrupted. Interestingly, a disruption of grasp by TMS over ventral premotor cortex was recently reported by Davare *et al.* (2006) when TMS was delivered 50 or 100 ms after the 'go' signal. Therefore it is possible that that the disruption of grasp by TMS over M1 described here may also reflect interference in premotor-M1 interactions and their reciprocal interconnections (Dum and Strick, 2005) at this key time point. This is not the same as saying inactivation of the two areas will produce the same deficit as these areas have different cortical and sub-cortical connections. The increased object contact time for the disc compared to the handle at these early time points may be due to the co-ordination of all five digits required to grasp the disc compared to the thumb and index finger opposition grasp required for the handle. In agreement with this, when rTMS was delivered to ventral premotor cortex, there was selective disruption of the positioning of the fingers on the object (Davare *et al.*, 2006). The significant main effect of object contact time was present for both single- and paired-pulse TMS, suggesting disruption to cortical elements from either TMS paradigms affected visuomotor grasp at these crucial time points. TMS can have two distinct actions in studies of the motor system: as a probe of cortical excitability and as a 'virtual lesion' (Merabet *et al.*, 2003). In this

study, TMS has been used as a probe. However, TMS immediately after object presentation may be additionally acting as a 'virtual lesion'.

In this light, it can be asked whether the increased object contact time was due to TMS delivery *per se*, or to the requirement for subjects to reach and grasp almost immediately after object presentation. Figure 6.4 demonstrates that there was no disruption of performance when sham TMS acted as an early 'go' signal at 50 ms. Therefore the explanation must lie in the disruptive effect of TMS itself. It seems likely that TMS at 50 and 100 ms may disrupt or prevent processing of the early visuomotor information required to *select* the appropriate reach-to-grasp movement. TMS delivery before visuomotor information has reached M1 may make it less able to respond to subsequent inputs thus delaying object contact.

6.10.4 Pattern of excitation during movement preparation

In principle the modulation of M1 outputs, prior to grasp could reflect sustained facilitation from 150 to 800 ms after object presentation by grasp-related visuomotor inputs. However, several arguments suggest that increased excitability is restricted to the period just before grasp. Firstly, while some premotor cortex neurones can show tonic set-related activity in a delayed response reach-to-grasp task (Crammond and Kalaska, 2000; Wise and Mauritz, 1985) the majority of neurones in ventral premotor area F5 show a phasic peak of firing after object presentation and then again for initiation of grasp (Murata *et al.*, 1997). A study of perceptual size illusion effects on human grasping concluded that the motor plan for grasping is formed just before

movement execution (Westwood and Goodale, 2003). Finally, TMS has been shown to delay voluntary reactions, while leaving the form of the response unaffected (Day *et al.*, 1989b). Taken together, these results suggests that the specific parameters for grasp may be stored 'upstream' of M1.

To investigate changes in the excitability of the cortico-cortical inputs to M1 in the period between visual presentation and cue to grasp, TMS was dissociated from the cue to grasp, and delivered at intervals which had previously produced MEP modulation. With the cue to grasp at 1200 ms, neither TMS at 150 nor at 800 ms produced an interaction in the MEP (Figure 6.7A, left), although the grasp-related EMG activity did show the usual interaction (Figure 6.7B, left). This suggests that the inputs to M1 have a peak of excitability at or just before the planned grasp, but not any earlier. The effect was also not present 400 ms prior to the 'go' signal. From Cattaneo *et al.* (2005), which used a 10% jitter in TMS stimulation time, it is known that this effect is present in a window of at least 100 ms around the time of the cue to grasp.

If transmission of the inputs conveying visuomotor information to M1 occurs just before movement onset, how can TMS, when it is given as the cue to move, evoke MEPs with such a significant modulation? It could be that in the blocked trials of Experiment 1, subjects anticipated the delivery of the TMS as the 'go' signal and therefore TMS probed the system just as subjects were about to execute the grasping action. Thus TMS was delivered in the period when visuomotor inputs had their greatest anticipatory influence on M1. In Experiment 3, random TMS was used to directly test

this 'predictability' hypothesis. Randomised TMS abolished the interaction effects seen in the MEP (Figure 6.7A, right). The subsequent grasp-related EMG activity was unaffected, showing the normal differential activation for the two objects (Fig. 5B, right). The results suggest that in self-paced grasp, excitatory inputs to M1 are only modulated just before the moment of grasp execution, rather than being maintained in a steady state for long periods prior to grasp.

6.10.5 Object observation

Recordings in macaque monkeys have shown firing of F5 neurones during object presentation when subsequent grasp was not required (Murata *et al.*, 1997; Raos *et al.*, 2006). Characteristically these neurones show a peak of firing on object presentation, and if there is an instruction to grasp the object, a second peak on movement initiation. In the present experiment, when subjects just observed the objects there was no task-related modulation in the corticospinal activity for any of the TMS timings used. The results suggest the excitability of inputs to M1 corresponds to the certainty of the up coming action. If subjects are not required to move, there is no need to send visuomotor signals to M1. In contrast prior to grasp, if the timing of the 'go' signal is predictable, visuomotor information is sent to M1 ready for execution of the movement.

6.10.6 The response to TMS over the ipsilateral motor cortex

The corpus callosum is the primary pathway connecting the two hemispheres and provides reciprocal connections between the two primary motor cortices (Jones and

Wise, 1977). Both excitatory and inhibitory responses are mediated by the corpus callosum. Reciprocal inhibition of M1 from the two hemispheres is thought to underlie unilateral movements of the limbs, whereas a callosotomy in patients with severe epilepsy helps to prevent spread of seizures, indicative of excitatory connections (Bloom and Hynd, 2005). With regards to motor tasks, disruption of ipsilateral M1 using rTMS interfered with the performance of grip-lift and step-tracking task, suggesting that the ipsilateral M1 contributes to the control of hand movements (Davare *et al.*, 2007). Early facilitatory responses had been recorded using double pulse TMS, a conditioning stimulus over ipsilateral M1 and a test stimulus over contralateral M1, at ISIs of 4-5 ms (Hanajima *et al.*, 2001). However, these are evoked only if medially directed currents were used for the conditioning stimulus and the test stimulus evoked I_3 waves. More often TMS studies have shown inhibitory responses, and these can be produced with less constrained conditions. Interhemispheric inhibition (IHI) has been reported in several studies using double pulse TMS over both primary motor cortex at ISIs of 6-50 ms (di Lazzaro *et al.*, 1999a; Duque *et al.*, 2007; Ferbert *et al.*, 1992; Hanajima *et al.*, 2001).

In the present study, single- and paired-pulse TMS was delivered to the ipsilateral motor cortex. Ipsilateral stimulation produced a reversal of the MEP facilitation ratio resulting in a significant object × muscle × hemisphere interaction when compared to contralateral stimulation (see Figure 6.7). The reversal of the MEP facilitation ratio from ipsilateral TMS was driven by the facilitation of the single-pulse MEP in ADM for the disc; all the other object-specificity indices had values of approximately 50%, so indicating no difference between the objects. Notably, the object-specificity index for

single-pulse stimulation in ADM was in the opposite direction as that elicited by contralateral stimulation in Experiment 1.

While the present results show contralateral *suppression* and ipsilateral *facilitation* of the single-pulse MEP, other studies have shown contralateral *facilitation* and ipsilateral *suppression* of the single-pulse MEP (Chen *et al.*, 1998; Duque *et al.*, 2005; Tomberg, 1995; van den Hurk *et al.*, 2007). The paradigms used in these studies differed in the predictability of the 'go' signal.

Facilitation of the contralateral MEP in the movement preparation period was noted in studies where there was knowledge of the movement, and the 'go' cue occurred at unpredictable times in a RT setting (Chen *et al.*, 1998; Tomberg, 1995; van den Hurk *et al.*, 2007). Here the 'go' cue was predictable and the movement to be performed was known, producing a decrease in corticospinal excitability in the movement preparation period as noted in pre-cued RT tasks (Hasbroucq *et al.*, 1997; Hasbroucq *et al.*, 1999; Touge *et al.*, 1998). In one study where subjects were not required to move, TMS itself, when delivered at predictable intervals, produced decreased corticospinal excitability, but this did not occur when the TMS was unpredictable and may be a mechanism to minimise involuntary movements evoked by TMS (Takei *et al.*, 2005).

The facilitation of the single-pulse MEP observed with ipsilateral stimulation may also be due to the timing of the TMS and the preparation level required by the task. Suppression of the ipsilateral MEP was observed when TMS was delivered in the RT

period, 70 ms before EMG onset (Duque *et al.*, 2005). In contrast, here TMS was delivered before the 'go' signal, producing facilitation of the MEP. In another RT study ipsilateral TMS was delivered in the preparation period, after the instruction cue (van den Hurk *et al.*, 2007), but unlike the present study, the timing of the 'go' signal was variable. The predictability of the 'go' signal may result in a reversal of the ipsilateral MEP response, facilitation when the 'go' signal is predictable and suppression when unpredictable; the opposite pattern of MEP facilitation to that from contralateral TMS. It has been suggested that the contralateral hemisphere inhibits the ipsilateral hemisphere to prevent mirror movement (Duque *et al.*, 2005).

6.10.7 Visual specificity of the object-specific MEP modulation

The facilitation of inputs to M1 by paired-pulse TMS is consistent with a role for these inputs in object-orientated grasp (Cattaneo *et al.*, 2005). This may reflect activity in visuomotor pathways influencing M1, or a more general neuronal transformation of the geometric properties of an object to hand-shape. In the last two experiments, objects were simultaneously presented and the degree of visual information manipulated to investigate the sensory input transmitted in the pathways facilitated by paired-pulse TMS. TMS at 1200 ms was the 'go' signal for both experiments, as this had previously produced the object-specific facilitation of the paired-pulse MEP (Cattaneo *et al.*, 2005).

If the paired-pulse paradigm is selectively enhancing inputs concerned with visuomotor grasp, the object-related facilitation should be restricted to when the target object is visible. However there is anatomical and physiological evidence for both area F5 and

M1 receiving somatosensory inputs. Anatomical studies in non-human primates have shown connections from the primary and secondary somatosensory regions to the ventral premotor cortex (Matelli *et al.*, 1986; Tanne-Gariepy *et al.*, 2002). M1 neurones also receive afferent inputs, there are indirect inputs from the primary and secondary somatosensory regions and possibly direct inputs from ascending somatosensory spinal projections (Ghosh *et al.*, 1987; Jones *et al.*, 1978; Porter and Lemon, 1993). Neural recordings from area F5 in macaque monkeys are consistent with the encoding of somatosensory information (Graziano *et al.*, 1997; Rizzolatti *et al.*, 1988). F5 neurones typically have a tactile receptive field that corresponds to their motor preference, for instance a neurone firing for precision grip having a tactile receptive field of the tip of the index finger and thumb (Rizzolatti *et al.*, 1988). Similarity, M1 neurones respond to tactile stimulation with neurones generally showing a tactile receptive field that matches the motor field (Lemon, 1981a; Lemon, 1981b). An M1 neurone that fires for passive stimulation can show inhibition during active touch or activation prior to hand contact during a motor task (Lemon, 1981a); which could differentiate sensations from movements initiated by the animal from those caused by an outside force (Jeannerod, 1997). This information may be used to provide sensory feedback on the position of the digits prior to or on contact of the object. When somatosensory feedback is prevented by local anaesthesia of the hand, there are deficits in pre-shaping of the hand and maximum grip aperture (Gentilucci *et al.*, 1997). However, while F5 and M1 may use somatosensory information to provide feedback on hand position during object contact, somatosensory information, from tactile exploration, could also be used to determine the hand shape required for grasp.

The importance of visual information for the object-specific modulation of the paired-pulse MEP was examined in Experiment 5. In the first block subjects had no visual information about the objects they were required to grasp. Instead subjects used somatosensory information, gained from haptic exploration before the experimental block, to grasp the target object. Without vision of the object there was no object-specific facilitation of the paired-pulse MEP even though the EMG activity during grasp had the typical crossed pattern of muscle activation (Figure 6.9A,B first column). This result could be interpreted as the paired-pulse paradigm selectively facilitating visuomotor inputs to M1 concerned grasp, but not those concerned with tactile information. The deficits observed when F5 was inactivated in non-human primates (Fogassi *et al.*, 2001) suggest the channel used to elaborate hand shape using vision is separate to that using tactile information. Hand shaping, after injection of muscimol in F5, was inappropriate for the size and shape of the object prior to grasp. However after tactile exploration the monkeys could grasp the object, therefore F5 inactivation produced impairment of the *visuomotor* transformation leading to grasp, but tactile sensory information could still be used to grasp the object.

Alternatively, the arbitrary cue used to designate the target object in Experiment 5 could have abolished the object × muscle interaction of the MEP. In an fMRI study, subjects pressed buttons in response to visual cues, when the instructional cue was arbitrary the ventral prefrontal, striatal and dorsal premotor cortex regions showed activation, when the instructional cue was congruent with the action there was activation of ventral premotor cortex (Toni *et al.*, 2001). In Experiment 5, when subjects could see

the object and the target object was designated by auditory tones, there was no object × muscle MEP interaction (Figure 6.9A, second column). Thus, even with vision of the object, if an arbitrary cue designates the target object the object-specific facilitation of the MEP was abolished. The importance of congruence between the cue to grasp and the subsequent grasp was directly tested when the target object was designated by object illumination for 200 ms at the start of the trial. Despite the cue to grasp being associative with the object to be grasped, there was still no object × muscle interaction of the MEP facilitation ratio (Figure 6.9A, third column). Therefore, although the vision of the object and congruence between cue and object may well be important factors in the pathway being facilitated by paired-pulse TMS, these cannot be the only reasons for the lack of an object × muscle interaction in the MEP.

There were three differences in the experimental protocol used here compared to that used by Cattaneo et al (2005), these differences may explain the absence of the object-specific MEP interaction. Firstly, in Experiment 5, the box which prevented vision of the object (Figure 5.2D) may have altered the kinematics of the reach to grasp movement. Even though subjects could easily reach and grasp the objects, the movement time, the time between homepad release and object contact, was greater when grasping without vision, so there was an extended reach-to-grasp phase compared to the subsequent blocks carried out with vision.

Secondly, the simultaneous presentation of two objects may have affected the inputs being facilitated by paired-pulse TMS. If the cortico-cortical inputs facilitated by

paired-pulse TMS are those used to transmit the motor plan to M1, it seems unlikely that that the presence of two simple shapes would obstruct transmission. Such a system would interfere with our daily functioning, as we are surrounded by, and interact with, a multitude of objects.

Thirdly, in all three conditions subjects had to remember which object to grasp, whereas previously, with serial presentation of the objects, the object to be grasped was immediately apparent. Studies in humans and non-human primates have shown different cortical regions involved in memory-cued and visually-driven grasp. Most ventral premotor cortex neurones recorded in non-human primates show object- and grasp-specific peaks of firing on initial presentation of the preferred 3D object, followed by a further peak of firing on movement initiation (Murata *et al.*, 1997). This phasic firing suggests the majority of ventral premotor cortex neurones do not maintain a 'memory' of the target object, but rely on its continued visibility throughout the delay period, similar to the visually-driven condition tested here (Expt. 6). Other premotor structures, such as the dorsal premotor cortex (Wise and Mauritz, 1985) and SMA (Halsband *et al.*, 1994; Mushiake *et al.*, 1991) may be involved in memory-cued grasp. These areas typically show set-activity, sustained firing in the period between the instruction signal and the 'go' cue (Halsband *et al.*, 1994; Kurata, 1993; Kurata and Hoffman, 1994; Mushiake *et al.*, 1991; Wise and Mauritz, 1985), presumably resulting in a very different response to TMS.

In the final experiment differences between visually-driven and memory-cued grasp were investigated. Here the target object was illuminated for either 200 ms (memory-cued condition) or for the entire 5 s trial (visually-driven condition). As in the previous experiment, in the memory-cued condition the differential pattern of the MEP facilitation ratio observed previously in Experiment 1, with increased activation of the MEP for ADM for the disc and for 1DI for the handle, was not present. However, in visually-driven condition there was an object-specific MEP interaction.

While there was no object-specific facilitation of the MEPs in the memory-cued task of Experiment 6, as expected from the results of the equivalent block in Experiment 5, the pattern of MEP modulation between these two experiments differed. In Experiment 5 object-specificity index for both muscles was the same within TMS pulse type. Single-pulse TMS produced greater facilitation for the disc in both ADM and 1DI and the paired-pulse MEP also showed the same pattern of facilitation for both muscles (Figure 6.9C, D, respectively). In the memory-cued condition of Experiment 6, the object-specificity indices differed between muscles. 1DI showed no preference for object in both single- and paired-pulse conditions while the paired-pulse MEP in ADM was greater for the handle and single-pulse for the disc (Figure 6.12A, B, respectively). The first block in Experiment 5 subjects were grasping objects hidden behind a box (Figure 5.2D), this may have altered the kinematics of the subsequent, visually-guided blocks. However as the reach trajectory and grasp kinematics were not recorded, this hypothesis can not be confirmed.

The absence of a task-related facilitation of the MEPs in the memory-cued condition in Experiments 6 cannot be explained by lack of visual information about the object, since both handle and disc were continuously visible. Moreover, analysis of reaction times to initiate grasping actions following the 'go' signal did not suggest any evidence that the sustained illumination in the visually-driven condition influenced MEPs indirectly, for example by effects of attention. The sustained illumination in the visually-driven condition could lead to subjects being more aroused or attending more selectively to the target object than in the memory-cued condition. For two reasons this seems unlikely. Firstly, any such effect should produce a shorter reaction time in visual-driven compared to a memory-cued condition. Secondly, attentional effects cannot easily explain the stronger suppression of the single-pulse MEP in the visually-driven compared to memory-cued condition.

Instead, the results suggest a distinction between two modes of selection for object-oriented action: an 'internally-guided' mode on the basis of a stored memory specifying which action to make, and a visually-driven mode which selects actions on the basis of *current* sensory information. Previously, characteristics of ventral stream processing, such as sensitivity to visual illusions, have been shown by visual occlusion of the target object on movement initiation (Westwood and Goodale, 2003). This study used a TMS paradigm that is believed to facilitate inputs from premotor cortex (Cattaneo *et al.*, 2005), though this requires further confirmation. Here the results show that even when the target object is visible, premotor cortex-M1 connectivity does not *maintain* information about the target object even over short intervals. In this study, a 1s delay

between object specification and action was sufficient to abolish the object-specific paired-pulse effects, suggesting task-related enhancement of premotor-motor connectivity reflects immediate information about an object and its affordance.

6.10.8 Conclusions

In a series of experiments it has been shown that, during the movement preparation period of self-paced visuomotor grasp, there are object and muscle specific changes in the excitability of M1. Depending on whether single- or paired-pulse TMS was delivered, the MEP in the muscle most activated during later pre-shaping of the hand for grasp was either suppressed or facilitated. Thus TMS can be used to measure contrasting patterns of corticospinal excitability during movement preparation. The study focussed particularly on the time course of these modulations. TMS over M1 delivered early, at 50 or 100 ms after object presentation, caused disruption of the subsequent movement whilst TMS delivered later, at 150 or 800 ms, elicited task-related modulation of the MEP. The effect for later TMS was abolished when stimulation was 400 ms or earlier from the imperative cue or if the time of the 'go' signal was unpredictable. This strongly indicates that the visuomotor grasping circuit modulates M1 outputs at moment of grasp execution rather than throughout the period from object presentation. The parietal-premotor circuit may prepare and then maintain grasp motor programmes during the delay period, forwarding them to primary motor cortex only at the time they are finally needed for action. The different preparatory pattern of corticospinal excitability prior to memory-cued and visually-driven grasp may be due to differences in premotor cortex activation. The premotor cortex functionally drives M1 when current sensory input specifies the appropriate action. A more complex interaction between ventral and dorsal stream visuomotor processing streams may be required when the object selected for action must be stored in memory.

7. Summary and Discussion

The relationship between the ventral premotor cortex and the primary motor cortex during grasp of a visually presented object was explored using three methodologies: single unit recording, ICMS and TMS. As the various results have been discussed in the relevant chapters, the present chapter will consider aspects that link the three studies.

7.1 Temporal changes in visuomotor encoding

In Chapter 3 single units from area F5 were recorded to elucidate object and grasp encoding at the different stages of a visuomotor grasping task. During visual presentation the majority of early-selective neurones showed object-related firing, this decreased as the trial progressed, while the number of neurones showing grasp-related firing increased during object presentation and reached a maximum during reach-to-grasp (Figure 3.11B). In the cortico-cortical visuomotor grasp circuit, AIP is believed to encode object affordance, while F5 encodes grasp and M1 is required for motor execution (Fagg and Arbib, 1998; Jeannerod *et al.*, 1995). The object-related activity of F5 neurones in the current study opens the possibility of F5 encoding object affordance. The M1 ranked population data was consistent with a role in motor execution; with an increase in the proportion of early- and late-selective neurones showing grasp-related activity during the movement phase (Figure 3.15B). Unlike the ranked population data recorded in F5, object-related data from M1 (which was only seen in a very small percentage of the sampled neurones) had no clear relationship to the different phases of the task. For both F5 and M1 populations there was a rise in the number of neurones

showing grasp-related activation which peaked during the reach-to-grasp movement. How these patterns of activation in M1 and F5 relate to motor output during object-orientated grasp was examined in two cortical stimulation studies.

The timing of cortical stimulation was driven by technical issues. Ongoing EMG is required to elicit an evoked response from M1 stimulation when using single-pulse ICMS (Cerri *et al.*, 2003; Shimazu *et al.*, 2004), therefore the stimulus was delivered during the movement phase of the task (Figure 4.1A). In contrast, MEPs are greatly affected by the level of ongoing muscle activity (Devanne *et al.*, 1997; Kischka *et al.*, 1993) (see also, Sections 1.4.4 and 6.2) so TMS was delivered prior to movement onset (Section 5.2, Methods 2).

The task performed by the monkeys in the ICMS study was the same as that for single unit recordings. The results discussed here are from one monkey that participated in both studies (M39). Single-pulse ICMS was delivered during the reach-to-grasp phase of the movement (Section 4.2.1, Chapter 4), the period when the number of neurones in F5 and M1 showing grasp-related activity was its highest level (Figure 3.11B and Figure 3.15B, respectively). Therefore the effect of F5 conditioning on the M1 test response would be expected to reflect the upcoming grasp. This was indeed the case with the largest facilitation of the test (T) response by conditioning (C) stimulation of F5 being found when the side grasp was required (Figure 4.9). There was also significant facilitation for the hook grip of the ring, but the conditioned response was not as prominent as that for the side grasps. The C-T response during the object presentation

phase of the task was not tested (for reasons stated above), however the results from the TMS study suggest that any significant conditioning effect would be confined to VP_3, the period just before the 'go' signal.

MEPs elicited from TMS delivered to M1 in healthy human volunteers reflected the pattern of EMG activity that was subsequently used to grasp the object (Figure 6.2A, B). This grasp-related facilitation of the MEP was highly specific only occurring: when grasp was required (not during object observation alone); if the time of movement onset was predictable; at one ISI; and when TMS was delivered close to the time of movement initiation. In relation to the single unit data, the time of TMS delivery that produced grasp-specific MEP facilitation is roughly equivalent to the VP_3 period, when over 50% of early-selective F5 neurones showed increased firing for object, and the number of neurones in F5 and M1 populations showing grasp-related activity was just starting to rise. When TMS was delivered earlier, for instance in Experiment 2 with TMS at 800 ms after object presentation and the 'go' cue (a tone) was at 1200 ms, there were no grasp-specific changes in the MEP amplitudes (Figure 6.5A). These results suggest that grasp-related activity is stored upstream and sent to M1 at the time of movement initiation. While the results are compatible with the ventral premotor cortex maintaining grasp-related information ready for transmission to M1, the origin of cortico-cortical inputs facilitated by paired-pulse TMS delivered to M1 remains unknown, though there is evidence for cortico-cortical inputs from the premotor cortex being able to modulate M1 corticospinal output (Amassian *et al.*, 1987; Shimazu *et al.*, 2004).

7.2 Effects of cortical stimulation

The stimulation studies support a role for the late I-wave pathways in the transmission of visuomotor information for object-orientated grasp. In the non-human primate study, the timing of significant peaks of facilitation from F5 conditioning of a M1 test stimulus occurred with a periodicity ~1 ms (Figure 4.7). This is compatible with the periodicity of I-wave generation in the corticospinal tract. Previously this ICMS paradigm has been shown to enhance the late I-wave components of the corticospinal volley in anaesthetized animals (Shimazu *et al.*, 2004). The present work extends this finding to show F5 conditioning also produces task-related enhancement during reach-to-grasp of a visible object. The TMS experiments in human subjects complemented and extended these findings. The late I-wave component of corticospinal volley can be facilitated by using a paired-pulse TMS paradigm (Amassian *et al.*, 1987; di Lazzaro *et al.*, 1999c; Hanajima *et al.*, 2002; Shimazu *et al.*, 2004). In Chapter 6 the resultant paired-pulse MEPs, elicited prior to grasp of a visually presented object was shown to reflect the upcoming pattern of muscle activation (Figure 6.2A, B). The pattern of grasp-specific facilitation is absent when making movements of the hand and digits without an object, even though this produced an equivalent differential EMG pattern (Cattaneo *et al.*, 2005); it is also absent if the object was not visible (Experiment 5, Section 6.8). Together these results, from humans and non-human primates, are consistent with the concept that cortical inputs from premotor areas transmit visuomotor information for object grasp to M1 corticospinal neurones via the late I-wave pathways.

The cognitive psychology literature emphasises the on-line nature of the dorsal visual processing stream. The rise and fall of the number of neurones with object- and grasp-related activity in M1 and F5 supports a phasic activation pattern. The TMS results further suggests grasp specification remains in the premotor cortex until just before movement execution. Furthermore, the task-related facilitation of the paired-pulse MEP only occurred if the target object was visually designated at the time of movement onset (Experiment 6, Section 6.9). These results suggest premotor-motor connectivity reflects immediate information about an object and its affordance, but does not *maintain* this information even over short intervals.

With cortical stimulation, the synchronised firing produced by electrical stimulation of the brain is far greater than that occurring in more natural conditions, and as noted by Ranck (1981), this may result in a disruption of normal function, mimicking of normal function or produce a result unrelated to normal function. As the findings presented here were those expected from the pattern of single unit activation, and as the evoked responses were also highly specific (with C-T facilitation from ICMS confined to certain muscles, objects/grasps and C-T intervals, and MEP facilitation confined to certain ISIs, muscles/grasps, timings from object presentation and tasks), it is unlikely that the pattern of evoked responses represent a general increase in excitability or that it is unrelated to function.

However, the results from single unit recordings do suggest caution when interpreting the TMS results. Activity recorded from both F5 and M1 showed that at any one time

single units exhibited a range of neuronal firing patterns, this included object- and grasp-related activity that could reflect facilitation or suppression. Therefore the evoked response represents the net effect of this activity along with any inputs from the peripheral nervous system.

The variety of patterns neuronal discharge in F5 and M1 may be reflected in the contrasting patterns of MEP suppression and facilitation observed when single- and paired-pulse TMS was delivered in the same block. The single-pulse MEP was suppressed whilst the paired-pulse MEP had the opposite pattern, facilitation in the muscle most activated by the task (Figure 6.2C). Thus TMS can highlight contrasting patterns of corticospinal activity. Notably, single-pulse TMS could also produce task-related facilitation in the movement preparation period if the task was RT and the 'go' cue unpredictable (Chen *et al.*, 1998; Mars *et al.*, 2007; Tomberg, 1995; van den Hurk *et al.*, 2007). MEPs from single- and paired-pulse TMS enhance different I-wave components. The single-pulse MEP has a prominent I_1-wave (Ilic *et al.*, 2002; Sakai *et al.*, 1997; Ziemann *et al.*, 1998a), whereas the late I-waves are facilitated by paired-pulse TMS (Amassian *et al.*, 1987; di Lazzaro *et al.*, 1999c; Hanajima *et al.*, 2002; Shimazu *et al.*, 2004). The mechanism behind the generation of the I-waves has not been resolved, but in one hypothesis the I-waves are produced by independent chains of interneurones (Day *et al.*, 1989a; Sakai *et al.*, 1997; Ziemann and Rothwell, 2000). In the monkey, intracortical stimulation of the deep layers of M1, near laminae V, produced a prominent D-wave, together with I_1-wave, whereas in the superficial layers later I-waves, such as I_3, were elicited (Amassian *et al.*, 1987; Patton and Amassian,

1954). Notably, laminae III also contains extensive cortico-cortical projections to M1 (Godschalk *et al.*, 1984; Muakkassa and Strick, 1979). It may be that neurones in lamina V are withholding the motor response, ensuring the movement occurs after the 'go' signal in a self-paced movement. In a RT task, when speed of the response is important, facilitation may aid a quick response. If differences in the firing patterns of neurones in the superficial and deep layers of the cortex are producing or contributing to the contrasting MEP amplitudes from single- and paired-pulse TMS, classification of single units by electrode depth may highlight inhibitory and facilitatory task-related activity in M1.

7.3 Task-related changes and performance levels

The present results indicate that the task subjects are asked to perform greatly influences the pattern of MEP facilitation. The primary motor cortex is considered the main cortical output stage for movement; therefore it could be hypothesised that if for two tasks the movement required is identical, a stimulus delivered to M1 would produce the same pattern of MEP modulation. This was not the case; task design greatly affected the results. The evoked response from TMS produced a grasp-specific pattern only if the 'go' signal (TMS) was predictable and if the object to be grasped was visually designated during movement initiation. This is likely to reflect, in part, the different strategies the subjects used when faced with the different tasks as well as the activation of different subsets of inputs to M1. As discussed in Chapter 6, the predictability of the 'go' signal and the speed at which the subjects were required to respond affect how prepared the subject needs to be to carry out the task, which in turn results in facilitation

or suppression of the MEP. For the work presented in this thesis, the role of F5 and M1 in natural actions was of particular interest. Therefore, both humans and non-human primates grasped simple shapes in a self-paced manner. In the monkey studies homepad release had to occur within 1 s of the 'go' cue and the time to reach, grasp and displace the object was 1 s, similarly human volunteers were asked to grasp the objects at a comfortable pace.

Task performance also needs to be considered. F5 neurones from the monkey that that always performed the correct grasp (M39) showed increased activity related to the object presented and grasp to be performed at appropriate times (Figure 3.11B). Conversely, the ranked population data for the monkey that had greater errors and made incorrect grasps (M40), did not show a systematic pattern of object- and grasp-related activity in the population data (Figure 3.11C).

7.4 The role of the ventral premotor cortex in the visuomotor grasp circuit

The results presented here suggest a wider role for F5 in the visuomotor grasp circuit then previously suggested (Fagg and Arbib, 1998; Jeannerod *et al.*, 1995). Some F5 single units showed object-related activity (Figure 3.12C) and there was an increase object-related activity present in the F5 population data during visual presentation (Figure 3.11B). This may represent the encoding of object affordance. In either case, this activity pattern has previously only been associated with neurones from AIP (Murata *et al.*, 2000; Sakata *et al.*, 1995; Taira *et al.*, 1990). Even M1 single units had a

very small amount of object-related activity (Figure 3.13C), although the population data showed a rather static proportion of neurones with increased activation for object across the seven periods of the task (Figure 3.15B). Whether the function of object encoding in F5 and M1 is different from that proposed for AIP, or if it reflects inputs from AIP remains to be seen.

7.5 Summary

The results from single unit recordings in F5 are in favour of a wider role for F5 than just encoding the grasp prototype. Single unit recordings provided evidence for F5 neurones first being activated by the visual characteristics of the object and then, later, representing the specific hand configuration for grasp of the same object. These results are compatible with visuomotor transformation for grasp occurring within area F5.

The pathways involved in the transmission of visuomotor information from F5 to M1 were examined using cortical stimulation techniques. Evidence from ICMS to area F5 and M1 in the macaque monkey during a grasping task suggested the involvement of the I-wave pathways in the transmission of the grasp prototype to M1. In human subjects, a TMS paradigm testing the excitability of cortico-cortical inputs to M1 strongly indicated that in self-paced grasp, motor programmes are sent to M1 at the time they are finally needed for action, not beforehand. The results also suggested that grasp specification only stays in the premotor cortex if there is visual drive to maintain it.

8. References

Aglioti S, DeSouza JF, Goodale MA (1995) Size-contrast illusions deceive the eye but not the hand. Curr Biol 5:679-685.

Amassian VE, Stewart M, Quirk GJ, Rosenthal JL (1987) Physiological basis of motor effects of a transient stimulus to cerebral cortex. Neurosurgery 20:74-93.

Andersen P, Hagan PJ, Phillips CG, Powell TP (1975) Mapping by microstimulation of overlapping projections from area 4 to motor units of the baboon's hand. Proc R Soc Lond B Biol Sci 188:31-36.

Ansuini C, Santello M, Massaccesi S, Castiello U (2006) Effects of end-goal on hand shaping. J Neurophysiol 95:2456-2465.

Armand J (1982) The origin, course and terminations of corticospinal fibers in various mammals. Prog Brain Res 57:329-360.

Armand J, Olivier E, Edgley SA, Lemon RN (1997) Postnatal development of corticospinal projections from motor cortex to the cervical enlargement in the macaque monkey. J Neurosci 17:251-266.

Asanuma H (1981) The pyramidal tract. In: Handbook of physiology: the nervous system (Brookhart JM, Mountcastle VB, eds), pp 703-733. Bethesda, MD: American Physiological Society.

Baker SN, Olivier E, Lemon RN (1998) An investigation of the intrinsic circuitry of the motor cortex of the monkey using intra-cortical microstimulation. Exp Brain Res 123:397-411.

Baker SN, Olivier E, Lemon RN (1995) Task-related variation in corticospinal output evoked by transcranial magnetic stimulation in the macaque monkey. J Physiol 488 (Pt 3):795-801.

Baker SN, Philbin N, Spinks R, Pinches EM, Wolpert DM, MacManus DG, Pauluis Q, Lemon RN (1999) Multiple single unit recording in the cortex of monkeys using independently moveable microelectrodes. J Neurosci Methods 94:5-17.

Baker SN, Spinks R, Jackson A, Lemon RN (2001) Synchronization in monkey motor cortex during a precision grip task. I. Task-dependent modulation in single-unit synchrony. J Neurophysiol 85:869-885.

Barker AT (1999) The history and basic principles of magnetic nerve stimulation. Electroencephalogr Clin Neurophysiol Suppl 51:3-21.

Barker AT (2002) The history and basic principles of magnetic nerve stimulation. In: Handbook of Transcranial Magnetic Stimulation (Pascual-Leone A, Davey NJ, Rothwell J, Wassermann EM, Puri BK, eds), pp 3-17. London: Arnold Publishers.

Barker AT, Jalinous R, Freeston IL (1985) Non-invasive magnetic stimulation of human motor cortex. Lancet 1:1106-1107.

Begliomini C, Wall MB, Smith AT, Castiello U (2007) Differential cortical activity for precision and whole-hand visually guided grasping in humans. Eur J Neurosci 25:1245-1252.

Bennett KM, Lemon RN (1994) The influence of single monkey cortico-motoneuronal cells at different levels of activity in target muscles. J Physiol 477 (Pt 2):291-307.

Bennett KM, Lemon RN (1996) Corticomotoneuronal contribution to the fractionation of muscle activity during precision grip in the monkey. J Neurophysiol 75:1826-1842.

Bernhard CG, Bohm E (1954a) Cortical representation of the cortico-motoneuronal system in monkeys. Experientia 10:312-315.

Bernhard CG, Bohm E (1954b) Monosynaptic corticospinal activation of fore limb motoneurones in monkeys (Macaca mulatta). Acta Physiol Scand 31:104-112.

Binkofski F, Buccino G, Posse S, Seitz RJ, Rizzolatti G, Freund H (1999) A fronto-parietal circuit for object manipulation in man: evidence from an fMRI-study. Eur J Neurosci 11:3276-3286.

Bloom JS, Hynd GW (2005) The role of the corpus callosum in interhemispheric transfer of information: excitation or inhibition? Neuropsychol Rev 15:59-71.

Borra E, Belmalih A, Calzavara R, Gerbella M, Murata A, Rozzi S, Luppino G (2007) Cortical Connections of the Macaque Anterior Intraparietal (AIP) Area. Cereb Cortex.

Brochier T, Spinks RL, Umilta MA, Lemon RN (2004) Patterns of muscle activity underlying object-specific grasp by the macaque monkey. J Neurophysiol 92:1770-1782.

Buccino G, Binkofski F, Fink GR, Fadiga L, Fogassi L, Gallese V, Seitz RJ, Zilles K, Rizzolatti G, Freund HJ (2001) Action observation activates premotor and parietal areas in a somatotopic manner: an fMRI study. Eur J Neurosci 13:400-404.

Burke D, Bartley K, Woodforth IJ, Yakoubi A, Stephen JP (2000) The effects of a volatile anaesthetic on the excitability of human corticospinal axons. Brain 123 (Pt 5):992-1000.

Burke D, Hicks R, Gandevia SC, Stephen J, Woodforth I, Crawford M (1993) Direct comparison of corticospinal volleys in human subjects to transcranial magnetic and electrical stimulation. J Physiol 470:383-393.

Buys EJ, Lemon RN, Mantel GW, Muir RB (1986) Selective facilitation of different hand muscles by single corticospinal neurones in the conscious monkey. J Physiol 381:529-549.

Canedo A (1997) Primary motor cortex influences on the descending and ascending systems. Prog Neurobiol 51:287-335.

Cattaneo L, Voss M, Brochier T, Prabhu G, Wolpert DM, Lemon RN (2005) A cortico-cortical mechanism mediating object-driven grasp in humans. Proc Natl Acad Sci U S A 102:898-903.

Cerri G, Shimazu H, Maier MA, Lemon RN (2003) Facilitation from ventral premotor cortex of primary motor cortex outputs to macaque hand muscles. J Neurophysiol 90:832-842.

Chen R, Yaseen Z, Cohen LG, Hallett M (1998) Time course of corticospinal excitability in reaction time and self-paced movements. Ann Neurol 44:317-325.

Chen R, Yung D, Li JY (2003) Organization of ipsilateral excitatory and inhibitory pathways in the human motor cortex. J Neurophysiol 89:1256-1264.

Cheney PD, Fetz EE (1985) Comparable patterns of muscle facilitation evoked by individual corticomotoneuronal (CM) cells and by single intracortical microstimuli in primates: evidence for functional groups of CM cells. J Neurophysiol 53:786-804.

Cheney PD, Fetz EE, Mewes K (1991) Neural mechanisms underlying corticospinal and rubrospinal control of limb movements. Prog Brain Res 87:213-252.

Civardi C, Cantello R, Asselman P, Rothwell JC (2001) Transcranial magnetic stimulation can be used to test connections to primary motor areas from frontal and medial cortex in humans. Neuroimage 14:1444-1453.

Crammond DJ, Kalaska JF (2000) Prior information in motor and premotor cortex: activity during the delay period and effect on pre-movement activity. J Neurophysiol 84:986-1005.

Daprati E, Sirigu A (2006) How we interact with objects: learning from brain lesions. Trends Cogn Sci 10:265-270.

Davare M, Andres M, Cosnard G, Thonnard J-L, Olivier E (2006) Dissociating the Role of Ventral and Dorsal Premotor Cortex in Precision Grasping. Journal of Neuroscience 26:2260-2268.

Davare M, Duque J, Vandermeeren Y, Thonnard JL, Olivier E (2007) Role of the ipsilateral primary motor cortex in controlling the timing of hand muscle recruitment. Cereb Cortex 17:353-362.

Day BL, Dressler D, Maertens de NA, Marsden CD, Nakashima K, Rothwell JC, Thompson PD (1989a) Electric and magnetic stimulation of human motor cortex: surface EMG and single motor unit responses. J Physiol 412:449-473.

Day BL, Rothwell JC, Thompson PD, Maertens de NA, Nakashima K, Shannon K, Marsden CD (1989b) Delay in the execution of voluntary movement by electrical or magnetic brain stimulation in intact man. Evidence for the storage of motor programs in the brain. Brain 112 (Pt 3):649-663.

Denny-Brown D (1979) Selected writings of Sir Charles Sherrington. Oxford: Oxford University Press.

Devanne H, Lavoie BA, Capaday C (1997) Input-output properties and gain changes in the human corticospinal pathway. Exp Brain Res 114:329-338.

di Lazzaro V, Oliviero A, Meglio M, Cioni B, Tamburrini G, Tonali P, Rothwell JC (2000) Direct demonstration of the effect of lorazepam on the excitability of the human motor cortex. Clin Neurophysiol 111:794-799.

di Lazzaro V, Oliviero A, Pilato F, Saturno E, Dileone M, Mazzone P, Insola A, Tonali PA, Rothwell JC (2004a) The physiological basis of transcranial motor cortex stimulation in conscious humans. Clin Neurophysiol 115:255-266.

di Lazzaro V, Oliviero A, Pilato F, Saturno E, Dileone M, Meglio M, Cioni B, Colosimo C, Tonali PA, Rothwell JC (2004b) Direct recording of the output of the motor cortex produced by transcranial magnetic stimulation in a patient with cerebral cortex atrophy. Clin Neurophysiol 115:112-115.

di Lazzaro V, Oliviero A, Pilato F, Saturno E, Insola A, Mazzone P, Tonali PA, Rothwell JC (2002) Descending volleys evoked by transcranial magnetic stimulation of the brain in conscious humans: effects of coil shape. Clin Neurophysiol 113:114-119.

di Lazzaro V, Oliviero A, Profice P, Insola A, Mazzone P, Tonali P, Rothwell JC (1999a) Direct demonstration of interhemispheric inhibition of the human motor cortex produced by transcranial magnetic stimulation. Exp Brain Res 124:520-524.

di Lazzaro V, Oliviero A, Profice P, Insola A, Mazzone P, Tonali P, Rothwell JC (1999b) Effects of voluntary contraction on descending volleys evoked by transcranial electrical stimulation over the motor cortex hand area in conscious humans. Exp Brain Res 124:525-528.

di Lazzaro V, Restuccia D, Oliviero A, Profice P, Ferrara L, Insola A, Mazzone P, Tonali P, Rothwell JC (1998) Effects of voluntary contraction on descending volleys evoked by transcranial stimulation in conscious humans. J Physiol 508 (Pt 2):625-633.

di Lazzaro V, Rothwell JC, Oliviero A, Profice P, Insola A, Mazzone P, Tonali P (1999c) Intracortical origin of the short latency facilitation produced by pairs of threshold magnetic stimuli applied to human motor cortex. Exp Brain Res 129:494-499.

Dum RP, Strick PL (1991) The origin of corticospinal projections from the premotor areas in the frontal lobe. J Neurosci 11:667-689.

Dum RP, Strick PL (2005) Frontal lobe inputs to the digit representations of the motor areas on the lateral surface of the hemisphere. J Neurosci 25:1375-1386.

Duque J, Mazzocchio R, Dambrosia J, Murase N, Olivier E, Cohen LG (2005) Kinematically specific interhemispheric inhibition operating in the process of generation of a voluntary movement. Cereb Cortex 15:588-593.

Duque J, Murase N, Celnik P, Hummel F, Harris-Love M, Mazzocchio R, Olivier E, Cohen LG (2007) Intermanual Differences in movement-related interhemispheric inhibition. J Cogn Neurosci 19:204-213.

Edgley SA, Eyre JA, Lemon RN, Miller S (1990) Excitation of the corticospinal tract by electromagnetic and electrical stimulation of the scalp in the macaque monkey. J Physiol 425:301-320.

Edgley SA, Eyre JA, Lemon RN, Miller S (1997) Comparison of activation of corticospinal neurons and spinal motor neurons by magnetic and electrical transcranial stimulation in the lumbosacral cord of the anaesthetized monkey. Brain 120 (Pt 5):839-853.

Eggermont JJ (1990) The Correlative Brain. Therory and Experiment in Neural Interaction. Berlin: Springer-Verlag.

Ehrsson HH, Fagergren A, Jonsson T, Westling G, Johansson RS, Forssberg H (2000) Cortical activity in precision- versus power-grip tasks: an fMRI study. J Neurophysiol 83:528-536.

Evarts EV (1981) Role of the motor cortex in voluntary movements in primates. In: Handbook of physiology: the nervous system (Brookhart JM, Mountcastle VB, eds), pp 1083-1120. Bethesda, MD: American Physiological Society.

Fagg AH, Arbib MA (1998) Modeling parietal-premotor interactions in primate control of grasping. Neural Netw 11:1277-1303.

Faillenot I, Toni I, Decety J, Gregoire MC, Jeannerod M (1997) Visual pathways for object-oriented action and object recognition: functional anatomy with PET. Cereb Cortex 7:77-85.

Ferbert A, Priori A, Rothwell JC, Day BL, Colebatch JG, Marsden CD (1992) Interhemispheric inhibition of the human motor cortex. J Physiol 453:525-546.

Fetz EE, Cheney PD (1980) Postspike facilitation of forelimb muscle activity by primate corticomotoneuronal cells. J Neurophysiol 44:751-772.

Flament D, Goldsmith P, Buckley CJ, Lemon RN (1993) Task dependence of responses in first dorsal interosseous muscle to magnetic brain stimulation in man. J Physiol 464:361-378.

Fogassi L, Ferrari PF, Gesierich B, Rozzi S, Chersi F, Rizzolatti G (2005) Parietal lobe: from action organization to intention understanding. Science 308:662-667.

Fogassi L, Gallese V, Buccino G, Craighero L, Fadiga L, Rizzolatti G (2001) Cortical mechanism for the visual guidance of hand grasping movements in the monkey: A reversible inactivation study. Brain 124:571-586.

Frey SH (2007) What puts the how in where? Tool use and the divided visual streams hypothesis. Cortex 43:368-375.

Frey SH, Vinton D, Norlund R, Grafton ST (2005) Cortical topography of human anterior intraparietal cortex active during visually guided grasping. Brain Res Cogn Brain Res 23:397-405.

Galea MP, Darian-Smith I (1994) Multiple corticospinal neuron populations in the macaque monkey are specified by their unique cortical origins, spinal terminations, and connections. Cereb Cortex 4:166-194.

Gallese V, Fadiga L, Fogassi L, Rizzolatti G (1996) Action recognition in the premotor cortex. Brain 119 (Pt 2):593-609.

Gallese V, Murata A, Kaseda M, Niki N, Sakata H (1994) Deficit of hand preshaping after muscimol injection in monkey parietal cortex. Neuroreport 5:1525-1529.

Gentilucci M, Fogassi L, Luppino G, Matelli M, Camarda R, Rizzolatti G (1988) Functional organization of inferior area 6 in the macaque monkey. I. Somatotopy and the control of proximal movements. Exp Brain Res 71:475-490.

Gentilucci M, Toni I, Daprati E, Gangitano M (1997) Tactile input of the hand and the control of reaching to grasp movements. Exp Brain Res 114:130-137.

Georgopoulos AP, Schwartz AB, Kettner RE (1986) Neuronal population coding of movement direction. Science 233:1416-1419.

Gerloff C, Cohen LG, Floeter MK, Chen R, Corwell B, Hallett M (1998) Inhibitory influence of the ipsilateral motor cortex on responses to stimulation of the human cortex and pyramidal tract. J Physiol 510 (Pt 1):249-259.

Gerschlager W, Siebner HR, Rothwell JC (2001) Decreased corticospinal excitability after subthreshold 1 Hz rTMS over lateral premotor cortex. Neurology 57:449-455.

Geyer S, Matelli M, Luppino G, Zilles K (2000) Functional neuroanatomy of the primate isocortical motor system. Anat Embryol (Berl) 202:443-474.

Ghosh S, Brinkman C, Porter R (1987) A quantitative study of the distribution of neurons projecting to the precentral motor cortex in the monkey (M. fascicularis). J Comp Neurol 259:424-444.

Ghosh S, Porter R (1988) Corticocortical synaptic influences on morphologically identified pyramidal neurones in the motor cortex of the monkey. J Physiol 400:617-629.

Godschalk M, Lemon RN, Kuypers HG, Ronday HK (1984) Cortical afferents and efferents of monkey postarcuate area: an anatomical and electrophysiological study. Exp Brain Res 56:410-424.

Godschalk M, Mitz AR, van DB, van der BH (1995) Somatotopy of monkey premotor cortex examined with microstimulation. Neurosci Res 23:269-279.

Goodale MA, Westwood DA (2004) An evolving view of duplex vision: separate but interacting cortical pathways for perception and action. Curr Opin Neurobiol 14:203-211.

Grafton ST, Arbib MA, Fadiga L, Rizzolatti G (1996a) Localization of grasp representations in humans by positron emission tomography. 2. Observation compared with imagination. Exp Brain Res 112:103-111.

Grafton ST, Fagg AH, Woods RP, Arbib MA (1996b) Functional anatomy of pointing and grasping in humans. Cereb Cortex 6:226-237.

Graziano MS, Hu XT, Gross CG (1997) Visuospatial properties of ventral premotor cortex. J Neurophysiol 77:2268-2292.

Graziano MS, Taylor CS, Moore T (2002a) Complex movements evoked by microstimulation of precentral cortex. Neuron 34:841-851.

Graziano MS, Taylor CS, Moore T, Cooke DF (2002b) The cortical control of movement revisited. Neuron 36:349-362.

Grezes J, Armony JL, Rowe J, Passingham RE (2003) Activations related to "mirror" and "canonical" neurones in the human brain: an fMRI study. Neuroimage 18:928-937.

Haaland KY, Harrington DL, Knight RT (2000) Neural representations of skilled movement. Brain 123 (Pt 11):2306-2313.

Halsband U, Matsuzaka Y, Tanji J (1994) Neuronal activity in the primate supplementary, pre-supplementary and premotor cortex during externally and internally instructed sequential movements. Neurosci Res 20:149-155.

Hanajima R, Ugawa Y, Machii K, Mochizuki H, Terao Y, Enomoto H, Furubayashi T, Shiio Y, Uesugi H, Kanazawa I (2001) Interhemispheric facilitation of the hand motor area in humans. J Physiol 531:849-859.

Hanajima R, Ugawa Y, Terao Y, Enomoto H, Shiio Y, Mochizuki H, Furubayashi T, Uesugi H, Iwata NK, Kanazawa I (2002) Mechanisms of intracortical I-wave facilitation elicited with paired-pulse magnetic stimulation in humans. J Physiol 538:253-261.

Hasbroucq T, Kaneko H, Akamatsu M, Possamai CA (1999) The time-course of preparatory spinal and cortico-spinal inhibition: an H-reflex and transcranial magnetic stimulation study in man. Exp Brain Res 124:33-41.

Hasbroucq T, Kaneko H, Akamatsu M, Possamai CA (1997) Preparatory inhibition of cortico-spinal excitability: a transcranial magnetic stimulation study in man. Brain Res Cogn Brain Res 5:185-192.

He SQ, Dum RP, Strick PL (1993) Topographic organization of corticospinal projections from the frontal lobe: motor areas on the lateral surface of the hemisphere. J Neurosci 13:952-980.

Heffner R, Masterton B (1975) Variation in form of the pyramidal tract and its relationship to digital dexterity. Brain Behav Evol 12:161-200.

Heffner RS, Masterton RB (1983) The role of the corticospinal tract in the evolution of human digital dexterity. Brain Behav Evol 23:165-183.

Hepp-Reymond M, Kirkpatrick-Tanner M, Gabernet L, Qi HX, Weber B (1999) Context-dependent force coding in motor and premotor cortical areas. Exp Brain Res 128:123-133.

Ilic TV, Meintzschel F, Cleff U, Ruge D, Kessler KR, Ziemann U (2002) Short-interval paired-pulse inhibition and facilitation of human motor cortex: the dimension of stimulus intensity. J Physiol 545:153-167.

Indovina I, Sanes JN (2001) On somatotopic representation centers for finger movements in human primary motor cortex and supplementary motor area. Neuroimage 13:1027-1034.

Jahanshahi M, Rothwell J (2000) Transcranial magnetic stimulation studies of cognition: an emerging field. Exp Brain Res 131:1-9.

Jankowska E (2001) Spinal interneuronal systems: identification, multifunctional character and reconfigurations in mammals. J Physiol 533:31-40.

Jankowska E, Padel Y, Tanaka R (1975) The mode of activation of pyramidal tract cells by intracortical stimuli. J Physiol 249:617-636.

Jeannerod M (1997) The cognitive neuroscience of action. Oxford: Blackwell Publishers.

Jeannerod M, Arbib MA, Rizzolatti G, Sakata H (1995) Grasping objects: the cortical mechanisms of visuomotor transformation. Trends Neurosci 18:314-320.

Johnson-Frey SH, Newman-Norlund R, Grafton ST (2005) A distributed left hemisphere network active during planning of everyday tool use skills. Cereb Cortex 15:681-695.

Jones EG, Coulter JD, Hendry SH (1978) Intracortical connectivity of architectonic fields in the somatic sensory, motor and parietal cortex of monkeys. J Comp Neurol 181:291-347.

Jones EG, Wise SP (1977) Size, laminar and columnar distribution of efferent cells in the sensory-motor cortex of monkeys. J Comp Neurol 175:391-438.

Kakei S, Hoffman DS, Strick PL (1999) Muscle and movement representations in the primary motor cortex. Science 285:2136-2139.

Kakei S, Hoffman DS, Strick PL (2003) Sensorimotor transformations in cortical motor areas. Neurosci Res 46:1-10.

Kakei S, Hoffman DS, Strick PL (2001) Direction of action is represented in the ventral premotor cortex. Nat Neurosci 4:1020-1025.

Kaneko K, Kawai S, Fuchigami Y, Morita H, Ofuji A (1996) The effect of current direction induced by transcranial magnetic stimulation on the corticospinal excitability in human brain. Electroencephalogr Clin Neurophysiol 101:478-482.

Kischka U, Fajfr R, Fellenberg T, Hess CW (1993) Facilitation of motor evoked potentials from magnetic brain stimulation in man: a comparative study of different target muscles. J Clin Neurophysiol 10:505-512.

Kurata K (1993) Premotor cortex of monkeys: set- and movement-related activity reflecting amplitude and direction of wrist movements. J Neurophysiol 69:187-200.

Kurata K, Hoffman DS (1994) Differential effects of muscimol microinjection into dorsal and ventral aspects of the premotor cortex of monkeys. J Neurophysiol 71:1151-1164.

Kurata K, Hoshi E (2002) Movement-related neuronal activity reflecting the transformation of coordinates in the ventral premotor cortex of monkeys. J Neurophysiol 88:3118-3132.

Kurata K, Tanji J (1986) Premotor cortex neurons in macaques: activity before distal and proximal forelimb movements. J Neurosci 6:403-411.

Kuypers HG (1962) Corticospinal connections: postnatal development in the rhesus monkey. Science 138:678-680.

Kuypers HG (1981) Anatomy of the descending pathways. In: Handbook of physiology: the nervous system (Brookhart JM, Mountcastle VB, eds), pp 597-666. Bethesda, MD: American Physiological Society.

Kwan HC, Mackay WA, Murphy JT, Wong YC (1978) Spatial organization of precentral cortex in awake primates. II. Motor outputs. J Neurophysiol 41:1120-1131.

Lawrence DG, Hopkins DA (1976) The development of motor control in the rhesus monkey: evidence concerning the role of corticomotoneuronal connections. Brain 99:235-254.

Lawrence DG, Kuypers HG (1968) The functional organization of the motor system in the monkey. I. The effects of bilateral pyramidal lesions. Brain 91:1-14.

Lemon R (2002) Basic physiology of transcranial magnetic stimulation. In: Handbook of Transcranial Magnetic Stimulation (Pascual-Leone A, Davey NJ, Rothwell J, Wassermann EM, Puri BK, eds), pp 61-77. London: Arnold Publishers.

Lemon RN (1984) Methods for neuronal recording in conscious animals. New York: John Wiley & Sons.

Lemon RN (1993) The G. L. Brown Prize Lecture. Cortical control of the primate hand. Exp Physiol 78:263-301.

Lemon RN (1981a) Functional properties of monkey motor cortex neurones receiving afferent input from the hand and fingers. J Physiol 311:497-519.

Lemon RN (1981b) Variety of functional organization within the monkey motor cortex. J Physiol 311:521-540.

Lemon RN, Griffiths J (2005) Comparing the function of the corticospinal system in different species: organizational differences for motor specialization? Muscle Nerve 32:261-279.

Lemon RN, Johansson RS, Westling G (1995) Corticospinal control during reach, grasp, and precision lift in man. J Neurosci 15:6145-6156.

Lemon RN, Kirkwood PA, Maier MA, Nakajima K, Nathan P (2004) Direct and indirect pathways for corticospinal control of upper limb motoneurons in the primate. Prog Brain Res 143:263-279.

Lemon RN, Muir RB, Mantel GW (1987) The effects upon the activity of hand and forearm muscles of intracortical stimulation in the vicinity of corticomotor neurones in the conscious monkey. Exp Brain Res 66:621-637.

Leocani L, Cohen LG, Wassermann EM, Ikoma K, Hallett M (2000) Human corticospinal excitability evaluated with transcranial magnetic stimulation during different reaction time paradigms. Brain 123 (Pt 6):1161-1173.

Lisanby SH, Gutman D, Luber B, Schroeder C, Sackeim HA (2001) Sham TMS: intracerebral measurement of the induced electrical field and the induction of motor-evoked potentials. Biol Psychiatry 49:460-463.

Liu CN, Chambers WW (1964) An experimental study of the cortico-spinal system in the monkey (Maca Mulatta). The spinal pathways ans preterminal distribution of degenerating fibred following discrte lesions of the pre- and postcentral gyri and bulbar pyramid. J Comp Neurol 123:257-283.

Luppino G, Murata A, Govoni P, Matelli M (1999) Largely segregated parietofrontal connections linking rostral intraparietal cortex (areas AIP and VIP) and the ventral premotor cortex (areas F5 and F4). Exp Brain Res 128:181-187.

Maier MA, Armand J, Kirkwood PA, Yang HW, Davis JN, Lemon RN (2002) Differences in the corticospinal projection from primary motor cortex and supplementary motor area to macaque upper limb motoneurons: an anatomical and electrophysiological study. Cereb Cortex 12:281-296.

Maier MA, Illert M, Kirkwood PA, Nielsen J, Lemon RN (1998) Does a C3-C4 propriospinal system transmit corticospinal excitation in the primate? An investigation in the macaque monkey. J Physiol 511 (Pt 1):191-212.

Manthey S, Schubotz RI, von Cramon DY (2003) Premotor cortex in observing erroneous action: an fMRI study. Brain Res Cogn Brain Res 15:296-307.

Mars RB, Bestmann S, Rothwell JC, Haggard P (2007) Effects of motor preparation and spatial attention on corticospinal excitability in a delayed-response paradigm. Exp Brain Res 182:125-129.

Matelli M, Camarda R, Glickstein M, Rizzolatti G (1986) Afferent and efferent projections of the inferior area 6 in the macaque monkey. J Comp Neurol 251:281-298.

Matelli M, Govoni P, Galletti C, Kutz DF, Luppino G (1998) Superior area 6 afferents from the superior parietal lobule in the macaque monkey. J Comp Neurol 402:327-352.

Matsumura M, Sawaguchi T, Oishi T, Ueki K, Kubota K (1991) Behavioral deficits induced by local injection of bicuculline and muscimol into the primate motor and premotor cortex. J Neurophysiol 65:1542-1553.

Merabet LB, Theoret H, Pascual-Leone A (2003) Transcranial magnetic stimulation as an investigative tool in the study of visual function. Optom Vis Sci 80:356-368.

Miller LE, van Kan PL, Sinkjaer T, Andersen T, Harris GD, Houk JC (1993) Correlation of primate red nucleus discharge with muscle activity during free-form arm movements. J Physiol 469:213-243.

Milner AD, Goodale MA (1995) The visual brain in action. Oxford University Press.

Mishkin M, Ungerleider LG (1982) Contribution of striate inputs to the visuospatial functions of parieto-preoccipital cortex in monkeys. Behav Brain Res 6:57-77.

Morecraft RJ, Louie JL, Herrick JL, Stilwell-Morecraft KS (2001) Cortical innervation of the facial nucleus in the non-human primate: a new interpretation of the effects of stroke and related subtotal brain trauma on the muscles of facial expression. Brain 124:176-208.

Muakkassa KF, Strick PL (1979) Frontal lobe inputs to primate motor cortex: evidence for four somatotopically organized 'premotor' areas. Brain Res 177:176-182.

Muir RB, Lemon RN (1983) Corticospinal neurons with a special role in precision grip. Brain Res 261:312-316.

Munchau A, Bloem BR, Irlbacher K, Trimble MR, Rothwell JC (2002) Functional connectivity of human premotor and motor cortex explored with repetitive transcranial magnetic stimulation. J Neurosci 22:554-561.

Murata A, Fadiga L, Fogassi L, Gallese V, Raos V, Rizzolatti G (1997) Object representation in the ventral premotor cortex (area F5) of the monkey. J Neurophysiol 78:2226-2230.

Murata A, Gallese V, Kaseda M, Sakata H (1996) Parietal neurons related to memory-guided hand manipulation. J Neurophysiol 75:2180-2186.

Murata A, Gallese V, Luppino G, Kaseda M, Sakata H (2000) Selectivity for the shape, size, and orientation of objects for grasping in neurons of monkey parietal area AIP. J Neurophysiol 83:2580-2601.

Mushiake H, Inase M, Tanji J (1991) Neuronal activity in the primate premotor, supplementary, and precentral motor cortex during visually guided and internally determined sequential movements. J Neurophysiol 66:705-718.

Nakamura H, Kitagawa H, Kawaguchi Y, Tsuji H (1996) Direct and indirect activation of human corticospinal neurons by transcranial magnetic and electrical stimulation. Neurosci Lett 210:45-48.

Napier JR (1956) The prehensile movements of the human hand. J Bone Joint Surg Br 38-B:902-913.

Nathan PW, Smith MC (1955) Long descending tracts in man. I. Review of present knowledge. Brain 78:248-303.

Nicolelis MA, Ghazanfar AA, Faggin BM, Votaw S, Oliveira LM (1997) Reconstructing the engram: simultaneous, multisite, many single neuron recordings. Neuron 18:529-537.

Nielsen J, Petersen N (1994) Is presynaptic inhibition distributed to corticospinal fibres in man? J Physiol 477 (Pt 1):47-58.

Nudo RJ, Masterton RB (1990a) Descending pathways to the spinal cord, III: Sites of origin of the corticospinal tract. J Comp Neurol 296:559-583.

Nudo RJ, Masterton RB (1990b) Descending pathways to the spinal cord, IV: Some factors related to the amount of cortex devoted to the corticospinal tract. J Comp Neurol 296:584-597.

Olivier E, Edgley SA, Armand J, Lemon RN (1997) An electrophysiological study of the postnatal development of the corticospinal system in the macaque monkey. J Neurosci 17:267-276.

Park MC, Belhaj-Saif A, Cheney PD (2004) Properties of primary motor cortex output to forelimb muscles in rhesus macaques. J Neurophysiol 92:2968-2984.

Park MC, Belhaj-Saif A, Gordon M, Cheney PD (2001) Consistent features in the forelimb representation of primary motor cortex in rhesus macaques. J Neurosci 21:2784-2792.

Patton HD, Amassian VE (1954) Single and multiple-unit analysis of cortical stage of pyramidal tract activation. J Neurophysiol 17:345-363.

Penfield W, Boldrey E (1937) Somatic motor and sensory representation in the cerebral cortex of man as studied by electrical stimulation. Brain 9:389-443.

Penfield W, Rasmussen T (1950) The cerebral cortex of man. New York: Macmillan.

Petrides M (2005) Lateral prefrontal cortex: architectonic and functional organization. Philos Trans R Soc Lond B Biol Sci 360:781-795.

Phillips, Porter R (1997) Corticospinal neurones their role in movement. London: Academic Press.

Picard N, Strick PL (2001) Imaging the premotor areas. Curr Opin Neurobiol 11:663-672.

Porter R, Lemon R (1993) Corticospinal function and voluntary movement. Oxford: Clarendon Press.

Prabhu G, Lemon R, Haggard P (2007a) On-Line Control of Grasping Actions: Object-Specific Motor Facilitation Requires Sustained Visual Input. J Neurosci 27:12651-12654.

Prabhu G, Shimazu H, Cerri G, Brochier T, Spinks RL, Maier MA, Lemon RN (2005) Modulation of primary motor cortex outputs from ventral premotor cortex during visually-guided grasp in the macaque monkey. J Physiol (Abstract) 565P, C109.

Prabhu G, Voss M, Brochier T, Cattaneo L, Haggard P, Lemon R (2007b) Excitability of human motor cortex inputs prior to grasp. J Physiol 581:189-201.

Ralston DD, Ralston HJ (1985) The terminations of corticospinal tract axons in the macaque monkey. J Comp Neurol 242:325-337.

Ranck JB (1981) Extracellular stimulation. In: Electrical stimulation techniques (Patterson MM, Kesner RP, eds), pp 1-36. Academic Press.

Raos V, Umilta MA, Murata A, Fogassi L, Gallese V (2006) Functional properties of grasping-related neurons in the ventral premotor area F5 of the macaque monkey. J Neurophysiol 95:709-729.

Rathelot JA, Strick PL (2006) Muscle representation in the macaque motor cortex: an anatomical perspective. Proc Natl Acad Sci U S A 103:8257-8262.

Rizzolatti G, Camarda R, Fogassi L, Gentilucci M, Luppino G, Matelli M (1988) Functional organization of inferior area 6 in the macaque monkey. II. Area F5 and the control of distal movements. Exp Brain Res 71:491-507.

Rizzolatti G, Fadiga L (1998) Grasping objects and grasping action meanings: the dual role of monkey rostroventral premotor cortex (area F5). Novartis Found Symp 218:81-95.

Rizzolatti G, Fadiga L, Gallese V, Fogassi L (1996) Premotor cortex and the recognition of motor actions. Brain Res Cogn Brain Res 3:131-141.

Rizzolatti G, Fogassi L, Gallese V (2002) Motor and cognitive functions of the ventral premotor cortex. Curr Opin Neurobiol 12:149-154.

Rizzolatti G, Luppino G (2001) The cortical motor system. Neuron 31:889-901.

Rizzolatti G, Luppino G, Matelli M (1998) The organization of the cortical motor system: new concepts. Electroencephalogr Clin Neurophysiol 106:283-296.

Rizzolatti G, Matelli M (2003) Two different streams form the dorsal visual system: anatomy and functions. Exp Brain Res 153:146-157.

Rizzolatti G, Scandolara C, Matelli M, Gentilucci M (1981) Afferent properties of periarcuate neurons in macaque monkeys. I. Somatosensory responses. Behav Brain Res 2:125-146.

Rockel AJ, Hiorns RW, Powell TP (1980) The basic uniformity in structure of the neocortex. Brain 103:221-244.

Rossini PM, Barker AT, Berardelli A, Caramia MD, Caruso G, Cracco RQ, Dimitrijevic MR, Hallett M, Katayama Y, Lucking CH, Maertens de Noordhout A, Marsden CD, Murray NMF, Rothwell J, Swash M, Tomberg C (1994) Non-invasive electrical and magnetic stimulation of the brain, spinal cord and roots: basic principles and procedures for routine clinical application. Report of an IFCN committee. Electroencephalogr Clin Neurophysiol 91:79-92.

Rothwell JC (1991) Physiological studies of electric and magnetic stimulation of the human brain. Electroencephalogr Clin Neurophysiol Suppl 43:29-35.

Roux S, Mackay WA, Riehle A (2006) The pre-movement component of motor cortical local field potentials reflects the level of expectancy. Behav Brain Res 169:335-351.

Ruohonen J, Ilmoniemi RJ (2002) Physical principles for transcranial magnetic stimulation. In: Handbook of Transcranial Magnetic Stimulation (Pascual-Leone A, Davey NJ, Rothwell J, Wassermann EM, Puri BK, eds), pp 18-29. London: Arnold Publishers.

Sakai K, Ugawa Y, Terao Y, Hanajima R, Furubayashi T, Kanazawa I (1997) Preferential activation of different I waves by transcranial magnetic stimulation with a figure-of-eight-shaped coil. Exp Brain Res 113:24-32.

Sakata H, Taira M, Kusunoki M, Murata A, Tsutsui K, Tanaka Y, Shein WN, Miyashita Y (1999) Neural representation of three-dimensional features of manipulation objects with stereopsis. Exp Brain Res 128:160-169.

Sakata H, Taira M, Murata A, Mine S (1995) Neural mechanisms of visual guidance of hand action in the parietal cortex of the monkey. Cereb Cortex 5:429-438.

Sawaguchi T, Yamane I, Kubota K (1996) Application of the GABA antagonist bicuculline to the premotor cortex reduces the ability to withhold reaching movements by well-trained monkeys in visually guided reaching task. J Neurophysiol 75:2150-2156.

Schieber MH (2001) Constraints on somatotopic organization in the primary motor cortex. J Neurophysiol 86:2125-2143.

Schieber MH (2000) Inactivation of the ventral premotor cortex biases the laterality of motoric choices. Exp Brain Res 130:497-507.

Schieber MH (1999) Somatotopic gradients in the distributed organization of the human primary motor cortex hand area: evidence from small infarcts. Exp Brain Res 128:139-148.

Schieber MH, Poliakov AV (1998) Partial inactivation of the primary motor cortex hand area: effects on individuated finger movements. J Neurosci 18:9038-9054.

Schluter ND, Rushworth MF, Passingham RE, Mills KR (1998) Temporary interference in human lateral premotor cortex suggests dominance for the selection of movements. A study using transcranial magnetic stimulation. Brain 121 (Pt 5):785-799.

Schwartz AB, Moran DW, Reina GA (2004) Differential representation of perception and action in the frontal cortex. Science 303:380-383.

Scott SH (2003) The role of primary motor cortex in goal-directed movements: insights from neurophysiological studies on non-human primates. Curr Opin Neurobiol 13:671-677.

Scott SH, Kalaska JF (1995) Changes in motor cortex activity during reaching movements with similar hand paths but different arm postures. J Neurophysiol 73:2563-2567.

Scott SH, Kalaska JF (1997) Reaching movements with similar hand paths but different arm orientations. I. Activity of individual cells in motor cortex. J Neurophysiol 77:826-852.

Shen L, Alexander GE (1997) Neural correlates of a spatial sensory-to-motor transformation in primary motor cortex. J Neurophysiol 77:1171-1194.

Sherrington C (1947) The integrative action of the nervous system. Cambridge University Press.

Shimazu H, Maier MA, Cerri G, Kirkwood PA, Lemon RN (2004) Macaque ventral premotor cortex exerts powerful facilitation of motor cortex outputs to upper limb motoneurons. J Neurosci 24:1200-1211.

Shinoda Y, Yokota J, Futami T (1981) Divergent projection of individual corticospinal axons to motoneurons of multiple muscles in the monkey. Neurosci Lett 23:7-12.

Stoney SD, Thompson WD, Asanuma H (1968) Excitation of pyramidal tract cells by intracortical microstimulation: effective extent of stimulating current. J Neurophysiol 31:659-669.

Taira M, Mine S, Georgopoulos AP, Murata A, Sakata H (1990) Parietal cortex neurons of the monkey related to the visual guidance of hand movement. Exp Brain Res 83:29-36.

Takei T, Hashimoto T, Hagura N, Matsumura M, Naito E (2005) Reduction of cortico-spinal excitability by transcranial magnetic stimulation at predictable timing. Jpn J Physiol 55:93-99.

Tanaka M, Lisberger SG (2001) Regulation of the gain of visually guided smooth-pursuit eye movements by frontal cortex. Nature 409:191-194.

Tanji J, Evarts EV (1976) Anticipatory activity of motor cortex neurons in relation to direction of an intended movement. J Neurophysiol 39:1062-1068.

Tanne-Gariepy J, Rouiller EM, Boussaoud D (2002) Parietal inputs to dorsal versus ventral premotor areas in the macaque monkey: evidence for largely segregated visuomotor pathways. Exp Brain Res 145:91-103.

Terao Y, Fukuda H, Ugawa Y, Hikosaka O, Hanajima R, Furubayashi T, Sakai K, Miyauchi S, Sasaki Y, Kanazawa I (1998a) Visualization of the information flow through human oculomotor cortical regions by transcranial magnetic stimulation. J Neurophysiol 80:936-946.

Terao Y, Ugawa Y (2002) Basic mechanisms of TMS. J Clin Neurophysiol 19:322-343.

Terao Y, Ugawa Y, Sakai K, Miyauchi S, Fukuda H, Sasaki Y, Takino R, Hanajima R, Furubayashi T, Putz B, Kanazawa I (1998b) Localizing the site of magnetic brain stimulation by functional MRI. Exp Brain Res 121:145-152.

Tokimura H, Ridding MC, Tokimura Y, Amassian VE, Rothwell JC (1996) Short latency facilitation between pairs of threshold magnetic stimuli applied to human motor cortex. Electroencephalogr Clin Neurophysiol 101:263-272.

Tokuno H, Nambu A (2000) Organization of nonprimary motor cortical inputs on pyramidal and nonpyramidal tract neurons of primary motor cortex: An electrophysiological study in the macaque monkey. Cereb Cortex 10:58-68.

Tomberg C (1995) Differential voluntary programming of fingers extensor commands revealed by non-invasive transcranial magnetic stimulation of the human brain. Neurosci Lett 185:41-43.

Toni I, Rushworth MF, Passingham RE (2001) Neural correlates of visuomotor associations. Spatial rules compared with arbitrary rules. Exp Brain Res 141:359-369.

Touge T, Taylor JL, Rothwell JC (1998) Reduced excitability of the cortico-spinal system during the warning period of a reaction time task. Electroencephalogr Clin Neurophysiol 109:489-495.

Tower SS (1940) Pyramidal lesions in the monkey. Brain 63:36-90.

Umilta MA, Brochier T, Spinks RL, Lemon RN (2007) Simultaneous recording of macaque premotor and primary motor cortex neuronal populations reveals different functional contributions to visuomotor grasp. J Neurophysiol 98:488-501.

van den Hurk P, Mars RB, van Elswijk G, Hegeman J, Pasman JW, Bloem BR, Toni I (2007) Online maintenance of sensory and motor representations: effects on corticospinal excitability. J Neurophysiol 97:1642-1648.

Walshe FMR (1943) On the mode of representation of movements in the motor cortex with special reference to "convulsions beginning unilaterally" (Jackson). Brain 66:104-139.

Wannier TM, Maier MA, Hepp-Reymond MC (1989) Responses of motor cortex neurons to visual stimulation in the alert monkey. Neurosci Lett 98:63-68.

Wehr M, Zador AM (2003) Balanced inhibition underlies tuning and sharpens spike timing in auditory cortex. Nature 426:442-446.

Weil A, Lassek A (1929) The quantitative distribution of the pyramidal tract in man. Archives of Neurology and Psychiatry 22:495-510.

Weinrich M, Wise SP (1982) The premotor cortex of the monkey. J Neurosci 2:1329-1345.

Werhahn KJ, Fong JK, Meyer BU, Priori A, Rothwell JC, Day BL, Thompson PD (1994) The effect of magnetic coil orientation on the latency of surface EMG and single motor unit responses in the first dorsal interosseous muscle. Electroencephalogr Clin Neurophysiol 93:138-146.

Westwood DA, Goodale MA (2003) Perceptual illusion and the real-time control of action. Spat Vis 16:243-254.

Wise SP (2006) The ventral premotor cortex, corticospinal region C, and the origin of primates. Cortex 42:521-524.

Wise SP, Kurata K (1989) Set-related activity in the premotor cortex of rhesus monkeys: effect of triggering cues and relatively long delay intervals. Somatosens Mot Res 6:455-476.

Wise SP, Mauritz KH (1985) Set-related neuronal activity in the premotor cortex of rhesus monkeys: effects of changes in motor set. Proc R Soc Lond B Biol Sci 223:331-354.

Ziemann U (1999) Intracortical inhibition and facilitation in the conventional paired TMS paradigm. Electroencephalogr Clin Neurophysiol Suppl 51:127-136.

Ziemann U, Rothwell JC (2000) I-waves in motor cortex. J Clin Neurophysiol 17:397-405.

Ziemann U, Tergau F, Wassermann EM, Wischer S, Hildebrandt J, Paulus W (1998a) Demonstration of facilitatory I wave interaction in the human motor cortex by paired transcranial magnetic stimulation. J Physiol 511 (Pt 1):181-190.

Ziemann U, Tergau F, Wischer S, Hildebrandt J, Paulus W (1998b) Pharmacological control of facilitatory I-wave interaction in the human motor cortex. A paired transcranial magnetic stimulation study. Electroencephalogr Clin Neurophysiol 109:321-330.